EXPLORING THE PROTEIN-PROTEIN INTERACTIONS OF *NEISSERIA GONORRHOEAE* CELL DIVISION PROTEINS FtsE, FtsX, FtsL AND FtsB

A Thesis Submitted to the

College of Graduate and Postdoctoral Studies

In Partial Fulfillment of the Requirements

For the Degree of Master of Science

In the Department of Biochemistry, Microbiology, and Immunology

University of Saskatchewan

Saskatoon, Saskatchewan

By

KRISTEN MIRANDA MITZEL

PERMISSION TO USE

In presenting this thesis in partial fulfillment of the requirements for a postgraduate degree from the University of Saskatchewan, I agree that the libraries of this University may make it freely available for inspection. I further agree that permission for copying of this thesis in any manner, in whole or in part, for scholarly purposes may be granted by the professor who supervised my thesis work or, in their absence, by the Head of the Department or the Dean of the College of in which my thesis work was done. It is understood that any copying or publication or use of this thesis or parts thereof for financial gain shall not be allowed without my written permission. It is also understood that due recognition shall be given to me and to the University of Saskatchewan in any scholarly use which may be made of any material in my thesis.

DISCLAIMER

Reference in this thesis to any specific commercial products, process, or service by trade name, trademark, manufacturer, or otherwise, does not constitute or imply its endorsement, recommendation, or favoring by the University of Saskatchewan. The views and opinions of the author expressed herein do not state or reflect those of the University of Saskatchewan, and shall not be used for advertising or product endorsement purposes. Requests for permission to copy or to make other uses of materials in this thesis/dissertation in whole or part should be addressed to:

Head of the Department of Biochemistry Microbiology and Immunology
GA20 Health Sciences, 107 Wiggins Road
University of Saskatchewan
Saskatoon, Saskatchewan S7N 5E5
Canada

OR:

Dean
College of Graduate and Postdoctoral Studies
116 Thorvaldson Building, 110 Science Place
University of Saskatchewan
Saskatoon, Saskatchewan S7N 5C9
Canada

ABSTRACT

Cell division is a vital process coordinated by both cell division proteins and an expansive network of protein-protein interactions. A previous study examined the interactions amongst cell division proteins in *Neisseria gonorrhoeae* (*N. gonorrhoeae*), a non-model organism, and identified several unique protein-protein interactions that are not observed in the model organism *Escherichia coli* (*E. coli)*. Studies of bacterial cell division are often performed in *E. coli,* but this previous study suggested that *N. gonorrhoeae* cell division may be distinct from *E. coli* cell division. However, this previous study of interactions amongst *N. gonorrhoeae* cell division proteins lacked information regarding the self-interactions of *N. gonorrhoeae* cell division proteins and the protein-protein interactions between cell division proteins FtsE, FtsX, FtsL, and FtsB, and the other gonococcal cell division proteins. My research investigated the interactions of these proteins using Bacterial-2-Hybrid (B2H) assays, GST pulldown assays, and affinity purification combined with mass spectrometry (AP-MS) experiments. My research detected nine protein-protein interactions (i.e., FtsE-FtsX, FtsE-FtsQ, FtsL-FtsX, FtsL-ZipA, FtsX-ZipA, FtsX-FtsK, FtsX-FtsW, FtsX-FtsN, and FtsB-FtsZ) and four self-interactions (i.e., self-interactions of FtsE, FtsW, FtsB, and FtsN). Only four of these 13 interactions are common interactions that are also observed in *E. coli* (i.e., FtsE-FtsX and the self-interactions of FtsE, FtsB, and FtsN), supporting the hypothesis that *N. gonorrhoeae* cell division proteins exhibit unique interactions. GST pulldown assays further examined the FtsE-FtsQ interaction; however, the interaction could not be confirmed. AP-MS experiments were used to examine potential interactions between *N. gonorrhoeae* FtsE and proteins in a *N. gonorrhoeae* whole cell lysate. These experiments identified over 300 possible proteins that may interact with FtsE, including the cell division proteins FtsI, FtsK, and FtsN. The Search Tool for the Retrieval of Interacting Genes/Proteins (STRING) database was also used to predict potential interactions between the proteins identified during AP-MS experiments. This analysis predicted the interactions observed between FtsE-FtsX and FtsB-FtsZ that were identified by B2H assays. My research provides new data regarding the interactions of FtsE, FtsX, FtsL, and FtsB with other cell division proteins in *N. gonorrhoeae* and indicates that *N. gonorrhoeae* has a distinct cell division interaction network.

ACKNOWLEDGEMENTS

I would like to thank my supervisor, Dr. Jo-Anne Dillon, for her unwavering support and mentorship. Thank you for fostering my love of science and always pushing me to be my best. I would also like to thank my committee members, Dr. George Katselis, Dr. Oleg Dmitriev, and Dr. Wei Xiao for their guidance and encouragement.

I would also like to thank all the current and past members of the Dillon laboratory that I had the pleasure of working with, especially Dr. Reema Singh for producing the *N. gonorrhoeae dcw* cluster map, Lyubov Pastushenko who assisted with GST pulldown experiments and Monisha Chakder who assisted with B2H experiments. I would also like to extend my sincere gratitude to the VIDO staff members I had the pleasure of interacting with, especially Neil Rawlyk and George Wong. Thank you for being kind, welcoming and always willing to answer my questions. I would also like to thank Paulo Chumala from Dr. Katselis' lab for his assistance with the mass spectrometry work that was performed in this thesis.

Thank you to both the Natural Sciences and Engineering Research Council of Canada (NSERC) and the College of Medicine for the scholarships they awarded me during my time here. I would also like to thank the Department of Biochemistry, Microbiology, and Immunology for their continuous and unwavering support. My love of science was fostered during my time as an undergraduate student in your department and your teachings helped me get to where I am today.

To Sumudu Perera, thank you for all your support and for always answering my questions, even the dumb ones. I am grateful to have met you and this thesis would not have been completed without you. To Kezia Fourie, thank you for being my sounding board; your advice and support was monumentally important to me. To Sean Lipsit, Maddie McCarthy, and Scott Dos Santos, thank you for being the most supportive and encouraging friends. I would also like to thank Paola Elizalde for being an amazing office mate and friend.

Lastly, I would like to thank my family for their sincere and steadfast support. You have always believed in me, even when I doubted myself, and I am grateful to you. Thank you for your love and guidance.

TABLE OF CONTENTS

LIST OF TABLES

LIST OF FIGURES

LIST OF ABBREVIATIONS

Abbreviation	Description
A1B1	resin + *N. gonorrhoeae* whole cell lysate
A2B2	resin + GST + *N. gonorrhoeae* whole cell lysate
A3B3	resin + GST-FtsE + *N. gonorrhoeae* whole cell lysate
A4B4	resin + interaction buffer
ABC	ATP binding cassette
AP-MS	affinity purification mass spectrometry
B2H	Bacterial-Two-Hybrid
BATCH	bacterial adenylate cyclase based two hybrid
BCA	bicinchoninic acid
B. subtilis	*Bacillus subtilis*
CAP	catabolite activator protein
DTT	Dithiothreitol
dca	division cluster competence associated
dcw	division cell wall cluster
EDTA	Ethylenediaminetetraacetic acid
E. coli and/or Ec	*Escherichia coli*
Fts	filamentous temperature sensitive
GST	glutathione S-transferase
I	Intensity
IPTG	Isopropyl β-D-1-thiogalactopyranoside
kDa	Kilodalton
LB	Luria Broth
MW	Molecular weight
NAATs	nucleic acid amplification tests
N. gonorrhoeae and/or Ng	*Neisseria gonorrhoeae*
OD	optical density
ONPG	ortho-nitrophenyl-β-galactoside
ORF	open reading frame
PBP(s)	penicillin binding protein(s)

PBS	phosphate buffered saline
PCR	polymerase chain reaction
rpm	revolutions per minute
SDS	sodium dodecyl sulphate
SDS-PAGE	sodium dodecyl sulphate polyacrylamide gel electrophoresis
SEDS	shape, elongation, division, sporulation
SpC	Spectral count
SPR	surface plasmon resonance
STRING	Search Tool for the Retrieval of Interacting Genes/Proteins
TAE	tris acetate EDTA
TBST	Tris-buffered saline + 0.05% Tween-20

1.0 INTRODUCTION

1.1 Introduction to *Neisseria gonorrhoeae*

1.1.1 Clinical Aspects of *Neisseria gonorrhoeae* – Infections and Treatment

Neisseria gonorrhoeae (N. gonorrhoeae) is a Gram-negative diplococcal bacterium and is the causative agent of the sexually transmitted infection gonorrhea (Dillon *et al.*, 2015; Sweet and Walker, 2011; Unemo *et al.*, 2019a). The World Health Organization reported 82.4 million new cases of gonorrhea worldwide in 2020 (World Health Organization, 2021). However, the prevalence of *N. gonorrhoeae* is likely under reported due to a combination of issues, including: a lack of laboratory diagnostic capability, that gonorrhea infections are often asymptomatic in women, and the presence of poor reporting systems (Dillon *et al.*, 2015; Sweet and Walker, 2011).

N. gonorrhoeae is a human-restricted pathogen that has evolved alongside its host organism (Sweet and Walker, 2011; Unemo and Shafer, 2014; Unemo *et al.*, 2019a). *N. gonorrhoeae* belongs to the *Neisseria* genus and is one of the two major pathogenic *Neisseria* species; the second pathogenic *Neisseria* species being *N. meningitidis* (Liu *et al.*, 2015; Unemo and Ison, 2013). The *Neisseria* genus includes approximately 30 understudied commensal species, including: *N. cinerea, N. sicca, N. lactamica, N. subflava,* and *N. mucosa* (Liu *et al.*, 2015; Unemo and Ison, 2013).

N. gonorrhoeae infects mucosal sites in humans which includes the pharynx, rectum, conjunctiva, and, most often, the male and female reproductive systems (Dillon *et al.*, 2015; Lenz and Dillard, 2018; Sweet and Walker, 2011). Infections in men often cause urethritis, while infections in women often cause both urethritis and cervicitis (Dillon *et al.*, 2015; Unemo and Shafer, 2014). Infections in women are often asymptomatic and, if left untreated, the infection may then spread to the upper genital tract in 10-20% of cases (Lenz and Dillard, 2018; Sweet and Walker, 2011; Unemo and Shafer, 2014; Unemo *et al.*, 2019a). Infections in the female upper genital tract may cause reproductive complications such as pelvic inflammatory disease. Pelvic inflammatory disease can increase the risk of ectopic pregnancy, involuntary infertility, and chronic pelvic pain (Dillon *et al.*, 2015; Lenz and Dillard, 2018; Sweet and Walker, 2011; Unemo *et al.*, 2019a). In men, untreated infections can also ascend to the upper genital tract, resulting in complications such as penile edema and epididymitis (Unemo and Shafer, 2014; Unemo *et al.*, 2019a).

N. gonorrhoeae infections are generally diagnosed by culturing methods or nucleic acid amplification tests (NAATs) (Sweet and Walker, 2011; Unemo and Shafer, 2014; Unemo *et al.*, 2019a). Culture was once the "gold standard" for the diagnosis of *N. gonorrhoeae* but it has been replaced by NAATs (Unemo and Ison, 2013; Unemo and Shafer, 2014; Unemo *et al.*, 2019a). In low-income settings *N. gonorrhoeae* infections are diagnosed either with culture or based on patient symptoms. Culture is used because it is inexpensive but, when there is a lack of laboratory capabilities, then the diagnosis of *N. gonorrhoeae* infections relies on syndromic management (Unemo and Shafer, 2014; Unemo *et al.*, 2019a). Culture methods requires the collection of *N. gonorrhoeae* isolates from infected mucosal sites for subsequent identification. In addition, since *N. gonorrhoeae* isolates are collected for culture diagnosis, this allows for antimicrobial resistance testing to be performed (Sweet and Walker, 2011; Unemo and Ison, 2013; Unemo and Shafer, 2014; Unemo *et al.*, 2019a). In contrast to culture methods, NAATs do not allow for antimicrobial resistance testing (Sweet and Walker, 2011; Unemo and Shafer, 2014; Unemo *et al.*, 2019a). NAATs are considered the standard diagnostic method because they are more sensitive than other methods for diagnosis (Sweet and Walker, 2011; Unemo and Shafer, 2014; Unemo *et al.*, 2019a).

Gonorrhea infections can only be treated with antibiotics because there are no vaccines available to prevent *N. gonorrhoeae* infections (Dillon *et al.*, 2015). However, *N. gonorrhoeae* has become resistant to every antibiotic used for treatment (Dillon *et al.*, 2015; Sweet and Walker, 2011). Before the invention of antibiotics, gonorrhea treatment consisted of hyperthermia, mercury compounds, or urethral irrigations (Unemo and Shafer, 2014). The first antimicrobials used to treat gonorrhea infections were sulfonamides but *N. gonorrhoeae* quickly developed resistance (Dillon *et al.*, 2015; Unemo and Shafer, 2014). Subsequently, penicillins, tetracyclines, spectinomycin, fluoroquinolones, and macrolides were all used as therapies for the treatment of *N. gonorrhoeae* infections, only for these antibiotics to also be abandoned upon the development of resistance (Dillon *et al.*, 2015; Unemo and Shafer, 2014). Extended spectrum cephalosporins (cefixime and ceftriaxone) were the recommended treatment for *N. gonorrhoeae* infections until resistant strains emerged and, in response, dual therapy treatments consisting of ceftriaxone and azithromycin were introduced (Dillon *et al.*, 2015; Unemo and Shafer, 2014). However, there have been recent reports of treatment failures due to resistance to both ceftriaxone and azithromycin (Unemo *et al.*, 2019b, 2019a). Therefore, the Center for Disease Control now recommends using single therapy treatment of high dose ceftriaxone for treatment (Workowski *et al.*, 2021; World Health Organization, 2020).

1.2 Bacterial Cell Division

1.2.1 Overview of Cell Division

Cell division is a crucial process where bacteria grow and divide into two daughter cells (Madigan *et al.*, 2003). For bacteria to divide properly, two critical events must occur during cell division. The first event involves the replication of bacterial DNA and the separation of chromosomes while the second event involves the formation of a septum at mid-cell and cellular separation (Lutkenhaus, 1993; Madigan *et al.*, 2003; Natale *et al.*, 2013; Rothfield and Justice, 1997). A large multi-protein complex known as the divisome coordinates the events of cell division until two daughter cells are created and these events include: the invagination of the cell wall and cell membrane, and the synthesis and hydrolysis of peptidoglycan (Du and Lutkenhaus, 2017; Egan and Vollmer, 2013; Madigan *et al.*, 2003; Natale *et al.*, 2013; Söderström and Daley, 2017).

1.2.2 Importance of Studying Cell Division

Bacterial cell division is often studied in model organisms. The model organism for Gram-negative bacteria is *Escherichia coli (E. coli)* while the model organism for Gram-positive bacteria is *Bacillus subtilis (B. subtilis)* (Eswara and Ramamurthi, 2017). Studies of cell division in *E. coli* have resulted in numerous groundbreaking discoveries regarding the fundamentals of cell division. One such discovery was in 1991 by Bi and Lutkenhaus when they were the first to show a cell division protein (FtsZ) could specifically localize to the mid-cell and assemble into a ring-like structure (i.e., the Z ring) (Bi and Lutkenhaus, 1991). Research of model organisms, like *E. coli*, has provided the basic knowledge of bacterial cell division. However, recent studies of non-model organisms have revealed alternative methods of cell division (Eswara and Ramamurthi, 2017).

In addition, knowledge of cell division can be used in the development of future antimicrobials (den Blaauwen *et al.*, 2014; Lock and Harry, 2008; Sass and Brötz-Oesterhelt, 2013; Vollmer, 2006). The rise of antimicrobial resistant bacteria has caused treatment of bacterial infections, including gonorrhea, to become more challenging and research has turned to developing new antibiotics (Dillon *et al.*, 2015; Lock and Harry, 2008; Sass and Brötz-Oesterhelt, 2013; Vollmer, 2006). Cell division proteins and the protein-protein interactions that occur between them have been explored as potential new antimicrobial targets (den Blaauwen *et al.*, 2014; Lock and Harry, 2008; Sass and Brötz-Oesterhelt, 2013; Vollmer, 2006). Since cell division proteins can often be essential for bacterial viability and tend to be highly conserved in bacteria (but absent in

eukaryotes), these proteins are considered promising antimicrobial targets (den Blaauwen *et al.*, 2014; Lock and Harry, 2008). In addition, as cell division proteins interact with each other, it has been proposed that protein-protein interactions amongst cell division proteins may also be utilized as targets for future antimicrobials (den Blaauwen *et al.*, 2014; Lock and Harry, 2008; Vollmer, 2006). The knowledge regarding *E. coli* cell division is extensive and has been used in the design of several antimicrobial drugs, most of which target the cell division protein FtsZ (den Blaauwen *et al.*, 2014; Lock and Harry, 2008; Sass and Brötz-Oesterhelt, 2013; Vollmer, 2006). In comparison, there is a limited amount of knowledge surrounding cell division in the non-model organism *N. gonorrhoeae.*

1.2.3 The *dcw* Cluster

Many of the genes that encode proteins involved in cell division or cell wall synthesis are frequently identified in a tightly grouped region known as the division cell wall (*dcw*) cluster (Ayala *et al.*, 1994). These *dcw* clusters have been identified in most Eubacteria. The gene content and the gene order is often highly conserved in *dcw* clusters, but it is unknown why this region is so highly conserved (Nikolaichik and Donachie, 2000; Vicente *et al.*, 1998). In fact, since the *dcw* cluster and its unique gene order can be identified in most Eubacteria, this suggests that the *dcw* cluster may have originated from a common ancestor millions of years ago (Nikolaichik and Donachie, 2000). Since this gene cluster has persisted for many years of evolution, it has been suggested that there may be some mechanism preventing the rearrangement of this gene cluster (Mingorance *et al.*, 2004; Nikolaichik and Donachie, 2000).

The *dcw* cluster in *E. coli* is a large cluster consisting of 16 genes (Figure 1.2.3) (Ayala *et al.*, 1994; Mingorance *et al.*, 2004; Vicente *et al.*, 1998). The gene products of the *E. coli dcw* cluster are involved in both cell division and peptidoglycan synthesis (Mingorance *et al.*, 2004). The Fts proteins (i.e., FtsZ, FtsA, FtsQ, FtsW, FtsL, and FtsI) are specifically involved in cell division (Du and Lutkenhaus, 2017). The *E. coli dcw* cluster may be transcribed as either one large transcript or in partial transcripts (Mingorance *et al.*, 2004; Vicente *et al.*, 1998). This is because the *E. coli dcw* cluster contains multiple internal promoters but only one transcriptional terminator, located downstream of *envA* (Mingorance *et al.*, 2004; Vicente *et al.*, 1998).

Figure 1.2.3: The *E. coli dcw* cluster. The *E. coli dcw* cluster consists of 16 genes and contains a promoter upstream of *mraZ* and one transcriptional terminator (stem loop) downstream of *envA*. Figure adapted with modifications from Mingorance *et al.* 2004. *J Mol Recognit.* 17(5). This figure is reproduced with permission from John Wiley and Sons.

1.2.4 Cell Division in *E. coli* – a Gram-negative Microorganism

1.2.4.1 Assembly of the *E. coli* Divisome

The *E. coli* divisome is a protein complex that works to execute cell division and as many as 3 dozen proteins have been identified as components of the divisome. However, only 12 are considered to be essential divisome proteins: FtsZ, ZipA, FtsA, FtsE, FtsX, FtsK, FtsQ, FtsL, FtsB, FtsW, FtsI and FtsN (Du and Lutkenhaus, 2017; Egan and Vollmer, 2013) (Figure 1.2.4.1). Genes encoding 6 of the 12 essential divisome proteins are found in the *E. coli dcw* cluster (i.e., *ftsZ*, *ftsA*, *ftsQ*, *ftsL*, *ftsI*, and *ftsW*) (Figure 1.2.3) (Du and Lutkenhaus, 2017; Mingorance *et al.*, 2004). These proteins are known as Fts proteins (filamentous temperature sensitive) because mutations in these genes have been observed to cause temperature-sensitive defects in cell division (de Boer *et al.*, 1990; Van De Putte *et al.*, 1964).

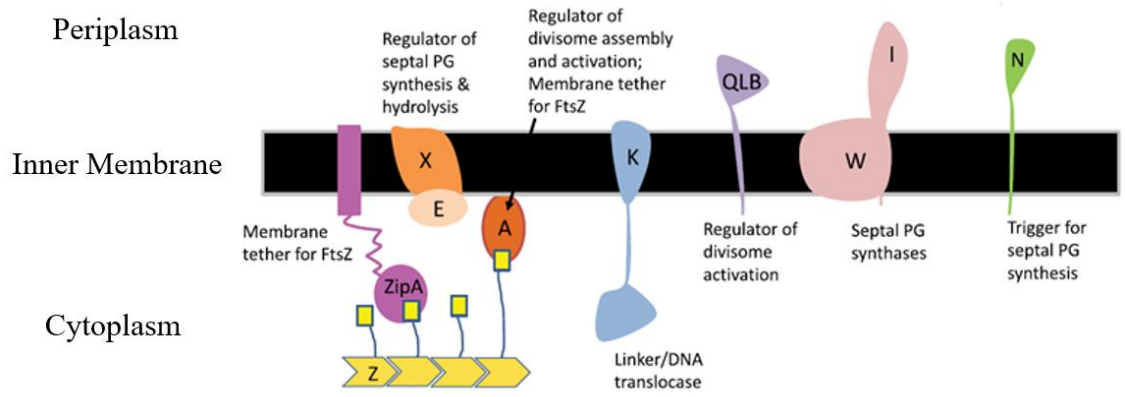

Figure 1.2.4.1: The *E. coli* Essential Divisome Proteins. The 12 essential cell division proteins of the *E. coli* divisome and their associated functions and the cellular locations. Figure adapted with modifications from Du and Lutkenhaus. 2017. *Mol Microbiol.* 105(2). This figure is reproduced with permission from John Wiley and Sons.

The bacterial divisome has been observed to assemble in two stages separated by a time delay (Aarsman *et al.*, 2005). In the first stage, FtsZ localizes to the mid-cell where it polymerizes

into the Z ring (Aarsman *et al.*, 2005; Du and Lutkenhaus, 2017). Once the Z ring has formed at mid-cell, it acts as a scaffold for the other divisome proteins to assemble onto (Du and Lutkenhaus, 2017; Söderström and Daley, 2017). Next, ZipA, FtsA, and the FtsEX complex are recruited to the divisome (Aarsman *et al.*, 2005; Du and Lutkenhaus, 2017; Pichoff and Lutkenhaus, 2002; Schmidt *et al.*, 2004). The recruitment of FtsA and ZipA requires the presence of FtsZ at the mid-cell, but ZipA and FtsA localize independently of each other (Pichoff and Lutkenhaus, 2002; Rothfield *et al.*, 1999). Together, these five proteins (i.e., FtsZ, FtsA, ZipA, FtsE, and FtsX) are considered the "early" divisome proteins (Du and Lutkenhaus, 2017). The second stage of divisome assembly begins after a time delay of approximately 17 minutes and the "late" divisome proteins (i.e., FtsK, FtsQ, FtsL, FtsB, FtsW, FtsI, and FtsN) assemble to the divisome (Aarsman *et al.*, 2005; Du and Lutkenhaus, 2017; Egan and Vollmer, 2013). The cause of this temporal delay between the first and second stages of divisome assembly is currently unknown (Aarsman *et al.*, 2005). The fully formed divisome then regulates peptidoglycan synthesis and hydrolysis, eventually leading to cell separation (Du and Lutkenhaus, 2017).

There are two ways in which the bacterial divisome can assemble itself: the linear (also known as the hierarchical) pathway or the alternative pathway (Du and Lutkenhaus, 2017). In the linear/hierarchical pathway, the divisome proteins are recruited in the following order: FtsZ → ZipA/FtsA → FtsEX → FtsK → FtsQ → FtsLB → FtsW →FtsI → FtsN (Buddelmeijer and Beckwith, 2002; Goehring *et al.*, 2006; Schmidt *et al.*, 2004). In the linear/hierarchical pathway, the recruitment of a given protein requires all the prior proteins to have localized properly to the divisome. In addition, the proper localization of that protein of interest is then required to recruit the downstream proteins as well (Goehring and Beckwith, 2005). For example, the localization of the FtsEX complex requires that FtsZ, ZipA, and FtsA have properly localized to the divisome themselves. Then, once FtsE and FtsX have been recruited to the Z ring, their presence is required for the recruitment of the downstream divisome proteins FtsK (Schmidt *et al.*, 2004) However, there are protein complexes identified in this linear recruitment pathway (i.e., the FtsQLB complex, the FtsLB subcomplex and the FtsWI complex) that can often be found pre-assembled prior to their localization to the divisome (Buddelmeijer and Beckwith, 2004; Goehring *et al.*, 2006).

The alternative pathway for divisome assembly is activated when the linear pathway has been disrupted, such as due to the absence of an early cell division protein (Pichoff *et al.*, 2018).

When FtsEX are absent, the FtsA-FtsN interaction is required to back recruit the remaining divisome proteins (Pichoff *et al.*, 2018). The presence of the alternative pathway was first identified through premature targeting experiments where late cell division proteins were forced to the divisome in the absence of early cell division proteins (Goehring *et al.*, 2006). For example, in cells where FtsW has been prematurely targeted to the divisome and FtsA has been depleted, it was found that FtsW can recruit most of the downstream divisome proteins and back recruit some upstream divisome proteins as well (Goehring *et al.*, 2006).

1.2.4.2 Characteristics of *E. coli* Early Divisome Proteins

FtsZ

FtsZ is the first cell division protein that is recruited to the divisome, where it forms a ring-like structure at mid-cell (Begg and Donachie, 1985; Bi and Lutkenhaus, 1991). FtsZ is a bacterial homolog to tubulin because, like tubulin, FtsZ is a GTPase that can bind GTP and hydrolyze it to GDP (de Boer *et al.*, 1992; Erickson, 1995; RayChaudhuri and Park, 1992). Upon binding GTP, FtsZ polymerizes into filaments, but these filaments disassemble once GTP is hydrolyzed into GDP. This cycle of assembly and disassembly suggests that the polymerization state of the Z ring is controlled by GTP hydrolysis (Mukherjee and Lutkenhaus, 1994, 1998). In addition, FtsZ and tubulin also have very similar three-dimensional structures (Löwe and Amos, 1998).

The N-terminal domain of FtsZ (i.e., the GTPase domain) binds to both GTP and other FtsZ proteins (Löwe and Amos, 1998; Wang *et al.*, 1997). Meanwhile, the C-terminal domain of FtsZ contains a small core region known as the conserved C-terminal peptide (CCTP) that mediates interactions with other cell division proteins, like ZipA and FtsA. Both ZipA and FtsA bind to the CCTP region of FtsZ, but they each have their own unique binding sites on the CCTP (Lutkenhaus and Du, 2017; Ma and Margolin, 1999; Wang *et al.*, 1997). FtsZ cannot associate to the cytoplasmic membrane on its own, so FtsA and ZipA, both membrane proteins, act as ‘anchors’ to allow for FtsZ filaments to associate to the cytoplasmic membrane. The presence of one of these proteins (i.e., FtsA or ZipA) is sufficient for Z ring formation (Hale and de Boer, 1997; Pichoff and Lutkenhaus, 2002, 2005).

FtsA

FtsA is an essential inner membrane cell division protein that binds ATP and is a member of the ATPase superfamily (Bork *et al.*, 1992; Lutkenhaus, 1993; Margolin, 2000; Pichoff and

Lutkenhaus, 2005; Pla *et al.*, 1990; Sánchez *et al.*, 1994). FtsA has two domains, known as domain 1 and domain 2, with the ATP binding site found in the cleft between these domains. These domains can be further divided into subdomains; there are 2 sub-domains for domain 1 (i.e., 1A and 1C) and 2 sub-domains for domain 2 (i.e., 2A and 2B) (van den Ent and Löwe, 2000). The 1C domain is necessary for the FtsA to self-interact and to recruit the downstream divisome proteins while domain 2B mediates the interaction with FtsZ (Pichoff and Lutkenhaus, 2007; Rico *et al.*, 2004).

The localization of FtsA to the divisome is dependent on the presence of the Z ring because, in the absence of the Z ring, FtsA cannot localize (Addinall and Lutkenhaus, 1996; Bramhill, 1997). FtsA is vital in recruiting proteins to the divisome in both the linear and alternative assembly pathways (Du *et al.*, 2016; Pichoff *et al.*, 2018). In the linear assembly pathway, FtsX of the FtsEX complex directly interacts with FtsA, causing the recruitment of downstream divisome proteins, including FtsK and FtsW (Du *et al.*, 2016). However, in cells lacking FtsEX, the alternative pathway is activated and FtsA interacts with FtsN, thereby allowing for the back recruitment of other division proteins (Pichoff *et al.*, 2018).

ZipA

ZipA (FtsZ interacting protein A) is a single-pass inner membrane protein that localizes to the divisome and the Z ring early in cell division. The N-terminal transmembrane domain of ZipA acts to anchor the protein in the inner membrane while the remainder of the protein is found in the cytoplasm (Hale and de Boer, 1997; Skoog and Daley, 2012). ZipA anchors the Z ring to the inner membrane through an interaction between the C-terminal peptide region of FtsZ and the FtsZ binding domain (FZB) located at the extreme C-terminus of ZipA (Egan and Vollmer, 2013; Skoog and Daley, 2012). Recently, cross-linking experiments determined that ZipA can self-interact and form dimers (Skoog and Daley, 2012).

The localization of ZipA to the divisome is dependent on the presence of FtsZ, like the localization of FtsA. However, ZipA can localize to the divisome independently of FtsA (Hale and de Boer, 1999; Liu *et al.*, 1999; Margolin, 2000). ZipA is also similar to FtsA in that ZipA also recruits downstream divisome proteins, including FtsK, FtsQ, FtsL and FtsN (Hale and de Boer, 2002). Therefore, both FtsA and ZipA are required to recruit downstream divisome proteins, but only one of these proteins is required for Z ring assembly. These proteins have overlapping roles

in Z ring assembly and formation of the divisome (Du *et al.*, 2016; Hale and de Boer, 2002; Margolin, 2000; Pichoff and Lutkenhaus, 2002).

FtsE/FtsX

In *E. coli*, *ftsE* and *ftsX* are considered conditionally essential cell division genes. These proteins are essential to cell division when *E. coli* is grown in low salt conditions but are not essential when *E. coli* is grown in high salt media (>0.5% NaCl). These proteins can be considered osmoremedial proteins since they are essential in low salt conditions (de Leeuw *et al.*, 1999; Reddy, 2007; Schmidt *et al.*, 2004).

FtsE and FtsX interact with each other to form the FtsEX complex, an inner membrane complex that has similar characteristics to an ATP binding cassette (ABC) type transporter. FtsX is a membrane protein while FtsE is a membrane associated protein due to its interaction with FtsX (Gill and Salmond, 1987; de Leeuw *et al.*, 1999).

FtsE and FtsX both localize to the Z ring, implying they are involved in cell division (Schmidt *et al.*, 2004). An initial study examining the localization ability for FtsE and FtsX found that FtsX targets the FtsEX complex to the divisome because FtsX can localize in the absence of FtsE, but FtsE cannot localize in the absence of FtsX (Arends *et al.*, 2009). However, a more recent study suggests that FtsE and FtsX localize to the division septum in a co-dependent manner. Du *et al.* found that the presence of one of the proteins (i.e., FtsE or FtsX) was required for the localization of the partner protein (i.e., FtsX or FtsE) to the division septum (Du *et al.*, 2019).

The FtsEX complex assists in building the divisome through the recruitment of downstream divisome proteins to the Z ring (Du *et al.*, 2016; Schmidt *et al.*, 2004). The FtsEX complex interacts with FtsA to trigger the recruitment of downstream divisome proteins (Du *et al.*, 2016; Pichoff *et al.*, 2019). The FtsEX complex localizes after the early divisome proteins FtsZ, ZipA and FtsA have localized to mid-cell but before the late divisome protein FtsK localizes to mid-cell (Schmidt *et al.*, 2004). If the FtsEX complex does not localize to the divisome, then downstream divisome proteins such as FtsK, FtsQ and FtsI do not localize (Schmidt *et al.*, 2004). The FtsEX complex also interacts with the amidase activator EnvC to recruit it to the divisome (Yang *et al.*, 2011).

The ATPase activity of the FtsEX complex appears to be involved in cell constriction and cell separation (Arends *et al.*, 2009; Du *et al.*, 2016, 2019; Yang *et al.*, 2011). Mutations in the

ATPase domain of FtsE are found to cause defects in cell constriction but there is no effect on either the ability of FtsE to localize to the Z ring or its ability to recruit downstream proteins (Arends *et al.*, 2009). These ATPase domain mutants act through FtsA to inhibit divisome activation because when the FtsX-FtsA interaction is abrogated, either by mutations in FtsA or deletion of the N-terminal cytoplasmic domain of FtsX, cell division is restored. (Du *et al.*, 2016, 2019). In addition, the ATPase activity of the FtsEX complex is required to activate the amidase EnvC for cell separation to occur because when the ATPase domain is mutated, cell separation does not occur (Yang *et al.*, 2011).

1.2.4.3 Characteristics of *E. coli* Late Divisome Proteins

FtsK

FtsK is a large (147 kDa) essential cell division protein and is considered the first of the "late" divisome proteins because it localizes to the Z ring after FtsZ and FtsA but before the remaining "late" proteins FtsQ, FtsI or FtsN (Begg *et al.*, 1995; Draper *et al.*, 1998; Wang and Lutkenhaus, 1998; Yu *et al.*, 1998). FtsK has an N-terminal domain with several membrane spanning regions and a C-terminal domain with nucleotide binding consensus sequence *(*Begg *et al.*, 1995). FtsK is a bi-functional protein involved in both cell division and chromosome segregation. The N-terminal domain of FtsK is involved in cell division while the C-terminal domain is involved in chromosome segregation (Draper *et al.*, 1998; Liu *et al.*, 1998). Only ~15% of the N-terminal of FtsK is required to both localize FtsK to the divisome and assist in cell division (Draper *et al.*, 1998; Yu *et al.*, 1998). Meanwhile, the C-terminal domain of FtsK is involved in chromosome segregation as it is a DNA translocase that is able to translocate dsDNA and activate Xer recombinases to perform chromosome dimer resolution (Aussel *et al.*, 2002; Liu *et al.*, 1998; Sherratt *et al.*, 2001).

FtsQ/FtsL/FtsB

FtsQ, FtsL and FtsB are highly conserved bitopic proteins that form the FtsQLB complex (Buddelmeijer and Beckwith, 2004; Gonzalez and Beckwith, 2009; Gonzalez *et al.*, 2010; Rothfield and Justice, 1997). FtsQ is a member of the POTRA (polypeptide transport associated domain) family (Sánchez-Pulido *et al.*, 2003). The C-terminal domain and transmembrane domains of FtsQ are crucial for self-interaction and its ability to interact with other cell division proteins, such as FtsL, FtsB, FtsW, FtsI and FtsN (D'Ulisse *et al.*, 2007). FtsL is a small essential cell

division protein (14 kDa) that consists of a cytoplasmic N-terminal, a single membrane spanning segment, and a periplasmic C-terminal domain that is predicted to contained leucine zippers (Guzman *et al.*, 1992). The periplasmic C-terminal domain of FtsL is required to interact with FtsQ while the cytoplasmic N-terminal domain of FtsL recruits FtsW (Gonzalez et al., 2010). FtsB is also a small single-pass inner membrane protein that consists of a cytoplasmic N-terminal domain, a single transmembrane domain, and a periplasmic C-terminal domain. The C-terminal of FtsB interacts with FtsQ while both the C-terminal and transmembrane domains of FtsB are required for its interaction with FtsL (Gonzalez and Beckwith, 2009; Robichon *et al.*, 2011). In addition, FtsB self-interacts through its transmembrane domain (LaPointe *et al.*, 2013).

FtsL and FtsB interact through their transmembrane domains to form a complex (FtsLB) prior to interacting with FtsQ (FtsQLB complex). Once the FtsQLB trimer complex has formed, the complex localizes to the divisome (Buddelmeijer and Beckwith, 2004; Khadria and Senes, 2013). The FtsLB subcomplex has been observed to exist as a heterotetramer (2:2) while the FtsQLB complex has been suggested to exist as either a trimer (1:1:1) or a hexamer (2:2:2) (Condon *et al.*, 2018; Villanelo *et al.*, 2011). Currently, it is thought that the FtsQLB complex assembles as follows: FtsB self-interacts, FtsL interacts with FtsB to form the subcomplex and, lastly, FtsQ binds to the FtsLB complex (LaPointe *et al.*, 2013).

The FtsQLB complex regulates septal peptidoglycan synthesis during cell division through activation of the FtsWI complex (Park *et al.*, 2020). Upon the arrival of FtsN to the divisome, a conformational change occurs in the FtsQLB complex and a region in the periplasmic domain of FtsL, known as the AWI (activation of FtsWI) domain, is available to interact with FtsI (Park *et al.*, 2020). The FtsL-FtsI interaction causes the FtsWI complex to become activated and septal peptidoglycan synthesis begins (Park *et al.*, 2020).

FtsW/FtsI

FtsW is a 46 kDa essential divisome protein with 10 transmembrane segments and both N- and C-terminal tails located in the cytoplasm (Boyle *et al.*, 1997; Lara and Ayala, 2002). FtsI (also known as PBP3 in *E. coli*) is essential for cell division and it is involved specifically in the synthesis of new cell wall during cell division (Botta and Park, 1981; Bramhill, 1997; Rothfield and Justice, 1997). FtsI is a single pass membrane protein that has a small cytoplasmic N-terminal domain, one transmembrane domain, and a large C-terminal domain located in the periplasm (Bowler and

Spratt, 1989). The transmembrane region allows FtsI to localize to the septal ring while the C-terminal domain assists in the recruitment of FtsN (Wissel and Weiss, 2004; Wissel *et al.*, 2005). FtsW and FtsI interact with each other to form the FtsWI complex (Fraipont *et al.*, 2011). FtsW and FtsI are several of the very last essential divisome proteins to localize to the divisome as they localize after FtsZ, FtsA, FtsQ and FtsL have already localized to the divisome (Mercer and Weiss, 2002; Wang *et al.*, 1998).

FtsW is a member of the SEDS family (shape, elongation, division and sporulation) (Henriques *et al.*, 1998; Mercer and Weiss, 2002). Initial studies of FtsW considered it to act as a flippase that would transport the cell wall precursor lipid II across the inner membrane during cell division (Mohammadi *et al.*, 2011, 2014). However, recent evidence suggests that FtsW is a peptidoglycan glycosyltransferase (Cho *et al.*, 2016; Meeske *et al.*, 2016). FtsW and FtsI work together as a subcomplex to perform the two major enzymatic activities required for peptidoglycan synthesis in the divisome: peptidoglycan glycosyltransferase and transpeptidation. FtsI, a transpeptidase, catalyzes the formation of peptide crosslinks in peptidoglycan while FtsW, a peptidoglycan glycosyltransferase, catalyzes the transfer of peptidoglycan precursor lipid II to the growing glycan strand (Cho *et al.*, 2016; Lutkenhaus and Du, 2017; Meeske *et al.*, 2016; Typas *et al.*, 2012).

The FtsWI complex must be activated for septal peptidoglycan synthesis to occur. In addition to the activation by the FtsQLB complex described above, the FtsWI complex can be activated by FtsN and FtsA (Park *et al.*, 2021). Upon the arrival of FtsN to the divisome, FtsN sends a signal through the cytoplasm that converts FtsA into an activated form (FtsA*) (Park *et al.*, 2021). FtsA* directly interacts with FtsW, thereby activating it and, subsequently, the FtsWI complex for septal peptidoglycan synthesis (Park *et al.*, 2021).

FtsN

FtsN is an essential single-pass inner membrane cell division protein. FtsN consists of a cytoplasmic N-terminal domain, a single transmembrane domain, and a periplasmic C-terminal domain (Dai *et al.*, 1993, 1996). The C-terminal domain is also known as the SPOR domain because it is able to bind peptidoglycan (Gerding *et al.*, 2009; Ursinus *et al.*, 2004). Localization studies suggest that FtsN is the last protein to be recruited to the divisome as it is found to localize after FtsZ, FtsA, FtsQ and FtsI have localized to the divisome (Addinall *et al.*, 1997; Goehring *et*

al., 2006). The essential function of FtsN in cell division can be performed by a small domain in the periplasmic region known as ^{E}FtsN (essential FtsN) (Gerding *et al.*, 2009). The main role of FtsN appears to be to regulate septal peptidoglycan synthesis as discussed previously (Park *et al.*, 2020, 2021).

Recent studies of FtsN showed that, during invagination of the cell septum, FtsN and FtsZ are spatially separated (Söderström *et al.*, 2018). FtsZ is observed near the leading edge of the invaginating cell septum while FtsN is found further back. These findings suggest that cell constriction is accomplished by two complexes that are spatially separated (Söderström *et al.*, 2018). This agrees with previous findings that the bacterial divisome is not one single ring but instead consists of multiple rings, with each ring layer having a specific function and cluster of proteins (Söderström and Daley, 2017).

1.2.4.4 Protein-Protein Interactions Amongst *E. coli* Divisome Proteins

Many protein-protein interactions have been observed to take place between the *E. coli* divisome proteins. These protein-protein interactions have been examined in several ways, including bacterial-two-hybrid (B2H) and co-immunoprecipitation assays. Amongst the 12 divisome proteins there have been 28 interactions and eight self-interactions identified (Figure 1.2.4.4 and Table 1.2.4.5) (Alexeeva *et al.*, 2010; Berezuk *et al.*, 2018, 2020; Buddelmeijer and Beckwith, 2004; Busiek *et al.*, 2012; Corbin *et al.*, 2007; Di Lallo *et al.*, 2003; Du *et al.*, 2016; D'Ulisse *et al.*, 2007; Fraipont *et al.*, 2011; Karimova *et al.*, 2005; LaPointe *et al.*, 2013; de Leeuw *et al.*, 1999; Liu *et al.*, 1999; Maggi *et al.*, 2008; Mukherjee and Lutkenhaus, 1994; Park *et al.*, 2021; Pichoff and Lutkenhaus, 2002; Skoog and Daley, 2012; Vega and Margolin, 2018; Yim *et al.*, 2000). The interaction map in Figure 1.2.4.4 is a representation of the identified interactions between *E. coli* cell division proteins and the self-interactions of the *E. coli* cell division proteins. Interactions were identified using either solely B2H assays, using alternative assays (i.e., co-immunoprecipitation assays, polymerization assays, cross-linking assays, pulldown assays, overlay assays or Fluorescence Resonance Energy Transfer (FRET) assays), or a combination of both B2H assays and alternative assays. However, the interaction map shown in Figure 1.2.4.4 lacks information regarding several protein-protein interactions. Table 1.2.4.5 summarizes which protein-protein interactions have been investigated amongst the *E. coli* divisome proteins and which have not.

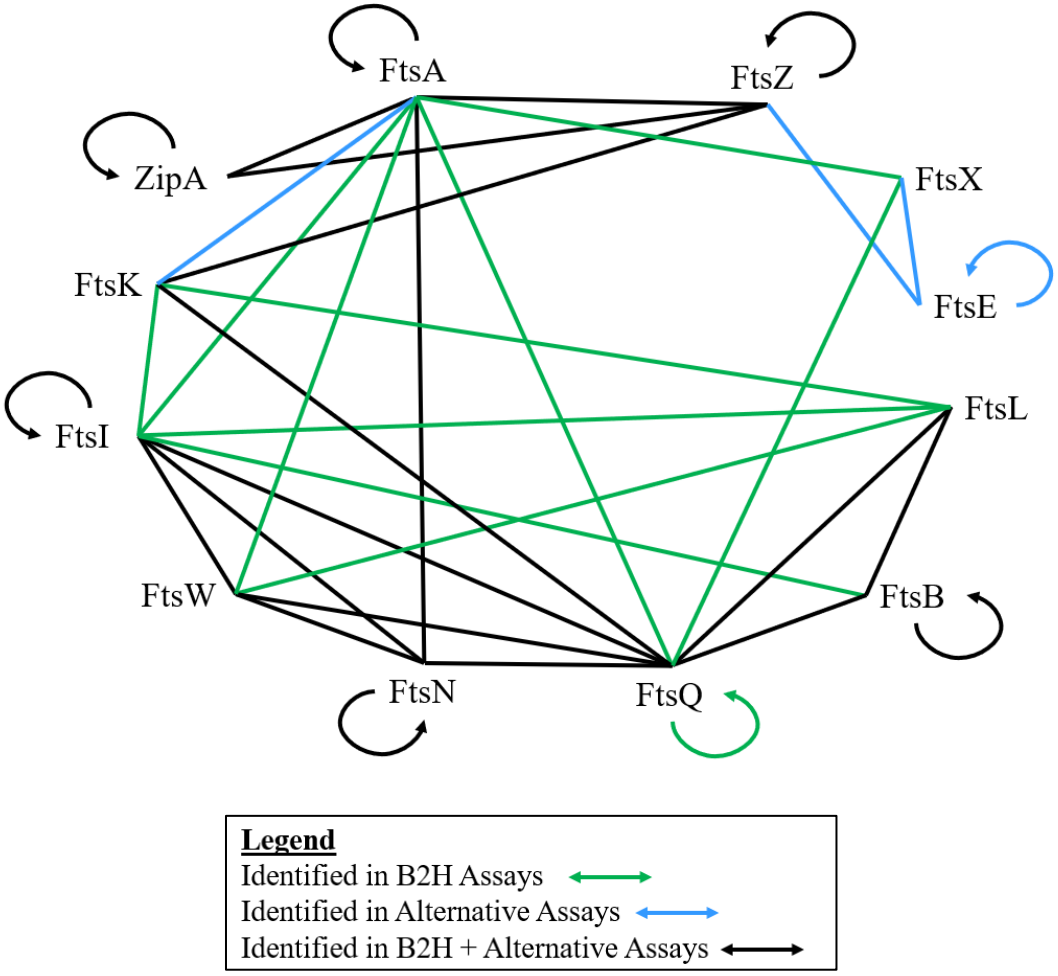

Figure 1.2.4.4: Protein-protein Interaction Map for *E. coli* Divisome Proteins. The map demonstrates the interactions that have been identified amongst the 12 *E. coli* essential divisome proteins. Self-interactions for the cell division proteins are indicated by curved arrows. Interactions identified through B2H assays are shown in green while interactions identified by alternative assays such as co-immunoprecipitation assays, pulldown assays, polymerization assays, cross-linking assays or FRET assays are shown in green. Interactions identified using both B2H assays and alternative assays are shown in black.

Table 1.2.4.5: Summary of the Protein-Protein Interactions Examined Amongst the *E. coli* Divisome Proteins.

	FtsZ	**FtsA**	**ZipA**	**FtsE**	**FtsX**	**FtsK**	**FtsQ**	**FtsL**	**FtsB**	**FtsW**	**FtsI**	**FtsN**
FtsZ	+											
FtsA	+	+										
ZipA	+	+	+									
FtsE	+	-	NT	+								
FtsX	-	+	NT	+	-							
FtsK	+	+	-	NT	NT	NT						
FtsQ	-	+	-	NT	+	+	+					
FtsL	-	-	-	NT	-	+	+	-				
FtsB	-	-	NT	NT	-	-	+	+	+			
FtsW	-	+	-	NT	-	-	+	+	-	-		
FtsI	-	+	-	NT	-	+	+	+	+	+	+	
FtsN	-	+	-	NT	-	-	+	-	-	+	+	+

NT = interaction has not tested; + = interaction has been examined and is present;
- = interaction has been examined but is not present

Although many of the interactions amongst the *E. coli* divisome proteins have been studied, there is very little data regarding the interactions between FtsE and the other cell division proteins (Table 1.2.4.5). FtsE has been found to interact with FtsZ, FtsX and to self-interact, but the interactions between FtsE and the remaining cell division proteins have not been studied (Corbin *et al.*, 2007; de Leeuw *et al.*, 1999). In addition, the FtsK self-interaction, the FtsX-ZipA, FtsX-FtsK, and FtsB-ZipA interactions have not been studied. Due to this lack of data, the role these proteins play in *E. coli* cell division are not fully understood.

1.2.4.5 Other *E. coli* Cell Division Proteins – The Min and Zap Proteins

Min Proteins

The Min protein system is an inhibitory system that works to assist in positioning the Z ring at mid-cell. There are three proteins that compose the Min protein system: MinC, MinD and MinE. MinC acts to inhibit FtsZ from polymerizing into the Z ring while MinD activates the

antagonization ability of MinC. MinE acts to regulate the position of the MinCD complex (Lutkenhaus, 2009; Lutkenhaus and Du, 2017; Snyder *et al.*, 2013). During the cell cycle the Min proteins oscillate from one cell pole to the other cell pole (Lutkenhaus, 2009; Lutkenhaus and Du, 2017; Snyder *et al.*, 2013). The oscillation pattern of MinC and MinD is driven by the oscillation of MinE. It has been suggested that the oscillation pattern of the Min proteins determines the location of the Z ring (Snyder *et al.*, 2013). The oscillation of MinE, MinC and MinD complex causes a higher concentration of MinC to exist at the cell poles and a lower concentration of MinC to exist at the mid-cell. The Z ring is prevented from forming at the cell poles due to the high concentration of MinC and, instead, the Z ring to forms at the mid-cell where the MinC concentration is the lowest (Snyder *et al.*, 2013).

Zap Proteins

There are five FtsZ associated proteins (Zap) observed in *E. coli:* ZapA, ZapB, ZapC, ZapD and ZapE. These Zap proteins interact with the FtsZ to crosslink the FtsZ filaments and, therefore, assist in combining the filaments into the Z ring (Lutkenhaus and Du, 2017; Ortiz *et al.*, 2016). The Zap protein of interest to this thesis is ZapA. The ZapA protein is the most conserved of all the five Zap proteins (Ortiz *et al.*, 2016). ZapA is able to crosslink FtsZ filaments through its dimerization ability. ZapA binds to FtsZ filaments as a monomer and then dimerizes with another ZapA monomer that is also bound to a FtsZ filament, thereby promoting FtsZ crosslinking (Lutkenhaus and Du, 2017; Ortiz *et al.*, 2016).

1.2.5 Cell Division in *N. gonorrhoeae* – Current Knowledge

N. gonorrhoeae is a diplococci bacterium that grows in 2 dimensions, thereby producing alternating division planes (Unemo *et al.*, 2019a; Westling-Häggström *et al.*, 1977). Growth in the first dimension occurs perpendicular to the previous cell septum while growth in the second dimension occurs parallel to the cell septum, resulting in the formation of tetrads (Westling-Häggström *et al.*, 1977). However, in a population of *N. gonorrhoeae* cells, tetrad cells are observed less frequently than either diplococci or monococcus cells (Li, 2011).

There is a limited amount of knowledge regarding *N. gonorrhoeae* cell division and the *N. gonorrhoeae* divisome proteins. The current knowledge of *N. gonorrhoeae* cell division is discussed below.

1.2.5.1 Division Cell Wall (*dcw*) Cluster of *N. gonorrhoeae*

The first genomic analysis of the *dcw* cluster found in *N. gonorrhoeae* determined that the *dcw* cluster contained 17 genes (i.e., *mraZ, mraW, ftsI, murE, hyp1, murF, mraY, hyp2, murD, ftsW, murG, murC, ddl, ftsQ, ftsA, ftsZ,* and *hyp3)* (Francis *et al.*, 2000). The three hypothetical genes (*hyp1, hyp2,* and *hyp3*) were novel as they had not been observed in other *dcw* clusters (Francis *et al.*, 2000). A later study by Snyder *et al.* characterized *hyp1* and re-named it *dca* (division cluster competence associated) (Snyder *et al.*, 2001). Dca encodes a putative inner membrane protein that is involved in competence in *N. gonorrhoeae*. If *dca* is lost, there is no observed effect on cell division but instead gonococci can no longer undergo transformation (Snyder *et al.*, 2001). Later studies of the *N. gonorrhoeae dcw* cluster also renamed the previously identified *hyp2* gene as *dcaC* (Snyder *et al.*, 2003). In addition, a previously unidentified open reading frame (ORF) was found between *murF* and *mraY* and subsequently named *dcaB* (Snyder *et al.*, 2001, 2003).

The initial genomic analysis of the *N. gonorrhoeae dcw* cluster by Francis *et al.* suggested that *ftsL* was not present, in contrast to the *E. coli dcw* cluster (Francis *et al.*, 2000). Francis *et al.* identified an ORF between *mraW* and *ftsI*, the same location that *ftsL* is observed in the *E. coli dcw* cluster (Francis *et al.*, 2000; Mingorance *et al.*, 2004). However, this ORF was not considered to be *ftsL* because it had low amino acid sequence similarity to *E. coli ftsL* (22%) (Francis *et al.*, 2000). A later study by Snyder *et al.* reiterated that this ORF between *mraW* and *ftsI* was *ftsL* because *ftsL* is often the least conserved gene in the *dcw* cluster (Snyder *et al.*, 2001). In addition, recent bioinformatic analysis of the *N. gonorrhoeae dcw* cluster further confirmed the presence of *ftsL* (Dillon and Singh, unpublished).

The *N. gonorrhoeae dcw* cluster has undergone recent bioinformatic analysis and is seen in Figure 1.2.5.1 (Dillon and Singh, unpublished). In contrast to the 16 gene *E. coli dcw* cluster (Figure 1.2.3), the *N. gonorrhoeae dcw* cluster contains 19 genes (Figure 1.2.5.1). The three additional genes include: *dca* (blue), located between *murE* and *murF*; *dcaB* (orange), located between *murF* and *mraY*; and *dcaC* (green), located between *mraY* and *murD* (Francis *et al.*, 2000; Snyder *et al.*, 2001, 2003). Unlike the *E. coli dcw* cluster (Figure 1.2.3), the *N. gonorrhoeae dcw* cluster has multiple transcriptional terminators (Figure 1.2.5.1). (Francis *et al.*, 2000; Dillon and Singh, unpublished). The initial study of the *N. gonorrhoeae dcw* cluster identified five

transcriptional terminators, four of which are internal transcriptional terminators (Francis *et al.*, 2000). However, recent analysis of the *N. gonorrhoeae dcw* cluster have identified has identified six terminators, five of which are internal transcriptional terminators. Since there are several internal transcriptional terminators in the *N. gonorrhoeae dcw* cluster, this suggests that multiple transcripts can be produced (Francis *et al.*, 2000; Dillon and Singh, unpublished).

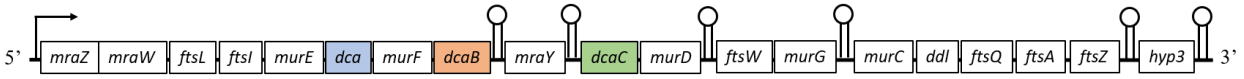

Figure 1.2.5.1: The *N. gonorrhoeae dcw* Cluster. The *N. gonorrhoeae dcw* cluster consists of 19 genes and includes multiple transcriptional terminators (stem loops). The *N. gonorrhoeae dcw* cluster has 3 genes which are not identified in the *E. coli dcw* cluster: *dca* (blue), *dcaB* (orange), and *dcaC* (green).

1.2.5.2 *N. gonorrhoeae* Divisome Proteins

N. gonorrhoeae encodes homologs to the *E. coli* divisome proteins (Zou *et al.*, 2017a). However, unlike *E. coli*, many of the *N. gonorrhoeae* divisome proteins have not been studied. The six *N. gonorrhoeae* divisome proteins that have been explored (i.e., FtsZ, FtsA, ZipA, FtsE, FtsX and FtsI) are discussed below. The remaining six *N. gonorrhoeae* divisome proteins (i.e., FtsK, FtsQ, FtsL, FtsB, FtsW, and FtsN) and their functions in *N. gonorrhoeae* cell division have not been studied.

FtsZ

The *ftsZ* ORF is located near the 3' end of the *N. gonorrhoeae dcw* cluster (Figure 1.2.5.1) and encodes FtsZ, a protein that has a predicted molecular weight of 41.5 kDa and is essential to *N. gonorrhoeae* survival (Francis *et al.*, 2000; Salimnia *et al.*, 2000). Sequence analysis of $FtsZ_{Ng}$ showed that this protein is similar to other existing FtsZ proteins, including *E. coli* FtsZ (67% similarity) (Salimnia *et al.*, 2000). Sequence analysis also revealed that $FtsZ_{Ng}$ contains the conserved GTP binding motif that is found in FtsZ homologs. When $FtsZ_{Ng}$ is expressed in *E. coli*, the protein is able to localize to the mid cell (Salimnia *et al.*, 2000). Therefore, these results suggest that *N. gonorrhoeae* FtsZ potentially exhibits similar characteristics as those observed in other FtsZ proteins (Salimnia *et al.*, 2000).

FtsA

A recent study of *N. gonorrhoeae* FtsA suggests that its function is species specific (Zou *et al.*, 2017b). Upon expression of $FtsA_{Ng}$ in *E. coli*, it was observed that *E. coli* cell division was disrupted and, in some cells, $FtsA_{Ng}$ could not properly localize to the *E. coli* division site *(Zou et al.*, 2017b). In addition, an *E. coli ftsA* mutant strain could not be complemented by the expression of $FtsA_{Ng}$. Using the B2H assay, the authors also found that $FtsA_{Ng}$ could only interact with $FtsN_{Ec}$, while *E. coli* $FtsA_{Ec}$ could interact with $FtsZ_{Ec}$, $FtsQ_{Ec}$, $FtsI_{Ec}$, and $FtsN_{Ec}$. Together, these results suggest that $FtsA_{Ng}$ has a different function than its *E. coli* homolog (Zou *et al.*, 2017b).

ZipA

N. gonorrhoeae ZipA is an essential protein that was identified during a genetic screen to detect proteins that use the signal recognition particle system for localizing to the inner membrane (Du and Arvidson, 2003). Sequence analysis of *N. gonorrhoeae* ZipA showed no significant primary sequence similarities to *E. coli* ZipA (Du and Arvidson, 2003). However, *N. gonorrhoeae zipA* and *E. coli zipA* have similar chromosomal locations and their encoded proteins have similar predicted secondary structures, like the hydrophobic region at the N-terminus (Du and Arvidson, 2003). In addition, *N. gonorrhoeae zipA* can complement an *E. coli* strain lacking ZipA, which indicates that *N. gonorrhoeae* encodes a functional ZipA homolog (Du and Arvidson, 2003).

FtsE and FtsX

ftsE and *ftsX* were identified through a combination of both manual and automated sequencing of pSB19, a plasmid created during the construction of a genomic library of *N. gonorrhoeae* CH811 (Bernatchez, 1997; Bernatchez et al., 2000). Sequence analysis of *ftsE* revealed that the gene is 651 bp long and encodes a protein with a predicted molecular weight of 23.8 kDa (Bernatchez *et al.*, 2000). When the *N. gonorrhoeae* FtsE sequence was aligned with other prokaryotic FtsE proteins, it was found that $FtsE_{Ng}$ has 71% similarity to its *E. coli* homolog (Bernatchez *et al.*, 2000). This sequence analysis also identified that *N. gonorrhoeae* FtsE contained the conserved motifs characteristic of ABC domains (Bernatchez *et al.*, 2000). Meanwhile, sequence analysis of *ftsX* found that *ftsX* is 918 bp and encodes a protein with a predicted molecular weight of 34.2 kDa (Bernatchez *et al.*, 2000). The sequence analysis of FtsX determined that this protein has 55% similarity to its *E. coli* homolog (Bernatchez *et al.*, 2000). In

addition, sequence analysis predicted that FtsX contained four transmembrane sequences (Bernatchez *et al.*, 2000). The authors suggest that FtsE and FtsX form an ABC transporter, with the FtsE acting as the cytoplasmic ATP binding component while FtsX acts as the membrane component (Bernatchez *et al.*, 2000).

When *N. gonorrhoeae ftsE* and *ftsX* are mutated through insertional inactivation, there is no effect on cell viability (Bernatchez *et al.*, 2000). Therefore, in contrast to *E. coli*, neither *ftsE* nor *ftsX* are essential for *N. gonorrhoeae* survival (Bernatchez *et al.*, 2000; Reddy, 2007). However, it has been suggested that *ftsE* and *ftsX* may be involved in cell division because *N. gonorrhoeae* cells with *ftsE* and *ftsX* insertion mutants are observed to have atypical division sites (Bernatchez *et al.*, 2000). These atypical division sites in *N. gonorrhoeae* cell division due to *ftsE* and *ftsX* mutants can be seen in Figure 1.2.5.2.

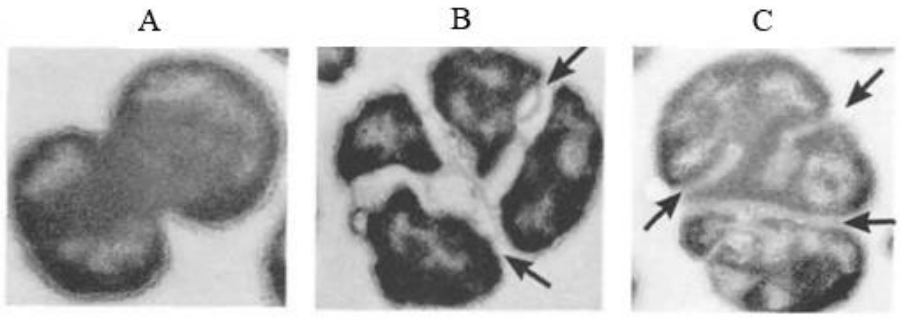

Figure 1.2.5.2: Transmission Electron Microscopy Examining the Effects of *ftsE* and *ftsX* Mutants on *N. gonorrhoeae* Cellular Morphology. (A) The wildtype *N. gonorrhoeae* CH811 strain, (B) *ftsE* mutant, and (C) the *ftsX* mutant. The arrows indicate sites where abnormal cell division has occurred. Figure is adapted with modifications from Bernatchez *et al.* 2000. 7(2). *DNA Res.* This figure is reproduced with permission from Oxford University Press.

FtsI

Penicillin binding proteins (PBPs) are proteins involved in the last stages of cell wall synthesis in bacteria as they are involved in both forming cross-links between glycan strands and polymerizing glycan strands (Powell *et al.*, 2009; Sauvage *et al.*, 2008). In addition, these PBPs are the targets of β-lactam antibiotics (Powell *et al.*, 2009; Stefanova *et al.*, 2003). Based on their molecular mass, the PBPs can be divided into either high molecular mass PBPs or low molecular mass PBPs (Sauvage *et al.*, 2008). The high molecular mass proteins can then be further classified as either class A or class B high molecular mass PBPs based on the activity of their N-terminal domains (Ghuysen, 1991; Sauvage *et al.*, 2008). The N-terminal domain of class A PBPs is a

glycosyltransferase that catalyzes the elongation of glycan strands (Ghuysen, 1991; Sauvage *et al.*, 2008). Meanwhile, the N-terminal domain of class B high molecular mass PBPs may interact with cell division proteins and, therefore, have a role in cell division (Sauvage *et al.*, 2008). In addition to being categorized by size, PBPs can also categorized based on activity. Class A PBPs are transpeptidases and glycosyltransferases that both form peptide crosslinks between peptidoglycan strands and cause the polymerization of glycan strands (Powell *et al.*, 2009). In contrast, Class B PBPs have only transpeptidase activity while Class C PBPs have only carboxypeptidase activity (Powell *et al.*, 2009).

There are four PBPs in *N. gonorrhoeae* (i.e., PBP1, PBP2, PBP3 and PBP4) (Barbour, 1981; Stefanova *et al.*, 2003, 2004). *N. gonorrhoeae* PBP1 and PBP2 are the major targets of β-lactam antibiotics (Barbour, 1981). PBP1 is a high molecular mass class A PBP that is encoded by *ponA* (Ropp and Nicholas, 1997). PBP1 is essential to *N. gonorrhoeae* viability because insertional inactivation leads to loss of viability (Ropp and Nicholas, 1997). In addition, PBP1 is the homolog of *E. coli* PBP1A (Ropp and Nicholas, 1997). PBP3 and 4 are low molecular mass PBPs that are not essential to viability (Stefanova *et al.*, 2003, 2004). PBP4 appears to play a role in cell wall synthesis and has no apparent transpeptidase activity (Stefanova *et al.*, 2004)

N. gonorrhoeae PBP2 (also known as FtsI) is encoded by *penA* and is a high molecular mass class B transpeptidase (Powell *et al.*, 2009). PBP2 is the homolog of *E. coli* PBP3 (FtsI) and appears to have a function in cell division (Barbour, 1981; Stefanova *et al.*, 2003). The crystal structure of PBP2 from a penicillin resistant strain of *N. gonorrhoeae* has been solved (Powell *et al.*, 2009). The function of the N-terminal domain of PBP2 is unknown but it has been suggested that it may target the protein to the mid-cell during cell division (Powell *et al.*, 2009). Meanwhile, the C-terminal domain is the transpeptidase domain that binds penicillin and mutations in this region lead to penicillin resistance (Powell *et al.*, 2009). A study of *N. gonorrhoeae* clinical samples from Saskatchewan determined that several mutation patterns in the transpeptidase domain of PBP2 can lead to varying susceptibility to penicillin (Thakur *et al.*, 2018).

1.2.5.3 Protein-protein Interactions Amongst *N. gonorrhoeae* Divisome Proteins

A preliminary cell division protein-protein interaction network for *N. gonorrhoeae* was characterized in 2017 by Zou *et al.* through several different methods including B2H assays,

glutathione S transferase (GST) pulldown assays and surface plasmon resonance (SPR) assays (Zou *et al.*, 2017a). A protein-protein interaction map was generated that summarizes the interactions amongst eight of the *N. gonorrhoeae* divisome proteins (i.e., FtsZ, FtsA, ZipA, FtsK, FtsQ, FtsI, FtsW, and FtsN) (Figure 1.2.5.3). Out of a total of 28 possible interactions studied, nine interactions were identified (Zou *et al.*, 2017a). B2H assays were used as an initial screen to identify protein-protein interactions and then GST pulldown assays and SPR assays were used to confirm three of those nine interactions (i.e., FtsA-FtsZ, FtsA-FtsQ and FtsA-FtsN) (Zou *et al.*, 2017a). Zou *et al.* identified four interactions that were unique to *N. gonorrhoeae* as they had not been observed amongst their *E. coli* homologs: FtsZ-FtsW, FtsA-FtsK, FtsA-FtsW and FtsK-FtsN (Zou *et al.*, 2017a). However, the FtsA-FtsK and FtsA-FtsW interactions have since been identified in *E. coli* (Berezuk *et al.*, 2020; Park *et al.*, 2021). In addition, Zou *et al.* found that ZipA did not interact with any other examined divisome proteins, unlike its *E. coli* homolog (Zou *et al.*, 2017a). Therefore, *N. gonorrhoeae* appears to have a distinct protein-protein interaction network *(Zou et al.*, 2017a).

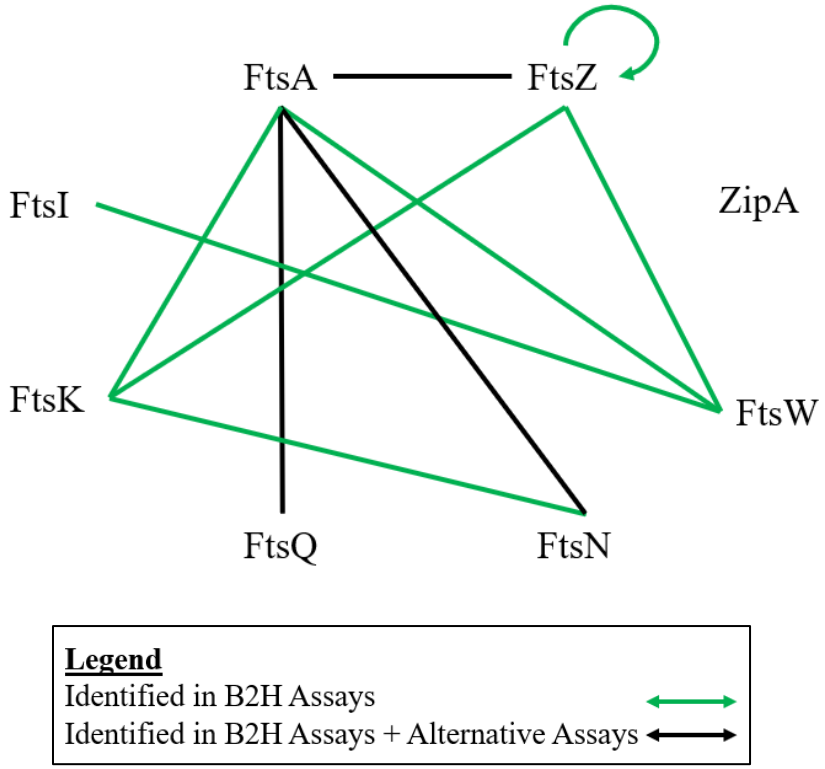

Figure 1.2.5.3: Protein-Protein Interaction Map for the *N. gonorrhoeae* Divisome Proteins. The map demonstrates the interactions that have been identified amongst the *N. gonorrhoeae* cell division proteins. Self-interactions for these proteins are indicated by curved arrows. Interactions that have been identified through B2H assays alone are shown in green while interactions identified by both B2H assays and alternative assays like GST pulldowns and/or SPR are shown in black.

The interaction network shown in Figure 1.2.5.3 is lacking crucial data regarding the self-interactions for all *N. gonorrhoeae* divisome proteins, except FtsZ, and the protein-protein interactions for four other *N. gonorrhoeae* divisome proteins (e.g., FtsB, FtsL, FtsE and FtsX). Table 1.2.5.4 summarizes the protein-protein interactions that were studied amongst *N. gonorrhoeae* divisome proteins (Zou *et al.*, 2017a). As seen in Table 1.2.5.4, the self-interaction ability for most *N. gonorrhoeae* divisome proteins have not been studied. In addition, the protein-protein interactions of FtsE, FtsX, FtsL and FtsB with the other divisome proteins have also not been studied. Therefore, the *N. gonorrhoeae* cell division interactome is not comprehensive because there is a large amount of data regarding potential protein-protein interactions amongst the *N. gonorrhoeae* divisome proteins that has not been examined.

Table 1.2.5.4: Summary of the Protein-Protein Interactions Examined Amongst *N. gonorrhoeae* Divisome Proteins

	FtsZ	**FtsA**	**ZipA**	**FtsE**	**FtsX**	**FtsK**	**FtsQ**	**FtsL**	**FtsB**	**FtsW**	**FtsI**	**FtsN**
FtsZ	+											
FtsA	+	NT										
ZipA	-	-	NT									
FtsE	NT	NT	NT	NT								
FtsX	NT	NT	NT	NT	NT							
FtsK	+	+	-	NT	NT	NT						
FtsQ	-	+	-	NT	NT	-	NT					
FtsL	NT	NT	NT	NT	NT	NT	NT	NT				
FtsB	NT	NT	NT	NT	NT	NT	NT	NT	NT			
FtsW	+	+	-	NT	NT	-	-	NT	NT	NT		
FtsI	-	-	-	NT	NT	-	-	NT	NT	+	NT	
FtsN	-	+	-	NT	NT	+	-	NT	NT	-	-	NT

NT = interaction has not tested; + = interaction has been examined and is present;
- = interaction has been examined but is not present

1.2.5.4 Other *N. gonorrhoeae* Cell Division Proteins – The Min Proteins

The three Min proteins (i.e., MinC, MinD, and MinE) are found in *N. gonorrhoeae* and they function to assist in cell division (Ramirez-Arcos *et al.*, 2001, 2002; Szeto *et al.*, 2001). When MinC or MinD are not present in *N. gonorrhoeae* cells, cell division is uncontrolled and the resulting cells have abnormal morphology and multiple division septa (Ramirez-Arcos *et al.*, 2001; Szeto *et al.*, 2001). MinC is a functional homolog of *E. coli* MinC because $MinC_{Ng}$ can restore the wildtype morphology to *E. coli* cells lacking $MinC_{Ec}$ (Ramirez-Arcos *et al.*, 2001). $MinD_{Ng}$ is a functional homolog to *E. coli* MinD because the proteins share 73% similarity and $MinD_{Ng}$ could partially restore the wildtype morphology to *E. coli* cells that lack $MinD_{Ec}$ (Szeto *et al.*, 2001). *N. gonorrhoeae* MinE is also a functional homolog to *E. coli* MinE because $MinE_{Ng}$, when expressed in an *E. coli* background, exhibits similar oscillation patterns as $MinE_{Ec}$. In addition, when $MinE_{Ng}$ and $MinD_{Ng}$ are expressed in *E. coli*, $MinE_{Ng}$ is able to activate the oscillation of $MinD_{Ng}$ (Ramirez-Arcos *et al.*, 2002).

1.3 Methods to Identify Protein-Protein Interactions

Proteins often do not perform their cellular functions on their own. Instead, proteins interact with other proteins, through either stable or transient protein-protein interactions, to form complexes and perform their cellular functions (Miura, 2018; Typas and Sourjik, 2015; Wissmueller *et al.*, 2011; Zhou *et al.*, 2016). Identifying these protein-protein interactions can either provide new knowledge or advance the current knowledge regarding the cellular function of these proteins (Brymora *et al.*, 2004; Wissmueller *et al.*, 2011). There are several methods that can be used to study protein-protein interactions and each method is unique in its specificity and its advantages and/or disadvantages. However, some of the most common ways to study protein-protein interactions include genetic methods (i.e., two-hybrid assays) and biochemical methods (i.e., co-immunoprecipitation, affinity pulldowns and mass spectrometry) (Miura, 2018; Typas and Sourjik, 2015; Zhou *et al.*, 2016).

1.3.1 Bacterial-Two-Hybrid: A Two-Hybrid Protein-Protein Interaction Assay

Two-hybrid systems are one of the most common methods to investigate protein-protein interactions *in vivo* (Berggård *et al.*, 2007; Typas and Sourjik, 2015). Two-hybrid systems are considered a genetic method for studying protein-protein interactions and the most widely known two-hybrid systems include the Yeast-Two-Hybrid (Y2H) and B2H systems (Berggård *et al.*, 2007; Typas and Sourjik, 2015). Both methods utilize protein fragment complementation to study potential interactions amongst proteins of interest. Briefly, the bait and prey proteins are each fused to one half of a modular protein. This modular protein only recovers its functionality and affects the transcription of a reporter gene upon an interaction between bait and prey proteins (Berggård *et al.*, 2007; Typas and Sourjik, 2015). There are two common B2H methods used to study protein-protein interactions, one designed by Karimova *et al.* and one designed by Di Lallo *et al.* (Di Lallo *et al.*, 1999; Karimova *et al.*, 1998). These systems have been used to examine the protein-protein interactions amongst cell division proteins (Di Lallo *et al.*, 2003; Karimova *et al.*, 2005).

The B2H method designed by Karimova *et al.* is known as the Bacterial Adenylate Cyclase based Two-Hybrid (BATCH) assay and this assay was designed around the ability to re-form a signal transduction pathway in *E. coli* (Ouellette *et al.*, 2017). In this method, the T25 and T18 fragments of the catalytic domain of adenylate cyclase from *Bordetella pertussis* are fused to the proteins of interest. If the two proteins of interest interact, then the T25 and T18 domains associate,

thereby reforming adenylate cycle and restoring the activity of the enzyme, leading to cAMP synthesis (Karimova *et al.*, 1998, 2000; Ouellette *et al.*, 2017). cAMP is a signaling molecule that binds to the catabolite activator protein (CAP), thereby forming a CAP-cAMP complex that controls the expression of several genes (Karimova *et al.*, 1998, 2000). Since the expression of the reporter gene *lacZ* can also be controlled by the CAP-cAMP complex, the amount of β-galactosidase produced can be a used to measure the potential interaction amongst proteins of interest (Ouellette *et al.*, 2017). The BATCH method relies on the use of a signaling cascade which allows the interactions of proteins that may not be near the transcriptional machinery (i.e., cytosolic or membrane bound proteins) to be examined (Karimova *et al.*, 1998, 2000).

The second most common B2H method was developed by Di Lallo *et al.* (Di Lallo *et al.*, 1999). The initial Di Lallo *et al.* B2H method was based on the reconstitution of a lambda repressor (i.e., a homodimer made from two repressor molecules) with the protein of interest fused to the C-terminal domain while the N-terminal region was involved in binding to the DNA operator (Di Lallo *et al.*, 1999). Therefore, if the protein of interest was able to dimerize, then the functional lambda repressor would reform and provide immunity to lambda infection (Di Lallo *et al.*, 1999). In addition, a *lacZ* reporter gene was placed under the control of the lambda promoter, thereby allowing the amount of β-galactosidase produced to indicate the presence or absence of an interaction between proteins of interest (Di Lallo *et al.*, 1999). Therefore, this system could measure the presence of a protein-protein interaction through both a β-galactosidase activity assay and immunity to lambda infections (Di Lallo *et al.*, 1999).

This B2H methodology was then modified so that a hybrid repressor could recognize a hybrid operator, thereby allowing for interactions between two different proteins to be studied (Di Lallo *et al.*, 2001). The current Di Lallo B2H methodology is summarized in Figure 1.3.1. Using the phage P22 and phage 434 operators, Di Lallo *et al.* created a hybrid operator that only a hybrid repressor would be able to bind (Di Lallo *et al.*, 2001). As seen in Figure 1.3.1, the hybrid repressor consists of two N-terminal regions that can bind DNA (i.e., P22 and 434) and two C-terminal regions which consists of the protein(s) of interest (i.e., A and B) (Di Lallo *et al.*, 2001). If the proteins of interest (i.e., A and B) interact, this causes the hybrid repressor to re-form and bind the hybrid operator, thereby repressing the synthesis of the reporter gene *lacZ* (Figure 1.3.1) (Di Lallo *et al.*, 2001).

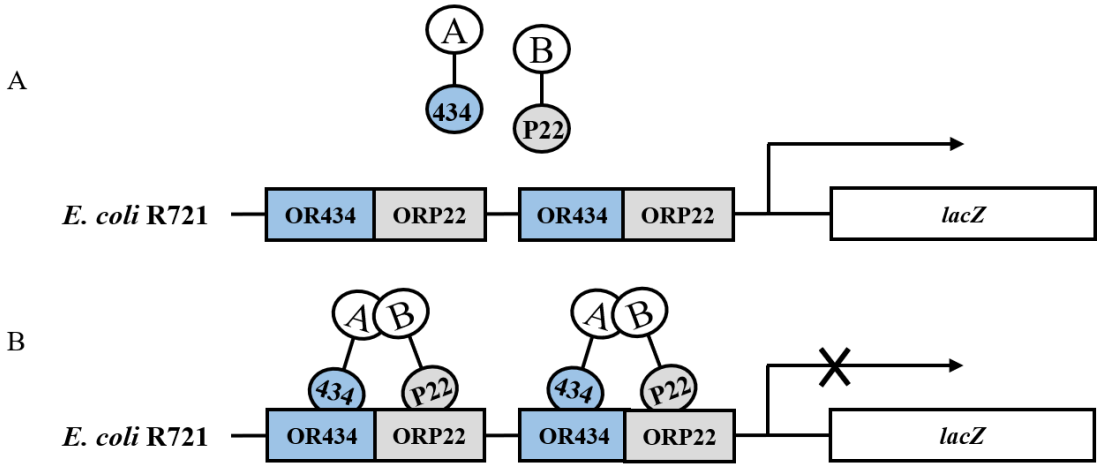

Figure 1.3.1: Di Lallo B2H Methodology. (A) The hybrid repressor is not formed when there is no interaction between proteins of interest and, therefore, *lacZ* expression is not affected; (B) The hybrid repressor is formed when there is an interaction between the proteins of interest. The hybrid repressor binds to the hybrid operator and *lacZ* expression is repressed. (Di Lallo et al., 2001). Figure is adapted with modifications from Di Lallo *et al.* 2001. 147(6). *Microbiology.*

The difference between the Di Lallo and Karimova B2H methodologies is that an interaction between two proteins causes a decrease in the production of β-galactosidase in the Di Lallo methodology but, during the Karimova methodology, an interaction between two proteins causes an increase in the production of β-galactosidase (Di Lallo *et al.*, 2001; Ouellette *et al.*, 2017).

1.3.2 GST Pulldowns – an Affinity Chromatography Methodology to Identify Protein-Protein Interactions

Affinity chromatography is a method that allows for a protein of interest to be purified from a sample based on the ability of the protein to specifically interact with another molecule (Zhou *et al.*, 2016). GST pulldowns are a common type of affinity chromatography methodology. GST pulldowns utilize the ability for the GST-tagged protein to bind to reduced glutathione that is immobilized on a solid support with both high affinity and high specificity (Luo *et al.*, 2014; Zhou *et al.*, 2016). GST pulldowns are an *in vitro* methodology to study the interaction between proteins of interest. This methodology can be used to identify unknown interactions or to confirm suspected interactions that were observed or predicted with other techniques (i.e., co-immunoprecipitation or B2H) (Luo *et al.*, 2014; Schäfer *et al.*, 2015; Wissmueller *et al.*, 2011; Zhou *et al.*, 2016).

The first step in the GST pulldown methodology involves the purification of the protein of interest, also known as the 'bait' protein. The bait protein is expressed with a GST tag and then

immobilized to GST affinity beads, thereby allowing the bait protein to be purified (Miura, 2018; Schäfer *et al.*, 2015; Zhou *et al.*, 2016). The GST-tagged protein of interest is immobilized to the matrix and potential protein interacting partners (i.e., 'prey' proteins) are added and incubated with the bait protein. The proteins that do not interact with the bait protein are washed away while the interacting partners remain bound to the bait protein. These interacting partners can then be identified by sodium dodecyl sulphate polyacrylamide gel electrophoresis (SDS-PAGE) analysis (Miura, 2018; Zhou *et al.*, 2016). This method can be used to examine either the interactions between two purified proteins or the interactions of proteins in a protein extract (Kim and Hakoshima, 2019; Miura, 2018). However, GST pulldown assays have disadvantages, including the potential for prey proteins to non-specifically bind to the affinity matrix of choice (i.e., agarose beads). Therefore, the presence of vigorous wash steps are crucial to assist in reducing non-specific protein interactions (Luo *et al.*, 2014).

1.3.3 Affinity Pulldowns coupled to Mass Spectrometry to Explore Protein Complexes

Mass spectrometry combined with affinity purification (AP-MS) is a methodology that is able to both expand the knowledge of the composition of protein complexes and identify protein-protein interactions, thereby further expanding the knowledge of the interactome (Dunham *et al.*, 2012; Gingras *et al.*, 2007). In general, AP-MS consists of two major steps: 1) the isolation of the tagged protein of interest and its interacting partners directly from cell lysates by affinity purification methods; and 2) the analysis and identification of the proteins by mass spectrometry (Dunham *et al.*, 2012; Gingras *et al.*, 2007). Affinity purification can be performed using antibodies to endogenous proteins as this allows for the protein of interest to be purified in its native condition. However, antibodies may not be available for every protein and, instead, an epitope tag may be fused to the protein of interest. The epitope tagged protein is then purified using affinity chromatography (Dunham *et al.*, 2012). However, the addition of an epitope tag can be problematic because improperly tagged proteins may misfold or be unable to localize properly (Dunham *et al.*, 2012). Once the proteins and their interacting partners have been captured, the proteins are processed and analyzed by mass spectrometry (Dunham *et al.*, 2012; Gingras *et al.*, 2007). Mass spectrometry is used for peptide sequencing because it is rapid, sensitive, and allows for peptides to be identified at extremely low levels (Gingras *et al.*, 2007). However, the proteins must be converted into peptides before being processed by the mass spectrometer. Trypsin, a protease,

digests the proteins on the carboxy-terminal side of the lysine and arginine residues, thereby creating understandable peptide fragmentation patterns (Gingras *et al.*, 2007; Steen and Mann, 2004).

There are three common methods used for protein digestion: in-gel, in-solution and on-bead digestion (Hedrick *et al.*, 2015). Briefly, during in-gel digestion the protein sample is separated by SDS-PAGE and the band(s) of interest are excised, de-stained and then digested. The peptides are then extracted from the digested gel fragments so they can be analyzed by mass spectrometry (Gundry *et al.*, 2009; Hedrick *et al.*, 2015; Turriziani *et al.*, 2014). However, the in-gel digestion method is time-consuming and low abundant proteins can be lost (Turriziani *et al.*, 2014). Therefore, either in-solution or on-bead digestion methods can be used instead. In comparison to in-gel digestion, during in-solution digestion the protein sample is digested immediately after the sample has been eluted from the affinity matrix instead of being separated by SDS-PAGE first (Gundry *et al.*, 2009; Hedrick *et al.*, 2015). However, during circumstances where the protein sample cannot be eluted from the affinity matrix (i.e., if the proteins of interest are resistant to elution or the proteins of interest are in low abundance), then the on-bead digestion methodology can be used instead of the in-solution digestion methodology. During this method, the protein samples are digested while they remain bound to the affinity matrix (Hedrick *et al.*, 2015).

There are three common components to all mass spectrometry instruments: the ionization source, the mass analyzer and the detector (Aebersold and Mann, 2003; Gundry *et al.*, 2009). The two most common ionization sources used to ionize the peptides are: matrix assisted laser desorption/ionization (MALDI) and electrospray ionization (ESI) (Aebersold and Mann, 2003; Gundry *et al.*, 2009). In MALDI, a laser is pulsed at a crystalized peptide mixture, thereby generating ionized peptides (Gundry *et al.*, 2009; Mehmood *et al.*, 2015). In contrast, ESI uses a high electric potential to create charged protein droplets that evaporate, producing the charged ions (Gundry *et al.*, 2009; Mehmood *et al.*, 2015).

Next, the mass analyzer measures the mass-to-charge ratio (*m/z*) of the generated ions and separates them based on this ratio (Aebersold and Mann, 2003; Gundry *et al.*, 2009). Finally, the detector converts the impact of the various ions into an electrical signal which is then used to determine the number of ions that can be identified for each *m/z* ratio (Aebersold and Mann, 2003; Gundry *et al.*, 2009). However, most mass spectrometers perform tandem mass spectrometry and

measure the *m/z* ratio over two steps (Dunham *et al.*, 2012). During the initial step, the mass spectrometer measures the *m/z* ratio of the entire peptide (also known as the precursor ion) (Dunham *et al.*, 2012; Steen and Mann, 2004). In the second step, several peptides of interest are fragmented, and the mass spectrometer determines the *m/z* ratio for the fragmented peptide (also known as the product ion) (Dunham *et al.*, 2012; Steen and Mann, 2004). The *m/z* values and intensities that were measured and recorded by the mass spectrometer are used to determine the peptide sequences of the proteins found in the provided sample (Steen and Mann, 2004). The proteins are then identified through the use of a large database that contains a wide collection of protein sequences. However, the protein database must be fairly expansive or the protein(s) of interest may not be identified (Gundry *et al.*, 2009).

There are several limitations to the AP-MS methodology. The first limitation is the co-purification of background and/or contaminant proteins that occurs when the prey proteins non-specifically bind to the solid matrix. Increasing the number or the stringency of the wash steps could be used to minimize the number of non-specific proteins detected. However, this can cause weak protein interactions to be lost, leading to false negative results (Dunham *et al.*, 2012). The second limitation to the AP-MS methodology is that transient interactions are often lost during the affinity purification steps (Dunham *et al.*, 2012; Yugandhar *et al.*, 2019). Lastly, the AP-MS methodology provides a list of proteins identified by the mass spectrometer but is unable to provide information regarding what protein complexes may be forming from this list of proteins (Gingras *et al.*, 2007).

1.4 Hypothesis and Objectives

1.4.1 Rationale

A previous study examined protein-protein interactions amongst *N. gonorrhoeae* cell division proteins (i.e., FtsZ, FtsA, ZipA, FtsK, FtsQ, FtsW, FtsI and FtsN) and identified several unique protein-protein interactions that are not observed between the homologous *E. coli* cell division proteins (Zou *et al.*, 2017a). However, this previous study did not examine the potential protein-protein interactions of four other *N. gonorrhoeae* cell division proteins (i.e., FtsE, FtsX, FtsL and FtsB). Therefore, there is a lack of information regarding the interactions of these four additional cell division proteins with the gonococcal cell division proteins FtsZ, FtsA, ZipA, FtsK, FtsQ, FtsW, FtsI and FtsN. In addition, data regarding the ability for the *N. gonorrhoeae* cell division proteins to self-interact was also not examined. Information regarding potential interactions amongst these additional cell division proteins could provide important information regarding the function of these cell division proteins.

1.4.2 Hypothesis

The protein-protein interaction network amongst *N. gonorrhoeae* divisome proteins includes additional proteins not previously investigated, such as FtsE, FtsX, FtsL, and FtsB. These additional divisome proteins participate in unique interactions with other cell division proteins. Identifying these unique interactions will provide context for the roles these divisome proteins play in cell division and expand knowledge of the current interactions amongst cell division proteins.

1.4.3 Objectives

To investigate this in detail we proposed the following objectives:

1. To explore the interactions of FtsE, FtsX, FtsL and FtsB with gonococcal cell division proteins (FtsZ, FtsA, ZipA, FtsE, FtsX, FtsK, FtsQ, FtsL, FtsB, FtsW, FtsI and FtsN), as well as the self-interactions of gonococcal cell division proteins using the Di Lallo B2H methodology;
2. To examine the potential interaction between *N. gonorrhoeae* cell division proteins FtsE and FtsQ using GST pulldown assays;
3. To explore potential interactions of *N. gonorrhoeae* FtsE with proteins derived from a gonococcal whole cell lysate using AP-MS assays

2.0 MATERIALS AND METHODS

2.1 Bacterial Strains and Growth Conditions

A list of all bacterial strains used in this study is provided in Table 2.1.

E. coli DH5α and *E. coli* XL1-Blue were used as cloning vector hosts for the various plasmids used in this study while *E. coli* BL21, *E. coli* C41 (DE3) and *E. coli* C43 (DE3) were used for protein overexpression and purification, as in Zou *et al.* (Zou *et al.*, 2017a). *E. coli* cultures were grown in Luria Broth (LB) medium (BD Difco, Mississauga, ON) for 18 hours at 37°C with shaking at 200 revolutions per minute (rpm). The following antibiotic concentrations were added as required: 100 μg/ml ampicillin (Sigma-Aldrich, Oakville, ON) or 50 μg/ml kanamycin (Sigma-Aldrich).

E. coli R721 was used for B2H assays and was grown in LB medium for 18 hours at 34°C with shaking at 200 rpm, as described previously (Di Lallo *et al.*, 2001). The following antibiotic concentrations were added as required: 34 μg/ml chloramphenicol (Sigma-Aldrich), 30 μg/ml kanamycin (Sigma-Aldrich), and 50 μg/ml ampicillin (Sigma-Aldrich).

N. gonorrhoeae CH811 was used for AP-MS assays and cloning experiments. Cultures were grown on GC medium base (BD Difco) supplemented with 1% Kellogg's defined supplement (GCMBK) (Kellogg *et al.*, 1963). Cultures were incubated in a humid environment at 37°C, with 5-7% CO_2, for 18-24 hours (Spence *et al.*, 2008; Unemo *et al.*, 2009).

All bacterial strains were stored at -80°C. *E. coli* strains were stored in LB plus 50% glycerol while *N. gonorrhoeae* strains were stored in Brain Heart Infusion (BHI) (BD Difco) plus 20% glycerol.

Table 2.1: Bacterial Strains Designed and Used in this Study

Strain Name	Relevant Genotype	Source/Reference
E. coli DH5α	F^- endA1 thi-1 recA1 relA1 gyrA96 φ80dlacZΔM15 Δ(lacZYA-argF)U169, hsdR17($r_K^- m_K^+$), λ^-	(Grant *et al.*, 1990)
E. coli XL1-Blue	recA1 endA1 gyrA96 thi-1 hsdR17 supE44 relA1 lac [F´ proAB $lacI^q$ ZΔM15 Tn10 (Tet^r)]	Stratagene
E. coli BL21 (DE3)	F^- ompT gal dcm lon $hsdS_B(r_B^- m_B^-)$ λ(DE3) pLysS	(Studier *et al.*, 1990)
E. coli C41 (DE3)	F^- ompT gal dcm $hsdS_B(r_B^- m_B^-)$(DE3)	(Miroux and Walker, 1996)
E. coli C43 (DE3)	F^- ompT gal dcm $hsdS_B(r_B^- m_B^-)$(DE3)	(Miroux and Walker, 1996)
E. coli R721	*supE thy D*(*lac-proAB*) F' [$proAB^+$ $lacI^q$ *lac*ZDM15] *glpT*::O-$_{P434/P22}$*lacZ*	(Di Lallo *et al.*, 2001)
N. gonorrhoeae CH811	Auxotype (A)/serotype (S)/plasmid content (P) class: nonrequiring/IB-2/plasmid-free, Str_r	(Picard and Dillon, 1989)
E. coli XL1-Blue pGEX2T	$Amp^R P_{tac}$::*gst*::*lacIq*	Amersham Bioscience, Uppsala, Sweden
E. coli DH5α pET30a	$Kan^R P_{T7}$::6Xhis	EMD Millipore, Billerica, MA
E. coli XL1-Blue pcI_{p22}	pC132 construct with N-terminal end of P22 repressor	This study
E. coli XL1-Blue pcI_{434}	pACYC177 construct with N-terminal end of 434 repressor	This study

Strains Related to GST pulldowns and Associated work		
Stain Name	**Relevant Genotype**	**Source/Reference**
E. coli BL21 (DE3) pGEX2T-FtsE	pGEX2T construct with the *ftsE*$_{Ng}$ gene	This study
E. coli BL21 (DE3) pGEX2T-FtsB	pGEX2T construct with the *ftsB*$_{Ng}$ gene	This study
E. coli BL21 (DE3) pET30a-FtsQ	pET30a construct with the *ftsQ*$_{Ng}$ gene	(Zou *et al.*, 2017a)
E. coli BL21 (DE3) pET30a-FtsL	pET30a construct with the *ftsL*$_{Ng}$ gene	This study
E. coli C43 (DE3) pET30a-FtsX	pET30a construct with the *ftsX*$_{Ng}$ gene	This study
E. coli C41 (DE3) pGEX2T	Amp^{R}P$_{tac}$::*gst*::*lacIq*	Amersham Bioscience, Uppsala, Sweden
Strains Related to B2H and Associated Work		
Stain Name	**Relevant Genotype**	**Source/Reference**
E. coli R721 pcI$_{p22}$-FtsB	pcIp22 construct with the *ftsB*$_{Ng}$ gene	This study
E. coli R721 pcI$_{434}$-FtsB	pcI434 construct with the *ftsB*$_{Ng}$ gene	This study
E. coli R721 pcI$_{p22}$-FtsK	pcIp22 construct with the *ftsK*$_{Ng}$ gene	This study
E. coli R721 pcI$_{434}$-FtsK	pcI434 construct with the *ftsK*$_{Ng}$ gene	(Zou *et al.*, 2017a)
E. coli R721 pcI$_{p22}$	pC132 construct with N-terminal end of P22 repressor	(Di Lallo *et al.*, 2001)
E. coli R721 pcI$_{434}$	pACYC177 construct with N-terminal end of 434 repressor	(Di Lallo *et al.*, 2001)
E. coli R721 pcI$_{p22}$-FtsE	pcI$_{p22}$ construct with the *ftsE*$_{Ng}$ gene	This study

E. coli R721 pcI$_{434}$-FtsE	pcI$_{434}$ construct with the *ftsE*$_{Ng}$ gene	This study
E. coli R721 pcI$_{p22}$-FtsX	pcI$_{p22}$ construct with the *ftsX*$_{Ng}$ gene	This study
E. coli R721 pcI$_{434}$-FtsX	pcI$_{434}$ construct with the *ftsX*$_{Ng}$ gene	This study
E. coli R721 pcI$_{p22}$-FtsL	pcI$_{p22}$ construct with the *ftsL*$_{Ng}$ gene	This study
E. coli R721 pcI$_{434}$-FtsL	pcI$_{434}$ construct with the *ftsL*$_{Ng}$ gene	This study
E. coli R721 pcI$_{p22}$-FtsZ	pcI$_{p22}$ construct with the *ftsZ*$_{Ng}$ gene	(Zou *et al.*, 2017a)
E. coli R721 pcI$_{434}$-FtsZ	pcI$_{434}$ construct with the *ftsZ*$_{Ng}$ gene	(Zou *et al.*, 2017a)
E. coli R721 pcI$_{p22}$-FtsA	pcI$_{p22}$ construct with the *ftsA*$_{Ng}$ gene	(Zou *et al.*, 2017a)
E. coli R721 pcI$_{434}$-FtsA	pcI$_{434}$ construct with the *ftsA*$_{Ng}$ gene	(Zou *et al.*, 2017a)
E. coli R721 pcI$_{p22}$-ZipA	pcI$_{p22}$ construct with the *ZipA*$_{Ng}$ gene	(Zou *et al.*, 2017a)
E. coli R721 pcI$_{434}$-ZipA	pcI$_{434}$ construct with the *ZipA*$_{Ng}$ gene	(Zou *et al.*, 2017a)
E. coli R721 pcI$_{p22}$-FtsQ	pcI$_{p22}$ construct with the *ftsQ*$_{Ng}$ gene	(Zou *et al.*, 2017a)
E. coli R721 pcI$_{434}$-FtsQ	pcI$_{434}$ construct with the *ftsQ*$_{Ng}$ gene	(Zou *et al.*, 2017a)
E. coli R721 pcI$_{p22}$-FtsW	pcI$_{p22}$ construct with the *ftsW*$_{Ng}$ gene	(Zou *et al.*, 2017a)
E. coli R721 pcI$_{434}$-FtsW	pcI$_{434}$ construct with the *ftsW*$_{Ng}$ gene	(Zou *et al.*, 2017a)
E. coli R721 pcI$_{p22}$-FtsI	pcI$_{p22}$ construct with the *ftsI*$_{Ng}$ gene	(Zou *et al.*, 2017a)

E. coli R721 pcI$_{434}$-FtsI	pcI$_{434}$ construct with the *ftsI*$_{Ng}$ gene	(Zou *et al.*, 2017a)
E. coli R721 pcI$_{p22}$-FtsN	pcI$_{p22}$ construct with the *ftsN*$_{Ng}$ gene	(Zou *et al.*, 2017a)
E. coli R721 pcI$_{434}$-FtsN	pcI$_{434}$ construct with the *ftsN*$_{Ng}$ gene	(Zou *et al.*, 2017a)
E. coli R721 pcI$_{p22}$-FtsE + pcI$_{434}$-FtsZ	pcI$_{p22}$-*ftsE*$_{Ng}$ construct + pcI$_{434}$-*ftsZ*$_{Ng}$ construct	This study
E. coli R721 pcI$_{434}$-FtsE + pcI$_{p22}$-FtsZ	pcI$_{434}$-*ftsE*$_{Ng}$ construct + pcI$_{p22}$-*ftsZ*$_{Ng}$ construct	This study
E. coli R721 pcI$_{p22}$-FtsE + pcI$_{434}$-FtsA	pcI$_{p22}$-*ftsE*$_{Ng}$ construct + pcI$_{434}$-*ftsA*$_{Ng}$ construct	This study
E. coli R721 pcI$_{434}$-FtsE + pcI$_{p22}$-FtsA	pcI$_{434}$-*ftsE*$_{Ng}$ construct + pcI$_{p22}$-*ftsA*$_{Ng}$ construct	This study
E. coli R721 pcI$_{p22}$-FtsE + pcI$_{434}$-ZipA	pcI$_{p22}$-*ftsE*$_{Ng}$ construct + pcI$_{434}$-*ZipA*$_{Ng}$ construct	This study
E. coli R721 pcI$_{434}$-FtsE + pcI$_{p22}$-ZipA	pcI$_{434}$-*ftsE*$_{Ng}$ construct + pcI$_{p22}$-*ZipA*$_{Ng}$ construct	This study
E. coli R721 pcI$_{p22}$-FtsE + pcI$_{434}$-FtsE	pcI$_{p22}$-*ftsE*$_{Ng}$ construct + pcI$_{434}$-*ftsE*$_{Ng}$ construct	This study
E. coli R721 pcI$_{p22}$-FtsE + pcI$_{434}$-FtsX	pcI$_{p22}$-*ftsE*$_{Ng}$ construct + pcI$_{434}$-*ftsX*$_{Ng}$ construct	This study
E. coli R721 pcI$_{434}$-FtsE + pcI$_{p22}$-FtsX	pcI$_{434}$-*ftsE*$_{Ng}$ construct + pcI$_{p22}$-*ftsX*$_{Ng}$ construct	This study
E. coli R721 pcI$_{p22}$-FtsE + pcI$_{434}$-FtsK	pcI$_{p22}$-*ftsE*$_{Ng}$ construct + pcI$_{434}$-*ftsK*$_{Ng}$ construct	This study
E. coli R721 pcI$_{434}$-FtsE + pcI$_{p22}$-FtsK	pcI$_{434}$-*ftsE*$_{Ng}$ construct + pcI$_{p22}$-*ftsK*$_{Ng}$ construct	This study
E. coli R721 pcI$_{p22}$-FtsE + pcI$_{434}$-FtsQ	pcI$_{p22}$-*ftsE*$_{Ng}$ construct + pcI$_{434}$-*ftsQ*$_{Ng}$ construct	This study
E. coli R721 pcI$_{434}$-FtsE + pcI$_{p22}$-FtsQ	pcI$_{434}$-*ftsE*$_{Ng}$ construct + pcI$_{p22}$-*ftsQ*$_{Ng}$ construct	This study

E. coli R721 pcI_{p22}-FtsE + pcI_{434}-FtsL	pcI_{p22}-*ftsE*$_{Ng}$ construct + pcI_{434}-*ftsL*$_{Ng}$ construct	This study
E. coli R721 pcI_{434}-FtsE + pcI_{p22}-FtsL	pcI_{434}-*ftsE*$_{Ng}$ construct + pcI_{p22}-*ftsL*$_{Ng}$ construct	This study
E. coli R721 pcI_{p22}-FtsE + pcI_{434}-FtsB	pcI_{p22}-*ftsE*$_{Ng}$ construct + pcI_{434}-*ftsB*$_{Ng}$ construct	This study
E. coli R721 pcI_{434}-FtsE + pcI_{p22}-FtsB	pcI_{434}-*ftsE*$_{Ng}$ construct + pcI_{p22}-*ftsB*$_{Ng}$ construct	This study
E. coli R721 pcI_{p22}-FtsE + pcI_{434}-FtsW	pcI_{p22}-*ftsE*$_{Ng}$ construct + pcI_{434}-*ftsW*$_{Ng}$ construct	This study
E. coli R721 pcI_{434}-FtsE + pcI_{p22}-FtsW	pcI_{434}-*ftsE*$_{Ng}$ construct + pcI_{p22}-*ftsW*$_{Ng}$ construct	This study
E. coli R721 pcI_{p22}-FtsE + pcI_{434}-FtsI	pcI_{p22}-*ftsE*$_{Ng}$ construct + pcI_{434}-*ftsI*$_{Ng}$ construct	This study
E. coli R721 pcI_{434}-FtsE + pcI_{p22}-FtsI	pcI_{434}-*ftsE*$_{Ng}$ construct + pcI_{p22}-*ftsI*$_{Ng}$ construct	This study
E. coli R721 pcI_{p22}-FtsE + pcI_{434}-FtsN	pcI_{p22}-*ftsE*$_{Ng}$ construct + pcI_{434}-*ftsN*$_{Ng}$ construct	This study
E. coli R721 pcI_{434}-FtsE + pcI_{p22}-FtsN	pcI_{434}-*ftsE*$_{Ng}$ construct + pcI_{p22}-*ftsN*$_{Ng}$ construct	This study
E. coli R721 pcI_{p22}-FtsX + pcI_{434}-FtsZ	pcI_{p22}-*ftsX*$_{Ng}$ construct + pcI_{434}-*ftsZ*$_{Ng}$ construct	This study
E. coli R721 pcI_{434}-FtsX + pcI_{p22}-FtsZ	pcI_{434}-*ftsX*$_{Ng}$ construct + pcI_{p22}-*ftsZ*$_{Ng}$ construct	This study
E. coli R721 pcI_{p22}-FtsX + pcI_{434}-FtsA	pcI_{p22}-*ftsX*$_{Ng}$ construct + pcI_{434}-*ftsA*$_{Ng}$ construct	This study
E. coli R721 pcI_{434}-FtsX + pcI_{p22}-FtsA	pcI_{434}-*ftsX*$_{Ng}$ construct + pcI_{p22}-*ftsA*$_{Ng}$ construct	This study
E. coli R721 pcI_{p22}-FtsX + pcI_{434}-ZipA	pcI_{p22}-*ftsX*$_{Ng}$ construct + pcI_{434}-*ZipA*$_{Ng}$ construct	This study
E. coli R721 pcI_{434}-FtsX + pcI_{p22}-ZipA	pcI_{434}-*ftsX*$_{Ng}$ construct + pcI_{p22}-*ZipA*$_{Ng}$ construct	This study

E. coli R721 pcI$_{p22}$-FtsX+ pcI$_{434}$-FtsX	pcI$_{p22}$-*ftsX*$_{Ng}$ construct + pcI$_{434}$-*ftsX*$_{Ng}$ construct	This study
E. coli R721 pcI$_{p22}$-FtsX + pcI$_{434}$-FtsK	pcI$_{p22}$-*ftsX*$_{Ng}$ construct + pcI$_{434}$-*ftsK*$_{Ng}$ construct	This study
E. coli R721 pcI$_{434}$-FtsX + pcI$_{p22}$-FtsK	pcI$_{434}$-*ftsX*$_{Ng}$ construct + pcI$_{p22}$-*ftsK*$_{Ng}$ construct	This study
E. coli R721 pcI$_{p22}$-FtsX + pcI$_{434}$-FtsQ	pcI$_{p22}$-*ftsX*$_{Ng}$ construct + pcI$_{434}$-*ftsQ*$_{Ng}$ construct	This study
E. coli R721 pcI$_{434}$-FtsX + pcI$_{p22}$-FtsQ	pcI$_{434}$-*ftsX*$_{Ng}$ construct + pcI$_{p22}$-*ftsQ*$_{Ng}$ construct	This study
E. coli R721 pcI$_{p22}$-FtsX + pcI$_{434}$-FtsL	pcI$_{p22}$-*ftsX*$_{Ng}$ construct + pcI$_{434}$-*ftsL*$_{Ng}$ construct	This study
E. coli R721 pcI$_{434}$-FtsX + pcI$_{p22}$-FtsL	pcI$_{434}$-*ftsX*$_{Ng}$ construct + pcI$_{p22}$-*ftsL*$_{Ng}$ construct	This study
E. coli R721 pcI$_{p22}$-FtsX + pcI$_{434}$-FtsB	pcI$_{p22}$-*ftsX*$_{Ng}$ construct + pcI$_{434}$-*ftsB*$_{Ng}$ construct	This study
E. coli R721 pcI$_{434}$-FtsX + pcI$_{p22}$-FtsB	pcI$_{434}$-*ftsX*$_{Ng}$ construct + pcI$_{p22}$-*ftsB*$_{Ng}$ construct	This study
E. coli R721 pcI$_{p22}$-FtsX + pcI$_{434}$-FtsW	pcI$_{p22}$-*ftsX*$_{Ng}$ construct + pcI$_{434}$-*ftsW*$_{Ng}$ construct	This study
E. coli R721 pcI$_{434}$-FtsX + pcI$_{p22}$-FtsW	pcI$_{434}$-*ftsX*$_{Ng}$ construct + pcI$_{p22}$-*ftsW*$_{Ng}$ construct	This study
E. coli R721 pcI$_{p22}$-FtsX + pcI$_{434}$-FtsI	pcI$_{p22}$-*ftsX*$_{Ng}$ construct + pcI$_{434}$-*ftsI*$_{Ng}$ construct	This study
E. coli R721 pcI$_{434}$-FtsX + pcI$_{p22}$-FtsI	pcI$_{434}$-*ftsX*$_{Ng}$ construct + pcI$_{p22}$-*ftsI*$_{Ng}$ construct	This study
E. coli R721 pcI$_{p22}$-FtsX + pcI$_{434}$-FtsN	pcI$_{p22}$-*ftsX*$_{Ng}$ construct + pcI$_{434}$-*ftsN*$_{Ng}$ construct	This study
E. coli R721 pcI$_{434}$-FtsX + pcI$_{p22}$-FtsN	pcI$_{434}$-*ftsX*$_{Ng}$ construct + pcI$_{p22}$-*ftsN*$_{Ng}$ construct	This study
E. coli R721 pcI$_{p22}$-FtsL + pcI$_{434}$-FtsZ	pcI$_{p22}$-*ftsL*$_{Ng}$ construct + pcI$_{434}$-*ftsZ*$_{Ng}$ construct	This study

E. coli R721 pcI$_{434}$-FtsL + pcI$_{p22}$-FtsZ	pcI$_{434}$-*ftsL*$_{Ng}$ construct + pcI$_{p22}$-*ftsZ*$_{Ng}$ construct	This study
E. coli R721 pcI$_{p22}$-FtsL + pcI$_{434}$-FtsA	pcI$_{p22}$-*ftsL*$_{Ng}$ construct + pcI$_{434}$-*ftsA*$_{Ng}$ construct	This study
E. coli R721 pcI$_{434}$-FtsL + pcI$_{p22}$-FtsA	pcI$_{434}$-*ftsL*$_{Ng}$ construct + pcI$_{p22}$-*ftsA*$_{Ng}$ construct	This study
E. coli R721 pcI$_{p22}$-FtsL + pcI$_{434}$-ZipA	pcI$_{p22}$-*ftsL*$_{Ng}$ construct + pcI$_{434}$-*ZipA*$_{Ng}$ construct	This study
E. coli R721 pcI$_{434}$-FtsL + pcI$_{p22}$-ZipA	pcI$_{434}$-*ftsL*$_{Ng}$ construct + pcI$_{p22}$-*ZipA*$_{Ng}$ construct	This study
E. coli R721 pcI$_{p22}$-FtsL + pcI$_{434}$-FtsK	pcI$_{p22}$-*ftsL*$_{Ng}$ construct + pcI$_{434}$-*ftsK*$_{Ng}$ construct	This study
E. coli R721 pcI$_{434}$-FtsL + pcI$_{p22}$-FtsK	pcI$_{434}$-*ftsL*$_{Ng}$ construct + pcI$_{p22}$-*ftsK*$_{Ng}$ construct	This study
E. coli R721 pcI$_{p22}$-FtsL + pcI$_{434}$-FtsQ	pcI$_{p22}$-*ftsL*$_{Ng}$ construct + pcI$_{434}$-*ftsQ*$_{Ng}$ construct	This study
E. coli R721 pcI$_{434}$-FtsL + pcI$_{p22}$-FtsQ	pcI$_{434}$-*ftsL*$_{Ng}$ construct + pcI$_{p22}$-*ftsQ*$_{Ng}$ construct	This study
E. coli R721 pcI$_{p22}$-FtsL + pcI$_{434}$-FtsL	pcI$_{p22}$-*ftsL*$_{Ng}$ construct + pcI$_{434}$-*ftsL*$_{Ng}$ construct	This study
E. coli R721 pcI$_{p22}$-FtsL + pcI$_{434}$-FtsB	pcI$_{p22}$-*ftsL*$_{Ng}$ construct + pcI$_{434}$-*ftsB*$_{Ng}$ construct	This study
E. coli R721 pcI$_{434}$-FtsL + pcI$_{p22}$-FtsB	pcI$_{434}$-*ftsL*$_{Ng}$ construct + pcI$_{p22}$-*ftsB*$_{Ng}$ construct	This study
E. coli R721 pcI$_{p22}$-FtsL + pcI$_{434}$-FtsW	pcI$_{p22}$-*ftsL*$_{Ng}$ construct + pcI$_{434}$-*ftsW*$_{Ng}$ construct	This study
E. coli R721 pcI$_{434}$-FtsL + pcI$_{p22}$-FtsW	pcI$_{434}$-*ftsL*$_{Ng}$ construct + pcI$_{p22}$-*ftsW*$_{Ng}$ construct	This study
E. coli R721 pcI$_{p22}$-FtsL + pcI$_{434}$-FtsI	pcI$_{p22}$-*ftsL*$_{Ng}$ construct + pcI$_{434}$-*ftsI*$_{Ng}$ construct	This study
E. coli R721 pcI$_{434}$-FtsL + pcI$_{p22}$-FtsI	pcI$_{434}$-*ftsL*$_{Ng}$ construct + pcI$_{p22}$-*ftsI*$_{Ng}$ construct	This study

E. coli R721 pcI$_{p22}$-FtsL + pcI$_{434}$-FtsN	pcI$_{p22}$-*ftsL*$_{Ng}$ construct + pcI$_{434}$-*ftsN*$_{Ng}$ construct	This study
E. coli R721 pcI$_{434}$-FtsL + pcI$_{p22}$-FtsN	pcI$_{434}$-*ftsL*$_{Ng}$ construct + pcI$_{p22}$-*ftsN*$_{Ng}$ construct	This study
E. coli R721 pcI$_{p22}$-FtsB + pcI$_{434}$-FtsZ	pcI$_{p22}$-*ftsB*$_{Ng}$ construct + pcI$_{434}$-*ftsZ*$_{Ng}$ construct	This study
E. coli R721 pcI$_{434}$-FtsB + pcI$_{p22}$-FtsZ	pcI$_{434}$-*ftsB*$_{Ng}$ construct + pcI$_{p22}$-*ftsZ*$_{Ng}$ construct	This study
E. coli R721 pcI$_{p22}$-FtsB + pcI$_{434}$-FtsA	pcI$_{p22}$-*ftsB*$_{Ng}$ construct + pcI$_{434}$-*ftsA*$_{Ng}$ construct	This study
E. coli R721 pcI$_{434}$-FtsB + pcI$_{p22}$-FtsA	pcI$_{434}$-*ftsB*$_{Ng}$ construct + pcI$_{p22}$-*ftsA*$_{Ng}$ construct	This study
E. coli R721 pcI$_{p22}$-FtsB + pcI$_{434}$-ZipA	pcI$_{p22}$-*ftsB*$_{Ng}$ construct + pcI$_{434}$-*ZipA*$_{Ng}$ construct	This study
E. coli R721 pcI$_{434}$-FtsB + pcI$_{p22}$-ZipA	pcI$_{434}$-*ftsB*$_{Ng}$ construct + pcI$_{p22}$-*ZipA*$_{Ng}$ construct	This study
E. coli R721 pcI$_{p22}$-FtsB + pcI$_{434}$-FtsK	pcI$_{p22}$-*ftsB*$_{Ng}$ construct + pcI$_{434}$-*ftsK*$_{Ng}$ construct	This study
E. coli R721 pcI$_{434}$-FtsB + pcI$_{p22}$-FtsK	pcI$_{434}$-*ftsB*$_{Ng}$ construct + pcI$_{p22}$-*ftsK*$_{Ng}$ construct	This study
E. coli R721 pcI$_{p22}$-FtsB + pcI$_{434}$-FtsQ	pcI$_{p22}$-*ftsB*$_{Ng}$ construct + pcI$_{434}$-*ftsQ*$_{Ng}$ construct	This study
E. coli R721 pcI$_{434}$-FtsB + pcI$_{p22}$-FtsQ	pcI$_{434}$-*ftsB*$_{Ng}$ construct + pcI$_{p22}$-*ftsQ*$_{Ng}$ construct	This study
E. coli R721 pcI$_{p22}$-FtsB + pcI$_{434}$-FtsB	pcI$_{p22}$-*ftsB*$_{Ng}$ construct + pcI$_{434}$-*ftsB*$_{Ng}$ construct	This study
E. coli R721 pcI$_{p22}$-FtsB + pcI$_{434}$-FtsW	pcI$_{p22}$-*ftsB*$_{Ng}$ construct + pcI$_{434}$-*ftsW*$_{Ng}$ construct	This study
E. coli R721 pcI$_{434}$-FtsB + pcI$_{p22}$-FtsW	pcI$_{434}$-*ftsB*$_{Ng}$ construct + pcI$_{p22}$-*ftsW*$_{Ng}$ construct	This study
E. coli R721 pcI$_{p22}$-FtsB + pcI$_{434}$-FtsI	pcI$_{p22}$-*ftsB*$_{Ng}$ construct + pcI$_{434}$-*ftsI*$_{Ng}$ construct	This study

E. coli R721 pcI$_{434}$-FtsB + pcI$_{p22}$-FtsI	pcI$_{434}$-*ftsB*$_{Ng}$ construct + pcI$_{p22}$-*ftsI*$_{Ng}$ construct	This study
E. coli R721 pcI$_{p22}$-FtsB + pcI$_{434}$-FtsN	pcI$_{p22}$-*ftsB*$_{Ng}$ construct + pcI$_{434}$-*ftsN*$_{Ng}$ construct	This study
E. coli R721 pcI$_{434}$-FtsB + pcI$_{p22}$-FtsN	pcI$_{434}$-*ftsB*$_{Ng}$ construct + pcI$_{p22}$-*ftsN*$_{Ng}$ construct	This study
E. coli R721 pcI$_{p22}$-FtsZ + pcI$_{434}$-FtsZ	pcI$_{p22}$-*ftZ*$_{Ng}$ construct + pcI$_{434}$-*ftsZ*$_{Ng}$ construct	(Zou *et al.*, 2017a)
E. coli R721 pcI$_{p22}$-FtsA + pcI$_{434}$-FtsA	pcI$_{p22}$-*ftsA*$_{Ng}$ construct + pcI$_{434}$-*ftsA*$_{Ng}$ construct	This study
E. coli R721 pcI$_{p22}$-ZipA + pcI$_{434}$-ZipA	pcI$_{p22}$-*ZipA*$_{Ng}$ construct + pcI$_{434}$-*ZipA*$_{Ng}$ construct	This study
E. coli R721 pcI$_{p22}$-FtsK + pcI$_{434}$-FtsK	pcI$_{p22}$-*ftsK*$_{Ng}$ construct + pcI$_{434}$-*ftsK*$_{Ng}$ construct	This study
E. coli R721 pcI$_{p22}$-FtsQ + pcI$_{434}$-FtsQ	pcI$_{p22}$-*ftsQ*$_{Ng}$ construct + pcI$_{434}$-*ftsQ*$_{Ng}$ construct	This study
E. coli R721 pcI$_{p22}$-FtsW + pcI$_{434}$-FtsW	pcI$_{p22}$-*ftsW*$_{Ng}$ construct + pcI$_{434}$-*ftsW*$_{Ng}$ construct	This study
E. coli R721 pcI$_{p22}$-FtsI + pcI$_{434}$-FtsI	pcI$_{p22}$-*ftsI*$_{Ng}$ construct + pcI$_{434}$-*ftsI*$_{Ng}$ construct	This study
E. coli R721 pcI$_{p22}$-FtsN + pcI$_{434}$-FtsN	pcI$_{p22}$-*ftsN*$_{Ng}$ construct + pcI$_{434}$-*ftsN*$_{Ng}$ construct	This study

2.2 Cloning Experiments – DNA Extraction, Primer Design and Creation of Constructs

2.2.1 Genomic and Plasmid DNA Extraction

N. gonorrhoeae CH811 DNA was extracted using a QIAamp DNA Mini Kit #51306 (Qiagen, Toronto, ON) according to the manufacturer's instructions and quantified using a NanoDrop One Spectrophotometer (Thermo Fisher Scientific Inc., Waltham, MA, USA). The final *N. gonorrhoeae* CH811 DNA concentration was adjusted to 50 ng/µL with ddH_2O for all polymerase chain reaction (PCR) experiments. Plasmid DNA was extracted from *E. coli* XL1-Blue pGEX2T, *E. coli* DH5α pET30a, *E. coli* XL1-Blue pcI_{p22}, and *E. coli* XL1-Blue pcI_{434} using a GeneJET Plasmid Miniprep Kit (Thermo Fisher Scientific) according to the manufacturer's instructions. Plasmid DNA was quantified using a NanoDrop One Spectrophotometer and the final concentration was adjusted to 20 ng/µL with ddH_2O for all cloning experiments. All DNA samples were stored at -20°C.

2.2.2 Primer Design

All primers were designed using Clone Manager version 9 (Clone Manger, Sci-Ed Software LLC, Westminster, CO, USA). Four primers (P1 to P4: fwSalI-*ftsB*, reBamHI-*ftsB*, fwSalI-*ftsK* and reBamHI-*ftsK*, respectively) were designed to clone *N. gonorrhoeae ftsB* and *ftsK* into pcIp22 and pcI434 vectors for use in B2H experiments (Table 2.2.2). Eight primers (P5 to P12: fwBamHI-*ftsE*, reEcoRI-*ftsE*, fwBamHI-*ftsB*, reEcoRI-*ftsB*, fwBglII-*ftsX*, reEcoRI-*ftsX*, fwBglII-*ftsL*, and reEcoRI-*ftsL*, respectively) were designed to clone *N. gonorrhoeae ftsE, ftsB, ftsL*, and *ftsX* into pGEX2T and pET30a vectors for GST pulldown assays (Table 2.2.3).

Table 2.2.2: Primers Designed for Use in B2H Experiments

Primer Name		**Sequence (5′-3′)***
P1	fwSalI-ftsB	GCGC**GTCGAC**CATGAAGTGGGTAACTGTCGTT
P2	reBamHI-ftsB	CGCG**GGATCC**TTACCGGTTATGCCTGATGAG
P3	fwSalI-ftsK	GCGC**GTCGAC**CATGTTTTGGATAGTTTTGATCGTTAT
P4	reBamHI-ftsK	CGCG**GGATCC**TCAAGCATTGTCCAAGGGGACGAG

*Enzyme recognition sequences are indicated in **bold**.

Table 2.2.3: Primers Designed for Use in GST Pulldown Experiments

Primer Name		**Sequence (5′-3′)***
P5	fwBamHI-ftsE	CGC**GGATCC**ATGATCCGTTTCGAACAAGTTTCCAAAACC
P6	reEcoRI-ftsE	CGC**GAATTC**TCATGCGAGTCGTCCTTTCGAGAGGC
P7	fwBamHI-ftsB	CGC**GGATCC**ATGAAGTGGGTAACTGTC
P8	reEcoRI-ftsB	CGC**GAATTC**TTACCGGTTATGCCTGATGAG
P9	fwBglII-ftsX	AGCCC**AGATCT**GATGAGCATCATCCACTACTTCTC
P10	reEcoRI-ftsX	ATATC**GAATTC**TTATTTTTTGGCTTTGAAGCAGAG
P11	fwBglII-ftsL	AGCCC**AGATCT**GATGAACAAATCGAATTTCTTTCTG
P12	reEcoRI-ftsL	ATATC**GAATTC**CTATCTTTGATGTTCCACCATAAAGG

*Enzyme recognition sequences are indicated in **bold**.

2.2.3 PCR Conditions and Creation of Constructs

The following conditions were applied to all PCR assays: Activation: 98°C (30 seconds), Denaturation: 98°C (10 secs), Annealing: 60°C (20 secs), Extension: 72°C (30 secs/kb) [for 30 cycles], Final Extension: 72°C (2 min), and Hold: 4°C (infinity). Each PCR reaction was carried out in 50 µL (final volume) mixtures containing 25 µL Q5 Master Mix (New England Biolabs Ltd, Whitby, ON), 2.5 µL forward primer (10 µM), 2.5 µL reverse primer (10 µM), 4 µL *N. gonorrhoeae* CH811 DNA (50 ng/µL), and 16 µL of ddH_2O.

2.2.4 Agarose Gels

Agarose gels were used to verify the results for all PCR experiments. Agarose gels were prepared at a 1% (w/v) solution, combining the required weight of agarose (Thermo Fisher Scientific) with the required volume of 1x Tris-acetate-ethylenediaminetetraacetic acid (EDTA) (TAE) buffer. Ethidium bromide was added to a final concentration of 0.2 µg/mL. The agarose gel was placed in a gel electrophoresis machine and submerged in 1x TAE buffer. The PCR products were loaded into the gel and the samples were subjected to electrophoresis at 100V for at least 30 minutes. After electrophoresis, the gel was imaged using the Bio-Rad Molecular Imager Gel Doc

XR+ (Bio-Rad, Bio-Rad Laboratories, Mississauga, ON). The molecular weight ladder used for all agarose gels was the 1 kb Plus DNA Ladder (Thermo Fisher Scientific).

2.2.5 Creation of Plasmid Constructs

For B2H experiments, full length *ftsB* and *ftsK* from *N. gonorrhoeae* CH811 were PCR amplified using primer pairs P1/P2 and P3/P4, respectively (Table 2.2.2). Amplicons were digested using *Sal*I and *BamH*I FastDigest enzymes (Thermo Fisher Scientific), according to manufacturer's protocol. *ftsB* and *ftsK* PCR products were ligated into pre-digested $pcIp_{22}$ and pcI_{434} from *E. coli* DH5α using T4 DNA ligase (Thermo Fisher Scientific), according to manufacturer's protocol. The pcI_{p22}-FtsB, pcI_{434}-FtsB, and pcI_{p22}-FtsK constructs were created for use in B2H assays. The pcI_{434}-FtsK construct was previously created by Zou *et al.* (Zou *et al.,* 2017a). The presence of the gene of interest within these constructs was verified through PCR amplification. The expected size amplicons were observed on a 1% TAE agarose gel.

For GST pulldown experiments, full length *ftsE* and *ftsB* from *N. gonorrhoeae* CH811 were PCR amplified primer pairs P5/P6 and P7/P8, respectively (Table 2.2.3). In addition, full length *ftsX* and *ftsL* from *N. gonorrhoeae* CH811 were PCR amplified using primer pairs P9/P10 and P11/P12 (Table 2.2.3), respectively. *ftsE* and *ftsB* PCR products were digested using *BamH*I and *EcoR*I FastDigest enzymes, following manufacturer's protocol (Thermo Fisher Scientific). *ftsE* and *ftsB* PCR products were ligated into pre-digested pGEX2T from *E. coli* DH5α with T4 DNA ligase (Thermo Fischer Scientific), according to manufacturer's protocol, thereby creating pGEX2T-FtsE and pGEX2T-FtsB constructs. *ftsL* and *ftsX* PCR products were digested using *Bgl*II and *EcoR*I FastDigest enzymes (Thermo Fisher Scientific), according to manufacturer's protocol. *ftsL* and *ftsX* PCR products were ligated into pre-digested pET30a from *E. coli* DH5α using T4 DNA ligase (Thermo Fisher Scientific), according to manufacturer's protocols, creating pET30a-FtsX and pET30a-FtsL constructs. The presence of the gene of interest within these constructs were verified by PCR amplification where the expected size amplicons were observed on a 1% TAE agarose gel. Constructs were also confirmed by DNA sequencing (Eurofins Genomics, Toronto, Ontario, Canada).

2.2.6 Creation of Competent Cells for Transformation

Competent cells were created for *E. coli* DH5α, *E. coli* BL21 (DE3), *E. coli* C43 (DE3) and *E. coli* R721 strains. The protocol from Sambrook and Russell was used with the following

modifications (Sambrook and Russell, 2001a). Briefly, the *E. coli* strain of interest was grown overnight at 37°C with shaking at 200 rpm. The culture was diluted 1:100 into fresh LB medium and incubated at 37°C with shaking at 200 rpm until the optical density at wavelength 600nm (OD_{600}) was approximately 0.5 on a spectrophotometer (Biochrom Libra S22 UV/Vis Spectrophotometer, Biochrom Ltd, Holliston, MA, USA). Cells were collected by centrifugation at 1000×*g* for 5 minutes (4°C) using the Sorvall Lynx 4000 superspeed centrifuge (Thermo Fisher Scientific). The pelleted cells were gently resuspended in Transformation Buffer 1 (100 mM RbCl, 50 mM $MnCl_2$, 30 mM potassium acetate, 10 mM $CaCl_2$, pH 5.8, 15% (v/v) glycerol), incubated on ice for 1 hour and re-pelleted using the centrifugation settings described above. The pellet was resuspended in Transformation Buffer 2 (75 mM $CaCl_2$, 10 mM MOPS, 10 mM RbCl, pH 8.0, 15% (v/v) glycerol) and aliquots of the competent cells were stored at -80°C.

2.2.7 Transformation of *E. coli* through Heat Shock Technique

All competent *E. coli* strains were transformed with plasmids using the heat shock protocol described by Sambrook and Russell, with the following modifications (Sambrook and Russell, 2001a). Briefly, 20 ng/µL plasmid DNA was gently mixed with the 50 µL of the *E. coli* competent cell strain of interest. The mixture was incubated on ice and then incubated in a heat block pre-warmed to 42°C for 30 seconds. The transformation mixtures were incubated in 1 mL of LB broth for 1 hour at 37°C with shaking at 200 rpm. The transformation samples were pelleted using a Microfuge 18 Centrifuge (Beckman Coulter, Brea, California, USA) for 3 minutes at 2000×*g*. The pellet was resuspended and spread onto the appropriate antibiotic containing LB plates. Plates were incubated overnight at 37°C and observed for colonies the next day. Potential transformants were confirmed by PCR as described above.

E. coli BL21 (DE3) competent cells were transformed with pGEX2T-FtsE and pGEX2T-FtsB as described above, creating *E. coli* BL21 (DE3) pGEX2T-FtsE and *E. coli* BL21 (DE3) pGEX2T-FtsB strains for protein expression and purification (Table 2.1). *E. coli* BL21 (DE3) and *E. coli* C43 (DE3) competent cells were both transformed with pET30a-FtsX, creating both *E. coli* BL21 (DE3) pET30a-FtsX and *E. coli* C43 (DE3) pET30a-FtsX strains for protein expression and purification (Table 2.1). *E. coli* BL21 (DE3) competent cells were transformed with pET30a-FtsL as described above, creating *E. coli* BL21 (DE3) pET30a-FtsL for protein expression and

purification. The pET30a-FtsQ construct had been previously designed and transformed into *E. coli* BL21 (DE3) (Zou *et al.*, 2017a).

In addition, *E. coli* R721 competent cells were transformed with pcI_{p22}-FtsB, pcI_{434}-FtsB and pcI_{p22}-FtsK constructs, creating *E. coli* R721 pcI_{p22}-FtsB, *E. coli* R721 pcI_{434}-FtsB, and *E. coli* R721 pcI_{p22}-FtsK strains for use in B2H experiments (Table 2.1). The *E. coli* R721 pcI_{434}-FtsK strain had been previously created (Zou *et al.*, 2017a).

2.3 Bacterial-2-Hybrid (B2H) Assays

The B2H assays described below were performed as described previously, but with the modifications described below (Di Lallo *et al.*, 2001, 2003). The B2H assay allows the study of two proteins and whether they interact, thereby repressing β-galactosidase production (Di Lallo *et al.*, 2001, 2003). The β-galactosidase produced through this assay is measured by the previously described protocol by Platt *et al.*, with the following modifications (Platt *et al.*, 1972). β-galactosidase assays measure the amount of β-galactosidase present in the sample that will convert colorless ortho-nitrophenyl-β-galactoside (ONPG) into the yellow o-nitrophenol product. By measuring the amount of yellow o-nitrophenol produced, the amount of β-galactosidase present can be indirectly determined (Platt *et al.,* 1972). The rate of conversion of ONPG to the yellow o-nitrophenol product is dependent on the concentration of β-galactosidase (Platt *et al.*, 1972).

Briefly, *E. coli* R721 cells containing the appropriate plasmids for the interaction under study were grown at 34°C with induction by 0.1 mM isopropyl β-D-1-thiogalactopyranoside (IPTG) until the OD_{600} read at least 0.2 on a spectrophotometer (Biochrom Ltd). The standardized log-phase *E. coli* samples were centrifuged at 3,000×*g* for 10 minutes. The pellet was resuspended in Z Buffer Complete (60 mM Na_2HPO_4, 40 mM NaH_2PO_4, 10 mM KCl, 1 mM $MgSO_4 \cdot 7H_2O$, pH 7.0, 0.3% (v/v) β-mercaptoethanol) and the OD_{600} was recorded. *E. coli* cells were permeabilized by the addition of 100% chloroform and 0.1% sodium dodecyl sulphate (SDS). After permeabilization, 200 µL of ONPG (4 mg/mL dissolved in 0.1 M Phosphate Buffer, pH 7.0) was added to all samples to initiate the β-galactosidase assay. The assay is halted by the addition of 1M Na_2CO_3 as this inactivates the β-galactosidase enzyme. The reaction time and the OD_{420} and OD_{550} are recorded for all samples.

The positive control for all B2H assays was the *N. gonorrhoeae* FtsZ-FtsZ self-interaction (Table 2.1) while the negative controls were recombinant plasmids containing cell division genes

transformed singly into *E. coli* R721 (i.e., pcI_{p22}-FtsE, pcI_{434}-FtsE, pcI_{p22}-FtsX, pcI_{434}-FtsX) where no interactions are possible (Table 2.1). The remaining *E. coli* R721 negative control strains included the following recombinant plasmids: pcI_{p22}-FtsL, pcI_{434}-FtsL, pcI_{p22}-FtsZ, pcI_{434}-FtsZ, pcI_{p22}-FtsA, pcI_{434}-FtsA, pcI_{p22}-ZipA, pcI_{434}-ZipA, pcI_{p22}-FtsQ, pcI_{434}-FtsQ, pcI_{p22}-FtsW, pcI_{434}-FtsW, pcI_{p22}-FtsI, pcI_{434}-FtsI, pcI_{p22}-FtsN, and pcI_{434}-FtsN (Table 2.1). In addition, the pcI_{p22}-FtsB, pcI_{434}-FtsB, pcI_{p22}-FtsK and pcI_{434}-FtsK constructs (Table 2.1) were also used as negative controls.

These single constructs were then transformed into *E. coli* R721 in various combinations to study the potential interaction between proteins of interest. These constructs were transformed in both "Forward" and "Reverse" configurations (i.e., *E. coli* R721 pcI_{p22}-FtsE + pcI_{434}-FtsZ and *E. coli* R721 pcI_{p22}-FtsZ, pcI_{434}-FtsE, etc.). A full list of all combinations of *E. coli* R721 strains studied during B2H assays is found in Table 2.1. All B2H assays were performed with two biological replicates and three technical replicates per biological replicate.

2.3.1 Statistical Analysis

To calculate the β-galactosidase activity, the values recorded during the β-galactosidase assay (i.e., the OD_{600}, OD_{550}, OD_{420}, and the reaction time) were input into Microsoft Excel 2016 (Microsoft Corporation, Redmond Washington, USA). The β-galactosidase activity for all samples can be calculated using the formula below (Platt *et al.*, 1972). Where T = the reaction time, in minutes, for the β-galactosidase assay and V = the volume of culture used in mL. The OD_{600} value provides the cell density of the sample prior to the β-galactosidase assay (Platt *et al.*, 1972). The OD_{420} value provides the absorbance of both the yellow o-nitrophenol and light scattering due to cellular debris (Platt *et al.*, 1972). To correct for the amount of light scattering caused by the cellular debris, the OD_{550} is measured as this value will provide the absorbance due solely to the cellular debris (Platt *et al.*, 1972). The units for β-galactosidase activity are known as Miller Units (Platt *et al.*, 1972).

$$\text{Miller Units} = \frac{1000 \times [OD_{420} - (1.75 \times OD_{550})]}{(T \times V \times OD_{600})}$$

Once β-galactosidase activity has been calculated for each sample, the standard deviation and standard error were calculated for each sample. The standard deviation was calculated using the =STDEV formula built into Microsoft Excel functions. The standard error was calculated by dividing the standard deviation by the square root of the sample size.

In addition, the percent β-galactosidase activity was calculated for all samples using the formula below. The percent β-galactosidase activity was calculated for each sample by dividing the Miller Units for the sample of interest by the Miller Units for the *E. coli* R721 baseline sample and multiplying by 100. The resulting value is the percentage β-galactosidase activity for the sample of interest.

$$\%\ \beta\text{-galactosidase Activity} = \frac{\text{Miller Units for Sample of Interest}}{\text{Miller Units for } \textit{E. coli} \text{ R721 Baseline Control}} \times 100$$

As recommended by Di Lallo *et al.*, a β-galactosidase activity of < 50% was interpreted to indicate the presence of an interaction (Di Lallo *et al.*, 2003). Di Lallo *et al.* chose 50% as the cutoff because when the assay was applied to previously identified protein-protein interactions, the protein-protein interactions would report values β-galactosidase values of < 50%. This 50% cutoff value has been used in several other papers when the Di Lallo B2H method is applied to examine protein-protein interactions including D'Ulisse *et al.*, Grenga *et al.*, Maggi *et al.*, and Zou *et al.* (D'Ulisse *et al.*, 2007; Grenga *et al.*, 2008; Maggi *et al.*, 2008; Zou *et al.*, 2017a). In addition, as per Di Lallo *et al.*, if any β-galactosidase activity value was over 100% (i.e., 130%), then the value was recorded as 100% (Di Lallo *et al.*, 2003).

2.4 Expression of GST- and His-tagged Fusion Proteins and GST Pulldown Assays

2.4.1 Expression and Purification of GST Fusion Proteins

GST and GST-tagged proteins GST-FtsE and GST-FtsB were purified from *E. coli* BL21 (DE3) following the "Purification of Proteins Fused to Glutathione S-Transferase" protocol, with the following modifications (Harper and Speicher, 2011). *E. coli* C41 pGEX2T, *E. coli* BL21 (DE3) pGEX2T-FtsE or *E. coli* BL21 (DE3) pGEX2T-FtsB were grown at 37°C until OD_{600} on the spectrophotometer (Biochrom Ltd) was 0.4. *E. coli* C41 pGEX2T, *E. coli* BL21 (DE3) pGEX2T-FtsE, or *E. coli* BL21 (DE3) pGEX2T-FtsB (Table 2.1) were induced with either 400 µM, 400 µM or 800 µM of IPTG, respectively, at 30°C for 3 hours. Cells were pelleted by centrifugation in a Sorvall Lynx 4000 superspeed centrifuge (Thermo Fisher Scientific) at 6,000×*g* for 10 minutes at 4°C. *E. coli* C41 pGEX2T pellets were resuspended in Phosphate Wash Buffer A (137 mM NaCl, 8 mM Na_2PO_4, 2.7 mM KCl, 1.5 mM KH_2PO_4, pH 7.4) while *E. coli* BL21 (DE3) pGEX2T-FtsE or *E. coli* pGEX2T-FtsB pellets were resuspended in Tris Wash Buffer A (150 mM NaCl, 50 mM Tris, pH 7.4). Samples were lysed by sonication using the Sonics VibraCell

Ultrasonic Processor (Sonics & Materials Inc., Newtown, Connecticut, USA) and centrifuged using the Sorvall Lynx 4000 superspeed centrifuge (Thermo Fisher Scientific) at 20,000×*g* for 20 minutes at 4°C.

For *E. coli* C41 pGEX2T, the GST protein was purified from the supernatant fraction. In contrast, for *E. coli* BL21 (DE3) pGEX2T-FtsE or *E. coli* BL21 (DE3) pGEX2T-FtsB, the GST-FtsE or GST-FtsB fusion proteins were purified from the pellet fraction. The pellet fraction was resuspended in Tris Wash Buffer A with the addition of 6 M urea and incubated on ice with agitation for 1 hour to solubilize the pellet. The samples were centrifuged using the Sorvall Lynx 4000 superspeed centrifuge (Thermo Fisher Scientific) at 16,000×*g* for 30 minutes at 4°C. GST-FtsE or GST-FtsB fusion proteins were dialyzed overnight at 4°C in Tris Wash Buffer A to remove the urea.

GST, GST-FtsE and GST-FtsB were purified from *E. coli* C41 pGEX2T, *E. coli* BL21 (DE3) pGEX2T-FtsE and *E. coli* BL21 (DE3) pGEX2T-FtsB cells, respectively. These proteins were purified using Pierce Glutathione Agarose (Thermo Fisher Scientific) in a gravity column, following the manufacturer's instructions. GST was eluted using Phosphate Elution Buffer A (137 mM NaCl, 8 mM Na_2PO_4, 2.7 mM KCl, 1.5 mM KH_2PO_4, 10 mM glutathione, pH 7.4) while GST-FtsE and GST-FtsB were eluted in Tris Elution Buffer A (150 mM NaCl, 50 mM Tris, 10 mM glutathione, pH 7.4). The purity of GST-FtsE, GST-FtsB and GST purifications determined by SDS-PAGE analysis, as described below. GST elution fractions were pooled and dialyzed overnight at 4°C into Phosphate Wash Buffer A for long term storage. GST-FtsE and GST-FtsB elution fractions were pooled and dialyzed overnight at 4°C into Tris Wash Buffer A to remove glutathione. GST, GST-FtsE, and GST-FtsB protein concentrations were measured using the Pierce bicinchoninic acid (BCA) protein Assay Kit (Thermo Fisher Scientific), according to manufacturer's protocol. GST and GST-FtsE were stored at -80°C.

2.4.2 Expression and Purification of His-tagged Proteins

His-tagged fusion proteins were purified following the protocol of Loughran and Walls, with the following modifications (Loughran and Walls, 2011). *E. coli* BL21 (DE3) pET30a-FtsL, *E. coli* BL21 (DE3) pET30a-FtsQ and *E. coli* C43 (DE3) pET30a-FtsX were grown at 37°C until the OD_{600} was 0.4 (Biochrom Ltd). Cells were then induced at 30°C for 3-4 hours with either 800 µM, 400 µM, or 400 µM of IPTG, respectively. *E. coli* BL21 (DE3) pET30a-FtsL, *E. coli* BL21

(DE3) pET30a-FtsQ and *E. coli* C43 (DE3) pET30a-FtsX cells were collected by centrifugation using the Sorvall Lynx 4000 superspeed centrifuge (Thermo Fisher Scientific) at 6,000×*g* for 10 minutes at 4°C. *E. coli* BL21 (DE3) pET30a-FtsL, *E. coli* BL21 (DE3) pET30a-FtsQ were resuspended in Tris Wash Buffer B (500 mM NaCl, 20 mM Tris, pH 7.4) while *E. coli* C43 (DE3) pET30a-FtsX was resuspended in Phosphate Wash Buffer B (1.5 M NaCl, 237 mM Na_2HPO_4, 12.8 mM NaH_2PO_4, pH 7.0). Samples were lysed by sonication using the Sonics VibraCell Ultrasonic Processor (Sonics & Materials Inc.) and centrifuged using the Sorvall Lynx 4000 superspeed centrifuge (Thermo Fisher Scientific) at 20,000×*g* for 20 minutes at 4°C.

For *E. coli* C43 (DE3) pET30a-FtsX, the His-FtsX fusion protein was purified from both the supernatant and pellet fraction. Meanwhile, for *E. coli* BL21 (DE3) pET30a-FtsQ or *E. coli* BL21 (DE3) pET30a-FtsL, the His-FtsQ or His-FtsL fusion proteins were purified from the pellet fraction alone. The pellet fraction containing His-FtsL or His-FtsQ fusion proteins was resuspended in Tris Wash Buffer B with the addition of 6 M urea while the pellet fraction containing His-FtsX fusion proteins was resuspended in Phosphate Wash Buffer B with the addition of 6 M urea. The samples were then incubated on ice with agitation for 1 hour to solubilize the pellet. The samples were centrifuged using a Sorvall Lynx 4000 superspeed centrifuge (Thermo Fisher Scientific) at 16,000×*g* for 30 minutes at 4°C.

His-FtsL, His-FtsQ, and His-FtsX were purified using metal affinity chromatography (His60 Ni Superflow Resin) (Takara Bio USA Inc, Mountain View, CA, USA) with a gravity column. His-FtsL and His-FtsQ proteins were eluted with Tris Elution Buffer B (6 M urea, 500 mM NaCl, 300 mM imidazole, 20 mM Tris, pH 7.4). Meanwhile, supernatant His-FtsX was eluted with Phosphate Elution Buffer B (1.5 M NaCl, 300 mM imidazole, 237 mM Na_2HPO_4, 12.8 mM NaH_2PO_4, pH 7.0) and pellet His-FtsX was eluted using Phosphate Elution Buffer B with the addition of 6 M urea. The purity of His-FtsL, His-FtsQ and His-FtsX was analyzed by SDS-PAGE analysis, as described below.

Eluted His-FtsQ, His-FtsL, and His-FtsX fusion proteins were pooled and dialyzed stepwise using several buffers (Figure 2.4.2). For the fusion protein His-FtsQ (Figure 2.4.2A), dialysis was performed at 4°C and four dialysis buffers were used to slowly remove the urea and imidazole before reaching the final buffer, Buffer Q5 (1.5 M NaCl, 20 mM Tris, pH 7.4), which was used for long term storage of His-FtsQ at -80°C. For His-FtsL (Figure 2.4.2B), dialysis was performed at

4°C and two dialysis buffers were used to remove the urea and imidazole before reaching Buffer L3 (500 mM NaCl, 20 mM Tris, pH 7.4) for long term storage at -80°C. Lastly, for His-FtsX (Figure 2.4.2C), dialysis was performed at room temperature and two dialysis buffers were used to gradually remove the urea and imidazole from the fusion protein. The last dialysis buffer for His-FtsX, Buffer X3 (1.5 M NaCl, 237 mM Na_2HPO_4, 12.8 mM NaH_2PO_4, pH 7.0), was used for long term storage of His-FtsX at -80°C. His-FtsQ and His-FtsX protein concentrations were measured using the Pierce BCA protein Assay Kit (Thermo Fisher Scientific), according to manufacturer's protocol.

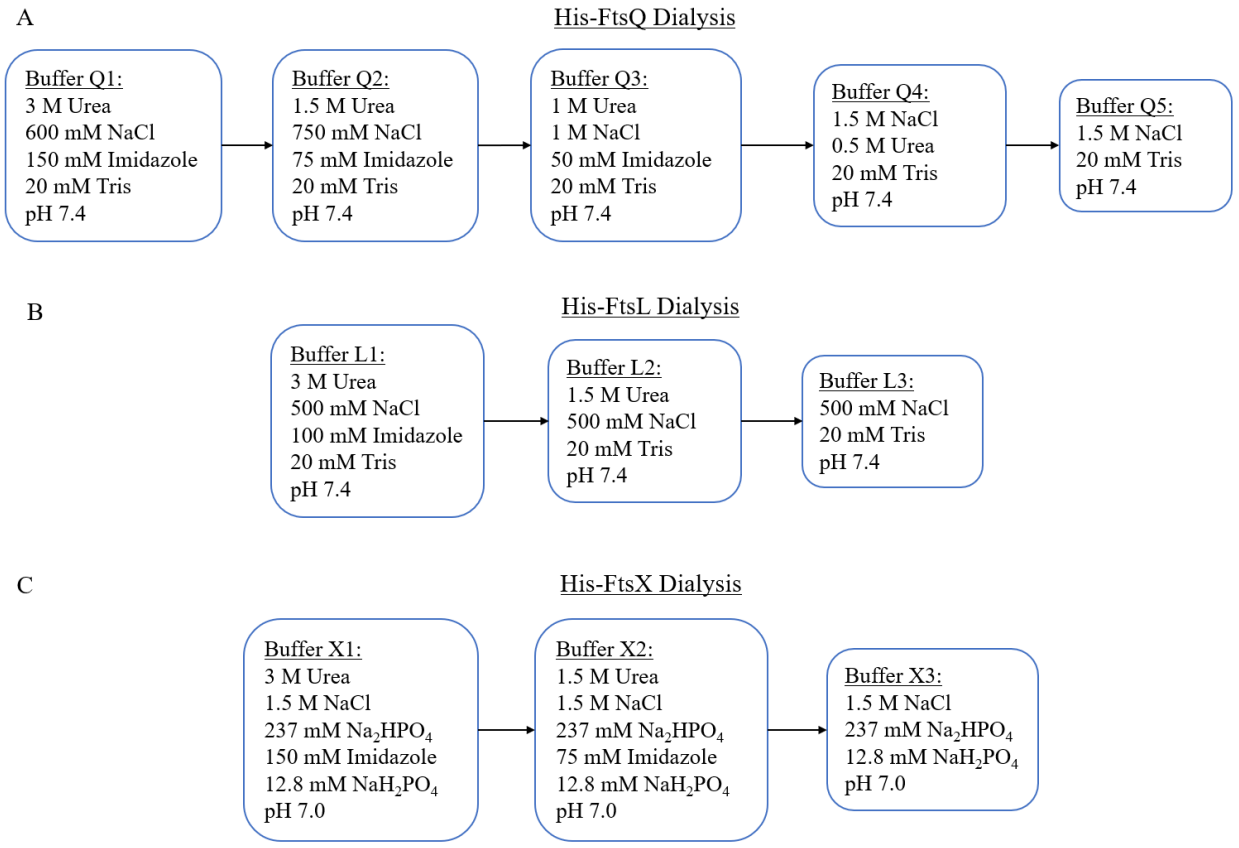

Figure 2.4.2: Dialysis Procedure for His-tagged Fusion Proteins. (A) Dialysis procedure for His-FtsQ fusion protein. (B) Dialysis procedure for His-FtsL fusion protein. (C) Dialysis procedure for His-FtsX fusion protein.

2.4.3 GST Pulldown Assays to Examine Protein-Protein Interactions

Pierce Glutathione Agarose (Thermo Fisher Scientific) was equilibrated with Pulldown Buffer A (50 mM KCl, 20 mM Tris, 0.5 mM EDTA, 1 mM dithiothreitol (DTT), pH 7.5, 10% (v/v)

glycerol, and 1% (v/v) Triton X-100) as per manufacturer's instructions. GST-FtsE (600 µg/mL) was incubated with glutathione resin for 1 hour at 4°C with end-over-end rotation before His-FtsQ (500 µg/mL) was added to the sample. GST-FtsE and His-FtsQ were incubated with glutathione resin and Pulldown Buffer A overnight at 4°C overnight with rotation. Two negative controls were used for all experiments, purified GST protein with His-FtsQ protein and His-FtsQ alone. The supernatant was collected following centrifugation using the Microfuge 18 Centrifuge (Beckman Coulter) for 5 minutes at 700×*g*. The glutathione resin was washed three times with Pulldown Buffer A to remove non-specific binding proteins. The supernatant fractions and the glutathione resin with bound proteins were boiled in 5X SDS-PAGE buffer and then separated by electrophoresis on SDS-PAGE gels for subsequent Western blot analysis, as described below.

Two additional interaction buffers were examined during GST pulldown assays to determine which buffer produced optimal conditions for the protein interaction under study. The first additional buffer tested was Pulldown Buffer B (137 mM NaCl, 8 mM Na_2PO_4, 2.7 mM KCl, 1.5 mM KH_2PO_4, 1 mM DTT, pH 7.4, 0.5% (v/v) Triton X-100) while the second additional buffer was Pulldown Buffer C (50 mM HEPES/KOH, 50 mM KCl, 1 mM ATP, pH 7.5, 0.5% (v/v) Triton X-100). Pulldown Buffer C was chosen based on a previous study which used a similar buffer to examine the ability for *E. coli* FtsE to bind to ATP (de Leeuw *et al.*, 1999). GST pulldown assays were performed in duplicate for each of the three interaction buffers examined.

2.5 Methods for Visualizing Proteins - SDS-PAGE and Western Blots

2.5.1 SDS-PAGE Analysis

SDS-PAGE gels were used to visualize purified proteins and results of GST pulldown experiments. SDS-PAGE experiments were performed following the protocol given by Sambrook and Russel, with the following modifications (Sambrook and Russell, 2001b). Samples were subject to electrophoresis at 90V for 2 hours. Gels were stained with Coomassie dye for 1 hour and de-stained with Destain Buffer (50% methanol, 10% acetic acid) for 3 hours. Gels were visualized using the Bio-Rad Molecular Imager Gel Doc XR+ (Bio-Rad). The molecular weight ladder used was a Precision Plus Protein™ Dual Xtra Pre-stained Protein Standards (Bio-Rad, Bio-Rad Laboratories, Mississauga, Ontario, Canada).

2.5.2 Western Blot Analysis

Western blots were performed for analyzing proteins in GST pulldown experiments. Primary antibodies used for Western blots included: anti-His monoclonal mouse antibody (Takara Bio) and an anti-GST polyclonal rabbit antibody (Thermo Fischer Scientific). Secondary antibodies used for Western blots included: IRDye 800CW goat anti-mouse secondary antibody and IRDye 800CW goat anti-rabbit secondary antibody (LI-COR Biosciences, Lincoln NE, USA).

Samples were boiled in 5x SDS-PAGE loading buffer and then separated by electrophoresis using SDS-PAGE gels. The SDS-PAGE gel, nitrocellulose membrane and filter paper were equilibrated in Towbin Transfer Buffer for 30 minutes. A Trans-Blot Semi Dry (Bio-Rad) machine was used to transfer the proteins from the SDS-PAGE gels to the nitrocellulose membranes, according to manufacturer's instructions. The nitrocellulose membranes were blocked for 2 hours at room temperature, while shaking, using 5% skim milk in Tris-buffered saline plus 0.05% Tween-20 (TBST) and then rinsed three times with TBST. Primary antibodies were added to the nitrocellulose membranes and incubated for 2 hours at room temperature with shaking. Membranes were washed three times with TBST and then the secondary antibodies were added to the nitrocellulose membranes and incubated for an additional 2 hours at room temperature with shaking. Primary antibodies were prepared using a 1:3,000 dilution in 5% skim milk in TBST while secondary antibodies were prepared using a 1:5,000 dilution in 2% skim milk in TBST. The nitrocellulose membranes and protein bands were visualized using an Odyssey CLX (LI-COR, Mandel Scientific, Guelph, Ontario, Canada).

2.6 Affinity Purification-Mass Spectrometry (AP-MS) for Identification of Protein Complexes in *N. gonorrhoeae*

A flow chart summarizing the steps performed during AP-MS experiments is provided in Figure 2.6. Before the AP-MS experiments between GST-FtsE and *N. gonorrhoeae* whole cell lysate could be performed, protein samples were prepared. The GST-FtsE bait was prepared following the method described in Section 2.4.1 "Expression and Purification of GST Fusion Proteins". The preparation of the *N. gonorrhoeae* whole cell lysate is described in Section 2.6.1 "Preparation of *N. gonorrhoeae* Whole Cell Lysate". Affinity purification experiments between GST-FtsE and *N. gonorrhoeae* whole cell lysate were performed in duplicate (i.e., replicate A and replicate B); samples and controls used during affinity purification are described in Section 2.6.2. The proteins captured during the affinity purification experiments were enzymatically digested

before being applied to the mass spectrometer for analysis and subsequent identification. The identified proteins were then subject to the data analysis described in Section 2.6.5 "Mass Spectrometry Data Analysis".

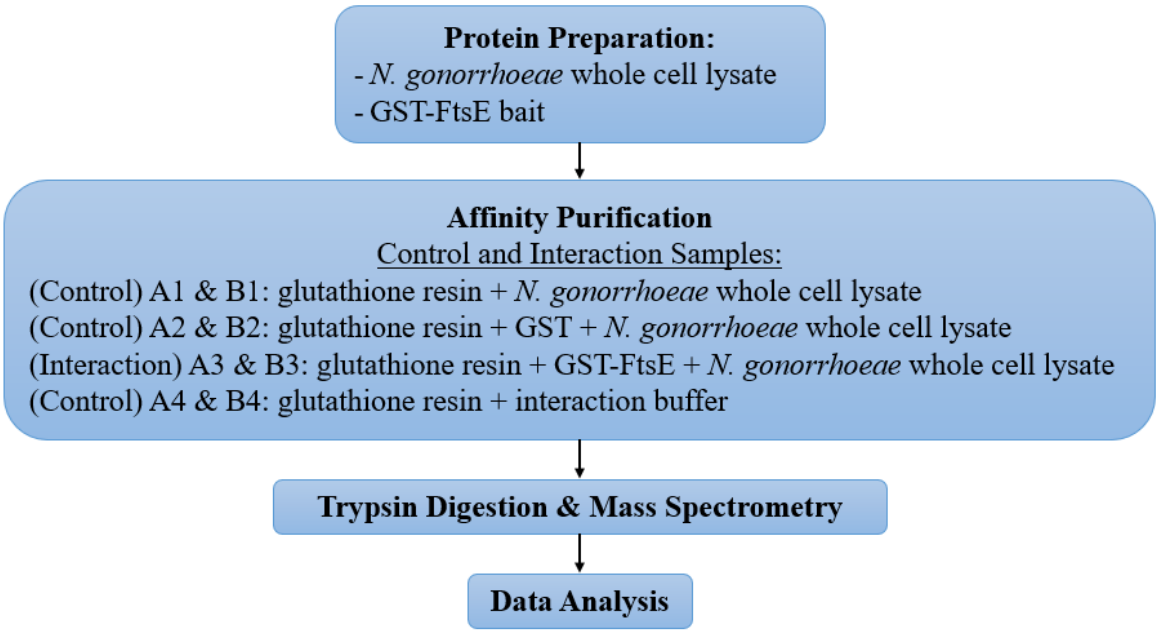

Figure 2.6: Workflow for AP-MS Experiments. The *N. gonorrhoeae* whole cell lysate and GST-FtsE bait protein are prepared prior to being subject to the affinity purification experiment. After the affinity purification experiment has been performed, the samples of interest are digested with trypsin and applied to the mass spectrometer and the resulting data is analyzed.

2.6.1 Preparation of *N. gonorrhoeae* Whole Cell Lysate

N. gonorrhoeae CH811 was collected from overnight growth on GCMBK agar plates with a sterile loop and resuspended in 150 mM NaCl, 50 mM Tris (pH 7.4) buffer. Cells were lysed by sonication using the Sonics VibraCell Ultrasonic Processor (Sonics & Materials Inc.) and centrifuged using the Sorvall Lynx 4000 superspeed centrifuge (ThermoFisher Scientific) at 20,000×*g* for 20 minutes at 4°C. The supernatant fraction of the *N. gonorrhoeae* cell lysate was stored at -80°C. *N. gonorrhoeae* whole cell lysate protein concentration was measured using the Pierce BCA protein Assay Kit (Thermo Fisher Scientific), according to manufacturer's protocol.

2.6.2 AP-MS to Study Interactions of GST-FtsE and *N. gonorrhoeae* Whole Cell Lysate

Four samples were used during AP-MS experiments (i.e., three negative control samples and one interaction sample) and AP-MS experiments were performed in duplicate (i.e., replicate A

and replicate B). The first negative control (samples A1 and B1) examined non-specific interactions occurring between *N. gonorrhoeae* whole cell lysate proteins and the glutathione resin. The second negative control (samples A2 and B2) was used to examine the presence of non-specific interactions that may occur between *N. gonorrhoeae* whole cell lysate proteins, the glutathione resin, and GST. This control allowed for the identification of proteins that were able to non-specifically interact with both GST and the glutathione resin. The third negative control, A4 and B4, consisted of the interaction buffer and the glutathione resin. Lastly, the interaction sample (A3 and B3) examined potential interactions between the bait protein GST-FtsE and proteins from *N. gonorrhoeae* whole cell lysate. The proteins identified in the three negative controls would allow for the discrimination between background/contaminant proteins from proteins that are true interacting partners with the bait GST-FtsE.

For mass spectrometry experiments, Pierce Glutathione Agarose (Thermo Fisher Scientific) was pre-equilibrated with AP-MS Interaction Buffer (500 mM NaCl, 50 mM Tris, 5 mM DTT, pH 7.9). Purified GST-FtsE (600 µg/mL) was incubated with glutathione resin overnight at 4°C with end-over-end rotation before the *N. gonorrhoeae* lysate (5,000 µg/mL) was added to the mixture. GST-FtsE and the *N. gonorrhoeae* cell lysate were incubated for 18 hours at 4°C with end-over-end rotation so the samples could mix. The supernatant containing the unbound proteins was collected by centrifugation at 700×*g* for 5 minutes (4°C) and was transferred to an Eppendorf tube for storage at -20°C. The glutathione resin and bound proteins were washed three times with AP-MS Interaction Buffer and centrifuged at 700×*g* for 5 minutes (4°C). The supernatant of each wash step was collected and transferred to an Eppendorf tube for storage at -20°C. The glutathione resin and bound proteins were also washed five times with 50 mM ammonium bicarbonate (pH 8.0) and centrifuged at 700×*g* for 5 minutes at 4°C. These samples were then transferred on ice to the Dr. Katselis Laboratory (Core MS Facility, University of Saskatchewan, 2D10 Health Science Building, 107 Wiggins Road, Saskatoon, SK, Canada) for enzymatic digestion and analysis by mass spectrometry.

2.6.3 On-Bead Proteins Tryptic Digestion

On-bead protein digestion was performed on the GST•Bind™ Resin (EMD Millipore). Protein digestion was performed as described previously by Nair *et al.*, but with the following modifications (Nair *et al.*, 2021). Briefly, the glutathione resin containing the bound protein

samples was washed three times with 25x bead volume 100 mM ammonium bicarbonate (Fisher Scientific, Fair Lawn, NJ, USA), and then the samples were resuspended in 100 mM ammonium bicarbonate. To denature the proteins which are bound to the glutathione resin, trifluoroethanol (Fisher Scientific) was added to the samples. To reduce the proteins, 1 M DTT was added to the samples and the samples were then placed in an Eppendorf Thermomixer (Eppendorf, Mississauga, ON) set at 60°C for 60 minutes with shaking at 300 rpm. While shaking, the on-bead protein samples were alkylated in the dark for 30 minutes at 37°C using 110 mM iodoacetamide (Fisher Scientific). The supernatant was collected and discarded following centrifugation of the samples at 5000×*g* for 3 minutes (Eppendorf Centrifuge 5430R, Eppendorf AG, Hamburg, Germany) and then the beads were washed twice with 25x bead volume of 100 mM ammonium bicarbonate. To the on-bead protein samples, a trypsin buffer solution (50 ng/µL trypsin in 1 mM HCl/100 mM ammonium bicarbonate) (Promega Corporation, Madison, WI, USA) was added at a 40:1 ratio (bead protein:trypsin volume solution) and then incubated at 37°C overnight with shaking at 300 rpm. The previous step was repeated, but with a 2-hour incubation performed. The supernatant was collected following centrifugation at 5000×*g* for 3 minutes and placed into a 1.5 mL low retention Eppendorf tube for storage. The beads were gently mixed with 100 mL HPLC grade water for 10 minutes at 300 rpm and, after centrifugation, the supernatant was collected and added to the previous supernatant fraction. To the peptide mixture, formic acid (10% stock solution, Fisher Scientific) was added until a 2% final concentration of formic acid was reached. The supernatant was carefully collected following centrifugation at 13,000×*g* for 5 minutes and then the samples were dried using a speed vac (Labconco, Kansas City, MO, USA) and stored at -80ºC until mass spectrometric analysis was performed.

2.6.4 Mass Spectrometry (MS) Workflow

The following mass spectrometry workflow was performed as described previously by Brandt *et al.*, but with the following modifications (Brandt *et al*., 2019). Briefly, the tryptic peptides were resuspended in mass spectrometry grade water:acetonitrile:formic acid (97:3:0.1 v/v), vortexed for 1-2 minutes and centrifuged at 18,000×*g* for 10 minutes at 4ºC. For each sample, a 15 µL aliquot was added to a mass spectrometry vial (Agilent Technologies Canada Ltd., Mississauga, ON) for analysis by liquid chromatography-tandem mass spectrometry (LC-MS/MS). An Agilent 6550 iFunnel quadrupole time-of-flight (QTOF) mass spectrometer equipped with an Agilent 1260

series liquid chromatography instrument and an Agilent Chip Cube LC-MS interface (Agilent Technologies Canada Ltd.) was used to perform all mass spectral analyses. All mass spectral analyses were performed in triplicate. The peptides were separated chromatographically with a high-capacity Agilent HPLC-Chip II: G4240-62030 Polaris-HR-Chip_3C18 that contained a 360 nL enrichment column and a 75 µm × 150 mm analytical column. Both the enrichment and analytical columns were packed with Polaris C18-A, 180Å, 3 µm stationary phase. The peptide samples were first added to the enrichment column with 0.1% formic acid in water at a flow rate of 2.0 µL/min and then transferred to the analytical column. In the analytical column, the peptide samples were separated with a linear gradient solvent system that consisted of solvent A (0.1% formic acid in water) and solvent B (0.1% formic acid in acetonitrile). The linear gradient solvent system was performed as follows: 3–25% solvent B for 105 min, 25–90% solvent B for 20 min with a flow rate of 0.3 µL/min. Using a capillary voltage set at 19000 V, an ion fragmentor set at 360 V, and the nitrogen gas (drying gas) set at 225°C with a flow rate of 12.0 L/min, the positive-ion electrospray mass spectral data was collected. Over a mass range of 250–1700 (mass/charge; m/z) at a scan rate of 8 spectra/sec, the spectra were collected. The tandem (MS/MS) data was collected using a set isolation width of 1.3 atomic mass units and over a range of 100–1700 m/z. For each MS scan, the top 20 most intense precursor ions were selected for tandem MS with active exclusion for 0.25 min.

2.6.5 Mass Spectrometry Data Analysis

The mass spectrometry data analysis was performed as described previously by Brandt *et al.*, with the following modifications (Brandt *et al.*, 2019). Using Spectrum Mill (Agilent Technologies Canada Ltd.) as the protein database search engine, the spectral data was searched against the SwissProt *Neisseria gonorrhoeae* database. For this search, the parameters were set as follows: carbamidomethyl as a fixed modification of cysteine, trypsin cleavage specificity, a fragment mass error of 50 ppm, and a parent mass error of 20 ppm. During various stages of the database search, the following were used as variable modifications: carbamylated lysine, acetyl lysine, oxidized methionine, pyroglutamic acid, deamidated asparagine and phosphorylated serine, threonine, and tyrosine. To improve protein identification during the database search, semi-trypsin non-specific C-terminus and semi-trypsin non-specific N-terminus were also used. Validation of the Spectrum Mill search was performed at both peptide and protein levels (1% false discovery

rate). Protein hits were exported into Microsoft Excel 2016 (Microsoft Corporation) for additional analysis. The additional analysis that was performed is summarized in Figure 2.6.5.

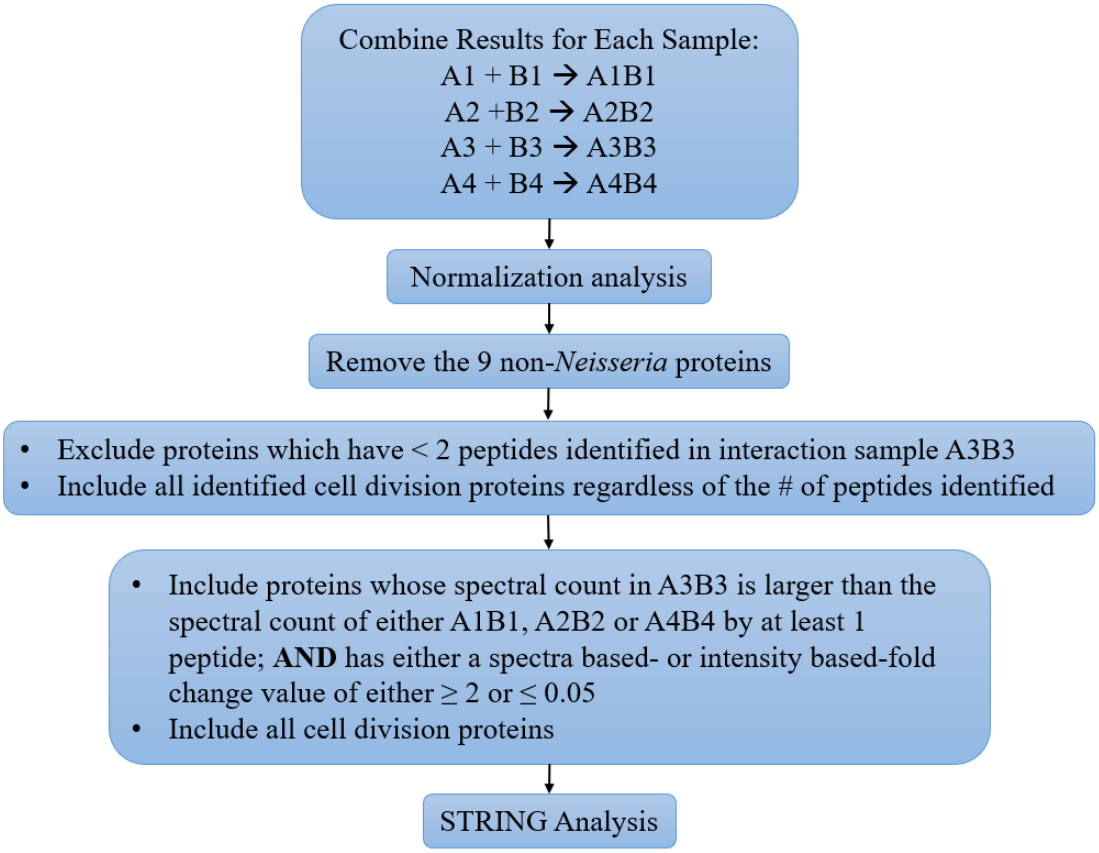

Figure 2.6.5: Additional Protein Analyses Performed on AP-MS Specimens. Data results from each replicate's sample are combined (i.e., A1 + B1 → A1B1) and a normalization analysis is performed. Proteins are subjected to an inclusion criterion and the proteins which meet the inclusion criteria are retained for analysis by STRING.

First, the proteins identified in each replicate were combined. For example, the proteins identified by AP-MS in control A1 and control B1 were combined to create control A1B1. This was repeated for the remaining controls and the interaction sample. Therefore, there are three control samples (A1B1, A2B2, and A4B4) and one interaction sample (A3B3).

Second, all proteins identified during AP-MS experiments were subjected to a normalization analysis wherein the spectral count-based and intensity-based fold change value was determined. This normalization analysis is fully described in Section 2.6.5.1. "Normalization Analysis". Third, proteins were excluded from further analysis if they did not meet the following inclusion criteria. First, only *Neisseria* species proteins were retained for further analysis. There

were nine non-*Neisseria* proteins identified that likely have high similarity to the corresponding *N. gonorrhoeae* proteins, but they were removed from further analysis.

Next, proteins with < 2 peptides in the interaction sample A3B3 were removed. However, all cell division proteins were retained for analysis, regardless of the number of peptides identified. For the remaining proteins, only proteins with a spectral count in the interaction sample (i.e., A3B3) that was larger than the spectral count of either of the negative controls (i.e., A1B1, A2B2, A4B4) by at least one peptide, AND had either a spectral count based- or intensity based-fold change value of either ≥ 2 or ≤ 0.05 were retained. Therefore, proteins with either a spectral based- or intensity based-fold change value of > 0.05 to < 2.0 were removed. The remaining proteins were analyzed by Search Tool for the Retrieval of Interacting Genes/Proteins (STRING) analysis to predict potential interactions.

2.6.5.1 Normalization Analysis

Two different fold change values were calculated; one using the spectral count data, and one using the intensity data. These fold change values were calculated in Microsoft Excel using the following formulas. First, the Spectral Abundance Factor (SAF), when based on spectral count data, was calculated by dividing the spectral count (SpC) by the protein's molecular weight (MW) in Daltons. However, when the SAF value was calculated based on intensity data, the intensity (I) was divided by the protein's molecular weight (MW) in Daltons.

$$\text{Based on Spectral Count:} \qquad SAF_{SpC} = \frac{SpC}{MW}$$

$$\text{Based on Intensity:} \qquad SAF_{I} = \frac{Intensity}{MW}$$

Next, the Normalized Spectral Abundance Factor (NSAF) was calculated by dividing the SAF values (based on spectral counts or intensity) for the protein of interest by sum of the SAF values (based on spectral counts or intensity) for all proteins in that sample. Where N equals the total number of proteins.

$$NSAF = \frac{SAF\ (\text{spectral count or intensity})}{\sum SAF_N\ (\text{spectral count or intensity})}$$

Then the Fold Change (FC), based on either spectral counts or intensity, was calculated by dividing the NSAF value for the interaction sample (i.e., A3B3) by the average NSAF value for all control samples (i.e., A1B1, A2B2 and A4B4).

$$\text{Fold Change} = \frac{\text{NSAF}_{\text{A3B3}}}{\text{NSAF}_{\text{AVG(A1B1, A2B2, A4B4)}}}$$

2.6.5.2 Identification of Homologous Cell Division Proteins through BLASTp

Several cell division proteins discovered during AP-MS experiments were identified solely as either 'cell division proteins' or 'putative cell division proteins'. The identity of these proteins and their potential homologs was further explored through a BLASTp search (https://blast.ncbi.nlm.nih.gov/Blast.cgi?PAGE=Proteins). First, the FASTA sequences for the cell division proteins of interest were extracted from Uniprot (https://www.uniprot.org/). These sequences were applied to BLASTp search with the database set to non-redundant (nr) protein sequences and the organism restricted to *N. gonorrhoeae*. The homologous proteins provided by the BLASTp search results were then used to identify the cell division proteins of interest.

2.6.5.3 STRING Analysis

Protein hits identified by mass spectrometry were analyzed by STRING software to create a network map for the protein-protein interactions (https://string-db.org/). The total list of proteins analyzed by STRING analysis is included in Appendix B (Table B.1). The Uniprot accession numbers for the proteins of interest to be analyzed by STRING were entered into the "Multiple Proteins" search engine and the organism was set to *N. gonorrhoeae* FA1090 strain. The minimum required interaction score was set to 0.400 (medium confidence) and the active interaction sources included all available options (i.e., neighborhood, experiments, gene fusion, databases, co-occurrence, and co-expression) but the text-mining source was excluded. The implication of the network edges was set to "confidence", so the line thickness would indicate the strength of the supporting data and, therefore, thicker lines indicate a strong amount of supporting data.

3.0 RESULTS

3.1 Bacterial-Two-Hybrid (B2H) Assays

3.1.1 Protein-Protein Interactions between FtsE, FtsX, FtsL, FtsB and other *N. gonorrhoeae* Divisome Proteins

There were 38 B2H assays performed to study protein-protein interactions between *N. gonorrhoeae* FtsE, FtsX, FtsL and FtsB and the other gonococcal cell division proteins (i.e., FtsZ, FtsA, ZipA, FtsK, FtsQ, FtsW, FtsI and FtsN). In accordance with B2H criteria, any interaction that reported an average β-galactosidase activity value of < 50% was considered to indicate that an interaction occurs between the proteins of interest. Meanwhile, any value of ≥ 50% was considered to indicate that no interaction occurs between the proteins of interest (Di Lallo *et al.*, 2003). The average β-galactosidase activity and standard deviation for each of these 38 protein-protein interactions studied are reported in Table 3.1.1. Of the 38 protein-protein interactions studied there were nine protein-protein interactions which reported an average β-galactosidase activity of < 50% and, therefore, indicate the presence of a protein-protein interaction (bold).

Table 3.1.1: Interactions of *N. gonorrhoeae* Cell Division Proteins with FtsE, FtsX, FtsL and FtsB

Average β-galactosidase Activity ± Standard Deviation (%)*											
	FtsX	**FtsL**	**FtsB**	**FtsZ**	**FtsA**	**ZipA**	**FtsK**	**FtsQ**	**FtsW**	**FtsI**	**FtsN**
FtsE	**45.2 ±2.1**	51.1 ±3.3	74.3 ±2.0	68.0 ±4.1	75.1 ±7.5	50.2 ±3.8	70.3 ±3.5	**42.7 ±4.0**	66.2 ±6.6	72.5 ±3.4	54.3 ±2.3
FtsX		**42.3 ±2.5**	58.3 ±2.4	55.3 ±2.7	55.3 ±2.7	**46.9 ±2.2**	**49.6 ±3.5**	60.9 ±4.5	**49.5 ±2.5**	68.0 ±4.9	**49.0 ±3.0**
FtsL			87.6 ±4.3	71.8 ±3.1	75.0 ±5.0	**48.9 ±2.9**	57.5 ±3.7	54.4 ±2.7	64.8 ±4.8	54.9 ±2.3	56.2 ±3.3
FtsB				**33.6 ±2.9**	68.5 ±3.5	89.6 ±4.0	64.8 ±9.1	79.8 ±4.3	85.2 ±9.1	52.2 ±6.2	75.3 ±5.6

*The values represent the average β-galactosidase activity ± standard deviation.
All B2H assays were performed with two biological replicates and three technical replicates per biological replicate.
Values with ≤ 50% β-galactosidase activity (**bold**) in comparison to control *E. coli* R721 represent protein-protein interactions between the proteins of interest.
Strong protein-protein interactions (i.e., values < 45% β-galactosidase activity) are shown in green. Probable protein-protein interactions (i.e., values with 45 to 50% β-galactosidase activity) are shown in dark blue. Values indicating the probable absence of a protein-protein interaction (i.e., 50 to 55% β-galactosidase activity) are shown in light blue while values indicating the strong absence of a protein-protein interaction (i.e., values > 55% β-galactosidase activity) are shown in white.

The interactions shown in Table 3.1.1 can be divided into four categories based on the reported average β-galactosidase activity. The first category, the 'strong protein-protein interactions', are B2H assays which reported < 45% β-galactosidase activity and suggest a protein-protein interaction has occurred. The 'strong protein-protein interactions' are highlighted in green (Table 3.1.1) and include: FtsB-FtsZ (33.6%), FtsX-FtsL (42.3%) and FtsE-FtsQ (42.7%). The second category, the 'probable protein-protein interactions', are B2H assays which reported 45 to 50% β-galactosidase activity. These interactions are highlighted in dark blue (Table 3.1.1) and include: FtsE-FtsX (45.2%), FtsX-ZipA (46.9%), FtsL-ZipA (48.9%), FtsX-FtsN (49.0%), FtsX-FtsW (49.5%), FtsX-FtsK (49.6%). The third category, the 'probable absence of a protein-protein interaction', include B2H assays which reported 50 to 55% β-galactosidase activity and, therefore, suggest that there may not be an interaction between the proteins of interest. The B2H assays in this group include: FtsE-ZipA (50.2%), FtsE-FtsL (51.1%), FtsB-FtsI (52.2%), FtsE-FtsN (54.3%), FtsL-FtsQ (54.4%), and FtsL-FtsI (54.9%). The assays identified in the second or third categories are considered 'probable' because the reported β-galactosidase activities are near the 50% cutoff value. The remaining interactions in Table 3.1.1 (white) are part of the 'absence of protein-protein interactions' category because the B2H assays report average β-galactosidase values of > 55%, which suggests no interaction can be detected amongst examined proteins. All interactions identified through B2H assays must be further examined with additional biochemical assays to be certain of the presence or absence of interactions. Future studies would especially focus on B2H assays which reported values around the 50% cutoff and were classified as either a probable interaction or probable absence of an interaction.

The values reported in Table 3.1.1 represent the average β-galactosidase activity for each protein-protein interaction under study. This value is the average of the 'forward' (i.e., pcI_{p22}-X + pcI_{434}-B) and the 'reverse' (i.e., pcI_{p22}-B + pcI_{434}-X) reactions. The β-galactosidase activity for both forward and reverse reactions is used to calculate the average β-galactosidase activity for the protein-protein interaction of study. For each interaction in either Table 3.1.1 or Table 3.1.3, a bar graph was produced that summarizes the average β-galactosidase data for the interaction. Figure 3.1.2 shows two bar graphs, one demonstrating the lack of an interaction between the proteins FtsX and FtsB (Figure 3.1.2A) and one demonstrating an interaction between the proteins FtsB and FtsZ (Figure 3.1.2B). The β-galactosidase activity (in Miller Units) and % β-galactosidase activity for all samples is shown. The 'forward' (i.e., $pcIp_{22}$-FtsB + pcI_{434}-FtsX) and 'reverse' (i.e., $pcIp_{22}$-FtsX

+ pcI$_{434}$-FtsB) interaction results and the results for the control samples are provided. For the interaction samples, the bar is colored green if the β-galactosidase activity is < 50% or red if the β-galactosidase activity is > 50%. Graphical analyzes for the additional interactions listed in Tables 3.1.1 and 3.1.3 are provided in Appendix A (Figure A.1).

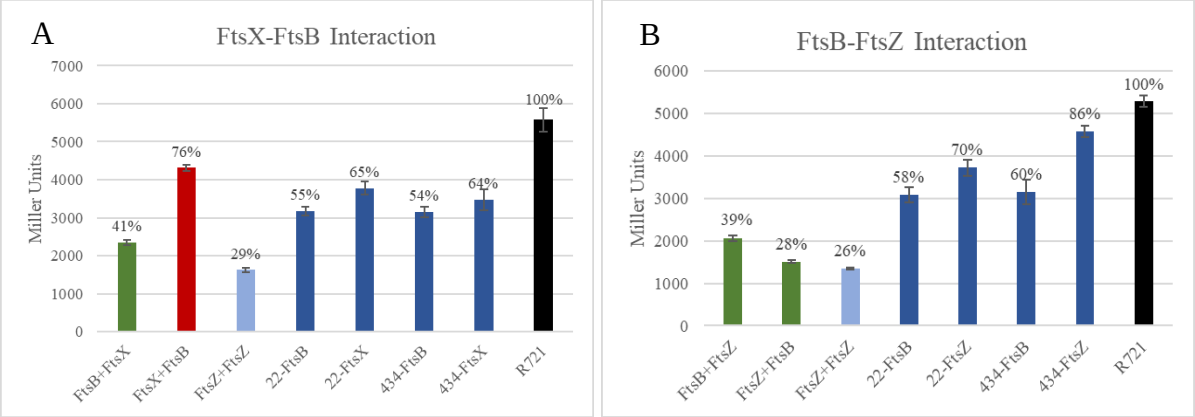

Figure 3.1.2: Bar Graph for the Two Potential Interactions Examined by B2H. The potential interaction between FtsX-FtsB (A) and the potential interaction between FtsB-FtsZ (B). The *N. gonorrhoeae* FtsZ-FtsZ self-interaction was used as a positive control (light blue). The negative controls were *E. coli* R721 with single plasmid transformants (dark blue) while the baseline control was *E. coli* R721 lacking any plasmid (black). For the interaction samples, values of <50% β-galactosidase in comparison to the baseline *E. coli* R721 indicate interactions between those proteins (green) while values of >50% indicate the absence of an interaction between those proteins (red).

3.1.2 B2H Assays Studying Self-Interactions Amongst *N. gonorrhoeae* Divisome Proteins

In addition to the 38 B2H assays that were performed to study interactions amongst *N. gonorrhoeae* divisome proteins, B2H assays were also used to study the ability of 11 divisome proteins (i.e., FtsA, ZipA, FtsE, FtsX, FtsK, FtsQ, FtsL, FtsB FtsW, FtsI and FtsN) to self-interact. The self-interactions for these *N. gonorrhoeae* cell division proteins had not been previously investigated. A total of 11 B2H assays were performed to study the self-interaction ability of the above proteins and the results are summarized in Table 3.1.3. In accordance with B2H criterium, any B2H assay that reports an average β-galactosidase activity value of < 50% suggests that a protein-protein interaction occurs between the proteins of interest. There are four proteins that report an average β-galactosidase activity of < 50%, suggesting that these proteins can self-interact. The four proteins that can self-interact are FtsE, FtsB, FtsW and FtsN. The protein with the strongest self-interaction ability according to B2H results was the FtsB-self interaction with an

average β-galactosidase activity of 29.9%. The remaining strong self-interactions, in order of strongest to weakest interaction, is the FtsW self-interaction (30.9%), the FtsE self-interaction (38.5%), and the FtsN self-interaction (42.7%). The remaining seven self-interactions that were studied report an average β-galactosidase activity of > 50%, indicating there no self-interaction could be detected.

Table 3.1.3: B2H Assays Examining the Self-Interactions of *N. gonorrhoeae* Cell Division Proteins

Average β-galactosidase Activity ± Standard Deviation (%)*											
	FtsA	**ZipA**	**FtsE**	**FtsX**	**FtsK**	**FtsQ**	**FtsL**	**FtsB**	**FtsW**	**FtsI**	**FtsN**
Self-Interactions	51.8 ±3.1	58.3 ±2.0	**38.5 ±2.5**	70.7 ±3.3	82.6 ±2.9	82.4 ±2.5	89.5 ±2.2	**29.9 ±2.9**	**30.9 ±2.0**	58.6 ±2.9	**42.7 ±1.0**

*The values represent the average β-galactosidase activity ± standard deviation.
All B2H assays were performed with two biological replicates and three technical replicates per biological replicate.
Values with ≤ 50% β-galactosidase activity (**bold**) in comparison to control *E. coli* R721 represent protein-protein interactions between the proteins of interest.
Strong protein-protein interactions (i.e., values < 45% β-galactosidase activity) are shown in green. Probable protein-protein interactions (i.e., values with 45 to 50% β-galactosidase activity) are shown in dark blue. Values indicating the probable absence of a protein-protein interaction (i.e., 50 to 55% β-galactosidase activity) are shown in light blue while values indicating the strong absence of a protein-protein interaction (i.e., values > 55% β-galactosidase activity) are shown in white.

The interactions in Table 3.1.3 can also be separated into four groups based on their average β-galactosidase activity, as described above. The FtsE, FtsB, FtsW and FtsN self-interactions are considered 'strong protein-protein interactions' as they report < 45% β-galactosidase activity. The FtsA self-interaction is part of the 'probable absence of a protein-protein interaction' category because it reports a β-galactosidase activity within the 50 to 55% β-galactosidase activity range. The remainder of the self-interactions listed in Table 3.1.3 are part of the 'strong absence of protein-protein interactions' because they report > 55% β-galactosidase activity.

3.2 GST Pulldown Assays

3.2.1 Purification of Fusion Proteins for GST Pulldown Assay

The B2H assays performed in this report identified several potential interactions between the *N. gonorrhoeae* cell division proteins, including: FtsE-FtsQ, FtsE-FtsX, and FtsB-FtsZ. The potential protein-protein interactions of FtsE-FtsQ, FtsE-FtsX and FtsB-FtsZ were chosen to be

further studied through GST pulldown assays. In addition, even though an FtsB-FtsL interaction was not identified during B2H assays, this interaction was chosen to be further examined because the FtsL-FtsB interaction is observed during formation of the *E. coli* FtsQLB complex (Buddelmeijer and Beckwith, 2004).

During GST pulldowns, the bait protein is tagged with GST while the potential interacting partner (i.e., prey protein) is tagged with 6xHis. To study the FtsE-FtsQ interaction, the GST-FtsE and His-FtsQ fusion proteins were created as described in the methodology. To study the second interaction of interest (i.e., the FtsE-FtsX interaction), the His-FtsX fusion protein was created as described in the methodology. For the third interaction under study (i.e., the FtsB-FtsZ interaction), the fusion protein GST-FtsB was created as described in the methodology while previously purified His-FtsZ would be utilized (Zou *et al.*, 2017a). Lastly, to study the FtsB-FtsL interaction, the His-FtsL fusion protein was created as described in the methodology. In addition, the negative control GST protein (*E. coli* C41 pGEX2T) was also purified for these experiments.

3.2.1.1 Purification of GST-tagged Bait Proteins and Negative Control GST

The bait protein GST-FtsE was overexpressed and purified from *E. coli* BL21 (DE3) pGEX2T-FtsE through affinity chromatography (Figure 3.2.1.1). In Figure 3.2.1.1, GST-FtsE was observed at approximately 50 kDa and was found in both the flowthrough (F) and elution (E1-E5) fractions. GST-FtsE has a molecular weight of 50 kDa because it is the combined size of *N. gonorrhoeae* FtsE (~24 kDa) and the GST tag (~26 kDa). There was a portion of GST-FtsE identified in the flowthrough but the majority of GST-FtsE was observed in the elution fractions, suggesting that this protein could bind to the glutathione resin during purification. This protein was collected and stored at -80°C until it was used for GST pulldown and mass spectrometry assays.

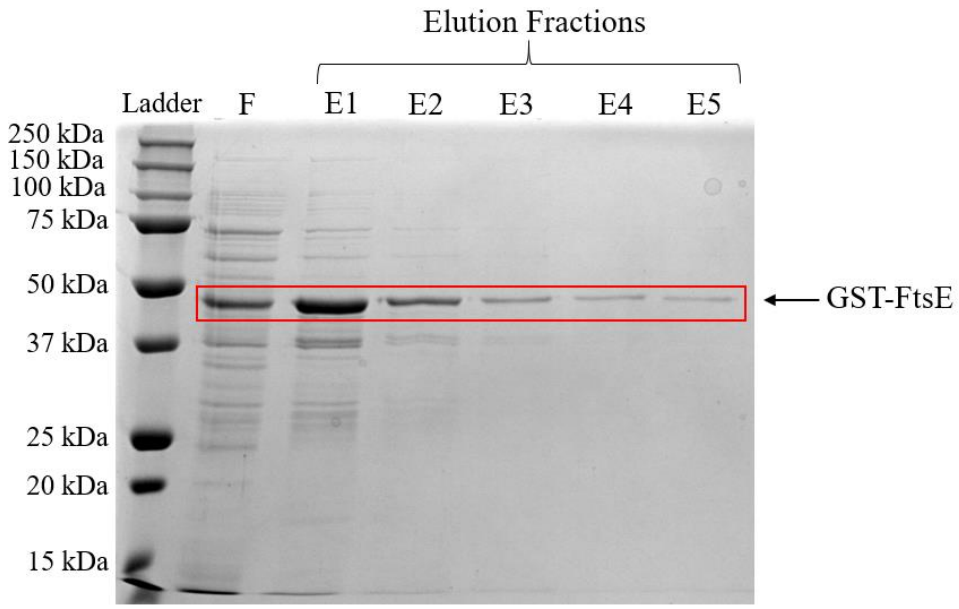

Figure 3.2.1.1: Coomassie Stained SDS-PAGE Gel Displaying the Purification of GST-FtsE. GST-FtsE was purified from *E. coli* BL21 (DE3) pGEX2T-FtsE through affinity chromatography using glutathione resin. The flowthrough (F) fraction and elution fractions (E1-E5) for the purification of GST-FtsE are shown. GST-FtsE (~50 kDa) is found in all fractions and has been indicated in red.

In addition, the bait protein GST-FtsB was overexpressed and purified from *E. coli* BL21 (DE3) pGEX2T-FtsB through affinity chromatography (Figure 3.2.1.2). GST-FtsB is a 36 kDa fusion protein that consists of the 10 kDa *N. gonorrhoeae* FtsB and the 26 kDa GST tag. GST-FtsB was successfully purified and was observed in the flowthrough (F), wash (W) and elution (E1-E5) fractions. However, most of GST-FtsB is observed in the flowthrough (F) fraction and, in comparison, the amount of GST-FtsB observed in either the wash (W) or elution (E1-E5) fractions was minimal. Since most of GST-FtsB is observed in the flowthrough fraction, this suggests the majority of the bait protein did not bind efficiently to the glutathione resin during protein purification. The elution fractions (E1-E5) indicate that only a minimal amount of GST-FtsB could bind to the glutathione resin.

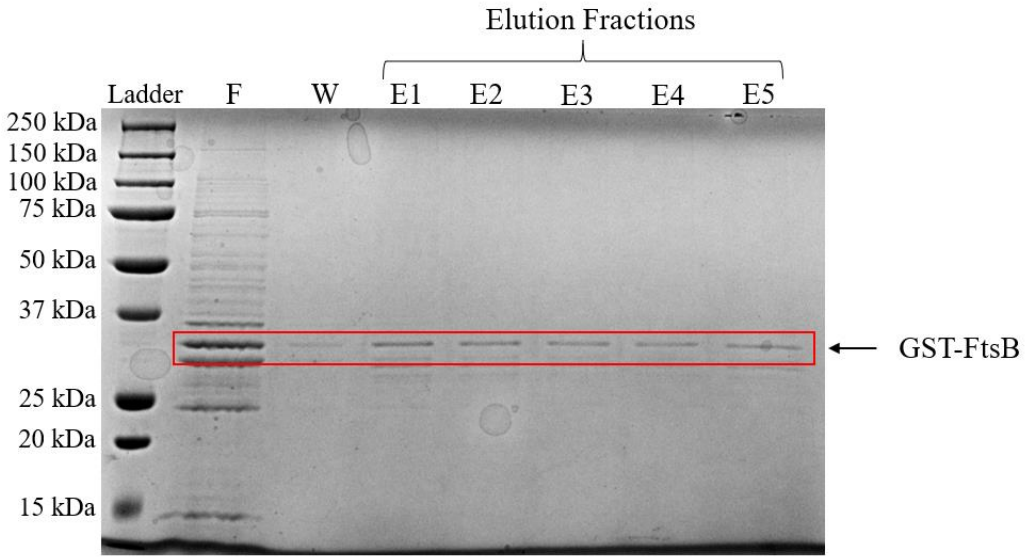

Figure 3.2.1.2: Coomassie Stained SDS-PAGE Gel Displaying the Purification of GST-FtsB. GST-FtsB was purified from *E. coli* BL21 (DE3) pGEX2T-FtsB through affinity chromatography using glutathione resin. The flowthrough (F) fraction and elution fractions (E1-E5) for the purification of GST-FtsB are shown. GST-FtsB (~36 kDa) is indicated in the elution fractions with a red box.

Several attempts were made to optimize the overexpression and purification of GST-FtsB. These attempts included extending the induction time in the presence of IPTG, different induction temperatures (i.e., 16°C and 37°C), and increasing the binding time between GST-FtsB and the glutathione resin to allow for better binding to the resin. However, none of these attempts were successful at significantly increasing the yield of GST-FtsB. Due to a limited quantity of protein, GST pulldown experiments to examine interactions of GST-FtsB with FtsZ or FtsL were unable to be completed.

The negative control protein GST was overexpressed and purified from *E. coli* C41 pGEX2T through affinity chromatography. In Figure 3.2.1.3, GST was observed at 26 kDa, which is the expected molecular weight of the protein. GST was observed in the flowthrough (F), wash (W) and elution (E1-E5) fractions. The vast majority of GST was observed in elution fractions 1 and 2, suggesting GST was able to strongly bind to the glutathione affinity column during the purification. This protein was collected and stored at -80°C until it could be used for GST pulldown assays and mass spectrometry experiments.

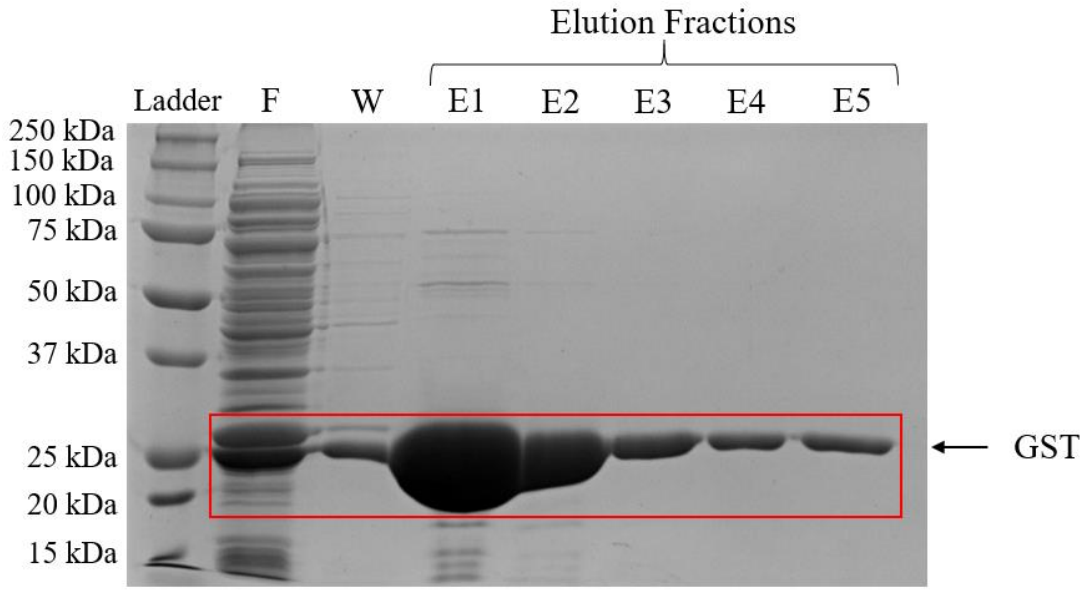

Figure 3.2.1.3: Coomassie Stained SDS-PAGE Gel Displaying the Purification of negative control protein GST. GST was purified from *E. coli* C41 pGEX2T through affinity chromatography using glutathione resin. The flowthrough (F), wash (W) and elution fractions (E1-E5) for the purification of GST are shown. GST (~26kda) was found in all elution fractions and is indicated in red.

3.2.1.2 Purification of His-tagged Prey Proteins

The His-tagged prey protein His-FtsQ was overexpressed and purified from *E. coli* BL21 (DE3) pET30a-FtsQ through affinity chromatography (Figure 3.2.1.4). In Figure 3.2.1.4, His-FtsQ was observed at the expected molecular weight of 29 kDa in the flowthrough (F), wash (W) and elution (E1-E5) fractions. However, the majority of His-FtsQ was found in the flowthrough and elution fractions. The presence of His-FtsQ in both the flowthrough and in the elution fraction suggests there may have been inefficient binding of His-FtsQ to the affinity column. However, because His-FtsQ was observed in the elution fractions as well, this suggests that some portion of His-FtsQ was able to bind to the nickel metal affinity column during purification. This protein was collected and stored at -80°C until it could be used in GST pulldown experiments.

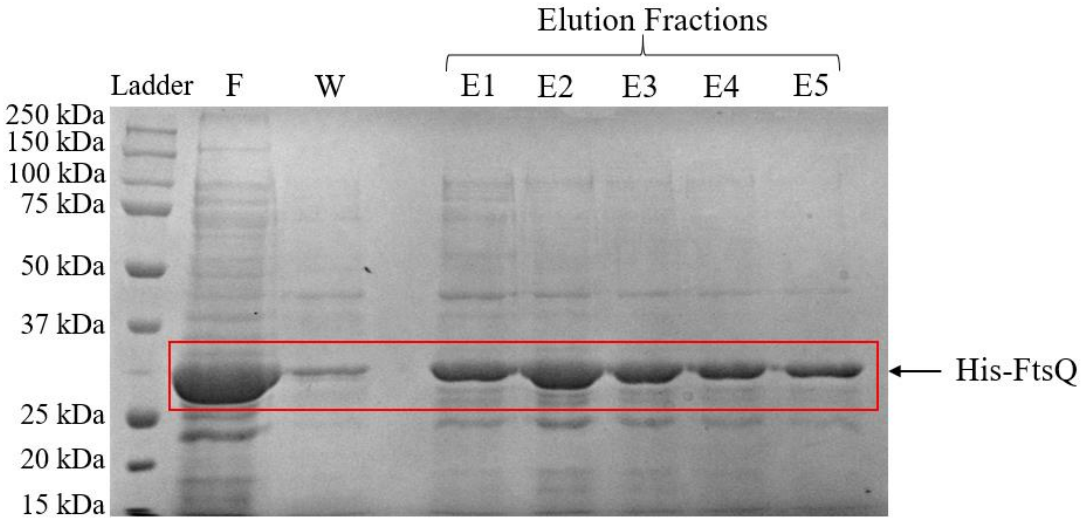

Figure 3.2.1.4: Coomassie Stained SDS-PAGE Gel Displaying the Purification of His-FtsQ. His-FtsQ was purified from *E. coli* BL21 (DE3) pET30a-FtsQ through metal affinity chromatography using nickel resin. The flowthrough (F), wash (F) and elution fractions (E1-E5) for the purification of His-FtsQ are shown. His-FtsQ (~29 kDa) is found in the flowthrough and all elution fractions. His-FtsQ is indicated in the elution fractions in red.

In addition, the His-tagged prey protein His-FtsL was overexpressed and purified from *E. coli* BL21 (DE3) pET30a-FtsL through affinity chromatography (Figure 3.2.1.5). His-FtsL is a fusion protein with a predicted molecular weight of approximately 10 kDa. His-FtsL was observed in the flowthrough (F) fraction and elution fractions (E1-E5) but was not seen in the wash (W) fractions. However, the observed molecular weight was closer to 14 kDa, almost 50% larger than expected (Figure 3.2.1.5). The *E. coli* homolog FtsL has been not been observed to form dimers and, if this size discrepancy was due to dimer formation, then the observed molecular weight of *N. gonorrhoeae* His-FtsL would be closer to 20 kDa (Karimova *et al.*, 2005).

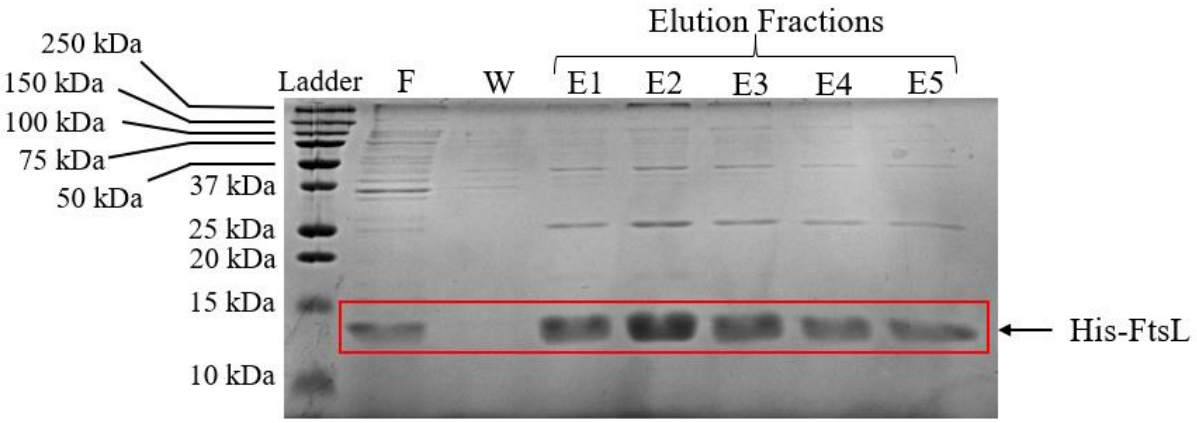

Figure 3.2.1.5: Coomassie Stained SDS-PAGE Gel Displaying the Purification of His-FtsL. His-FtsL was purified from *E. coli* BL21 (DE3) pET30a-FtsL through metal affinity chromatography using nickel resin. The flowthrough (F) fraction and elution fractions (E1-E5) for the purification of His-FtsL are shown. His-FtsL (~13 kDa) is indicated in the elution fractions with a red box.

In addition, when His-FtsL was subject to dialysis to remove the urea and imidazole necessary for purification experiments, the fusion protein would consistently precipitate. Attempts were made to optimize dialysis of His-FtsL, including dialysis at various temperatures (i.e., 4°C vs. room temperature). An additional dialysis buffer was also attempted in an effort to decrease the concentration of urea and imidazole more gradually to prevent precipitation. However, none of these attempts were successful at preventing the precipitation of His-FtsL. Due to the unexpected size of His-FtsL and the failure to prevent precipitation during dialysis, further experiments with this protein were unable to be completed.

Lastly, the His-tagged fusion protein His-FtsX was overexpressed and purified. Initially, pET30a-FtsX was transformed into *E. coli* BL21 for overexpression. However, His-FtsX was toxic to *E. coli* BL21 upon induction with IPTG. Therefore, pET30a-FtsX was transformed into *E. coli* C43 because this strain is used for proteins that are found to be toxic in *E. coli* BL21 (Miroux and Walker, 1996).

His-FtsX has a predicted molecular weight of 36 kDa. However, after purification, the most abundant band observed has a molecular weight of approximately 46 kDa (Figure 3.2.1.6A). This unexpected band is highly concentrated when compared to contamination bands, suggesting it is

binding to the metal affinity resin. The potential His-FtsX protein purified in Figure 3.2.1.6A was then analyzed by Western blot with anti-His primary antibodies (Figure 3.2.1.6B) to verify that the observed 46 kDa band was the His-tagged FtsX fusion protein. However, the 46 kDa band was not visualized upon Western blot analysis (Figure 3.2.1.6B), suggesting that the 46 kDa band that was purified was not His-FtsX.

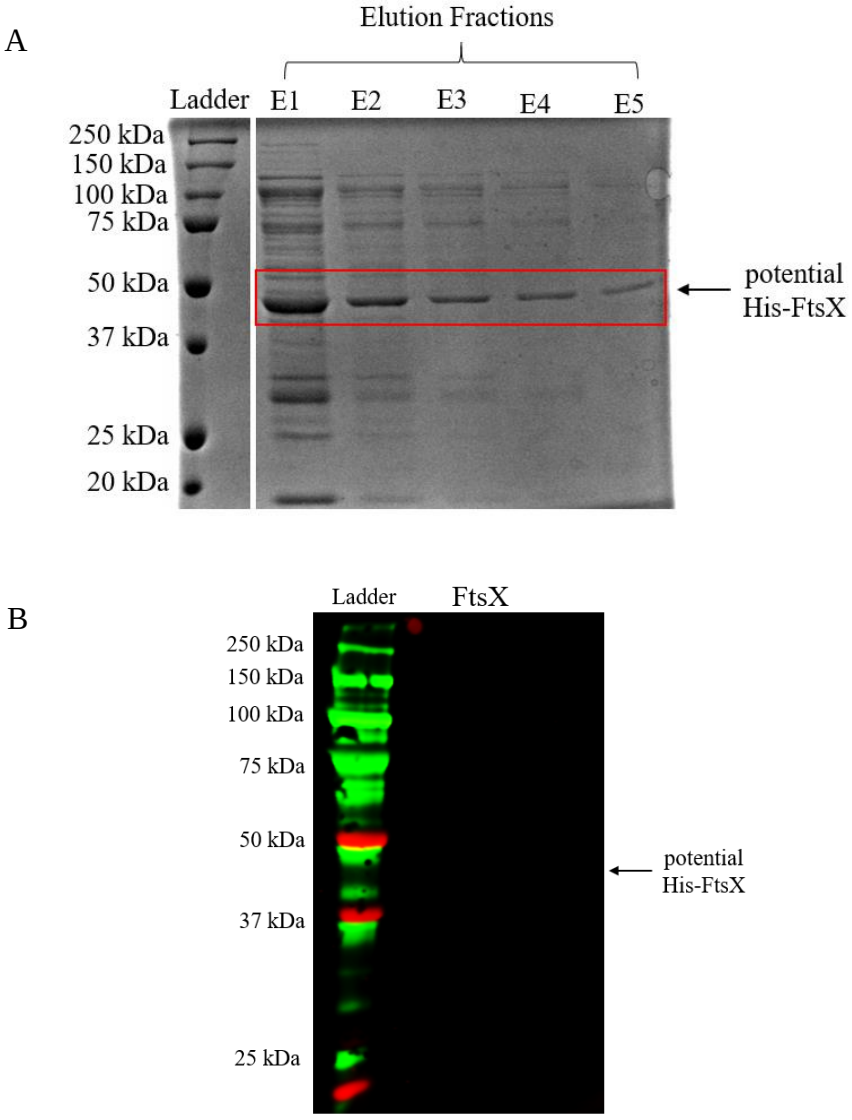

Figure 3.2.1.6: Purification and Attempted Identification of Potential His-FtsX Fusion Protein. A) Coomassie stained SDS-PAGE gel of His-FtsX purification through metal affinity chromatography using nickel resin. The elution fractions (E1-E5) for the purification of His-FtsX are shown and the 46 kDa band of interest is indicated in red. B) Western blot of His-FtsX using anti-His primary antibodies. The expected location of the potential His-FtsX protein is indicated by the arrow.

Therefore, the purification of His-FtsX from *E. coli* C43 pET30a-FtsX was repeated, and both the supernatant and inclusion body fractions were subjected to metal affinity purification to purify the His-FtsX fusion protein (Figure 3.2.1.7). Once again, for both the inclusion body and supernatant fraction purifications, the most abundant band observed in the elution fractions was a 46 kDa band, instead of a 36 kDa band that corresponds to the predicted molecular weight of His-FtsX. The 46 kDa band in Figure 3.2.1.7 was the same band that was seen in Figure 3.2.1.6A, suggesting the same protein had been purified for a second time.

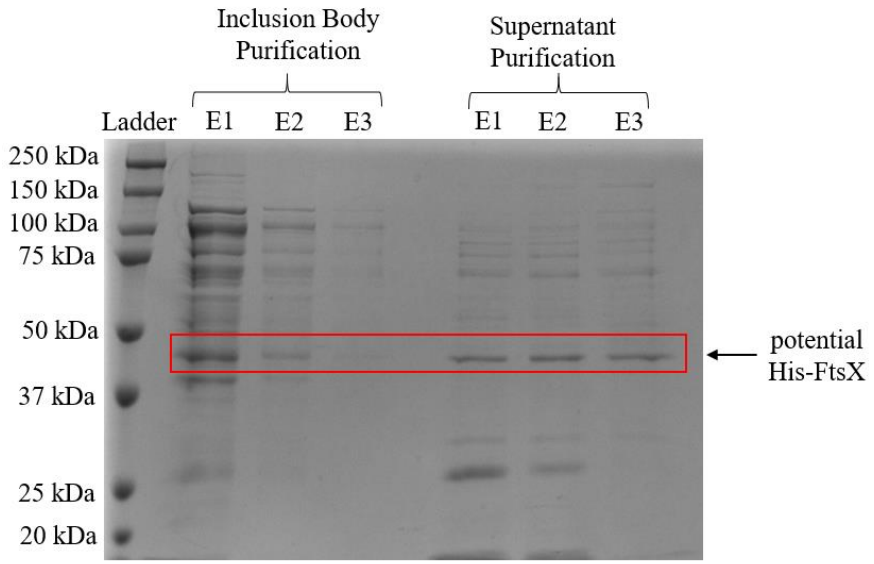

Figure 3.2.1.7: Purification of His-FtsX Fusion Protein from Supernatant and Inclusion Body Fractions. Coomassie stained SDS-PAGE gel of His-FtsX purification from the inclusion body and supernatant fractions of *E. coli* C43 pET30a-FtsX using metal affinity chromatography using nickel resin. From L to R the samples include: the elution fractions (E1-E3) for the inclusion body purification and the elution fractions (E1-E3) for the supernatant fraction purification. The potential His-FtsX fusion protein is indicated with a red box.

A Western blot using anti-His primary antibodies was performed to verify whether the 46 kDa band observed in Figure 3.2.1.7 was the His-tagged FtsX fusion protein (Figure 3.2.1.8). However, the 46 kDa band was not observed on the anti-His primary antibody Western blot. Instead, a band of approximately 36 kDa was observed in the "Inclusion Body Purification - Elution Fraction #1" sample (Figure 3.2.1.8). The 36 kDa band observed on the anti-His Western blot was most likely the His-FtsX fusion protein because it corresponds to the predicted size of His-FtsX and is the only band that can be observed when subject to an anti-His Western blot. However, the

36 kDa His-FtsX seen in Figure 3.2.1.8 was not observed in the corresponding Coomassie gel (Figure 3.2.1.7). This indicates that His-FtsX was either unable to be expressed at high concentrations or was unable to be highly purified. Due to the failure to purify His-FtsX, further experiments with this protein were unable to be completed.

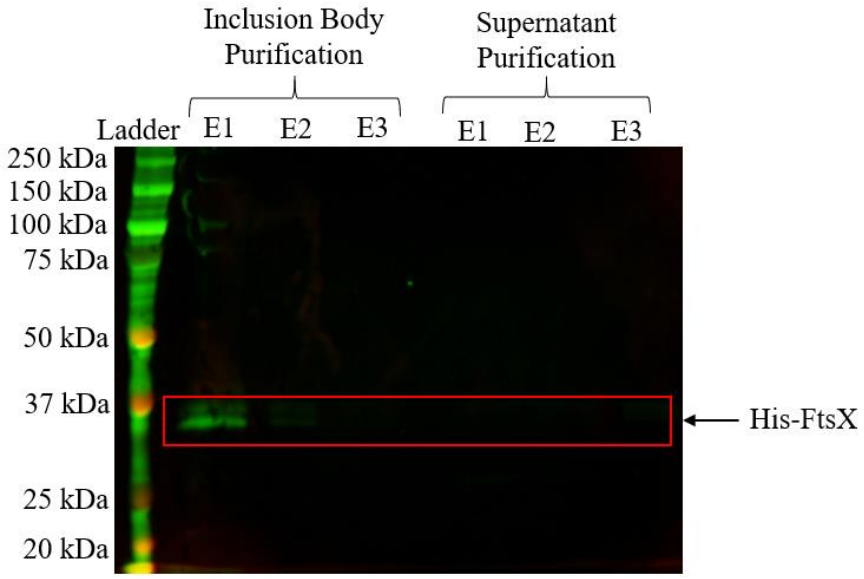

Figure 3.2.1.8: Identification of His-FtsX Fusion Protein. Anti-His Western blot of the purification of His-FtsX from both the inclusion body and supernatant fractions of *E. coli* C43 pET30a-FtsX. From L to R the samples for both gels are as follows: elution fractions 1-3 (E1-E3) from the inclusion body purification and elution fractions 1-3 (E1-E3) from the supernatant purification. The His-FtsX fusion protein is indicated in red.

3.2.2 GST Pulldown for Exploring the FtsE-FtsQ Interaction

After GST-FtsE, GST and His-FtsQ were purified, GST pulldowns were performed to study the potential FtsE-FtsQ interaction. Two negative controls were used for all GST pulldown assays: 1) glutathione resin with His-FtsQ prey protein and 2) glutathione resin with the GST protein + His-FtsQ prey protein. These controls were used to determine if His-FtsQ would bind non-specifically to either the glutathione resin or GST protein.

GST pulldowns to study the FtsE-FtsQ interaction were performed in the presence of several different interaction buffers. Three different interaction buffers were examined to determine which buffer produced the optimal experimental conditions to study the FtsE-FtsQ interaction: Pulldown Buffer A (50 mM KCl, 20 mM Tris, 1 mM DTT, 0.5 mM EDTA, pH 7.5, 10% (v/v)

glycerol, and 1% (v/v) Triton X-100), Pulldown Buffer B (137 mM NaCl, 8 mM Na_2PO_4, 2.7 mM KCl, 1.5 mM KH_2PO_4, 1 mM DTT, pH 7.4, 0.5% (v/v) Triton X-100) and Pulldown Buffer C (50 mM HEPES/KOH, 50 mM KCl, 1 mM ATP, pH 7.5, 0.5% (v/v) Triton X-100). The Pulldown Buffer C is similar to the one used by de Leeuw *et al.* when the authors studied the ability for *E. coli* FtsE to bind ATP (de Leeuw *et al.*, 1999). As *N. gonorrhoeae* FtsE is also predicted to bind ATP, this buffer was used in an attempt to provide optimal conditions for the FtsE-FtsQ interaction (Bernatchez *et al.*, 2000).

However, the FtsE-FtsQ interaction could not be confirmed in the presence of any of the above interaction buffers. Figure 3.2.2 shows the Coomassie stained gel (Figure 3.2.2A) and the corresponding anti-His and anti-GST Western blot (Figure 3.2.2.B) demonstrating the lack of observable interaction between GST-FtsE and His-FtsQ in the presence of Pulldown Buffer C. For both Figure 3.2.2A and Figure 3.2.2B, lanes 1 and 4 show the resulting flowthrough and resin fractions for the negative control His-FtsQ + glutathione resin interaction sample, respectively. His-FtsQ (~29 kDa) is observed in the flowthrough fraction (lane 1) and is not observed in the resin fraction (lane 4), indicating that this fusion protein does not bind non-specifically to the glutathione resin. The results of the second negative control sample, GST + His-FtsQ, are shown in lanes 2 and 5 with lane 2 representing the resin fraction and lane 5 representing the flowthrough fraction. The GST moiety (~25 kDa) is observed in the resin fraction (lane 2) while His-FtsQ (~29 kDa) is observed in the flowthrough fraction (lane 5), indicating that His-FtsQ was successfully removed during the washing steps and, therefore, cannot bind to the GST tag. In summary, His-FtsQ was unable to bind to either negative control sample. There is an additional band (~45 kDa) found in lanes 1, 5 and 6 of the Coomassie gel (Figure 3.2.2A) that is not observed in the corresponding Western blot (Figure 3.2.2B). This additional band is most likely a contaminating protein that was purified with His-FtsQ as it can also be seen during purification of His-FtsQ (Figure 3.2.1.4). The results of the interaction sample, GST-FtsE + His-FtsQ, are shown in lanes 3 and 6 with lane 3 representing the resin fraction and lane 6 representing the flowthrough fraction. GST-FtsE (~50 kDa) is observed in the resin fraction (lane 3) along with a degrading GST tag found at 26 kDa, but His-FtsQ is not observed in this fraction. Instead, His-FtsQ is observed in the flowthrough fraction (lane 6), suggesting that His-FtsQ was unable to bind to GST-FtsE during the GST pulldown assay. Therefore, these results suggest that GST-FtsE and His-FtsQ do not interact with each other under the conditions tested.

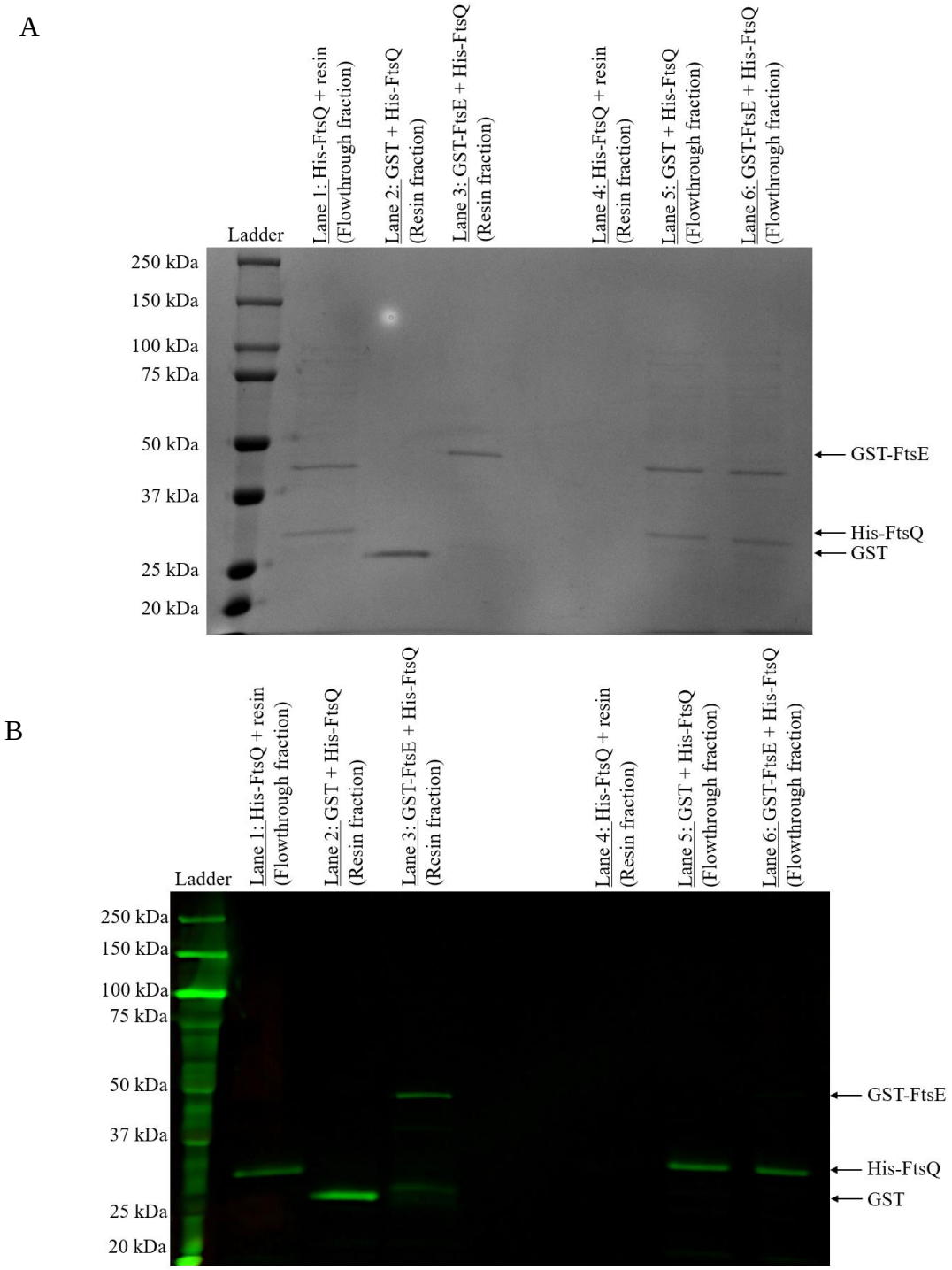

Figure 3.2.2: GST Pulldown Assay Examining the GST-FtsE + His-FtsQ Interaction. (A) The Coomassie stained gel and (B) the corresponding anti-His and anti-GST Western Blot. The GST pulldown assay was performed in the presence of Pulldown Buffer C (50 mM HEPES/KOH, 50 mM KCl, 1 mM ATP, pH 7.5, 0.5% (v/v) Triton X-100). The lanes for both gels are as follows: Lane 1: His-FtsQ + glutathione resin negative control (flowthrough fraction); Lane 2: GST + His-FtsQ negative control (resin fraction); Lane 3: GST-FtsE + His-FtsQ interaction

sample (resin fraction); Lane 4: His-FtsQ + glutathione resin negative control (resin fraction); Lane 5: GST + His-FtsQ negative control (flowthrough fraction); Lane 6: GST-FtsE + His-FtsQ interaction sample (flowthrough fraction).

3.3 Exploring the Interactions between GST-FtsE and *N. gonorrhoeae* Lysate through Affinity Purification Mass Spectrometry (AP-MS)

AP-MS experiments were performed to examine potential interactions between the bait protein GST-FtsE, and proteins found in a *N. gonorrhoeae* whole cell lysate. AP-MS experiments initially identified 1850 proteins that potentially interacted with GST-FtsE, but the majority were removed because they did not meet the inclusion criteria described in Section 2.6.5 "Protein Analysis". The 305 that met the inclusion criteria were considered to be proteins that could be potential interacting partners of FtsE. These 305 proteins included 36 cell division proteins that were retained for further analysis. The full list of these 305 proteins and their corresponding spectral count value, intensity value and the corresponding spectral count and spectra based- and intensity-based fold change values are provided in Table B.1 (Appendix B).

3.3.1 Cell Division Proteins Identified During AP-MS Experiments

Mass spectrometry identified 36 cell division proteins amongst the 305 total proteins identified in the AP-MS experiments. The cell division proteins can be grouped into two categories based on their likelihood of interacting with FtsE (Table 3.3.1). Table 3.3.1 provides the spectral count (SpC), intensity (I), and the corresponding spectral count based- or intensity-based fold change for all 36 proteins identified in AP-MS experiments. The first category, "Probable Interacting Partners", are proteins that meet the following criteria: larger spectral count in the interaction sample A3B3 than the spectral count of the negative controls, AND the protein exhibited either a spectral-based or intensity-based fold change value of either ≥ 2 or ≤ 0.05. The second category, "Other Cell Division Proteins Identified in AP-MS Experiments", includes the remaining cell division proteins that do not fall into the "Probably Interacting Partners" category. These cell division proteins were identified in AP-MS experiments but are most likely not interacting with FtsE because they do not meet the above criteria.

Table 3.3.1: Cell Division Proteins Identified in AP-MS Experiments

	Protein Name	Neg Control A1B1		Neg Control A2B2		Interaction Sample A3B3		Neg Control A4B4		SpC Based Fold Change	I Based Fold Change
		SpC	I	SpC	I	SpC	I	SpC	I		
Probable Interacting Partners	Probable PenA (FtsI)	3	1.03E+07	3	1.83E+06	6	3.69E+07	3	6.30E+07	0.07	0.05
	Cell division protein (likely FtsN)[%]	0	0.00E+00	0	0.00E+00	2	8.46E+05	0	0.00E+00	[$]N/A	N/A
	Putative cell-division protein (likely FtsK)[%]	0	0.00E+00	0	0.00E+00	1	7.43E+05	0	0.00E+00	N/A	N/A
	Putative cell-division protein (likely FtsK)[%]	0	0.00E+00	0	0.00E+00	1	2.95E+04	0	0.00E+00	N/A	N/A
Other Cell Division Proteins Identified in AP-MS Experiments	GMP synthase (likely FtsE)*	4	4.31E+06	5	6.93E+06	466	1.11E+10	0	0.00E+00	61.10	665.71
	FtsE-like protein*	4	4.31E+06	4	5.26E+06	380	1.05E+10	0	0.00E+00	55.76	727.44
	Septum site-determining protein MinD	128	5.50E+08	166	7.19E+08	168	6.78E+08	0	0.00E+00	0.67	0.36
	Cell division protein FtsZ	186	7.05E+08	201	8.07E+08	165	6.16E+08	0	0.00E+00	0.50	0.27
	Cell division protein FtsZ	176	6.81E+08	198	7.93E+08	164	6.07E+08	0	0.00E+00	0.52	0.27
	Cell division protein FtsZ	121	4.08E+08	152	5.16E+08	124	3.53E+08	0	0.00E+00	0.54	0.25
	Cell division topological specificity factor (MinE)	71	6.72E+08	77	1.08E+09	77	1.15E+09	0	0.00E+00	0.61	0.44
	Cell division protein FtsA	83	2.03E+08	81	1.85E+08	70	1.36E+08	0	0.00E+00	0.50	0.23
	Cell division protein FtsA	74	1.96E+08	75	1.82E+08	63	1.31E+08	0	0.00E+00	0.50	0.23

	Cell division protein ZipA	41	1.01E+08	54	1.15E+08	41	6.92E+07	0	0.00E+00	0.51	0.21
	Cell division protein ZapA	26	5.17E+07	36	6.14E+07	34	6.27E+07	0	0.00E+00	0.65	0.37
	Cell division topological specificity factor (MinE)	27	2.42E+08	14	2.91E+08	19	3.88E+08	0	0.00E+00	0.54	0.48
	Probable septum site-determining protein MinC	19	8.35E+06	23	1.68E+07	17	6.40E+06	0	0.00E+00	0.48	0.17
	Cell division protein FtsK	7	8.64E+06	10	1.29E+07	10	7.59E+07	0	0.00E+00	0.70	2.36
	Probable PenA (FtsI)	5	5.31E+07	4	4.36E+07	9	1.34E+08	4	3.92E+07	0.08	0.22
	Cell division protein FtsN	8	1.03E+07	2	1.82E+06	7	4.25E+07	0	0.00E+00	0.80	2.12
	UDP-N-acetylglucosamine 1-carboxyvinyltransferase (MurA)	7	5.89E+06	8	1.14E+06	7	2.03E+06	0	0.00E+00	0.55	0.17
	Probable PenA (FtsI)	3	1.03E+07	2	1.78E+06	6	3.44E+07	2	3.29E+07	0.11	0.09
	Probable PenA (FtsI)	5	1.13E+07	2	1.78E+06	5	3.45E+07	2	3.29E+07	0.09	0.09
	Cell division protein FtsK	7	4.35E+06	6	2.91E+06	5	1.50E+06	0	0.00E+00	0.45	0.13
	Cell division protein (likely Fic/Doc family protein)[%]	2	6.83E+06	3	6.36E+06	4	1.32E+07	0	0.00E+00	0.95	0.65
	Probable PenA (FtsI)	0	0.00E+00	0	0.00E+00	3	2.77E+07	2	3.29E+07	0.06	0.07
	Probable PenA (FtsI)	4	1.36E+07	2	2.80E+05	3	2.95E+07	3	3.29E+07	0.04	0.07
	Probable PenA (FtsI)	4	1.18E+07	2	1.78E+06	3	2.53E+07	2	3.29E+07	0.05	0.06

	Cell division protein FtsX	1	1.74E +06	3	8.78E +06	3	4.93E +05	0	0.00E +00	0.90	0.03
	Cell division protein (likely Fic/Doc family protein)[%]	3	6.85E +06	3	6.36E +06	3	1.23E +07	0	0.00E +00	0.59	0.61
	Probable PenA (FtsI)	4	1.03E +07	2	2.80E +05	2	2.52E +07	3	3.29E +07	0.02	0.06
	Penicillin-binding protein 2 (FtsI)	5	1.03E +07	3	1.83E +06	1	1.50E +05	0	0.00E +00	0.15	0.01
	Penicillin binding protein (Fragment) (FtsI)	4	3.47E +06	0	0.00E +00	0	0.00E +00	0	0.00E +00	0.00	0.00
	Probable PenA (FtsI)	4	2.55E +06	3	1.83E +06	0	0.00E +00	0	0.00E +00	0.00	0.00
	Cell division protein FtsN	3	2.32E +06	2	1.58E +06	0	0.00E +00	0	0.00E +00	0.00	0.00
	Cell division protein FtsB	1	1.94E +06	0	0.00E +00	0	0.00E +00	0	0.00E +00	0.00	0.00

SpC, spectral count; I, intensity

[$]N/A = fold change value is not applicable. This note occurs when the spectral-based or intensity-based fold change is calculated for proteins which have no peptides and no intensity values recorded for all negative control samples. The fold change is calculated by dividing the NSAF for the A3B3 sample by the average NSAF for the negative controls (i.e., $NSAF_{(A3B3)}/NSAF_{AVG(A1B1, A2B2, A4B4)}$). When the negative controls have a spectral count and intensity value of 0, then the average NSAF for the negative controls will be zero.

[%]The likely identity of these non-specific cell division proteins was determined through BLASTp (Appendix B).

*FtsE is listed in the "Other Cell Division Proteins Identified in AP-MS Experiments" category because the increased amount of FtsE peptides in the interaction sample (A3B3) is due to the addition of the GST-FtsE bait protein to the sample.

Four proteins in the "Probable Interacting Partners" are most likely interacting with FtsE in these AP-MS experiments. These proteins include: FtsI, a "cell division protein" which is likely FtsN and the two "putative cell division proteins" that are likely FtsK. Therefore, these experiments suggest that FtsE interacts with FtsI, FtsN and FtsK. The FtsN and FtsK proteins are the only cell division proteins in all of Table 3.3.1 that were found solely in the interaction sample A3B3 and, therefore, were most likely pulled down by interacting with FtsE.

The remaining cell division proteins are found in the final category "Other Cell Division Proteins Identified in AP-MS Experiments" category (Table 3.3.1). These proteins are most likely not interacting partners of FtsE and, instead, are most likely background contamination proteins. Many of these proteins were found at similar abundances in the negative controls and interaction sample or were more abundant in the negative control than the interaction sample. For example, there were 200 FtsZ peptides identified in the negative control A2B2 (i.e., resin + GST + Ng lysate) in comparison to the 165 peptides identified in the interaction sample A3B3 (i.e., resin + GST-FtsE + Ng lysate) (Table 3.3.1). It appears that many of these proteins are background proteins that are non-specifically binding to the resin or the GST tag and most likely do not interact with FtsE.

In addition, two FtsE proteins were categorized as "Other Cell Division Proteins Identified in AP-MS Experiments", even though they meet the criteria for being placed in the "Probable Interacting Partners" category (i.e., increased spectral count in interaction sample A3B3 and either a spectral-based or intensity-based fold change value of either ≥ 2 or ≤ 0.05). This was done because the increased amount of FtsE found in the interaction sample (A3B3) is due to the addition of the GST-FtsE bait protein to that sample.

3.3.2 Potential Protein-Protein Interactions as Ascertained by STRING Analysis

STRING was used to predict potential interactions amongst the 305 proteins identified by AP-MS experiments, with a specific interest in the predicted interaction amongst the cell division proteins. An initial STRING analysis of the 305 proteins and the predicted interactions are shown in Appendix B (Figure B.2). However, the network map (Figure B.2) does not include all the cell division proteins that were identified in AP-MS experiments; only a handful of cell division proteins can be observed (i.e., FtsA, MinC, MinE, FtsE, ZapA, FtsK, MurA and FtsN) while the remaining cell division proteins (i.e., FtsZ, ZipA, FtsX, FtsI, and MinD) were not observed in the STRING network map. This discrepancy is because the cell division proteins FtsA, MinC, MinE,

FtsE, ZapA, FtsK, FtsN and cell wall proteins MurA were identified in *N. gonorrhoeae* FA1090 during data analysis, while the remaining cell division proteins were not identified in *N. gonorrhoeae* FA1090. STRING is only able to recognize and provide data for *N. gonorrhoeae* proteins who have Uniprot accession numbers corresponding to the FA1090 strain. The cell division proteins that are not observed in Figure B.2 instead have Uniprot accession numbers that correspond to other *N. gonorrhoeae* strains. Therefore, the FA1090 strain accession numbers were determined for the cell division proteins that were not initially observed in the STRING map in Figure B.2 (i.e., FtsZ, ZipA, FtsX, FtsI, and MinD). In addition, the FA1090 strain accession numbers were determined for the cell division proteins that were not observed in AP-MS experiments (i.e., FtsQ, FtsL, and FtsW). These accession numbers are provided in Appendix B (Table B.3).

STRING was used to predict interactions amongst the 305 proteins identified during AP-MS experiments and the cell division proteins described above (i.e., FtsZ, FtsA, FtsE, MinD, MinE, ZipA, ZapA, MinC, FtsK, FtsI, FtsX, FtsN, FtsB, FtsQ, FtsL, FtsW, and MurA). The resulting STRING network map shows a cell division cluster in which cell division proteins (FtsZ, ZipA, FtsQ, FtsI, FtsX, FtsW, and MinD) form an expected cell division cluster with the previously identified cell division proteins (i.e., FtsN, ZapA, FtsE, FtsA, FtsB, MinC, MinE, MurA (Figure 3.3.2). The full STRING network is provided in Appendix B (Figure B.4). There are several interactions predicted in this network, including: FtsE-FtsX, FtsB-FtsZ, FtsZ-FtsA, MinC-MinD, FtsW-FtsI, ZipA-FtsI, ZipA-FtsN.

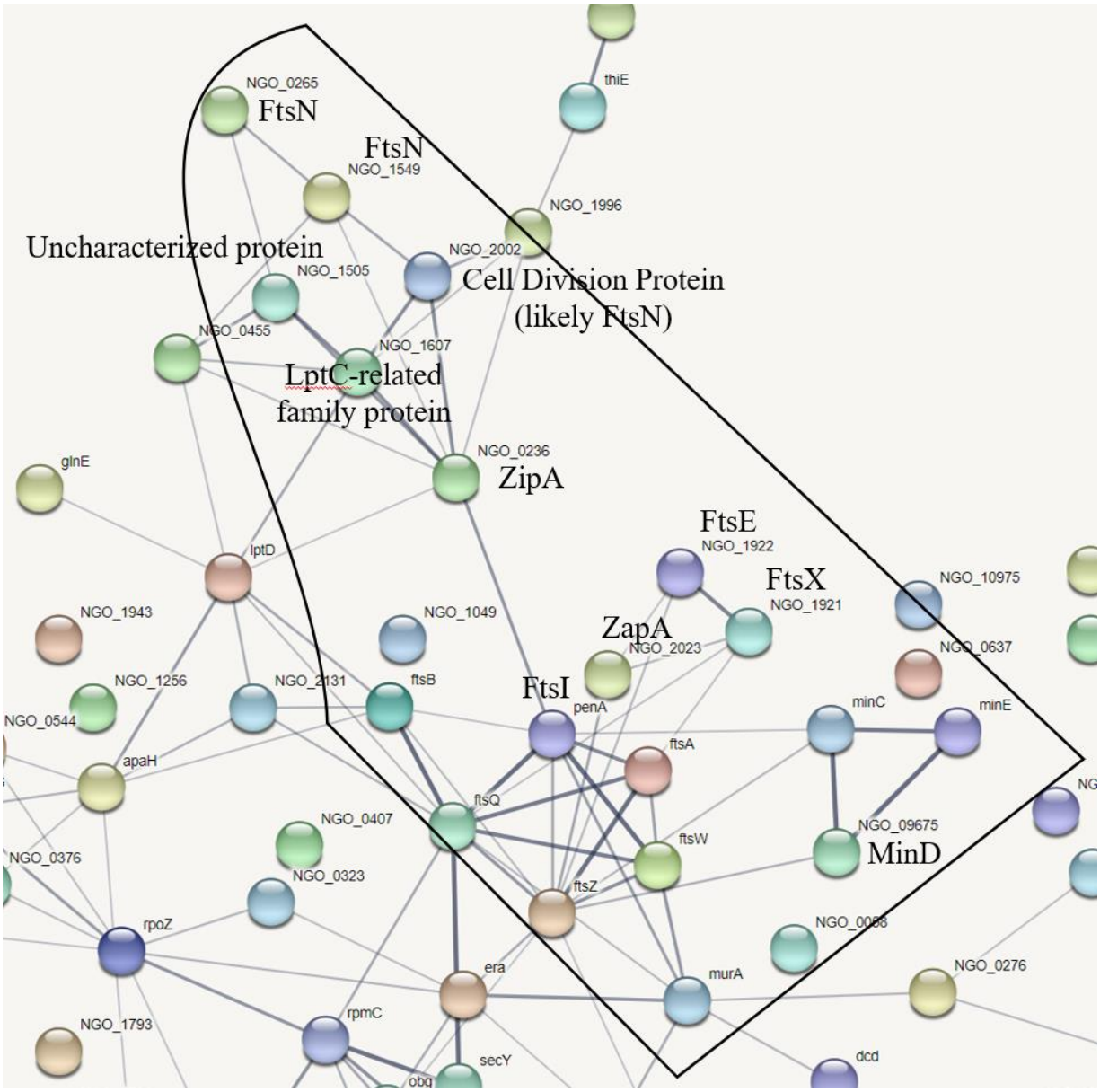

Figure 3.3.2: Cell Division Cluster Predicted by STRING Analysis. STRING analysis was performed on the 305 proteins identified in AP-MS experiments and additional cell division proteins (i.e., FtsZ, MinD, ZipA, FtsX, FtsI, FtsQ, FtsL, and FtsW). The minimum interaction score was set to 0.4 and all interaction sources were included except the text-mining data source. The line thickness is indicative of the strength of the predicted interaction; thicker lines indicate more confidence in the prediction.

4.0 DISCUSSION

4.1 Bacterial-Two-Hybrid (B2H) Assays

B2H assays are often used to study protein-protein interactions and they have been used to study the interactions of *N. gonorrhoeae* cell division proteins prior to this current study (Zou *et al.*, 2017a). In 2017, Zou *et al.* examined protein-protein interactions amongst 8 gonococcal cell division proteins (i.e., FtsZ, FtsA, ZipA, FtsK, FtsI, FtsQ, FtsW and FtsN) using B2H, GST pulldowns and surface plasmon resonance methodologies. The results of this examination determined that *N. gonorrhoeae* cell division proteins exhibit unique interactions that were not observed in *E. coli*, the Gram-negative model organism (Zou *et al.*, 2017a). However, four gonococcal cell division proteins, FtsE, FtsX, FtsL and FtsB, were not studied at that time. In addition, the self-interactions of the cell division proteins FtsA, ZipA, FtsE, FtsX, FtsK, FtsQ, FtsL, FtsB, FtsW, FtsI and FtsN were not studied at that time. Therefore, to fully compare the *E. coli* and *N. gonorrhoeae* divisomes, the self-interactions of the *N. gonorrhoeae* cell division proteins and the protein-protein interactions of *N. gonorrhoeae* FtsE, FtsX, FtsL and FtsB were investigated in this study using B2H assays.

4.1.1 The Interactions of *N. gonorrhoeae* FtsE

B2H assays revealed that *N. gonorrhoeae* FtsE can self-interact and can interact with the *N. gonorrhoeae* cell division proteins FtsX and FtsQ. The protein-protein interactions for both *E. coli* and *N. gonorrhoeae* FtsE are compared in Figure 4.1.1. In *E. coli,* FtsE can self-interact and can also interact with *E. coli* cell division proteins FtsZ and FtsX (Figure 4.1.1.A) (Corbin *et al.*, 2007; de Leeuw *et al.*, 1999). The FtsE self-interaction is common to both *E. coli* and *N. gonorrhoeae* (Figure 4.1.1). The ability for FtsE to self-interact in *E. coli* was determined through dimerization studies where they found the *E. coli* FtsE forms a strong dimer that can only be converted to a monomer in the presence of the denaturing agent DTT at 100°C (de Leeuw *et al.*, 1999). According to B2H assays, *N. gonorrhoeae* FtsE is also predicted to self-interact (38.5% β-galactosidase activity).

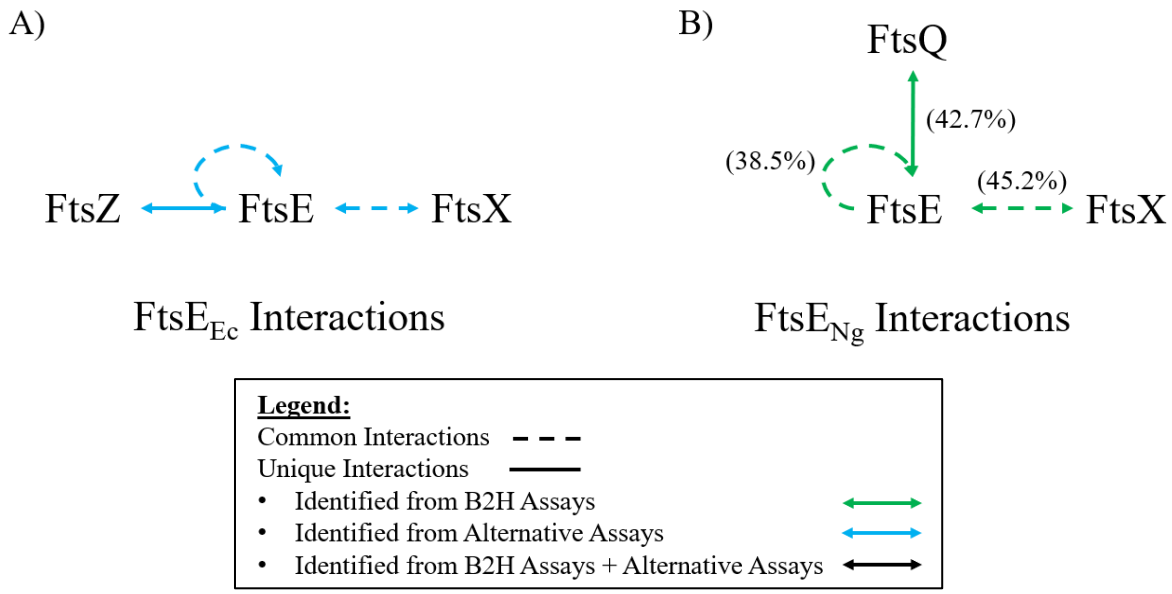

Figure 4.1.1: Comparison of Protein-Protein interactions for FtsE in both (A) *E. coli* and (B) *N. gonorrhoeae*. Common interactions between *N. gonorrhoeae* and *E. coli* are shown with dashed lines. Unique interactions to one of the two organisms are indicated with solid lines. Interactions identified by B2H experiments are shown in green while interactions identified from alternative experiments like co-immunoprecipitation assays, cross-linking assays, etc. are shown in blue. Interactions identified using both B2H data and alternative experiments are shown in black. Data from B2H assays performed in this thesis are provided in brackets next to the interaction it represents.

In *E. coli*, FtsE and FtsX interact to form a complex (FtsEX complex) that is involved in assisting in building the divisome and regulating peptidoglycan synthesis and hydrolysis (Figure 4.1.1A) (Du *et al.*, 2016; de Leeuw *et al.*, 1999; Pichoff *et al.*, 2019; Schmidt *et al.*, 2004). This *E. coli* FtsEX complex was identified through co-immunoprecipitation experiments (de Leeuw *et al.*, 1999). Both the FtsE and FtsX proteins had been previously identified in *N. gonorrhoeae* and were found to be highly similar to their *E. coli* homologs (Bernatchez *et al.*, 2000). The presence of the FtsE-FtsX interaction in *N. gonorrhoeae* suggests that the FtsEX complex may form (Figure 4.1.1B). However, the role of this complex in *N. gonorrhoeae* and whether this role is similar to that the role of the *E. coli* FtsEX complex remains to be explored.

As shown in Figure 4.1.1.A, there is an interaction between *E. coli* FtsE and FtsZ. This interaction was identified through co-immunoprecipitation experiments (Corbin *et al.*, 2007). In contrast, the B2H assay performed in this thesis that studied the *N. gonorrhoeae* FtsE-FtsZ interaction reported a β-galactosidase activity of 68.0%, suggesting that FtsE and FtsZ do not

interact. This discrepancy may be because the B2H assay is an *in vivo* methodology while the co-immunoprecipitation assay is an *in vitro* methodology. Recently, Du *et al.* performed a B2H assay to further explore the *E. coli* FtsE-FtsZ interaction and they discovered that, like the results reported in this thesis, *E. coli* FtsE and FtsZ did not interact. However, the authors found that the co-expression of FtsX would allow for the *E. coli* FtsE-FtsZ interaction to occur (Du *et al.*, 2019). According to this recent study by Du *et al.*, it appears that FtsX should be co-expressed when the interactions of *E. coli* FtsE are studied using the B2H methodology, as the presence of FtsX appears to allow FtsE to properly localize prior to interacting with potential protein partners (Du *et al.*, 2019). If co-expression is beneficial, a decrease in β-galactosidase activity will be observed. The addition of *N. gonorrhoeae* FtsX may be required during future B2H experiments involving FtsE in order for additional interactions with other potential protein partners to be identified.

The FtsE-FtsQ interaction identified by B2H (Figure 4.1.1B) may be unique to *N. gonorrhoeae*. However, an interaction between FtsE and FtsQ have not yet been studied or observed in *E. coli*, so it is not possible to be certain that the FtsE-FtsQ interaction is unique to *N. gonorrhoeae*. In *E. coli*, FtsQ is part of a trimer (FtsQLB complex) that is involved in regulating septal peptidoglycan synthesis (den Blaauwen and Luirink, 2019; Park *et al.*, 2020). $FtsE_{Ec}$ and $FtsQ_{Ec}$ both regulate septal peptidoglycan synthesis but through different pathways and mechanisms. $FtsQ_{Ec}$ regulates peptidoglycan synthesis through interactions with the FtsWI complex while $FtsE_{Ec}$ regulates peptidoglycan synthesis indirectly by influencing the activity of FtsA (den Blaauwen and Luirink, 2019; Du *et al.*, 2016; de Leeuw *et al.*, 1999; Park *et al.*, 2020; Pichoff *et al.*, 2019; Schmidt *et al.*, 2004). However, even though both FtsE and FtsQ can regulate peptidoglycan synthesis, their potential ability to interact has not been investigated in *E. coli*. This hinders the ability to determine whether the FtsE-FtsQ interaction is truly unique to *N. gonorrhoeae* and what the role of this interaction may be. It can be speculated that since *N. gonorrhoeae* FtsE and FtsQ interact, perhaps they act to regulate septal peptidoglycan synthesis together. These speculations and the role of the FtsE-FtsQ interaction need to be clarified through additional experiments.

There is a serious limitation to the comparison of the protein-protein interaction network for *E. coli* and *N. gonorrhoeae* FtsE. To date, there have only been a few studies that have examined the ability for *E. coli* FtsE to interact with other cell division proteins. A study by Corbin *et al.*

identified the FtsE-FtsZ interaction while another study by de Leeuw *et al.* identified both the FtsE-FtsX interaction and the FtsE self-interaction (Corbin *et al.*, 2007; de Leeuw *et al.*, 1999). The true breadth of interactions that *E. coli* FtsE is involved in is not fully known. There could be additional interactions that *E. coli* FtsE is involved in that have not been investigated yet, including FtsQ.

4.1.2 The Interactions of *N. gonorrhoeae* FtsX

The B2H assays revealed that *N. gonorrhoeae* FtsX interacted with 5 divisome proteins: FtsL, ZipA, FtsK, FtsW, and FtsN. Out of these 5 interactions, the only interaction that is common to both *N. gonorrhoeae* and *E. coli* is the FtsX-FtsE interaction, as discussed above. The remaining interactions (i.e., FtsX-FtsL, FtsX-ZipA, FtsX-FtsK, FtsX-FtsW and FtsX-FtsN) are unique to *N. gonorrhoeae* because they have not been observed in *E. coli.*

The protein-protein interaction network for both *E. coli* and *N. gonorrhoeae* FtsX are compared in Figure 4.1.2. As shown in Figure 4.1.2A, *E. coli* FtsX interacts with FtsE, FtsQ and FtsA (Du *et al.*, 2016; Karimova *et al.*, 2005; de Leeuw *et al.*, 1999). The interaction between *E. coli* FtsX and FtsE was determined through co-immunoprecipitation experiments and was discussed in depth above (de Leeuw *et al.*, 1999). Karimova *et al*. used a B2H methodology to study the interactions of *E. coli* FtsX with FtsA, FtsX, FtsQ, FtsL, FtsB, FtsW, FtsI, and FtsN. This assay allowed Karimova *et al.* to identify the presence of the FtsX-FtsA and FtsX-FtsQ interactions (Figure 4.1.2A) (Karimova *et al.*, 2005). Du *et al.* also identified the *E. coli* FtsX-FtsA interaction through a B2H assay (Figure 4.1.2A) (Du *et al.*, 2016). However, Karimova *et al.* did not identify interactions between *E. coli* FtsX and FtsL, FtsB, FtsW, FtsI and FtsN or the FtsX self-interaction. Therefore, the presence of the *N. gonorrhoeae* FtsX-FtsL, FtsX-FtsW and FtsX-FtsN interactions but absence of these same interactions in *E. coli* is notable. It is not known what roles the FtsX-FtsL, FtsX-FtsW, and FtsX-FtsN protein-protein interactions (Figure 4.1.2B) may be performing in *N. gonorrhoeae* cell division. In *E. coli*, the FtsL, FtsW and FtsN proteins are involved in regulating peptidoglycan synthesis (Park *et al.*, 2020, 2021). Perhaps these unique *N. gonorrhoeae* FtsX interactions (i.e., FtsX-FtsL, FtsX-FtsW, and FtsX-FtsN) may also be involved in peptidoglycan synthesis. The exact role the *N. gonorrhoeae* FtsX-FtsL, FtsX-FtsW and FtsX-FtsN interactions play in *N. gonorrhoeae* cell division would need to be clarified through additional experiments.

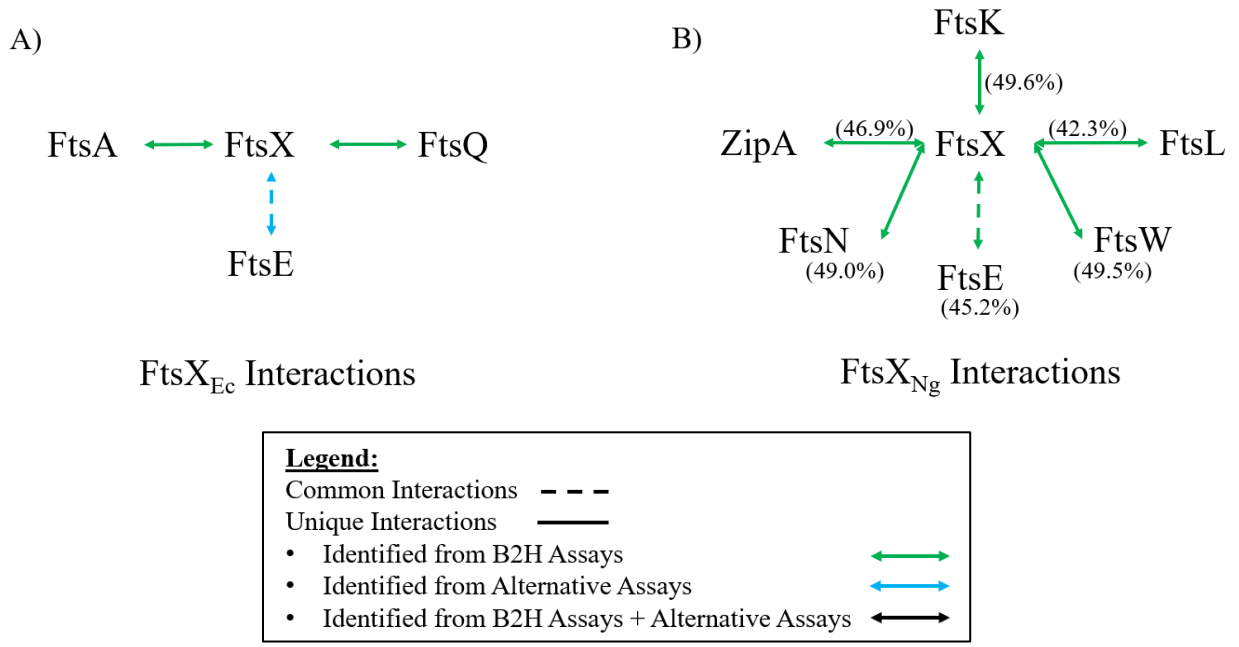

Figure 4.1.2: Comparison of Protein-Protein interactions for FtsX in both (A) *E. coli* and (B) *N. gonorrhoeae*. Common interactions between *N. gonorrhoeae* and *E. coli* are shown with dashed lines. Unique interactions to one of the two organisms are indicated with solid lines. Interactions identified by B2H experiments are shown in green while interactions identified from alternative experiments like co-immunoprecipitation assays, cross-linking assays, etc. are shown in blue. Interactions identified using both B2H data and alternative experiments are shown in black. Data from B2H assays performed in this thesis are provided in brackets next to the interaction it represents.

When Karimova *et al.* studied the interactions of *E. coli* FtsX, the authors did not include *E. coli* divisome proteins FtsZ, ZipA, and FtsK in their investigation (Karimova *et al.*, 2005). Therefore, the *N. gonorrhoeae* FtsX-ZipA and FtsX-FtsK interactions that were identified in this study (Figure 4.1.2B) may also exist in *E. coli*, but they have not been currently investigated. The role the *N. gonorrhoeae* FtsX-ZipA and FtsX-FtsK protein-protein interactions play in cell division would also have to be further studied with future experimentations.

In *E. coli*, the FtsX-FtsA interaction (Figure 4.1.2A) is important in recruiting downstream divisome proteins and regulating cell wall hydrolysis and synthesis (Du *et al.*, 2016; de Leeuw *et al.*, 1999; Pichoff *et al.*, 2019; Schmidt *et al.*, 2004). However, the B2H assay performed in this thesis for the *N. gonorrhoeae* FtsX-FtsA interaction reported a 55.3% β-galactosidase activity, suggesting there is no interaction between these proteins. The absence of this interaction and its effects on *N. gonorrhoeae* cell division would need to be studied. A recent study by Zou *et al.* reported that *N. gonorrhoeae* FtsA seems to have a species-specific function (Zou *et al.*, 2017b).

The authors discovered that *N. gonorrhoeae* FtsA could not complement an *E. coli* strain depleted in FtsA (Zou *et al.*, 2017b). In addition, the authors noted that while $FtsA_{Ec}$ can self-interact and interact with several cell division proteins, including $FtsZ_{Ec}$, $FtsQ_{Ec}$, $FtsI_{Ec}$, $FtsN_{Ec}$, *N. gonorrhoeae* FtsA could not interact with $FtsZ_{Ec}$, $FtsQ_{Ec}$, or $FtsI_{Ec}$ and instead could only interact with $FtsN_{Ec}$ (Zou *et al.*, 2017b). Zou *et al.* suggests that *N. gonorrhoeae* FtsA does not behave in same manner seen with that *E. coli* FtsA (Zou *et al.*, 2017b). Therefore, the lack of a *N. gonorrhoeae* FtsX-FtsA interaction may be due to the species-specific function of *N. gonorrhoeae* FtsA. In addition, the lack of an FtsX-FtsA interaction may also be due to the absence of FtsE. As discussed above, Du *et al.* discovered that the co-expression of FtsX was beneficial when examining the FtsE-FtsZ interaction by B2H assays (Du *et al.*, 2019). Perhaps the FtsX-FtsA interaction should be re-examined in the presence of co-expressed FtsE. If the amount of β-galactosidase produced during the FtsX-FtsA interaction decreases when FtsE is co-expressed, this would indicate that co-expression of FtsE is beneficial when examining protein-protein interactions involving FtsX.

4.1.3 The Interactions of *N. gonorrhoeae* FtsL

The B2H assays performed in this thesis also revealed that *N. gonorrhoeae* FtsL interacts with the divisome proteins FtsX and ZipA. The *N. gonorrhoeae* FtsL-FtsX interaction has been discussed in depth above. Figure 4.1.3 compares the observed protein-protein interactions of *E. coli* and *N. gonorrhoeae* FtsL. As shown in Figure 4.1.3A, *E. coli* FtsL interacts with FtsK, FtsQ, FtsB, FtsW and FtsI (Buddelmeijer and Beckwith, 2004; Di Lallo *et al.*, 2003; Karimova *et al.*, 2005; Maggi *et al.*, 2008). The *E. coli* FtsL-FtsQ and FtsL-FtsB interactions have been observed with both B2H assays and co-immunoprecipitation assays (Figure 4.1.3A) (Buddelmeijer and Beckwith, 2004; Di Lallo *et al.*, 2003; Karimova *et al.*, 2005; Maggi *et al.*, 2008). Meanwhile, the *E. coli* FtsL-FtsK, FtsL-FtsW and FtsL-FtsI interactions have only been identified through B2H assays (Figure 4.1.3A) (Di Lallo *et al.*, 2003; Karimova *et al.*, 2005). *N. gonorrhoeae* FtsL was found to interact with ZipA in the B2H assays performed in this thesis (Figure 4.1.3B). Di Lallo *et al.* examined the potential ability for *E. coli* FtsL to interact with ZipA and did not observe an interaction between these proteins during their B2H assays (Di Lallo *et al.*, 2003). In *E. coli*, FtsL assists in activating septal peptidoglycan synthesis while ZipA assists in anchoring the Z ring to the inner membrane (Park *et al.*, 2020; Pichoff and Lutkenhaus, 2002). Therefore, the *N. gonorrhoeae* FtsL-ZipA interaction observed in this thesis is notable (Figure 4.1.3B). The role of

this unique interaction in *N. gonorrhoeae* cell division is unknown and further experiments should be performed to examine this interaction.

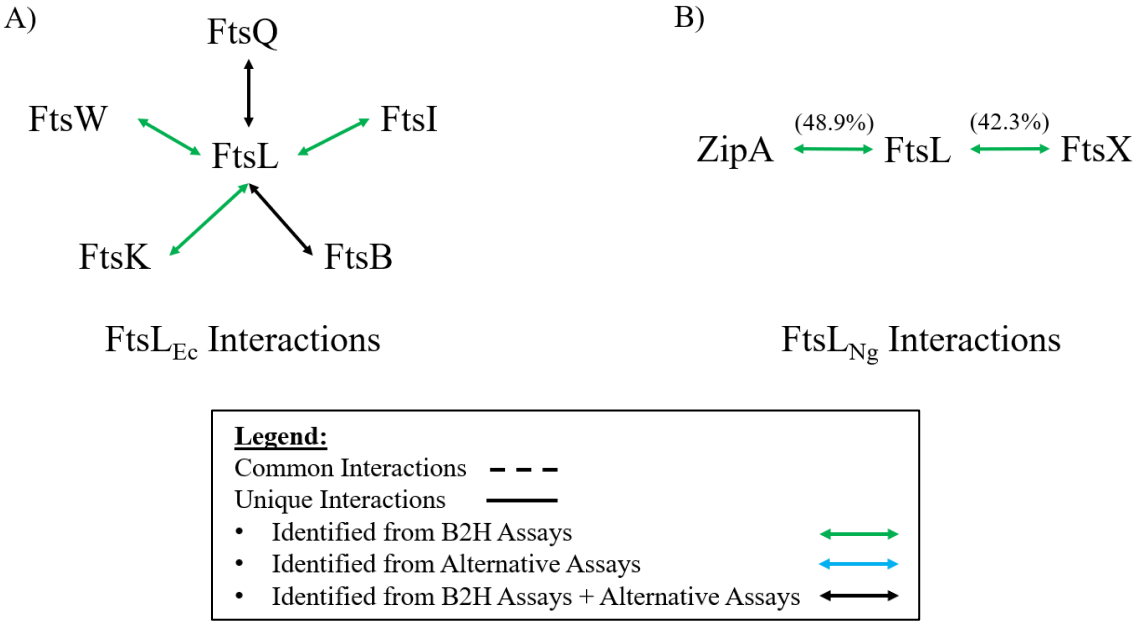

Figure 4.1.3: Comparison of Protein-Protein interactions for FtsL in both (A) *E. coli* and (B) *N. gonorrhoeae*. Common interactions between *N. gonorrhoeae* and *E. coli* are shown with dashed lines. Unique interactions to one of the two organisms are indicated with solid lines. Interactions identified by B2H experiments are shown in green while interactions identified from alternative experiments like co-immunoprecipitation assays, cross-linking assays, etc. are shown in blue. Interactions identified using both B2H data and alternative experiments are shown in black. Data from B2H assays performed in this thesis are provided in brackets next to the interaction it represents.

The interactions of FtsL with FtsQ and FtsB proteins are well studied in *E. coli*, through both co-immunoprecipitation experiments and B2H experiments (Buddelmeijer and Beckwith, 2004; Karimova *et al.*, 2005). These three proteins form a trimer known as the FtsQLB complex (Buddelmeijer and Beckwith, 2004; Gonzalez and Beckwith, 2009; Gonzalez *et al.*, 2010; Rothfield and Justice, 1997). The absence of a protein-protein interaction between FtsL and both FtsB and FtsQ in *N. gonorrhoeae* is notable. The *N. gonorrhoeae* FtsL-FtsQ interaction reports a 54.4% β-galactosidase activity which suggests the lack of an interaction between these proteins because the B2H assay value is over the 50% cutoff value. However, as this value is close to the 50% cutoff, this is considered to represent the probable absence of an interaction. The B2H assay performed in this thesis which examined the *N. gonorrhoeae* FtsL-FtsB interaction reports an 87.6% β-galactosidase activity, indicating an absence of an interaction. However, Karimova *et al*.

discovered that co-expression of *E. coli* FtsL could enhance the interaction detected between *E. coli* FtsB and FtsQ (Karimova *et al.*, 2005). A similar B2H experiment could be performed to study the interactions between *N. gonorrhoeae* FtsL, FtsB and FtsQ where FtsL is co-expressed during the FtsB-FtsQ interaction, FtsB is co-expressed during the FtsL-FtsQ interaction and FtsQ is co-expressed during the FtsL-FtsB interaction. The overexpression of one of the three proteins may enhance the binding of the other two proteins. If the amount of β-galactosidase produced during the assay decreases, this would be indicative that co-expression is beneficial to studying the interactions amongst these proteins.

4.1.4 The Interactions of *N. gonorrhoeae* FtsB

Lastly, B2H experiments involving *N. gonorrhoeae* FtsB suggest that *N. gonorrhoeae* FtsB only interacts with one other divisome protein, FtsZ, and performs a self-interaction. The protein-protein interaction maps for both *E. coli* and *N. gonorrhoeae* are compared in Figure 4.1.4. For *E. coli* FtsB, B2H assays were used to identify the FtsB-FtsI interaction, while the FtsB self-interaction, FtsB-FtsQ and FtsB-FtsL interactions were identified using both B2H assays and either cross-linking assays or co-immunoprecipitation assays (Figure 4.1.4A) (Buddelmeijer and Beckwith, 2004; Karimova *et al.*, 2005; LaPointe *et al.*, 2013; Maggi *et al.*, 2008). The only interaction common to both *E. coli* and *N. gonorrhoeae* is the FtsB self-interaction (Figure 4.1.4) (LaPointe *et al.*, 2013; Maggi *et al.*, 2008). *N. gonorrhoeae* FtsB was not found to interact with FtsL, FtsQ or FtsI during B2H experiments performed in this thesis (Figure 4.1.4B). As described above, *E. coli* FtsB is part of a trimer protein complex known as the FtsQLB complex (Buddelmeijer and Beckwith, 2004; Gonzalez and Beckwith, 2009; Gonzalez *et al.*, 2010; Rothfield and Justice, 1997). Therefore, the absence of an FtsB-FtsL or FtsB-FtsQ interaction in *N. gonorrhoeae* is notable as this suggests the conserved FtsQLB complex may not be forming, or the methodology used in this study was not optimal to capture the interaction. As discussed above, Karimova *et al.* discovered that the interaction between two proteins could be enhanced when a third protein was co-expressed during B2H assays (Karimova *et al.*, 2005). Therefore, the FtsB-FtsL and FtsB-FtsQ interactions should be examined again with the co-expression of FtsQ and FtsL, respectively.

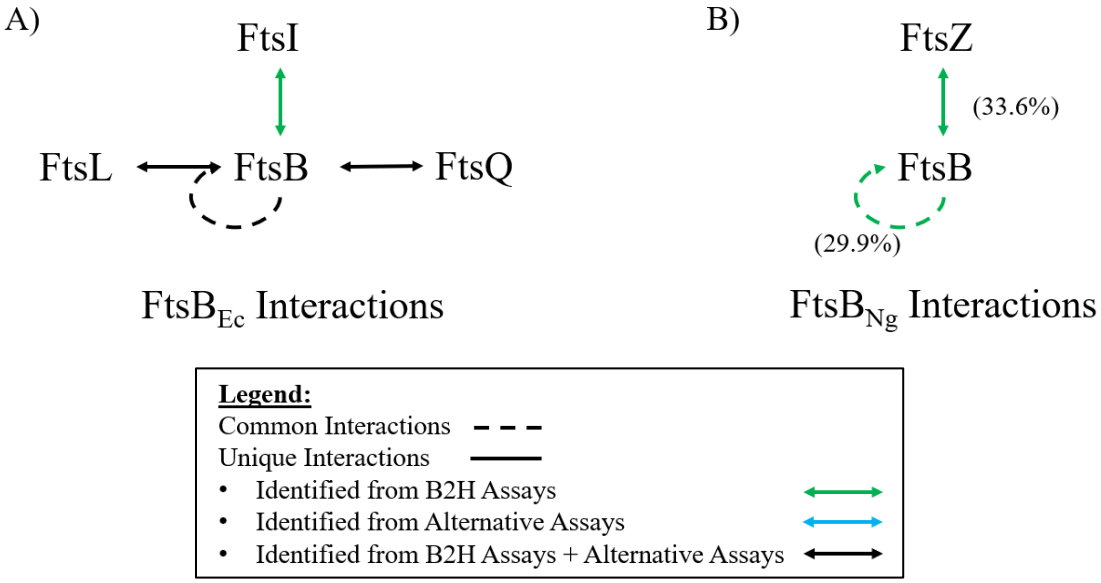

Figure 4.1.4: Comparison of Protein-Protein interactions for FtsB in both (A) *E. coli* and (B) *N. gonorrhoeae*. Common interactions between *N. gonorrhoeae* and *E. coli* are shown with dashed lines. Unique interactions to one of the two organisms are indicated with solid lines. Interactions identified by B2H experiments are shown in green while interactions identified from alternative experiments like co-immunoprecipitation assays, cross-linking assays, etc. are shown in blue. Interactions identified using both B2H data and alternative experiments are shown in black. Data from B2H assays performed in this thesis are provided in brackets next to the interaction it represents.

The FtsB-FtsZ interaction that was identified in *N. gonorrhoeae* (Figure 4.1.4B) appears to be a unique protein-protein interaction. Maggi *et al.* did not observe an interaction between *E. coli* FtsB and FtsZ during the B2H assays they performed (Maggi *et al.*, 2008). Therefore, the role of the FtsB-FtsZ interaction in *N. gonorrhoeae* is unknown and would require further study.

4.1.5 The Self-Interactions of *N. gonorrhoeae* Divisome Proteins

The only self-interaction amongst *N. gonorrhoeae* divisome proteins that was previously studied was the FtsZ self-interaction (Zou *et al.*, 2017a). In this thesis, B2H assays were used to study whether the remaining *N. gonorrhoeae* divisome proteins (i.e., FtsA, ZipA, FtsE, FtsX, FtsK, FtsQ, FtsL, FtsB, FtsW, FtsI and FtsN) were able to self-interact. Only four *N. gonorrhoeae* divisome proteins are able to self-interact: FtsE, FtsB, FtsW and FtsN. The FtsE self-interaction (Figure 4.1.1B), FtsB self-interaction (Figure 4.1.4B) and the FtsN self-interactions are observed in both *E. coli* and *N. gonorrhoeae,* making these common interactions between the two microorganisms (Di Lallo *et al.*, 2003; Karimova *et al.*, 2005; LaPointe *et al.*, 2013; de Leeuw *et*

al., 1999). However, the FtsW self-interaction is unique to *N. gonorrhoeae* as it has not been identified in *E. coli* (Karimova *et al.*, 2005).

4.1.6 Limitations to B2H Assays

B2H assays are often used to screen and identify protein-protein interactions. However, these assays have serious limitations and interactions identified by these assays should be confirmed through additional experiments. One of these limitations includes the occurrence of false positive and false negative results. Due to the occurrence of false positives and false negatives, the B2H methodology should be used as an initial screening assay that is then combined with additional biochemical methods (i.e., GST pulldowns or mass spectrometry) to identify protein-protein interactions (Karimova *et al.*, 2002).

In addition, a limitation to using the B2H methodology created by Di Lallo *et al.* is due to the 50% cutoff value used for determining the presence or absence of a protein-protein interaction (Di Lallo *et al.*, 2003). When Di Lallo *et al.* created their B2H assay, they chose a 50% cut off value based on observations that protein pairs that were known to interact often exhibited β-galactosidase activity values of 13 to 43% (Di Lallo *et al.*, 2003). Therefore, the authors considered that β-galactosidase values of less than 50% indicative of the presence of an interaction while values above 50% were indicative of the absence of an interaction (Di Lallo *et al.*, 2003). However, some protein-protein interactions in this thesis report β-galactosidase values close to the 50% cutoff value. For example, many of the B2H interactions involving FtsX that were examined in this thesis (i.e., FtsX-ZipA, FtsX-FtsK, FtsX-FtsW and FtsX-FtsN) all report β-galactosidase values just below the 50% cutoff value. These interactions could be false positives, or they could be weak and transient interactions. Further study with additional experiments such as co-immunoprecipitation or mass spectrometry could reveal the true nature of these interactions. Protein-protein interactions that were identified through B2H assays should be confirmed by additional biochemical methods. Protein-protein interactions which report β-galactosidase values in the range of 45-55% should especially be confirmed with additional assays because the reported β-galactosidase value is too close to the 50% cutoff to be certain the interaction is present or absent.

4.2 GST Pulldown Experiment to Study the Potential FtsE-FtsQ Interaction

GST pulldowns are often used as an additional method to study previously identified protein-protein interactions or to identify new interactions (Schäfer *et al.*, 2015). GST pulldowns

are *in vitro* assays that study the ability for two proteins to interact without the potential interference of other cellular molecules that may occur during in *in vivo* assays. Therefore, GST pulldowns can be used to determine if the interaction of interest is a direct interaction or an indirect interaction caused by an adaptor molecule acting to connect the two proteins together (Kim and Hakoshima, 2019; Wissmueller *et al.*, 2011).

GST pulldowns were used to further study the FtsE-FtsQ interaction, but repeated GST pulldown assays reported no observable interaction between GST-FtsE and His-FtsQ. The absence of the FtsE-FtsQ interaction could be due to a variety of factors, one factor being the presence of non-optimal experimental conditions. GST pulldown assays were performed in the presence of multiple different interaction buffers in an attempt to optimize the conditions required for a potential interaction between FtsE and FtsQ. Three interaction buffers were examined in order to determine which would be optimal for an interaction between FtsE and FtsQ: a Tris based buffer (20 mM Tris, 50 mM KCl, 0.5 mM EDTA, 1 mM DTT, 10% glycerol, 1% Triton X-100, pH 7.5), a PBS based buffer (1xPBS, 0.5% Triton X-100, 1 mM DTT, pH 7.4), and a HEPES based buffer with 1 mM ATP (50 mM HEPES/KOH, 50 mM KCl, 0.5% Triton X-100, 1 mm ATP, pH 7.5). However, the FtsE-FtsQ interaction could not be confirmed in the presence of any of these interaction buffers.

Studies of *E. coli* FtsE have found that FtsE can perform different functions based on whether ATP hydrolysis has occurred. For example, prior to ATP hydrolysis, FtsEX will promote recruitment of divisome proteins. But upon ATP hydrolysis, the role of FtsEX is to initiate peptidoglycan synthesis/hydrolysis and cell constriction (Du *et al.*, 2016; Pichoff *et al.*, 2019). Therefore, the ability for FtsE to bind and use ATP is important to its function. Another previous study used a HEPES buffer to examine the ability for *E. coli* FtsE to bind ATP (de Leeuw *et al.*, 1999). A similar buffer was used to provide *N. gonorrhoeae* FtsE with ATP in an attempt to provide more optimal experimental conditions and allow the FtsE-FtsQ interaction to occur. However, the FtsE-FtsQ interaction could not be confirmed in the presence of this buffer.

In previous GST pulldowns in our laboratory, a similar situation has occurred when studying the interaction between FtsZ and FtsA. GST pulldowns were used to study the *N. gonorrhoeae* FtsZ-FtsA interaction and GTP was added to promote polymerization of FtsZ experiment (Zou *et al.*, 2017a). However, the FtsZ-FtsA interaction could not be observed with

GST pulldowns. The FtsZ-FtsA interaction could only be confirmed through a surface plasmon resonance experiment (Zou *et al.*, 2017a). Perhaps something similar is occurring between *N. gonorrhoeae* FtsE and FtsQ and surface plasmon resonance studies may be able to identify the FtsE-FtsQ interaction.

Another reason the FtsE-FtsQ interaction may not occur during a GST pulldown assay is because FtsX is not present. In *E. coli*, FtsE and FtsX form a complex (i.e., FtsEX complex) that works to act on other cell division proteins to trigger cellular functions such as divisome assembly and to regulate peptidoglycan synthesis (Du *et al.*, 2016; Pichoff *et al.*, 2019; Schmidt *et al.*, 2004). It could be suggested that FtsE and FtsX must form the FtsEX complex prior to triggering these cellular functions. Therefore, when $FtsX_{Ng}$ is not present and the *N. gonorrhoeae* FtsEX complex is not formed, perhaps $FtsE_{Ng}$ is unable to interact with its other cell division protein partners. This reasoning could also explain why the FtsE-FtsQ interaction is observed in B2H assays but not in the GST pulldown assay. As B2H assays are an *in vivo* assay, the *N. gonorrhoeae* FtsE and FtsQ proteins are expressed in *E. coli* and their protein-protein interaction is studied. *N. gonorrhoeae* FtsE has high homology to *E. coli* FtsE (Bernatchez *et al.*, 2000), so it could potentially bind to *E. coli* FtsX, forming the FtsEX complex, and then interact with FtsQ. Therefore, the presence of FtsX and whether it influences the FtsE-FtsQ interaction should be studied. To initially investigate this, FtsX could be co-expressed during a B2H assay examining the FtsE-FtsQ interaction, as described above. Du *et al*. performed a similar experiment and demonstrated that the co-expression of *E. coli* FtsX would assist in the FtsE-FtsZ interaction could increase the interaction between FtsB and FtsQ (Du *et al.*, 2019).

One final factor that may explain why the FtsE-FtsQ interaction is not visualized with GST pulldowns is that the FtsE-FtsQ interaction may be a weak interaction. According to B2H assays, the FtsE-FtsQ interaction has 42.7% β-galactosidase activity and, suggesting the presence of a protein-protein interaction. It is a stronger interaction than the majority of protein-protein interactions studied by B2H in this report, but it is possible that this interaction could be a weak interaction. Affinity chromatography methods, including GST pulldown assays, tend to be biased towards detecting protein-protein interactions that have a high affinity with each other (Berggård *et al.*, 2007; Zhou *et al.*, 2016). In addition, weak interactions may be lost during the washing steps of this assay (Berggård *et al.*, 2007; Luo *et al.*, 2014). Therefore, this method may not ideal for

studying potentially weak protein-protein interactions (Berggård *et al.*, 2007). One such methodology to study weak protein-protein interactions could include BioID (proximity dependent biotin identification). BioID is a type of proximity dependent labelling method where the protein of interest is fused to BirA*, a mutant biotin ligase that attaches a biotin tag to any nearby proteins (Gingras *et al.*, 2019; Smits and Vermeulen, 2016; Varnaitė and MacNeill, 2016). All biotinylated proteins are then collected and identified through mass spectrometry (Gingras *et al.*, 2019; Varnaitė and MacNeill, 2016). This method could be able to identify any transient or weak interactions that cannot be identified using affinity purification techniques where weak interactions may be washed away (Berggård *et al.*, 2007; Gingras *et al.*, 2019; Varnaitė and MacNeill, 2016).

4.3 AP-MS Assay to Identifying Interacting Partners of FtsE

4.3.1 Potential Interactions Between FtsE and Cell Division Proteins Identified by AP-MS Experiments

B2H experiments performed in this thesis indicated that FtsE interacts with itself, FtsX and FtsQ. The AP-MS experiments were performed in this thesis to observe and/or confirm some of these interactions and potentially identify new protein-protein interactions. However, FtsQ was not identified during these experiments, and, therefore, the FtsE-FtsQ interaction observed in B2H assays could not be confirmed.

According to AP-MS experiments, there were four proteins that are probable interacting partners of FtsE (Table 3.3.1). These four proteins include: FtsI, a cell division protein that has homology to a SPOR domain protein (most likely FtsN) and the two putative cell division proteins which are homologous to FtsK. Interactions between FtsE with FtsI, FtsN or FtsK were not observed in B2H experiments performed in this thesis. However, the absence of these interactions may be because FtsX was not co-expressed during the B2H assays. As discussed above, the co-expression of FtsX has been found to improve the results of B2H assays involving FtsE (Du *et al.*, 2019). Future experiments could examine whether the co-expression of FtsX would improve the interactions between FtsE and FtsI, FtsN or FtsK.

B2H experiments also showed that FtsE is able to self-interact. However, based on the current AP-MS experimental design, the ability for FtsE to self-interact could not be confirmed. The amount of FtsE peptides identified in the interaction sample A3B3 (i.e., GST-FtsE + *N. gonorrhoeae* lysate) is larger in comparison to the amount of FtsE peptides identified in the

negative controls A1B1 (i.e., resin + *N. gonorrhoeae* lysate) or A2B2 (i.e., resin + GST + *N. gonorrhoeae* lysate) (Table B.1). However, the increased number of peptides identified in the interaction sample is most likely due to the addition of the bait protein GST-FtsE. Therefore, the current experimental design cannot conclude whether dimerization has occurred between GST-FtsE and any FtsE proteins from the *N. gonorrhoeae* lysate. Future experiments should consider the addition of a negative control containing resin and GST-FtsE as this could provide a baseline level for how much GST-FtsE can be identified by mass spectrometry without the *N. gonorrhoeae* whole cell lysate present. Therefore, if there are more FtsE peptides identified in the resin + GST-FtsE + *N. gonorrhoeae* lysate interaction sample than in the resin + GST-FtsE control, this might suggest the presence of a FtsE self-interaction.

As discussed previously, there is a severe lack of knowledge concerning the ability for *E. coli* FtsE to interact with other cell division proteins. The only interactions identified for *E. coli* FtsE are the FtsE self-interaction and the FtsE-FtsX and FtsE-FtsZ interactions (Corbin *et al.*, 2007; de Leeuw *et al.*, 1999). The interactions of *E. coli* FtsE with FtsI, FtsN and FtsK have not been investigated previously. Therefore, whether these interactions are common to both *E. coli* and *N. gonorrhoeae* cannot be determined.

Many of the cell division proteins that are considered probable interacting partners of FtsE have a spectral count in the interaction sample A3B3 that is only one to four values larger than the spectral count of the negative controls (Table 3.3.1). The low number of spectral count values for a majority of the cell division proteins identified in AP-MS experiments could be caused by the following factors. First, many of the cell division proteins are membrane proteins that may have been lost during sonication and centrifugation to generate the *N. gonorrhoeae* whole cell lysate. In the future, a method to collect the membrane proteins of *N. gonorrhoeae* whole cell lysate and use these proteins during AP-MS experiments could be examined. This could allow the cell division proteins more ability to interact with each other without other proteins that are not usually found in the same cellular location to also be there. A protocol to collect the inner membrane proteins of Gram-negative bacterium is described by Cian *et al*. (Cian *et al.*, 2020).

Second, the low number of cell division proteins identified may be due to the design of the affinity purification experiment. In my experimental design, GST-FtsE and *N. gonorrhoeae* whole cell lysate were purified separately and then combined in an *in vitro* assay to study potential

interactions. This may have influenced the amount of cell division proteins identified as potential interacting partners since the bait was not expressed in its native environment and allowed to interact with other proteins within the cell. Thus, AP-MS experiments might be performed where the GST-tagged bait protein is expressed in *N. gonorrhoeae*, allowing for the bait protein to interact with prey proteins *in vivo*. After lysis of the host cell the bait protein and its interacting protein partners would be purified away from the background cellular proteins through affinity purification (Dunham *et al.*, 2012; Gingras *et al.*, 2007).

4.3.2 STRING Analysis to Predict Potential Interactions Amongst Proteins Identified During AP-MS Experiments

STRING was used to predict potential interactions among proteins identified during AP-MS experiments, with a specific focus on the potential interactions between cell division proteins (Figure 3.3.2). The STRING network map in Figure 3.3.2 (and Figure B.4) provides the predicted interactions of all cell division proteins identified during AP-MS experiments, plus the addition of the three cell division proteins that were not identified in these experiments (e.g., FtsQ, FtsL, FtsW). Several predicted interactions observed in Figure 3.3.2 that have also been identified through experimental methods such as B2H or GST pulldowns in *N. gonorrhoeae* including: FtsZ-FtsA, FtsA-FtsI, FtsW-FtsI, MinC-MinD and MinC-FtsZ (Greco-Stewart *et al.*, 2007; Zou *et al.*, 2017a). In addition, some of the predictions in the STRING map (Figure 3.3.2) agree with B2H data reported in this thesis, including the FtsB-FtsZ and FtsE-FtsX interactions. However, there were also several experimentally determined interactions between proteins that were not seen in the STRING network map (Figure 3.3.2), including: FtsA-FtsK and FtsK-FtsN (Zou *et al.*, 2017a). The B2H experiments performed in this thesis identified several interactions that were also not predicted by STRING (Figure 3.3.2), including: FtsX-FtsW, FtsX-FtsL and FtsX-FtsN. Additionally, the AP-MS experiment performed in this thesis appears to suggest interactions of FtsE with FtsI, FtsN and FtsK, but none of these interactions are observed in either the B2H experiments reported in this thesis or in the STRING network map (Figure 3.3.2). Therefore, while some of the experimentally identified interactions amongst *N. gonorrhoeae* cell division proteins were also predicted by STRING, others were not (Figure 3.3.2).

Contradictions regarding putative interactions may be due to the STRING software itself. STRING is an online database that collects publicly available data regarding protein-protein interactions from several sources, including text-mining, biochemical experimental data, genomic

context information, gene co-expression, and databases of protein-complexes. This collection of publicly available data is then used to computationally predict protein-protein interactions (Szklarczyk *et al.*, 2019). Each data source contains information from two subsections, one that contains the data for the organism of interest and the other is data observed in other organisms, like *E. coli* (Szklarczyk *et al.*, 2019). There is no *N. gonorrhoeae* specific protein-protein interaction data in the *N. gonorrhoeae* subsection of the experimental data source, such as data published by Zou *et al.* or Greco-Stewart *et al.* regarding protein-protein interactions amongst *N. gonorrhoeae* cell division proteins (i.e., FtsZ-FtsA, FtsW-FtsI, FtsZ-MinC, etc.) (Greco-Stewart *et al.*, 2007; Zou *et al.*, 2017a). Therefore, the predicted interactions seen in Figure 3.3.2 are based solely on the experimental data subsection that reports similar interactions in other organisms, such as *E. coli*. However, as discussed above, the *N. gonorrhoeae* protein-protein interaction network is unique because many interactions have been identified in *N. gonorrhoeae* that are not observed in *E. coli* (Zou *et al.*, 2017a). This may be the reason why STRING cannot predict several experimentally identified interactions reported in either this thesis (i.e., FtsX-FtsW, FtsX-FtsL) or by Zou *et al.* (i.e., FtsK-FtsN) because these interactions are unique to *N. gonorrhoeae* (Zou *et al.*, 2017a).

STRING can be a helpful tool that can provide several options regarding potential protein-protein interactions to examine because this software is able to combine data from multiple sources to predict interactions amongst a given set of proteins (Szklarczyk *et al.*, 2019). Therefore, STRING is able to predict interactions between proteins of interest that may not have been considered previously, such as FtsX-FtsL. These interactions may or may not occur in *N. gonorrhoeae,* but they are potential avenues of interest that would then be later verified with either *in vivo* or *in vitro* experiments. B2H experiments could be used as a method to screen several of these interactions quickly and then either BioID or GST pulldown experiments could be used to further verify the interactions.

4.3.3 A Limitation to the Uniprot Database for Use in Identifying Proteins

The number of reviewed proteins for an organism of interest can be a limitation when using the Uniprot database. For example, the *N. gonorrhoeae* database is not as well annotated as the *E. coli* database on Uniprot. When '*Neisseria gonorrhoeae*' is used as the search term on the Uniprot website and results are filtered to only include reviewed proteins, then there are 423 reviewed

proteins for NEIG1 (i.e., *N. gonorrhoeae* strain FA1090). In contrast, when the same search parameters are applied to the search term '*Escherichia coli*', then there are 4,529 reviewed proteins that are listed for *E. coli* strain K-12. The smaller number of *N. gonorrhoeae* proteins available on the Uniprot database may introduce a bias during peptide identification following mass spectrometry because there are proteins that may not be annotated in the database. Therefore, if a peptide cannot be matched to a protein provided in the database, then this protein is left unidentified. In addition, there were a handful of proteins that were identified on Uniprot, but as an 'uncharacterized protein'. The role and/or function of these uncharacterized proteins are not known, so the reason behind its interaction with the cell division protein FtsE cannot be determined.

4.4 *N. gonorrhoeae* Protein-Protein Interaction Map

The protein-protein interactions amongst *N. gonorrhoeae* cell division proteins FtsZ, FtsA, ZipA, FtsK, FtsQ, FtsL, FtsB, FtsW, FtsI and FtsN have been previously studied through B2H, GST pulldowns and surface plasmon resonance (Zou *et al.*, 2017a). A protein-protein interaction map was created for *N. gonorrhoeae* using the data reported by Zou *et al.* (Figure 1.2.5.3) (Zou *et al.*, 2017a). However, this interaction network lacked data pertaining to both potential interactions of FtsE, FtsX, FtsL and FtsB with the above *N. gonorrhoeae* cell division proteins and the self-interactions of these cell division proteins. Figure 4.4 summarizes the current knowledge of protein-protein interactions amongst *N. gonorrhoeae* divisome proteins and demonstrates both the present results from investigations in this thesis and the previous results from the investigation by Zou *et al.* (Figure 4.4) (Zou *et al.*, 2017a). The FtsE-FtsQ interaction is indicated by a dashed line to reflect the contradictory results between B2H assays and GST pulldown experiments because this interaction was identified during B2H assays but could not be observed in GST pulldown experiments. This expanded interactome now includes interactions between all 12 gonococcal divisome proteins and the self-interactions of these 12 divisome proteins.

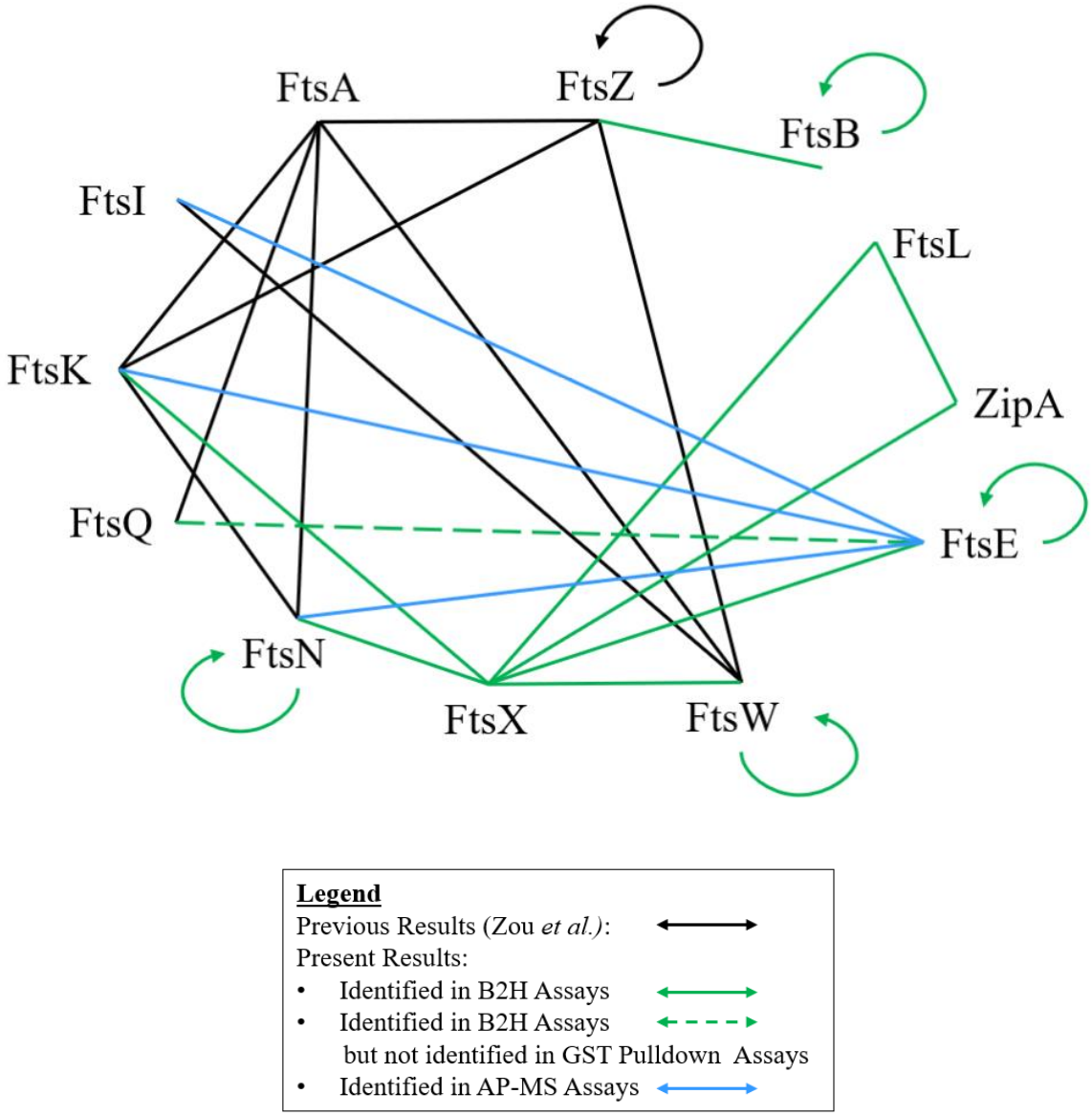

Figure 4.4: Interaction Map for *N. gonorrhoeae* Cell Division Proteins. The map demonstrates both the interactions that have been identified amongst the *N. gonorrhoeae* cell division proteins in this thesis (present results) and the interactions that have been identified by Zou *et al.* (previous results) (Zou *et al.*, 2017a). Present interaction results reported in this thesis are indicated in green (B2H results) or blue (AP-MS results). The presence of the FtsE-FtsQ interaction during B2H assays but the absence of this interaction in GST pulldown assays is represented by a green, dashed line. Previous interaction results reported by Zou *et al.* are indicated in black (Zou *et al.*, 2017a). Self-interactions are indicated by curved arrows.

The protein-protein interactions examined amongst *N. gonorrhoeae* divisome proteins (Figure 4.4) can be compared to the protein-protein interactions examined amongst *E. coli* divisome proteins (Figure 1.2.4.4 and Table 1.2.4.5). Table 4.4.1 provides a summary the comparison of the protein-protein interactions amongst the 12 divisome proteins of *E. coli* and *N. gonorrhoeae*. The protein-protein interactions amongst *E. coli* divisome proteins were examined in several studies and are described in further detail in Figure 1.2.4.4 and Table 1.2.4.5 (Alexeeva *et al.*, 2010; Berezuk *et al.*, 2018, 2020; Buddelmeijer and Beckwith, 2004; Busiek *et al.*, 2012; Corbin et al., 2007; Di Lallo *et al.*, 2003; Du *et al.*, 2016; D'Ulisse *et al.*, 2007; Fraipont *et al.*, 2011; Karimova *et al.*, 2005; LaPointe *et al.*, 2013; de Leeuw *et al.*, 1999; Liu *et al.*, 1999; Maggi *et al.*, 2008; Mukherjee and Lutkenhaus, 1994; Park *et al.*, 2021; Pichoff and Lutkenhaus, 2002; Skoog and Daley, 2012; Vega and Margolin, 2018; Yim *et al.*, 2000). The protein-protein interactions amongst the corresponding *N. gonorrhoeae* proteins were examined in this thesis and by Zou *et al.* (Zou *et al.*, 2017a). Table 4.4.1 shows that there are 12 interactions common (blue) to both *E. coli* and *N. gonorrhoeae*: FtsZ-FtsA, FtsZ-FtsK, FtsA-FtsK, FtsA-FtsQ, FtsA-FtsW, FtsA-FtsN, FtsE-FtsX, FtsW-FtsI, and the self-interactions of FtsZ, FtsE, FtsB and FtsN. Meanwhile, there are 14 interactions that were identified in *N. gonorrhoeae* alone (green): FtsZ-FtsB, FtsZ-FtsW, ZipA-FtsX, ZipA-FtsL, FtsE-FtsK, FtsE-FtsQ, FtsE-FtsI, FtsE-FtsN, FtsX-FtsK, FtsX-FtsL, FtsX-FtsW, FtsX-FtsN, FtsK-FtsN, and the FtsW self-interaction. The remaining interactions summarized in Table 4.4.1 are either unique to *E. coli*, have not been examined in *E. coli*, or are not observed in either organism. The large number of unique interactions amongst *N. gonorrhoeae* cell division proteins supports the previous finding that *N. gonorrhoeae* and its cell division proteins may form unique interactions as compared to the model organism *E. coli* (Zou *et al.*, 2017a).

Table 4.4.1: Comparison of the Protein-Protein Interactions Examined Amongst *E. coli* and *N. gonorrhoeae* Cell Division Proteins

Ec \ Ng	FtsZ	FtsA	ZipA	FtsE	FtsX	FtsK	FtsQ	FtsL	FtsB	FtsW	FtsI	FtsN
FtsZ	+ / +											
FtsA	+ / +	- / +										
ZipA	- / +	- / +	- / +									
FtsE	- / +	- / -	- / NT	+ / +								
FtsX	- / -	- / +	+ / NT	+ / +	- / -							
FtsK	+ / +	+ / +	- / -	+/- / NT	+ / NT	- / NT						
FtsQ	- / -	+ / +	- / -	+/- / NT	- / +	- / +	- / +					
FtsL	- / -	- / -	+ / -	- / NT	+ / -	- / +	- / +	- / -				
FtsB	+ / -	- / -	- / NT	- / NT	- / -	- / -	- / +	- / +	+ / +			
FtsW	+ / -	+ / +	- / -	- / NT	+ / -	- / -	- / +	- / +	- / -	+ / -		
FtsI	- / -	- / +	- / -	+/- / NT	- / -	- / +	- / +	- / +	- / +	+ / +	- / +	
FtsN	- / -	+ / +	- / -	+/- / NT	+ / -	+ / -	- / +	- / -	- / -	- / +	- / +	+ / +

NT = interaction has not tested; + = interaction has been examined and is present;
- = interaction has been examined but is not present
+/- = contradictory results from B2H assays and GST pulldowns or AP-MS experiments
Blue = interactions common to Ec and Ng; green = interactions identified only in Ng

4.5 Conclusion

The interactions of *N. gonorrhoeae* divisome proteins were examined through several methods, including B2H, GST pulldowns and AP-MS. B2H assays were performed to identify previously unknown self-interactions and interactions between gonococcal cell division proteins and the cell division proteins FtsE, FtsX, FtsL and FtsB. The B2H assays revealed the presence of nine protein-protein interactions (i.e., FtsE-FtsX, FtsE-FtsQ, FtsL-FtsX, FtsL-ZipA, FtsX-ZipA, FtsX-FtsK, FtsX-FtsW, FtsX-FtsN and FtsB-FtsZ) and the self-interactions of the cell division proteins FtsE, FtsW, FtsB, FtsN. Of the 13 interactions identified through B2H assays, only the FtsE-FtsX interaction and the self-interactions of FtsE, FtsB and FtsN are common to both *N. gonorrhoeae* and *E. coli*. GST pulldowns were performed to further study the FtsE-FtsQ interaction that was identified through B2H assays. However, a FtsE-FtsQ interaction was not observed,

suggesting that FtsE and FtsQ do not interact. This could be due to non-optimal experimental conditions or, perhaps, a different biochemical method should be used to further study the interaction. In addition, affinity purification mass spectrometry experiments were performed to identify potential interactions between *N. gonorrhoeae* FtsE and proteins from an *N. gonorrhoeae* CH811 whole cell lysate. The AP-MS experiments identified probable interactions between FtsE and the cell division proteins FtsI, FtsN and FtsK that were not observed during B2H assays performed in this work. As the interactions of *E. coli* FtsE with $FtsI_{Ec}$, $FtsN_{Ec}$ and $FtsK_{Ec}$ have not been examined, it cannot be determined whether these interactions identified during AP-MS experiments are common to *E. coli* and *N. gonorrhoeae*. In addition, a STRING analysis was performed to predict potential interactions amongst the proteins identified during AP-MS experiments. This STRING analysis predicted several interactions of interest, including the FtsE-FtsX and FtsB-FtsZ interactions that were also identified during B2H assays performed in this thesis.

In all, the interactions of *N. gonorrhoeae* FtsE, FtsX, FtsL and FtsB were examined in this thesis and several previously unknown protein-protein interactions were identified. The work in this thesis supports previous findings that the cell division proteins for the non-model organism *N. gonorrhoeae* exhibit unique protein-protein interactions not observed in the Gram-negative model organism *E. coli*. Therefore, further research of non-model organisms is crucial to expanding the knowledge regarding how various cellular mechanisms, such as cell division, are performed.

APPENDICES

Appendix A: Detailed B2H Methodology

B2H experiments have at least eight samples for every protein-protein interaction studied: one positive control, four negative controls, one baseline control and two samples for the protein-protein interaction of interest. For this study, the *N. gonorrhoeae* FtsZ self-interaction was used as a positive control. The four negative controls are the genes for the protein of interest cloned into either pcI_{p22} and pcI_{434} vectors and transformed into *E. coli* R721 singly (i.e., pcI_{p22}-FtsE, pcI_{434}-FtsZ, pcI_{p22}-FtsZ, and pcI_{434}-FtsE). The negative controls ensure one of the proteins of interest is not binding to the hybrid operator on its own and generating a false positive result. A baseline control is also used for B2H experiments. The baseline control is *E. coli* R721 lacking any plasmids as this reports the base level of β-galactosidase produced. This baseline control is used as the comparison for all the samples and controls. Lastly, B2H experiments have two samples for the protein-protein interaction of interest, one known as the forward reaction and the other as the reverse interaction (i.e., pcI_{p22}-FtsE + pcI_{434}-FtsZ and pcI_{p22}-FtsZ + pcI_{434}-FtsE).

Experimental Tips

E. coli samples are grown at 34°C until OD_{600} reads at least 0.2. According to the protocol by Platt *et al.*, the bacteria should be in their exponential growth phase so that the β-galactosidase assay can be performed with precision (Platt *et al.*, 1972). If the recorded OD_{600} is greater than 0.7, the experiment should be restarted. Once the samples have reached the range of 0.2-0.7 OD_{600}, the cultures are standardized to a common OD_{600} and the experiment can proceed.

Additional B2H Data

The B2H data provided in the results section is a summary of the β-galactosidase activity for each interaction. For each interaction there was a graph made for the average β-galactosidase activity for all samples across both replicates. These graphs are included for all samples below in Figure A.1.

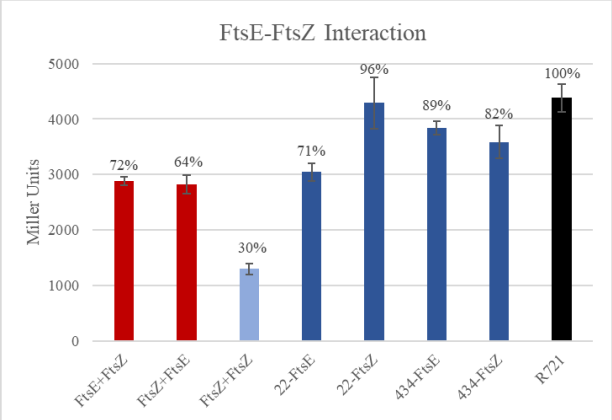
FtsE-FtsZ Interaction
Miller Units
5000
4000
3000
2000
1000
0
72%
64%
30%
71%
96%
89%
82%
100%
FtsE+FtsZ
FtsZ+FtsE
FtsZ+FtsZ
22-FtsE
22-FtsZ
434-FtsE
434-FtsZ
R721

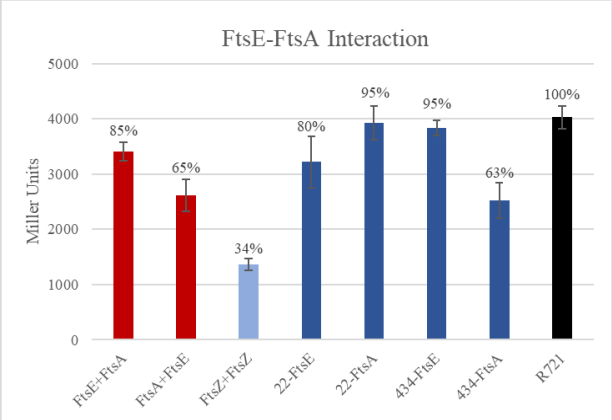
FtsE-FtsA Interaction
Miller Units
5000
4000
3000
2000
1000
0
85%
65%
34%
80%
95%
95%
63%
100%
FtsE+FtsA
FtsA+FtsE
FtsZ+FtsZ
22-FtsE
22-FtsA
434-FtsE
434-FtsA
R721

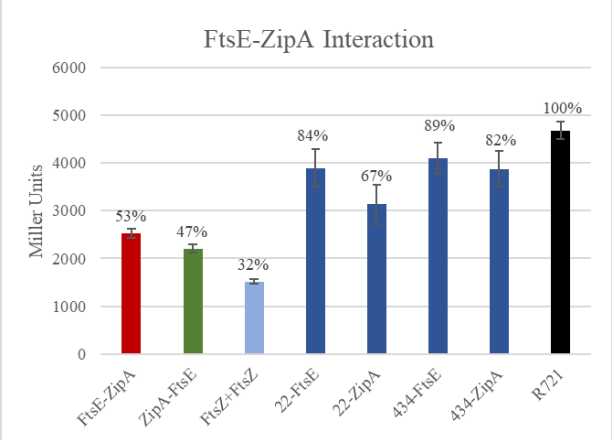
FtsE-ZipA Interaction
Miller Units
6000
5000
4000
3000
2000
1000
0
53%
47%
32%
84%
67%
89%
82%
100%
FtsE-ZipA
ZipA-FtsE
FtsZ+FtsZ
22-FtsE
22-ZipA
434-FtsE
434-ZipA
R721

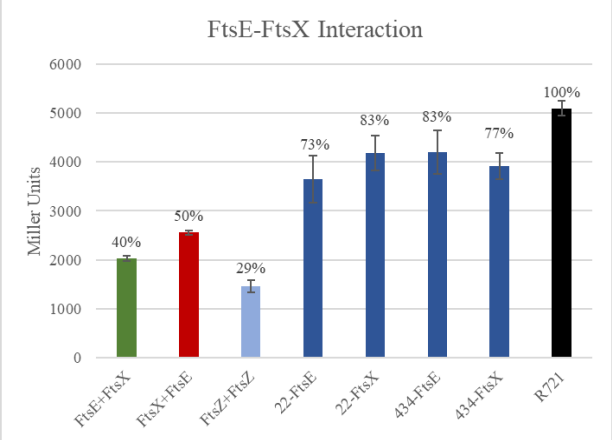
FtsE-FtsX Interaction
Miller Units
6000
5000
4000
3000
2000
1000
0
40%
50%
29%
73%
83%
83%
77%
100%
FtsE+FtsX
FtsX+FtsE
FtsZ+FtsZ
22-FtsE
22-FtsX
434-FtsE
434-FtsX
R721

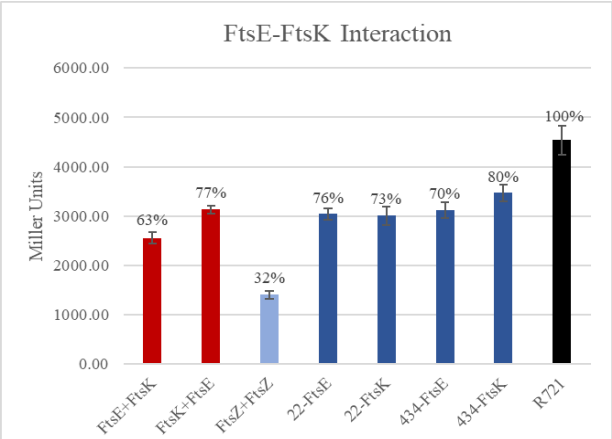
FtsE-FtsK Interaction
Miller Units
6000.00
5000.00
4000.00
3000.00
2000.00
1000.00
0.00
63%
77%
32%
76%
73%
70%
80%
100%
FtsE+FtsK
FtsK+FtsE
FtsZ+FtsZ
22-FtsE
22-FtsK
434-FtsE
434-FtsK
R721

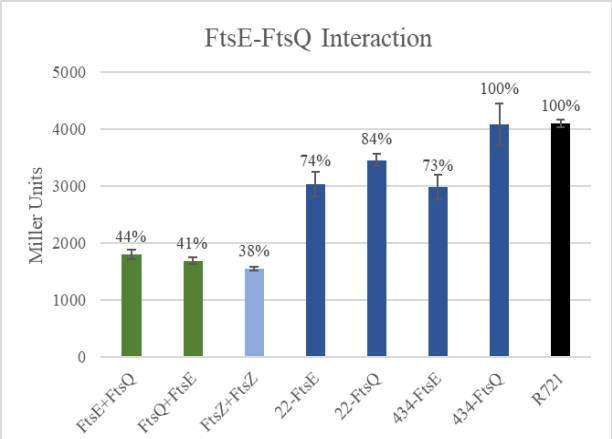
FtsE-FtsQ Interaction
Miller Units
5000
4000
3000
2000
1000
0
44%
41%
38%
74%
84%
73%
100%
100%
FtsE+FtsQ
FtsQ+FtsE
FtsZ+FtsZ
22-FtsE
22-FtsQ
434-FtsE
434-FtsQ
R721

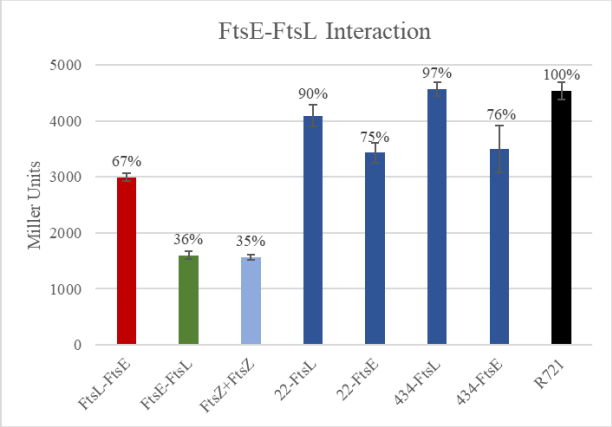
FtsE-FtsL Interaction
Miller Units
5000
4000
3000
2000
1000
0
67%
36%
35%
90%
75%
97%
76%
100%
FtsL-FtsE
FtsE-FtsL
FtsZ+FtsZ
22-FtsL
22-FtsE
434-FtsL
434-FtsE
R721

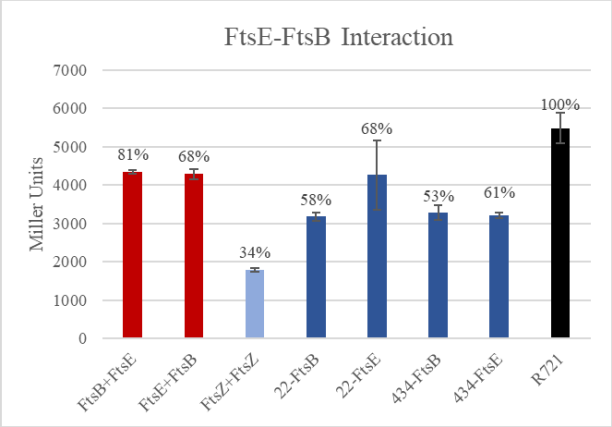
FtsE-FtsB Interaction
Miller Units
7000
6000
5000
4000
3000
2000
1000
0
81%
68%
34%
58%
68%
53%
61%
100%
FtsB+FtsE
FtsE+FtsB
FtsZ+FtsZ
22-FtsB
22-FtsE
434-FtsB
434-FtsE
R721

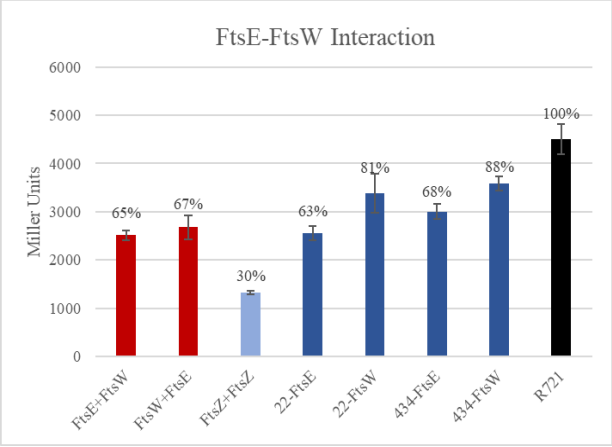
FtsE-FtsW Interaction
Miller Units
6000
5000
4000
3000
2000
1000
0
65%
67%
30%
63%
81%
68%
88%
100%
FtsE+FtsW
FtsW+FtsE
FtsZ+FtsZ
22-FtsE
22-FtsW
434-FtsE
434-FtsW
R721

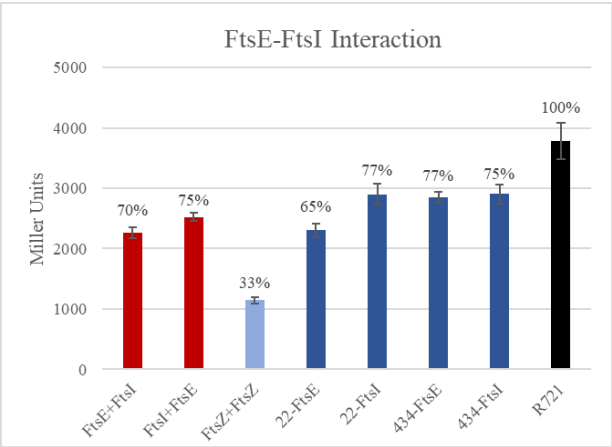
FtsE-FtsI Interaction
Miller Units
5000
4000
3000
2000
1000
0
70%
75%
33%
65%
77%
77%
75%
100%
FtsE+FtsI
FtsI+FtsE
FtsZ+FtsZ
22-FtsE
22-FtsI
434-FtsE
434-FtsI
R721

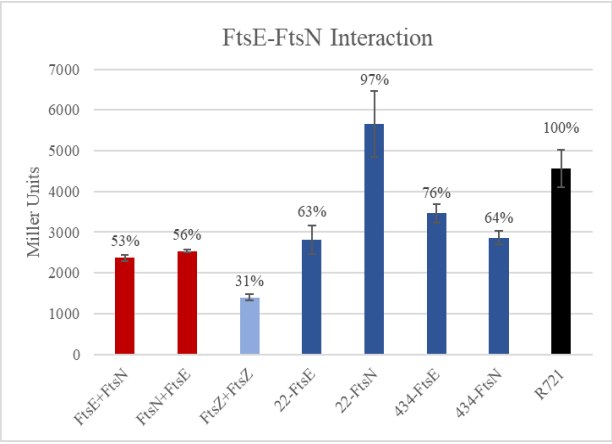
FtsE-FtsN Interaction
Miller Units
7000
6000
5000
4000
3000
2000
1000
0
53%
56%
31%
63%
97%
76%
64%
100%
FtsE+FtsN
FtsN+FtsE
FtsZ+FtsZ
22-FtsE
22-FtsN
434-FtsE
434-FtsN
R721

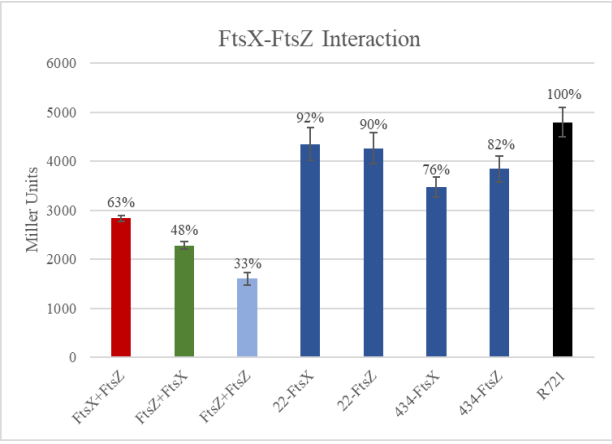
FtsX-FtsZ Interaction
Miller Units
6000
5000
4000
3000
2000
1000
0
63%
48%
33%
92%
90%
76%
82%
100%
FtsX+FtsZ
FtsZ+FtsX
FtsZ+FtsZ
22-FtsX
22-FtsZ
434-FtsX
434-FtsZ
R721

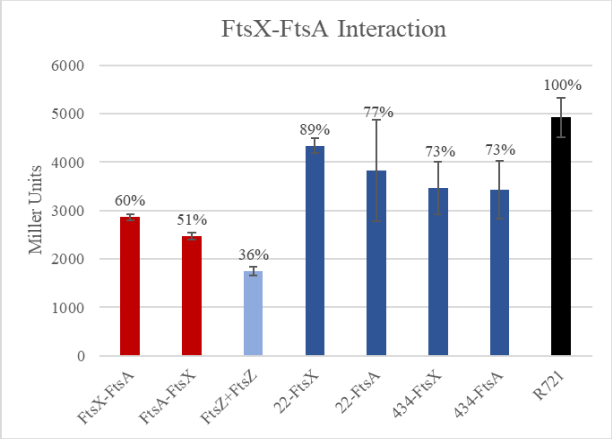
FtsX-FtsA Interaction
Miller Units
6000
5000
4000
3000
2000
1000
0
60%
51%
36%
89%
77%
73%
73%
100%
FtsX-FtsA
FtsA-FtsX
FtsZ-FtsZ
22-FtsX
22-FtsA
434-FtsX
434-FtsA
R721

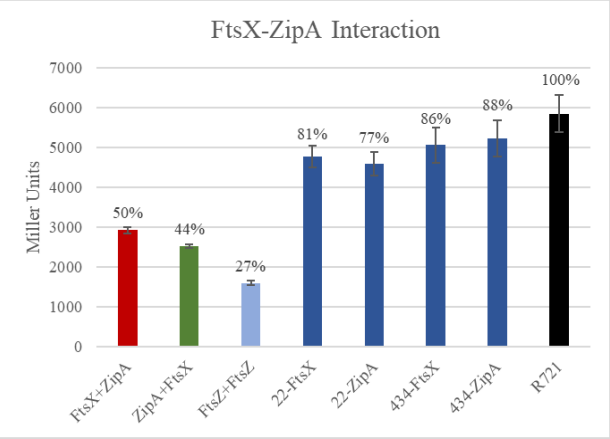
FtsX-ZipA Interaction
Miller Units
7000
6000
5000
4000
3000
2000
1000
0
50%
44%
27%
81%
77%
86%
88%
100%
FtsX-ZipA
ZipA-FtsX
FtsZ-FtsZ
22-FtsX
22-ZipA
434-FtsX
434-ZipA
R721

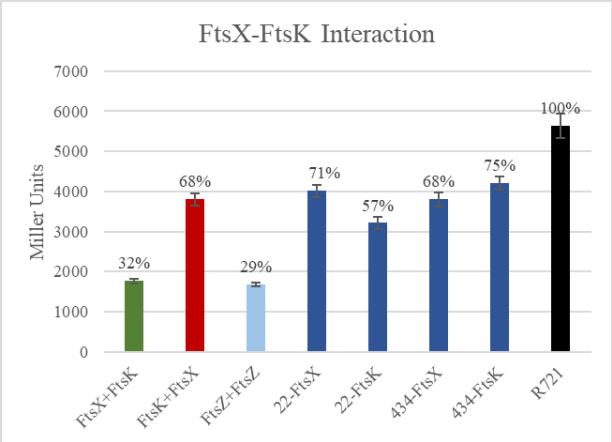
FtsX-FtsK Interaction
Miller Units
7000
6000
5000
4000
3000
2000
1000
0
32%
68%
29%
71%
57%
68%
75%
100%
FtsX-FtsK
FtsK-FtsX
FtsZ-FtsZ
22-FtsX
22-FtsK
434-FtsX
434-FtsK
R721

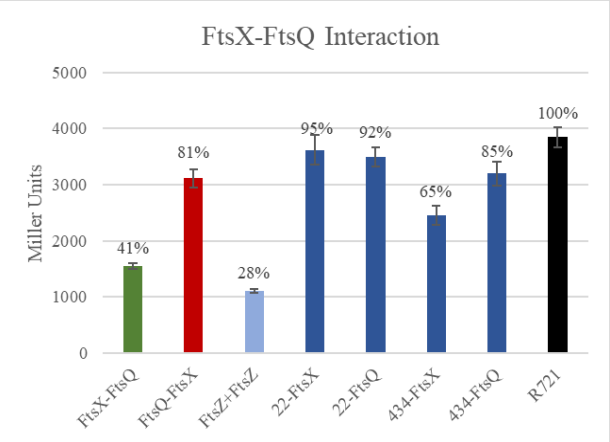
FtsX-FtsQ Interaction
Miller Units
5000
4000
3000
2000
1000
0
41%
81%
28%
95%
92%
65%
85%
100%
FtsX-FtsQ
FtsQ-FtsX
FtsZ-FtsZ
22-FtsX
22-FtsQ
434-FtsX
434-FtsQ
R721

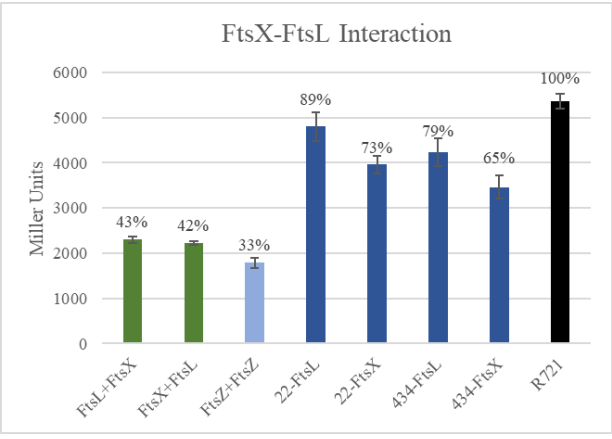
FtsX-FtsL Interaction
Miller Units
6000
5000
4000
3000
2000
1000
0
43%
42%
33%
89%
73%
79%
65%
100%
FtsL-FtsX
FtsX-FtsL
FtsZ-FtsZ
22-FtsL
22-FtsX
434-FtsL
434-FtsX
R721

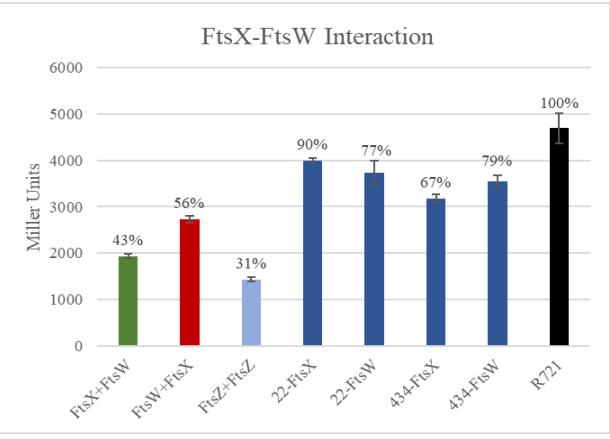
FtsX-FtsW Interaction
Miller Units
6000
5000
4000
3000
2000
1000
0
43%
56%
31%
90%
77%
67%
79%
100%
FtsX-FtsW
FtsW-FtsX
FtsZ-FtsZ
22-FtsX
22-FtsW
434-FtsX
434-FtsW
R721

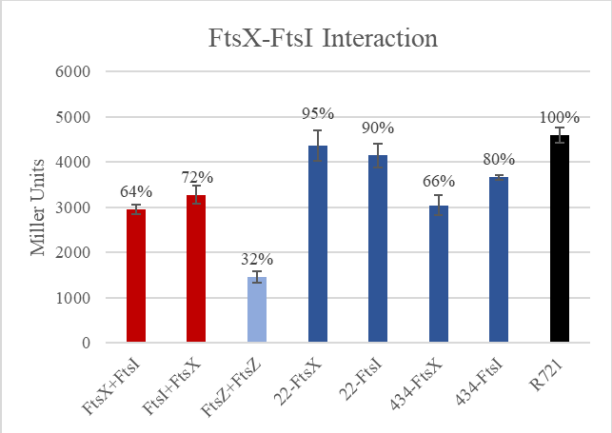
FtsX-FtsI Interaction
Miller Units
6000
5000
4000
3000
2000
1000
0
64%
72%
32%
95%
90%
66%
80%
100%
FtsX+FtsI
FtsI+FtsX
FtsZ+FtsZ
22-FtsX
22-FtsI
434-FtsX
434-FtsI
R721

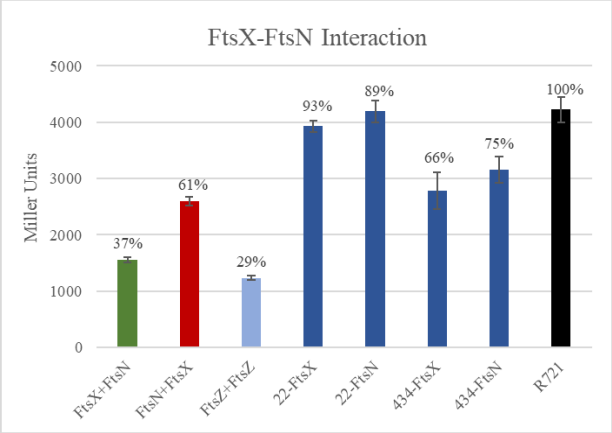
FtsX-FtsN Interaction
Miller Units
5000
4000
3000
2000
1000
0
37%
61%
29%
93%
89%
66%
75%
100%
FtsX+FtsN
FtsN+FtsX
FtsZ+FtsZ
22-FtsX
22-FtsN
434-FtsX
434-FtsN
R721

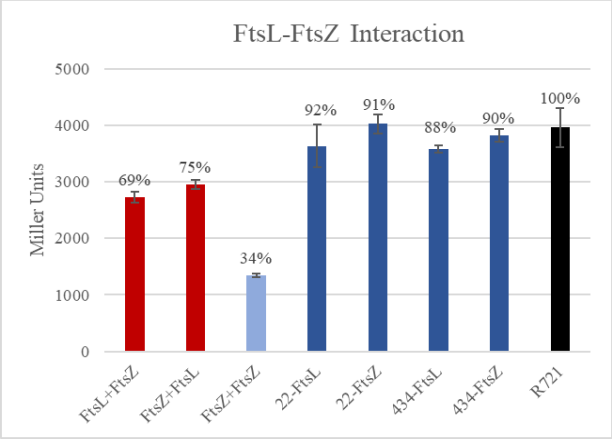
FtsL-FtsZ Interaction
Miller Units
5000
4000
3000
2000
1000
0
69%
75%
34%
92%
91%
88%
90%
100%
FtsL+FtsZ
FtsZ+FtsL
FtsZ+FtsZ
22-FtsL
22-FtsZ
434-FtsL
434-FtsZ
R721

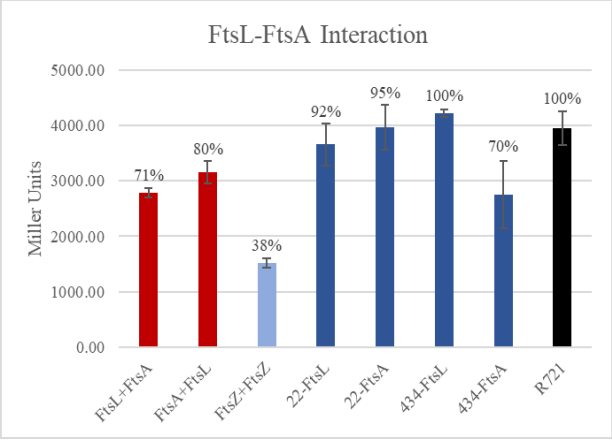
FtsL-FtsA Interaction
Miller Units
5000.00
4000.00
3000.00
2000.00
1000.00
0.00
71%
80%
38%
92%
95%
100%
70%
100%
FtsL+FtsA
FtsA+FtsL
FtsZ+FtsZ
22-FtsL
22-FtsA
434-FtsL
434-FtsA
R721

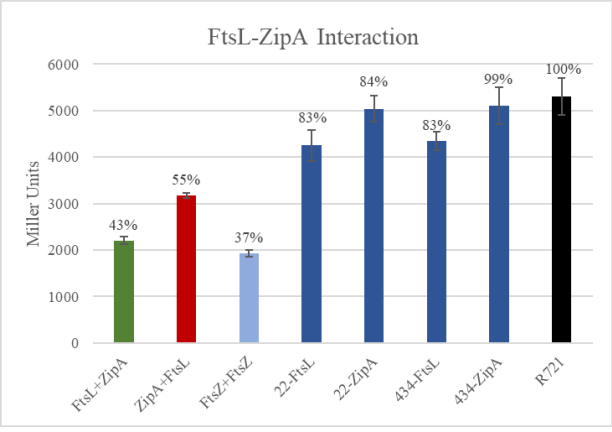
FtsL-ZipA Interaction
Miller Units
6000
5000
4000
3000
2000
1000
0
43%
55%
37%
83%
84%
83%
99%
100%
FtsL+ZipA
ZipA+FtsL
FtsZ+FtsZ
22-FtsL
22-ZipA
434-FtsL
434-ZipA
R721

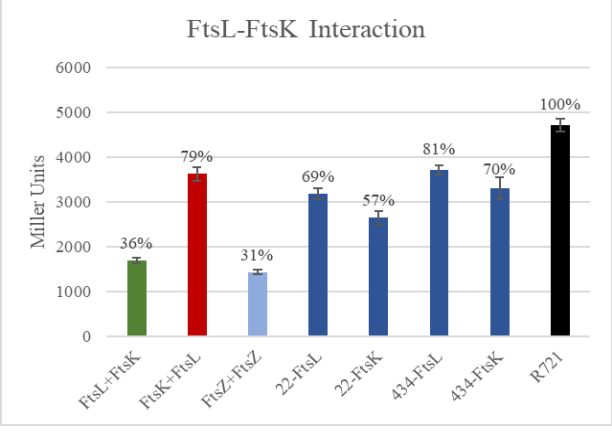
FtsL-FtsK Interaction
Miller Units
6000
5000
4000
3000
2000
1000
0
36%
79%
31%
69%
57%
81%
70%
100%
FtsL+FtsK
FtsK+FtsL
FtsZ+FtsZ
22-FtsL
22-FtsK
434-FtsL
434-FtsK
R721

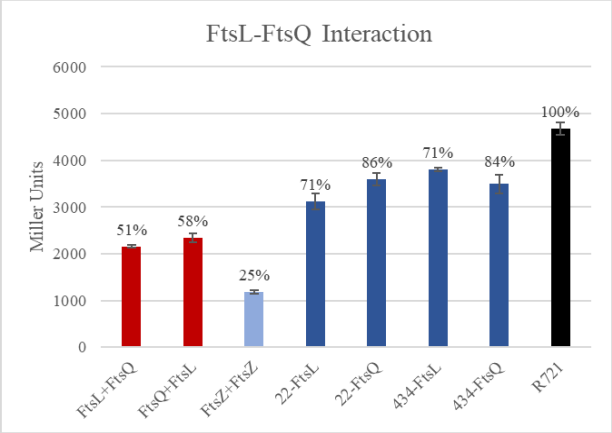
FtsL-FtsQ Interaction
Miller Units
6000
5000
4000
3000
2000
1000
0
51%
58%
25%
71%
86%
71%
84%
100%
FtsL+FtsQ
FtsQ+FtsL
FtsZ+FtsZ
22-FtsL
22-FtsQ
434-FtsL
434-FtsQ
R721

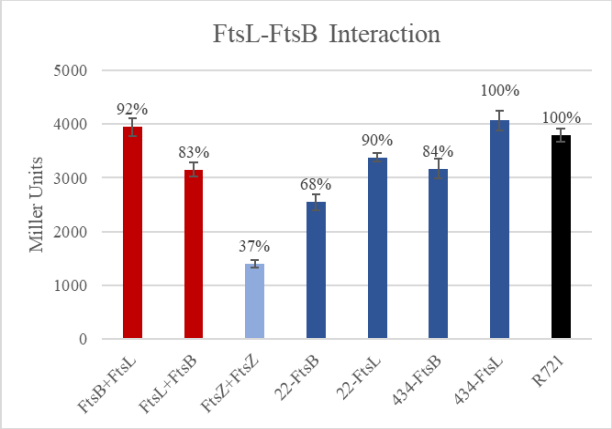
FtsL-FtsB Interaction
Miller Units
5000
4000
3000
2000
1000
0
92%
83%
37%
68%
90%
84%
100%
100%
FtsB+FtsL
FtsL+FtsB
FtsZ+FtsZ
22-FtsB
22-FtsL
434-FtsB
434-FtsL
R721

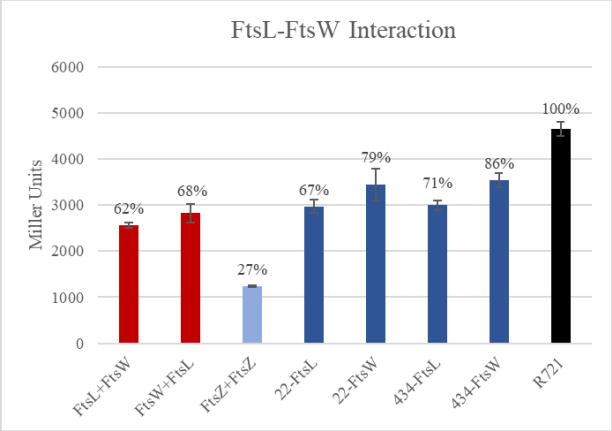
FtsL-FtsW Interaction
Miller Units
6000
5000
4000
3000
2000
1000
0
62%
68%
27%
67%
79%
71%
86%
100%
FtsL+FtsW
FtsW+FtsL
FtsZ+FtsZ
22-FtsL
22-FtsW
434-FtsL
434-FtsW
R721

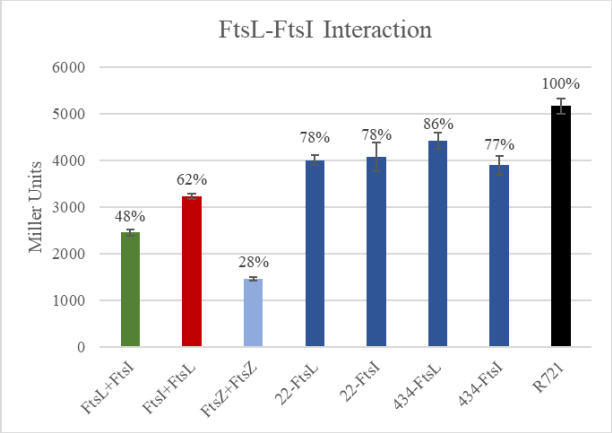
FtsL-FtsI Interaction
Miller Units
6000
5000
4000
3000
2000
1000
0
48%
62%
28%
78%
78%
86%
77%
100%
FtsL+FtsI
FtsI+FtsL
FtsZ+FtsZ
22-FtsL
22-FtsI
434-FtsL
434-FtsI
R721

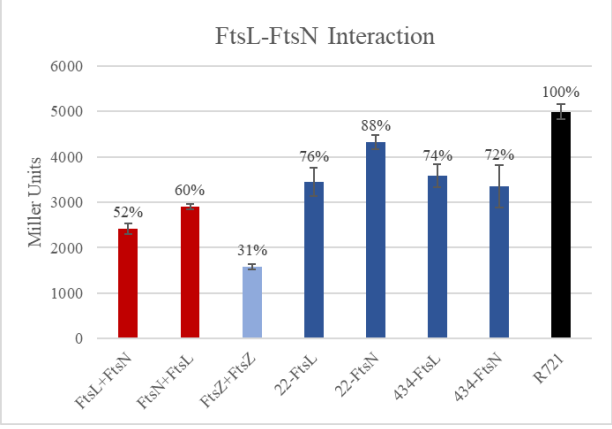
FtsL-FtsN Interaction
Miller Units
6000
5000
4000
3000
2000
1000
0
52%
60%
31%
76%
88%
74%
72%
100%
FtsL+FtsN
FtsN+FtsL
FtsZ+FtsZ
22-FtsL
22-FtsN
434-FtsL
434-FtsN
R721

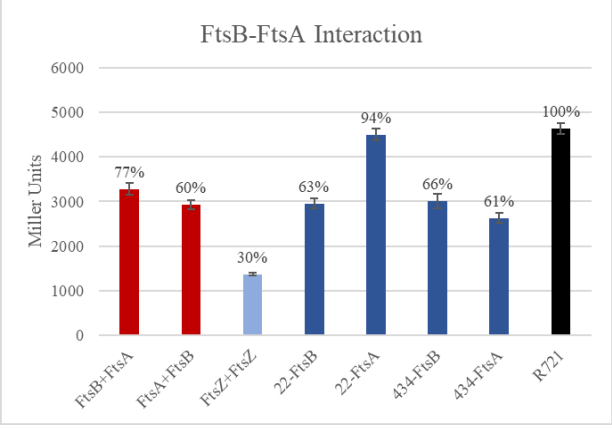
FtsB-FtsA Interaction
Miller Units
6000
5000
4000
3000
2000
1000
0
77%
60%
30%
63%
94%
66%
61%
100%
FtsB+FtsA
FtsA+FtsB
FtsZ+FtsZ
22-FtsB
22-FtsA
434-FtsB
434-FtsA
R721

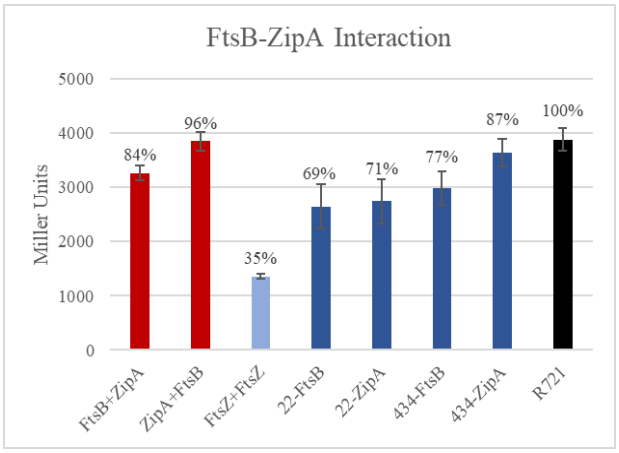
FtsB-ZipA Interaction
Miller Units
5000
4000
3000
2000
1000
0
84%
96%
35%
69%
71%
77%
87%
100%
FtsB+ZipA
ZipA+FtsB
FtsZ+FtsZ
22-FtsB
22-ZipA
434-FtsB
434-ZipA
R721

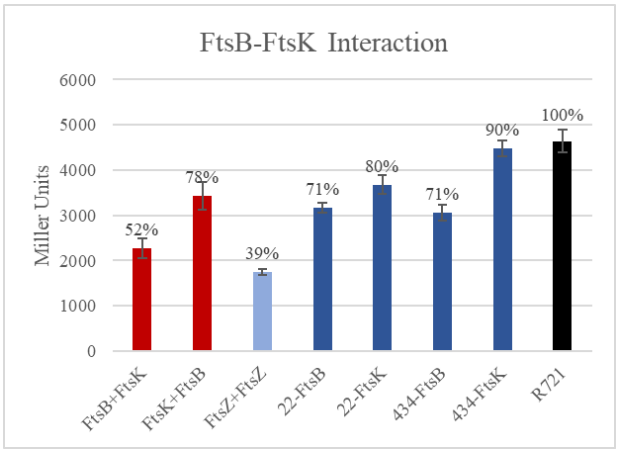
FtsB-FtsK Interaction
Miller Units
6000
5000
4000
3000
2000
1000
0
52%
78%
39%
71%
80%
71%
90%
100%
FtsB+FtsK
FtsK+FtsB
FtsZ+FtsZ
22-FtsB
22-FtsK
434-FtsB
434-FtsK
R721

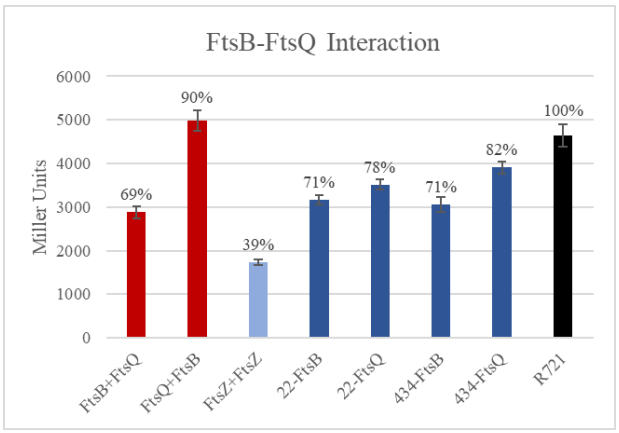
FtsB-FtsQ Interaction
Miller Units
6000
5000
4000
3000
2000
1000
0
69%
90%
39%
71%
78%
71%
82%
100%
FtsB+FtsQ
FtsQ+FtsB
FtsZ+FtsZ
22-FtsB
22-FtsQ
434-FtsB
434-FtsQ
R721

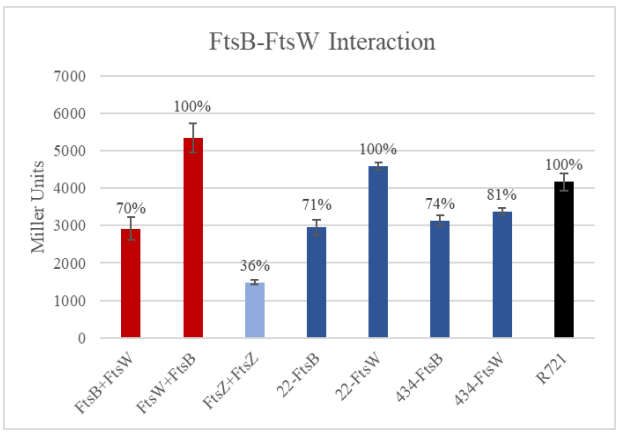
FtsB-FtsW Interaction
Miller Units
7000
6000
5000
4000
3000
2000
1000
0
70%
100%
36%
71%
100%
74%
81%
100%
FtsB+FtsW
FtsW+FtsB
FtsZ+FtsZ
22-FtsB
22-FtsW
434-FtsB
434-FtsW
R721

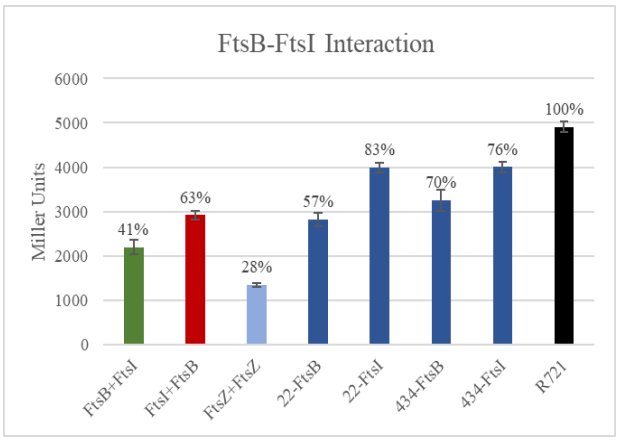
FtsB-FtsI Interaction
Miller Units
6000
5000
4000
3000
2000
1000
0
41%
63%
28%
57%
83%
70%
76%
100%
FtsB+FtsI
FtsI+FtsB
FtsZ+FtsZ
22-FtsB
22-FtsI
434-FtsB
434-FtsI
R721

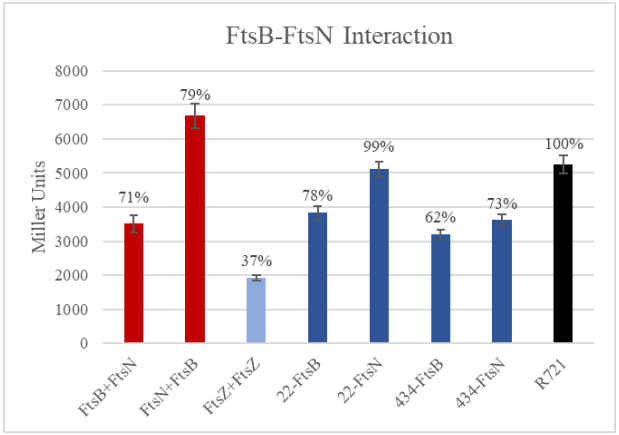
FtsB-FtsN Interaction
Miller Units
8000
7000
6000
5000
4000
3000
2000
1000
0
71%
79%
37%
78%
99%
62%
73%
100%
FtsB+FtsN
FtsN+FtsB
FtsZ+FtsZ
22-FtsB
22-FtsN
434-FtsB
434-FtsN
R721

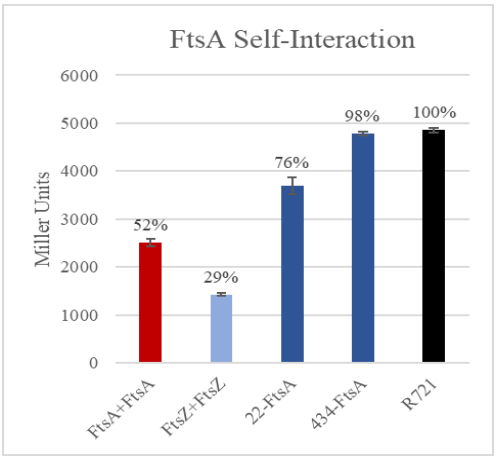
FtsA Self-Interaction
Miller Units
6000
5000
4000
3000
2000
1000
0
52%
29%
76%
98%
100%
FtsA+FtsA
FtsZ+FtsZ
22-FtsA
434-FtsA
R721

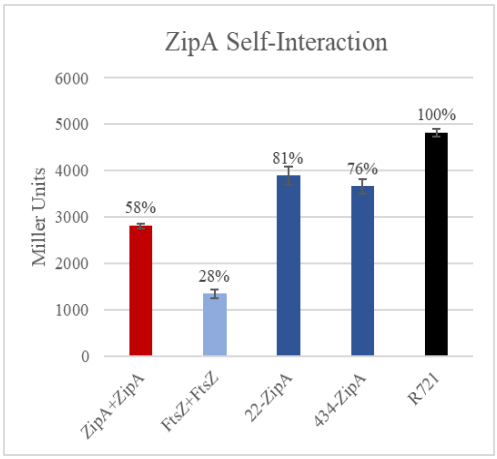
ZipA Self-Interaction
Miller Units
6000
5000
4000
3000
2000
1000
0
58%
28%
81%
76%
100%
ZipA+ZipA
FtsZ+FtsZ
22-ZipA
434-ZipA
R721

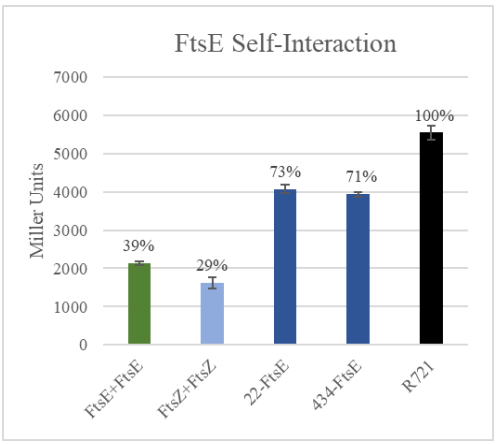
FtsE Self-Interaction
Miller Units
7000
6000
5000
4000
3000
2000
1000
0
39%
29%
73%
71%
100%
FtsE+FtsE
FtsZ+FtsZ
22-FtsE
434-FtsE
R721

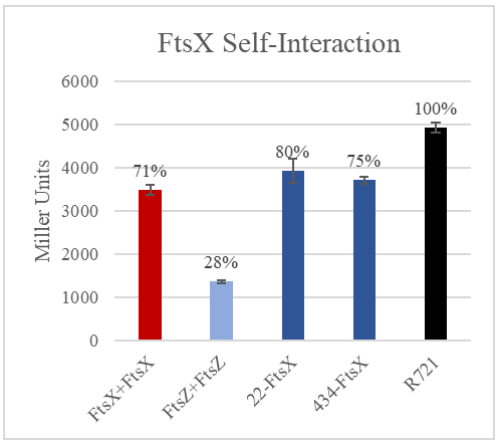
FtsX Self-Interaction
Miller Units
6000
5000
4000
3000
2000
1000
0
71%
28%
80%
75%
100%
FtsX+FtsX
FtsZ+FtsZ
22-FtsX
434-FtsX
R721

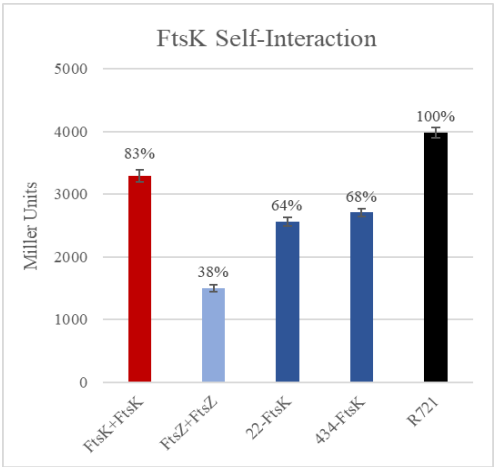
FtsK Self-Interaction
Miller Units
5000
4000
3000
2000
1000
0
83%
38%
64%
68%
100%
FtsK+FtsK
FtsZ+FtsZ
22-FtsK
434-FtsK
R721

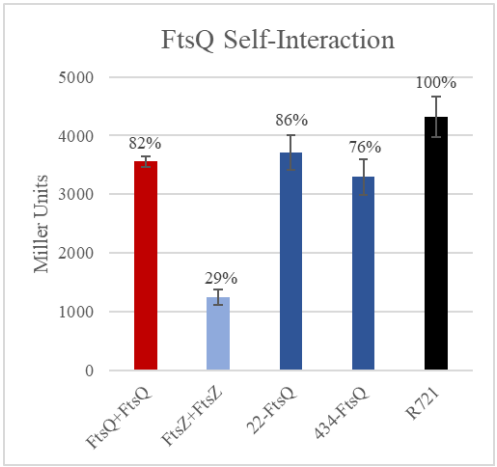
FtsQ Self-Interaction
Miller Units
5000
4000
3000
2000
1000
0
82%
29%
86%
76%
100%
FtsQ+FtsQ
FtsZ+FtsZ
22-FtsQ
434-FtsQ
R721

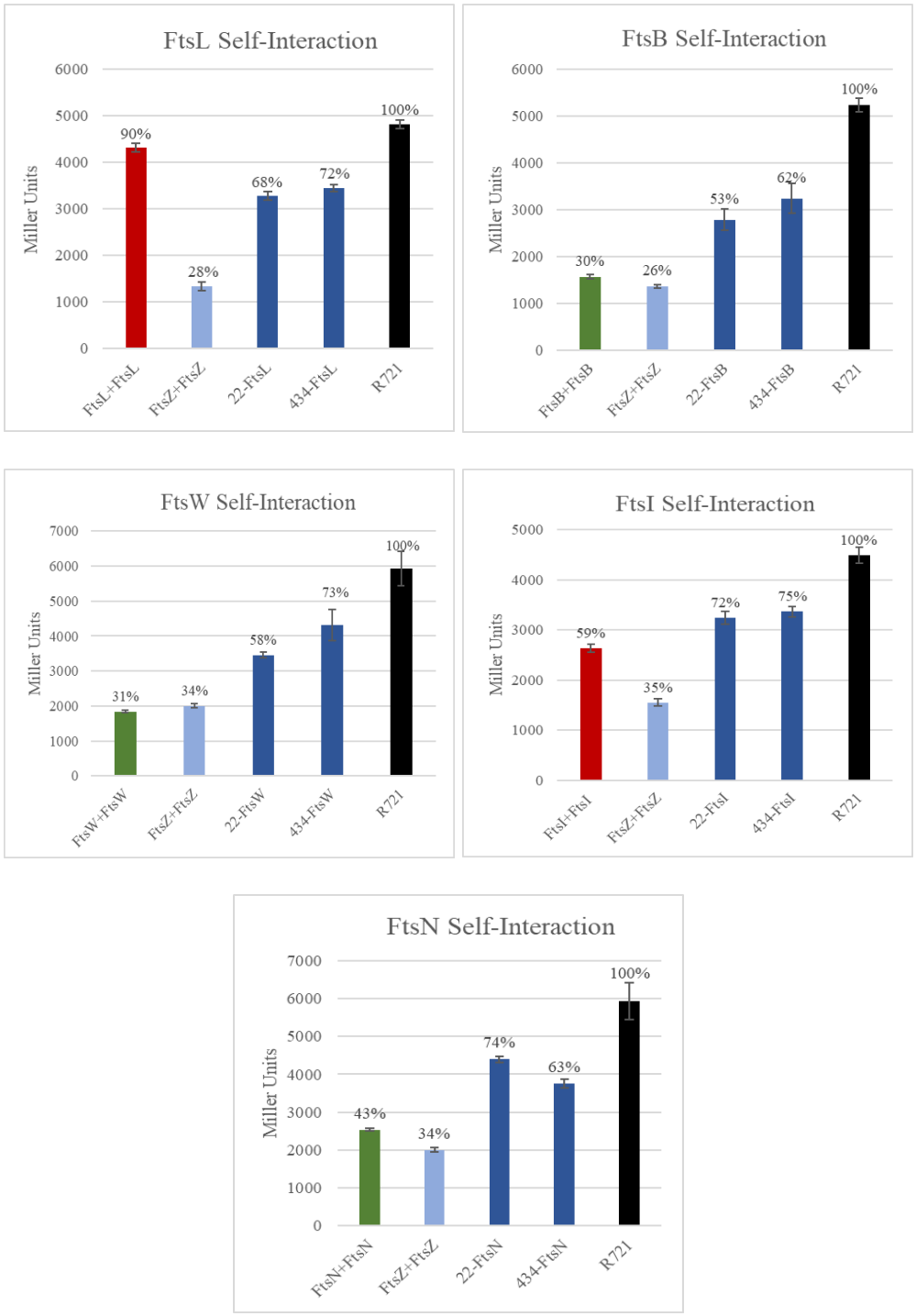

Figure A.1: Additional B2H Graphs. The *N. gonorrhoeae* FtsZ-FtsZ self-interaction was used as a positive control (light blue). The negative controls were *E. coli* R721 with single plasmid transformants (dark blue) while the baseline control was *E. coli* R721 lacking any plasmid (black). For the interaction samples, values of <50% β-galactosidase in comparison to the baseline *E. coli* R721 indicate interactions between those proteins (green) while values of >50% indicate the absence of an interaction between those proteins (red).

Appendix B: Additional AP-MS Experimental Data

Additional data from AP-MS experiments is provided in this section. Table B.1 provides a list of all 305 potential interacting partners of FtsE. The table is organized in descending order of the spectral count in interaction sample A3B3 (i.e., resin + GST-FtsE + *N. gonorrhoeae* lysate). Table B.1 provides the protein name, the spectral count (SpC) and intensity (I) for all four samples, and the spectral count-based and intensity-based fold change values. Figure B.2 is the resulting STRING network map analyzing the protein-protein interactions of the 305 proteins provided in Table B.1. Table B.3 provides the list of additional cell division proteins and their corresponding Uniprot accession number for the protein in the *N. gonorrhoeae* FA1090 strain. Figure B.4 is the STRING network examining interactions amongst the 305 proteins (Table B.1) and the additional cell division proteins (Table B.3).

Table B.1: List of 305 Proteins Identified During AP-MS Experiments

Protein Name	Neg Control A1B1		Neg Control A2B2		Interaction Sample A3B3		Neg Control A4B4		SpC Based Fold Change	I Based Fold Change
	SpC	I	SpC	I	SpC	I	SpC	I		
GMP synthase (likely FtsE)	4	4.31E+06	5	6.93E+06	466	1.11E+10	0	0.00E+00	61.10	665.71
FtsE-like protein	4	4.31E+06	4	5.26E+06	380	1.05E+10	0	0.00E+00	55.76	727.44
Septum site-determining protein MinD	128	5.50E+08	166	7.19E+08	168	6.78E+08	0	0.00E+00	0.67	0.36
Cell division protein FtsZ	186	7.05E+08	201	8.07E+08	165	6.16E+08	0	0.00E+00	0.50	0.27
Cell division protein FtsZ	176	6.81E+08	198	7.93E+08	164	6.07E+08	0	0.00E+00	0.52	0.27
Cell division protein FtsZ	121	4.08E+08	152	5.16E+08	124	3.53E+08	0	0.00E+00	0.54	0.25
Cell division topological specificity factor (MinE)	71	6.72E+08	77	1.08E+09	77	1.15E+09	0	0.00E+00	0.61	0.44
Cell division protein FtsA	83	2.03E+08	81	1.85E+08	70	1.36E+08	0	0.00E+00	0.50	0.23
Cell division protein FtsA	74	1.96E+08	75	1.82E+08	63	1.31E+08	0	0.00E+00	0.50	0.23
Peptidase	0	0.00E+00	0	0.00E+00	45	9.31E+07	0	0.00E+00	N/A	N/A
Cell division protein ZipA	41	1.01E+08	54	1.15E+08	41	6.92E+07	0	0.00E+00	0.51	0.21
Riboflavin biosynthesis protein	17	1.05E+07	26	2.44E+07	36	3.18E+07	5	1.30E+08	0.22	0.02
Cell division protein ZapA	26	5.17E+07	36	6.14E+07	34	6.27E+07	0	0.00E+00	0.65	0.37

Riboflavin biosynthesis protein	18	1.16E+07	26	2.44E+07	32	3.15E+07	5	1.30E+08	0.20	0.02
Pilus assembly protein PilX	14	4.01E+07	19	9.68E+06	21	3.26E+07	4	1.10E+08	0.16	0.02
Multidrug transporter MatE	5	8.77E+05	8	2.19E+06	21	9.54E+06	0	0.00E+00	1.92	2.15
Cell division topological specificity factor (MinE)	27	2.42E+08	14	2.91E+08	19	3.88E+08	0	0.00E+00	0.54	0.48
Pilus assembly protein	13	3.91E+07	16	6.10E+06	17	3.56E+07	3	9.51E+07	0.17	0.03
Probable septum site-determining protein MinC	19	8.35E+06	23	1.68E+07	17	6.40E+06	0	0.00E+00	0.48	0.17
10 kDa chaperonin	2	5.91E+06	7	1.54E+07	16	3.70E+07	0	0.00E+00	2.14	1.20
Pilus assembly protein PilX	9	3.97E+07	8	8.38E+06	15	3.24E+07	4	9.51E+07	0.13	0.03
Uncharacterized protein	0	0.00E+00	2	1.14E+05	15	1.08E+07	0	0.00E+00	9.23	70.64
Peptidyl-prolyl cis-trans isomerase	2	9.28E+04	8	5.01E+05	14	5.34E+06	0	0.00E+00	1.69	6.43
Succinate dehydrogenase flavoprotein subunit	7	3.09E+06	8	6.63E+06	14	8.72E+07	0	0.00E+00	1.10	6.15
Uncharacterized protein	9	8.89E+06	7	3.28E+06	13	4.99E+06	2	2.25E+07	0.20	0.02
Malonyl-[acyl-carrier protein] O-methyltransferase	2	2.41E+08	0	0.00E+00	13	5.84E+08	0	0.00E+00	7.29	1.42
Cytochrome C biogenesis protein CcdA	4	3.13E+06	2	4.29E+04	12	4.98E+07	0	0.00E+00	2.31	9.19
Probable protein kinase UbiB	2	6.64E+06	3	1.24E+07	11	7.43E+06	0	0.00E+00	2.61	0.27
Probable protein kinase UbiB	1	5.90E+06	3	1.24E+07	11	7.06E+06	0	0.00E+00	3.31	0.26

Cell division protein FtsK	7	8.64E+06	10	1.29E+07	10	7.59E+07	0	0.00E+00	0.70	2.36
NAD(P) transhydrogenase subunit alpha	7	1.76E+09	7	1.31E+09	10	1.79E+07	0	0.00E+00	0.84	0.00
Uncharacterized protein	3	9.07E+06	2	7.46E+06	10	5.95E+07	0	0.00E+00	2.33	2.33
Acetate kinase	3	2.03E+06	2	2.32E+04	10	8.84E+05	0	0.00E+00	2.33	0.25
PTS IIA-like nitrogen regulatory protein PtsN	0	0.00E+00	4	3.58E+07	10	1.63E+07	0	0.00E+00	3.08	0.34
LysR family transcriptional regulator (Fragment)	0	0.00E+00	4	7.17E+06	10	3.70E+07	0	0.00E+00	3.08	3.85
Multifunctional fusion protein	6	2.63E+06	0	0.00E+00	9	1.16E+07	0	0.00E+00	1.68	2.58
Probable peptidoglycan D,D-transpeptidase PenA (FtsI)	5	5.31E+07	4	4.36E+07	9	1.34E+08	4	3.92E+07	0.08	0.22
Phosphoglycerate kinase	1	4.93E+05	2	1.87E+07	9	3.59E+07	0	0.00E+00	3.58	1.38
Phosphoglycerate kinase	0	0.00E+00	2	1.87E+07	9	3.58E+07	0	0.00E+00	5.54	1.43
Membrane protein	5	2.88E+07	6	3.77E+07	9	6.63E+07	7	1.39E+08	0.05	0.04
FMN-binding protein	0	0.00E+00	5	1.76E+05	9	1.84E+07	0	0.00E+00	2.22	77.95
Holo-[acyl-carrier-protein] synthase	0	0.00E+00	3	5.69E+06	9	1.35E+07	0	0.00E+00	3.69	1.77
ATP-binding protein Uup	3	2.25E+05	4	2.68E+05	8	6.60E+06	0	0.00E+00	1.35	8.86
DNA topoisomerase	2	1.03E+07	0	0.00E+00	8	5.58E+07	0	0.00E+00	4.49	3.16
Membrane protein	2	1.10E+07	6	4.30E+08	8	1.76E+07	0	0.00E+00	1.20	0.03

Repetitive large surface protein	1	3.43E+05	1	3.68E+05	8	1.43E+07	0	0.00E+00	4.70	13.23
Yfa	5	2.94E+07	2	4.62E+07	8	2.45E+08	7	2.11E+08	0.04	0.10
Transferrin-binding protein B (Fragment)	1	3.32E+04	2	8.37E+07	8	5.49E+06	1	2.24E+04	0.29	0.05
Fe3+ dicitrate ABC transporter permease	1	1.69E+05	2	8.10E+06	8	1.50E+07	0	0.00E+00	3.18	1.34
UDP-N-acetylglucosamine 1-carboxyvinyltransferase (MurA)	7	5.89E+06	8	1.14E+06	7	2.03E+06	0	0.00E+00	0.55	0.17
GatB/Yqey domain-containing protein	1	2.94E+04	1	5.44E+05	7	2.13E+07	0	0.00E+00	4.11	27.31
GatB/YqeY domain-containing protein	0	0.00E+00	4	1.91E+07	7	2.28E+07	0	0.00E+00	2.15	0.89
Putative MafB alternative C-terminus	0	0.00E+00	1	1.15E+06	7	2.04E+07	0	0.00E+00	8.62	13.23
AhpC/TSA family protein	0	0.00E+00	4	4.90E+06	7	1.21E+06	0	0.00E+00	2.15	0.18
Cell division protein FtsN	8	1.03E+07	2	1.82E+06	7	4.25E+07	0	0.00E+00	0.80	2.12
Phage associated protein	0	0.00E+00	0	0.00E+00	7	1.65E+07	0	0.00E+00	N/A	N/A
Na(+)-translocating NADH-quinone reductase subunit B	0	0.00E+00	0	0.00E+00	7	5.23E+07	0	0.00E+00	N/A	N/A
dTDP-4-dehydrorhamnose reductase	1	2.02E+04	2	1.91E+06	7	7.13E+07	0	0.00E+00	2.78	27.46
IS110 family transposase	0	0.00E+00	0	0.00E+00	7	1.17E+07	0	0.00E+00	N/A	N/A
Homoprotocatechuate degradative operon repressor	3	1.06E+07	0	0.00E+00	7	1.74E+07	0	0.00E+00	2.62	0.96
Ribosome maturation factor RimM	0	0.00E+00	0	0.00E+00	7	1.99E+07	0	0.00E+00	N/A	N/A

Outer membrane protein H.8	5	1.90E+05	0	0.00E+00	7	7.13E+05	0	0.00E+00	1.57	2.19
Uncharacterized protein	2	5.50E+06	1	3.16E+06	7	3.37E+07	0	0.00E+00	2.70	2.47
zf-HC2 domain-containing protein	0	0.00E+00	0	0.00E+00	7	9.11E+06	0	0.00E+00	N/A	N/A
Probable peptidoglycan D,D-transpeptidase PenA (FtsI)	3	1.03E+07	3	1.83E+06	6	3.69E+07	3	6.30E+07	0.07	0.05
Probable peptidoglycan D,D-transpeptidase PenA (FtsI)	3	1.03E+07	2	1.78E+06	6	3.44E+07	2	3.29E+07	0.11	0.09
Bifunctional glutamine synthetase adenylyltransferase/adenylyl-removing enzyme	0	0.00E+00	0	0.00E+00	6	2.00E+07	0	0.00E+00	N/A	N/A
Transcription-repair-coupling factor	1	3.05E+06	3	5.81E+06	6	5.36E+05	0	0.00E+00	1.80	0.04
Enoyl-[acyl-carrier-protein] reductase [NADH]	0	0.00E+00	3	2.72E+06	6	6.07E+06	0	0.00E+00	2.46	1.66
Uncharacterized protein	2	1.18E+05	0	0.00E+00	6	5.65E+06	0	0.00E+00	3.36	27.96
DUF560 domain-containing protein	0	0.00E+00	0	0.00E+00	6	1.22E+07	0	0.00E+00	N/A	N/A
Acetate kinase	0	0.00E+00	0	0.00E+00	6	1.71E+07	0	0.00E+00	N/A	N/A
Aminopeptidase N	1	1.69E+05	0	0.00E+00	6	5.84E+06	0	0.00E+00	6.73	20.18
Uncharacterized protein	2	9.22E+06	0	0.00E+00	6	5.60E+07	0	0.00E+00	3.36	3.55
Uncharacterized protein	1	1.06E+06	0	0.00E+00	6	1.66E+07	0	0.00E+00	6.73	9.15
Putative type I restriction enzyme EcoR124II R protein	2	7.10E+04	0	0.00E+00	6	5.92E+06	0	0.00E+00	3.36	48.70
O-succinylhomoserine sulfhydrolase	0	0.00E+00	0	0.00E+00	6	4.75E+06	0	0.00E+00	N/A	N/A

O-succinylhomoserine sulfhydrylase	0	0.00E+00	0	0.00E+00	6	3.03E+06	0	0.00E+00	N/A	N/A
Citrate synthase	0	0.00E+00	0	0.00E+00	6	3.45E+06	0	0.00E+00	N/A	N/A
Methionine aminopeptidase	0	0.00E+00	0	0.00E+00	6	4.07E+06	0	0.00E+00	N/A	N/A
MBL fold metallo-hydrolase (Fragment)	1	1.82E+06	0	0.00E+00	6	4.14E+07	0	0.00E+00	6.73	13.29
Probable peptidoglycan D,D-transpeptidase PenA (FtsI)	5	1.13E+07	2	1.78E+06	5	3.45E+07	2	3.29E+07	0.09	0.09
Cell division protein FtsK	7	4.35E+06	6	2.91E+06	5	1.50E+06	0	0.00E+00	0.45	0.13
GatB/Yqey domain-containing protein	0	0.00E+00	2	6.09E+05	5	5.97E+06	0	0.00E+00	3.08	7.31
Transferrin-binding protein B (Fragment)	3	2.43E+08	3	8.41E+07	5	1.67E+06	0	0.00E+00	0.98	0.00
Transferrin-binding protein B	1	3.32E+04	4	1.68E+08	5	5.92E+06	0	0.00E+00	1.21	0.03
Ligand-gated channel	0	0.00E+00	3	2.20E+06	5	1.67E+06	0	0.00E+00	2.05	0.57
Phosphoribosylaminoimidazole-succinocarboxamide synthase	2	2.80E+06	1	8.69E+05	5	2.71E+07	0	0.00E+00	1.93	4.55
Glutamine--tRNA ligase	0	0.00E+00	3	5.38E+05	5	1.15E+07	0	0.00E+00	2.05	15.94
Putative serotype-1-specific antigen	0	0.00E+00	0	0.00E+00	5	6.05E+06	0	0.00E+00	N/A	N/A
Valine--tRNA ligase	0	0.00E+00	0	0.00E+00	5	1.36E+07	0	0.00E+00	N/A	N/A
Uncharacterized protein	0	0.00E+00	0	0.00E+00	5	1.02E+07	0	0.00E+00	N/A	N/A
LPS-assembly protein LptD	0	0.00E+00	4	1.30E+07	5	1.98E+05	0	0.00E+00	1.54	0.01

Cytochrome C oxidase subunit II	0	0.00E+00	0	0.00E+00	5	7.28E+06	0	0.00E+00	N/A	N/A
Uncharacterized protein	0	0.00E+00	0	0.00E+00	5	6.54E+06	0	0.00E+00	N/A	N/A
TonB-dependent receptor	0	0.00E+00	0	0.00E+00	5	2.05E+08	0	0.00E+00	N/A	N/A
TraU	0	0.00E+00	0	0.00E+00	5	8.37E+06	0	0.00E+00	N/A	N/A
Type I restriction enzyme R Protein	3	3.19E+07	0	0.00E+00	5	1.10E+08	0	0.00E+00	1.87	2.01
50S ribosomal protein L29	0	0.00E+00	1	5.22E+04	5	2.61E+06	0	0.00E+00	6.16	37.28
Hemoglobin receptor	0	0.00E+00	0	0.00E+00	5	1.66E+07	0	0.00E+00	N/A	N/A
Putative ferredoxin-NADP+ reductase (Fragment)	0	0.00E+00	0	0.00E+00	5	1.75E+07	0	0.00E+00	N/A	N/A
Uncharacterized protein	0	0.00E+00	0	0.00E+00	5	1.31E+07	0	0.00E+00	N/A	N/A
Uncharacterized protein	1	1.81E+06	1	1.16E+06	5	8.26E+06	0	0.00E+00	2.93	1.77
Putative ATP-binding protein (Fragment)	0	0.00E+00	2	5.00E+04	4	1.14E+06	0	0.00E+00	2.46	17.00
Transferrin-binding protein B	1	3.32E+04	1	9.44E+04	4	5.21E+06	0	0.00E+00	2.35	28.40
Transferrin-binding protein B (Fragment)	1	3.32E+04	3	1.68E+08	4	2.43E+06	0	0.00E+00	1.20	0.01
Phosphoribosylaminoimidazole-succinocarboxamide synthase	2	2.80E+06	2	8.95E+05	4	2.69E+07	0	0.00E+00	1.17	4.49
Regulatory protein NosR	0	0.00E+00	0	0.00E+00	4	1.21E+07	0	0.00E+00	N/A	N/A
Threonine synthase	0	0.00E+00	2	1.46E+06	4	1.30E+07	0	0.00E+00	2.46	6.64

Toxin	0	0.00E+00	2	1.30E+06	4	1.31E+07	0	0.00E+00	2.46	7.51
Branched-chain-amino-acid transaminase	0	0.00E+00	0	0.00E+00	4	1.55E+07	0	0.00E+00	N/A	N/A
Diadenosine tetraphosphatase	0	0.00E+00	3	4.21E+05	4	1.26E+08	0	0.00E+00	1.64	223.15
Phage replication initiation protein	1	7.79E+05	0	0.00E+00	4	9.16E+06	0	0.00E+00	4.49	6.87
Crossover junction endodeoxyribonuclease RuvC	2	2.91E+05	0	0.00E+00	4	4.93E+07	0	0.00E+00	2.24	98.95
Outer membrane protein OmpU	0	0.00E+00	0	0.00E+00	4	4.77E+06	0	0.00E+00	N/A	N/A
Hemoglobin receptor component HpuA	1	4.88E+06	0	0.00E+00	4	1.26E+08	0	0.00E+00	4.49	15.08
tRNA(Ile)-lysidine synthase	0	0.00E+00	0	0.00E+00	4	1.53E+07	0	0.00E+00	N/A	N/A
Putative TonB-dependent receptor protein	0	0.00E+00	2	5.26E+06	4	1.87E+08	0	0.00E+00	2.46	26.51
AmpG protein	2	8.15E+04	0	0.00E+00	4	2.06E+06	0	0.00E+00	2.24	14.76
Uncharacterized protein	0	0.00E+00	0	0.00E+00	4	6.27E+06	0	0.00E+00	N/A	N/A
Thiamine-phosphate synthase	1	3.49E+03	0	0.00E+00	4	9.39E+05	0	0.00E+00	4.49	157.14
Phosphoribosylglycinamide formyltransferase	0	0.00E+00	0	0.00E+00	4	4.38E+06	0	0.00E+00	N/A	N/A
Antibiotic resistance efflux pump component	3	9.26E+07	2	3.08E+06	4	4.55E+06	0	0.00E+00	0.93	0.03
GTPase Era	0	0.00E+00	2	3.24E+06	4	1.02E+06	0	0.00E+00	2.46	0.23
Phosphoheptose isomerase	0	0.00E+00	2	3.02E+06	4	1.04E+07	0	0.00E+00	2.46	2.57

PqiA family protein	0	0.00E+00	0	0.00E+00	4	3.50E+05	0	0.00E+00	N/A	N/A
SbmA protein	0	0.00E+00	0	0.00E+00	4	2.39E+06	0	0.00E+00	N/A	N/A
TonB-dependent receptor	0	0.00E+00	0	0.00E+00	4	2.28E+07	0	0.00E+00	N/A	N/A
Type IV pilus assembly protein PilA (Fragment)	0	0.00E+00	0	0.00E+00	4	3.43E+07	0	0.00E+00	N/A	N/A
Phage head morphogenesis, SPP1 gp7 family domain protein	0	0.00E+00	0	0.00E+00	4	1.13E+08	0	0.00E+00	N/A	N/A
Phosphoribosylglycinamide formyltransferase	0	0.00E+00	2	1.95E+06	4	3.44E+06	0	0.00E+00	2.46	1.32
Uncharacterized protein	0	0.00E+00	0	0.00E+00	4	3.34E+06	0	0.00E+00	N/A	N/A
Cell division protein (likely Fic/DOC family protein)[%]	2	6.83E+06	3	6.36E+06	4	1.32E+07	0	0.00E+00	0.95	0.65
Uncharacterized protein	0	0.00E+00	0	0.00E+00	4	8.30E+05	0	0.00E+00	N/A	N/A
Peptidase	0	0.00E+00	0	0.00E+00	4	3.77E+06	0	0.00E+00	N/A	N/A
dTDP-glucose 4,6-dehydratase	0	0.00E+00	0	0.00E+00	4	8.56E+06	0	0.00E+00	N/A	N/A
3-deoxy-D-manno-octulosonic acid transferase	0	0.00E+00	0	0.00E+00	4	1.26E+06	0	0.00E+00	N/A	N/A
Uncharacterized protein (Fragment)	0	0.00E+00	1	6.38E+06	4	1.93E+07	0	0.00E+00	4.93	2.26
Replication initiation factor	0	0.00E+00	0	0.00E+00	4	4.76E+06	0	0.00E+00	N/A	N/A
Putative GpT-like prophage major head subunit protein	0	0.00E+00	2	1.26E+06	4	2.31E+06	0	0.00E+00	2.46	1.37
Exodeoxyribonuclease 7 large subunit	1	1.47E+06	0	0.00E+00	4	1.00E+07	0	0.00E+00	4.49	3.97

Tyrosine recombinase XerD	1	9.48E+04	0	0.00E+00	4	6.70E+05	0	0.00E+00	4.49	4.13
P(-)rp(+) fimbrial protein	0	0.00E+00	1	1.77E+05	4	2.36E+06	0	0.00E+00	4.93	9.94
Large pilS cassette protein	0	0.00E+00	0	0.00E+00	4	1.90E+07	0	0.00E+00	N/A	N/A
TraL	0	0.00E+00	0	0.00E+00	4	1.72E+05	0	0.00E+00	N/A	N/A
Ohr family peroxiredoxin	3	2.06E+05	2	1.60E+05	4	4.95E+06	0	0.00E+00	0.93	8.73
Uncharacterized protein	0	0.00E+00	2	6.96E+06	4	8.21E+06	0	0.00E+00	2.46	0.88
Segregation and condensation protein A	0	0.00E+00	2	1.27E+07	4	2.46E+07	0	0.00E+00	2.46	1.44
Permease	1	1.81E+06	0	0.00E+00	4	5.53E+06	0	0.00E+00	4.49	1.78
Chromosomal replication initiation protein	1	1.68E+05	0	0.00E+00	3	2.91E+06	0	0.00E+00	3.36	10.12
Outer-membrane protein assembly factor Omp85	2	9.62E+05	0	0.00E+00	3	1.19E+07	0	0.00E+00	1.68	7.22
Probable peptidoglycan D,D-transpeptidase PenA (FtsI)	0	0.00E+00	0	0.00E+00	3	2.77E+07	2	3.29E+07	0.06	0.07
Probable peptidoglycan D,D-transpeptidase PenA (FtsI)	4	1.36E+07	2	2.80E+05	3	2.95E+07	3	3.29E+07	0.04	0.07
Probable peptidoglycan D,D-transpeptidase PenA (FtsI)	4	1.18E+07	2	1.78E+06	3	2.53E+07	2	3.29E+07	0.05	0.06
tRNA pseudouridine synthase A	0	0.00E+00	0	0.00E+00	3	2.42E+06	0	0.00E+00	N/A	N/A
ModA13 (Fragment)	1	9.02E+04	0	0.00E+00	3	4.14E+06	0	0.00E+00	3.36	26.81
Uncharacterized protein	1	8.21E+04	1	8.37E+05	3	8.66E+06	0	0.00E+00	1.76	6.86

P-type cation-transporting ATPase	2	2.78E+07	0	0.00E+00	3	2.18E+06	0	0.00E+00	1.68	0.05
Ribonuclease R	0	0.00E+00	0	0.00E+00	3	1.64E+07	1	5.09E+04	0.12	27.88
Glycosyltransferase family 25 protein	0	0.00E+00	2	1.58E+06	3	8.77E+06	0	0.00E+00	1.85	4.14
Bis(5'-nucleosyl)-tetraphosphatase, symmetrical	0	0.00E+00	2	3.55E+05	3	1.26E+08	0	0.00E+00	1.85	264.64
Putative hemolysin activation protein HecB	2	4.71E+04	0	0.00E+00	3	1.10E+06	0	0.00E+00	1.68	13.64
Methionine--tRNA ligase	0	0.00E+00	1	3.16E+04	3	1.29E+07	0	0.00E+00	3.69	304.38
Adenylosuccinate synthase	2	7.75E+07	0	0.00E+00	3	2.77E+06	0	0.00E+00	1.68	0.02
NAD-dependent succinate-semialdehyde dehydrogenase	0	0.00E+00	0	0.00E+00	3	4.77E+06	0	0.00E+00	N/A	N/A
Acetate kinase	0	0.00E+00	1	3.25E+04	3	6.23E+04	2	2.13E+07	0.06	0.00
TonB-dependent receptor	0	0.00E+00	0	0.00E+00	3	1.79E+08	0	0.00E+00	N/A	N/A
IS1016 group transposase	2	9.79E+05	0	0.00E+00	3	2.28E+07	0	0.00E+00	1.68	13.60
IS1016 transposase	0	0.00E+00	0	0.00E+00	3	2.25E+07	0	0.00E+00	N/A	N/A
Transposase	0	0.00E+00	0	0.00E+00	3	4.81E+07	0	0.00E+00	N/A	N/A
Cytosine-specific methyltransferase	1	3.93E+06	0	0.00E+00	3	1.66E+06	0	0.00E+00	3.36	0.25
Type IV pilus assembly protein PilE	1	2.15E+04	0	0.00E+00	3	2.39E+06	0	0.00E+00	3.36	64.92
Uncharacterized protein (Fragment)	0	0.00E+00	1	2.51E+04	3	2.10E+06	0	0.00E+00	3.69	62.38

YkuD domain-containing protein	2	2.03E+06	0	0.00E+00	3	1.26E+07	0	0.00E+00	1.68	3.63
Phage associated protein	0	0.00E+00	0	0.00E+00	3	9.71E+06	0	0.00E+00	N/A	N/A
Probable IS1016 transposase	2	7.76E+04	2	4.71E+04	3	4.10E+06	0	0.00E+00	0.88	20.91
Uncharacterized protein (Fragment)	2	7.48E+05	0	0.00E+00	3	4.37E+06	0	0.00E+00	1.68	3.41
Pilin	0	0.00E+00	0	0.00E+00	3	4.60E+06	0	0.00E+00	N/A	N/A
Pilin	0	0.00E+00	0	0.00E+00	3	3.80E+06	0	0.00E+00	N/A	N/A
UPF0056 inner membrane protein	0	0.00E+00	0	0.00E+00	3	1.56E+06	0	0.00E+00	N/A	N/A
NAD(P) transhydrogenase subunit beta	0	0.00E+00	1	5.08E+04	3	4.08E+06	0	0.00E+00	3.69	59.88
Cell division protein FtsX	1	1.74E+06	3	8.78E+06	3	4.93E+05	0	0.00E+00	0.90	0.03
Putative phage associated protein	0	0.00E+00	0	0.00E+00	3	2.29E+06	0	0.00E+00	N/A	N/A
Ferric siderophore receptor protein	0	0.00E+00	0	0.00E+00	3	1.56E+06	0	0.00E+00	N/A	N/A
Phosphoenolpyruvate-protein phosphotransferase	0	0.00E+00	1	7.92E+04	3	1.49E+07	0	0.00E+00	3.69	140.27
Competence protein ComA	0	0.00E+00	2	3.65E+04	3	1.16E+06	0	0.00E+00	1.85	23.70
GTPase Obg	1	6.91E+04	0	0.00E+00	3	5.90E+06	0	0.00E+00	3.36	49.87
Divalent metal cation transporter	0	0.00E+00	0	0.00E+00	3	1.31E+06	0	0.00E+00	N/A	N/A
ADP-L-glycero-D-manno-heptose-6-epimerase	0	0.00E+00	0	0.00E+00	3	2.13E+08	0	0.00E+00	N/A	N/A

ATP-dependent DNA helicase DinG	0	0.00E+00	2	1.29E+06	3	3.66E+06	0	0.00E+00	1.85	2.12
Fimbrial protein	0	0.00E+00	0	0.00E+00	3	1.28E+07	0	0.00E+00	N/A	N/A
Pilin	0	0.00E+00	0	0.00E+00	3	6.68E+06	0	0.00E+00	N/A	N/A
Pilin (Fragment)	0	0.00E+00	0	0.00E+00	3	8.80E+06	0	0.00E+00	N/A	N/A
Cell division protein (likely Fic/DOC family protein)[%]	3	6.85E+06	3	6.36E+06	3	1.23E+07	0	0.00E+00	0.59	0.61
YfeB	0	0.00E+00	0	0.00E+00	3	9.84E+07	0	0.00E+00	N/A	N/A
Protein translocase subunit SecY	0	0.00E+00	1	5.67E+05	3	6.34E+06	0	0.00E+00	3.69	8.34
Pilin	0	0.00E+00	0	0.00E+00	3	1.02E+07	0	0.00E+00	N/A	N/A
ATP-dependent RNA helicase HrpA	1	1.64E+05	2	1.97E+05	3	1.76E+06	0	0.00E+00	1.19	3.23
AAA family ATPase (Fragment)	1	2.97E+05	0	0.00E+00	3	2.29E+06	0	0.00E+00	3.36	4.50
Type IV secretion system lytic transglycosylase VirB1	0	0.00E+00	1	1.32E+05	3	1.09E+07	0	0.00E+00	3.69	61.57
Pyridoxine/pyridoxamine 5'-phosphate oxidase	0	0.00E+00	0	0.00E+00	3	9.75E+05	0	0.00E+00	N/A	N/A
Sulfatase domain-containing protein	0	0.00E+00	0	0.00E+00	3	3.95E+05	0	0.00E+00	N/A	N/A
Uncharacterized protein	0	0.00E+00	0	0.00E+00	3	4.60E+06	0	0.00E+00	N/A	N/A
Uncharacterized protein rth49	0	0.00E+00	0	0.00E+00	3	8.96E+05	0	0.00E+00	N/A	N/A
Outer membrane protein assembly factor BamD	0	0.00E+00	0	0.00E+00	3	2.43E+05	0	0.00E+00	N/A	N/A

Acyl carrier protein	1	3.93E+05	0	0.00E+00	3	9.84E+05	0	0.00E+00	3.36	1.46
Pilin	0	0.00E+00	0	0.00E+00	3	8.05E+06	0	0.00E+00	N/A	N/A
Threonyl-tRNA synthetase	1	1.67E+07	0	0.00E+00	3	1.03E+08	0	0.00E+00	3.36	3.60
Integral membrane protein	0	0.00E+00	1	2.39E+05	3	2.15E+06	0	0.00E+00	3.69	6.71
Peptidyl-prolyl cis-trans isomerase	0	0.00E+00	0	0.00E+00	2	7.70E+06	0	0.00E+00	N/A	N/A
Toxin CdiA	0	0.00E+00	0	0.00E+00	2	3.75E+06	0	0.00E+00	N/A	N/A
Peptidyl-prolyl cis-trans isomerase B	0	0.00E+00	1	1.21E+05	2	4.97E+04	0	0.00E+00	2.46	0.31
ATP-binding protein (Fragment)	0	0.00E+00	0	0.00E+00	2	1.75E+05	0	0.00E+00	N/A	N/A
Autotransporter outer membrane beta-barrel domain-containing protein	0	0.00E+00	0	0.00E+00	2	2.17E+06	0	0.00E+00	N/A	N/A
Probable peptidoglycan D,D-transpeptidase PenA (FtsI)	4	1.03E+07	2	2.80E+05	2	2.52E+07	3	3.29E+07	0.02	0.06
Cytochrome biogenesis protein	0	0.00E+00	1	9.98E+05	2	1.37E+05	0	0.00E+00	2.46	0.10
MafB-like protein	0	0.00E+00	0	0.00E+00	2	2.88E+07	0	0.00E+00	N/A	N/A
Uncharacterized protein	0	0.00E+00	0	0.00E+00	2	2.87E+07	0	0.00E+00	N/A	N/A
ABC transporter ATP-binding protein	0	0.00E+00	0	0.00E+00	2	2.30E+06	0	0.00E+00	N/A	N/A
Acetate/propionate family kinase	0	0.00E+00	0	0.00E+00	2	5.74E+06	0	0.00E+00	N/A	N/A
Citrate synthase (unknown stereospecificity)	0	0.00E+00	1	1.91E+04	2	6.41E+06	0	0.00E+00	2.46	250.23

Plasmid replicase	1	1.55E+06	1	8.11E+04	2	3.60E+07	0	0.00E+00	1.17	13.03
Acetylornithine/succinyldiaminopimelate aminotransferase (ACOAT succinyldiaminopimelate transferase DapATase)	1	3.50E+06	0	0.00E+00	2	2.66E+06	0	0.00E+00	2.24	0.44
Transposase IS1016	0	0.00E+00	0	0.00E+00	2	2.46E+06	0	0.00E+00	N/A	N/A
DNA (cytosine-5-)-methyltransferase	0	0.00E+00	0	0.00E+00	2	4.80E+06	0	0.00E+00	N/A	N/A
DNA polymerase IV	0	0.00E+00	1	3.87E+08	2	3.12E+06	0	0.00E+00	2.46	0.01
Putative acetyltransferase	1	1.76E+06	0	0.00E+00	2	7.23E+05	0	0.00E+00	2.24	0.24
Large pilS cassette	0	0.00E+00	1	5.15E+06	2	2.88E+06	0	0.00E+00	2.46	0.42
Putative iron-sulfur cluster insertion protein ErpA	0	0.00E+00	0	0.00E+00	2	6.18E+06	0	0.00E+00	N/A	N/A
PqiA family protein	1	2.14E+06	0	0.00E+00	2	2.63E+05	0	0.00E+00	2.24	0.07
Type III pantothenate kinase	0	0.00E+00	1	7.31E+06	2	9.31E+05	0	0.00E+00	2.46	0.09
Lipopolysaccharide export system permease protein LptF	0	0.00E+00	1	2.17E+06	2	8.83E+05	0	0.00E+00	2.46	0.30
Precorrin-2 dehydrogenase	0	0.00E+00	0	0.00E+00	2	9.38E+06	0	0.00E+00	N/A	N/A
Tripartite tricarboxylate transporter substrate binding protein (Fragment)	1	2.05E+06	0	0.00E+00	2	2.11E+06	0	0.00E+00	2.24	0.60
ADP-L-glycero-D-manno-heptose-6-epimerase	0	0.00E+00	0	0.00E+00	2	2.10E+08	0	0.00E+00	N/A	N/A
Ornithine carbamoyltransferase	1	2.79E+06	0	0.00E+00	2	5.47E+06	0	0.00E+00	2.24	1.15

Peptidase M61	0	0.00E+00	0	0.00E+00	2	5.07E+05	0	0.00E+00	N/A	N/A
CMP-N-acetylneuraminate-beta-galactosamide-alpha-2,3-sialyltransferase	1	1.03E+05	0	0.00E+00	2	1.86E+06	0	0.00E+00	2.24	10.55
Ybi	1	1.32E+04	0	0.00E+00	2	7.18E+06	0	0.00E+00	2.24	317.68
Excinuclease	1	3.80E+06	0	0.00E+00	2	4.05E+06	0	0.00E+00	2.24	0.62
dTDP-glucose 4,6-dehydratase	1	3.02E+05	0	0.00E+00	2	8.54E+06	0	0.00E+00	2.24	16.52
Flagellar motor protein MotA (Fragment)	1	8.49E+04	0	0.00E+00	2	3.09E+06	0	0.00E+00	2.24	21.26
Lipopolysaccharide-assembly, LptC-related family protein	0	0.00E+00	1	3.80E+06	2	6.12E+06	0	0.00E+00	2.46	1.20
Peptidyl-prolyl cis-trans isomerase	0	0.00E+00	0	0.00E+00	2	1.01E+06	0	0.00E+00	N/A	N/A
Putative phage associated protein	0	0.00E+00	0	0.00E+00	2	1.33E+07	0	0.00E+00	N/A	N/A
Terminase	0	0.00E+00	1	2.62E+06	2	5.33E+05	0	0.00E+00	2.46	0.15
Indolepyruvate ferredoxin oxidoreductase family protein (Fragment)	0	0.00E+00	0	0.00E+00	2	3.08E+04	0	0.00E+00	N/A	N/A
Pilin (Fragment)	0	0.00E+00	0	0.00E+00	2	3.25E+07	0	0.00E+00	N/A	N/A
dCTP deaminase	0	0.00E+00	0	0.00E+00	2	1.93E+06	0	0.00E+00	N/A	N/A
Ydf	0	0.00E+00	0	0.00E+00	2	2.59E+05	0	0.00E+00	N/A	N/A
Uncharacterized protein	0	0.00E+00	1	6.48E+04	2	3.00E+06	0	0.00E+00	2.46	34.52

Meta-pathway of phenol degradation family protein	0	0.00E+00	0	0.00E+00	2	3.52E+05	0	0.00E+00	N/A	N/A
Cell division protein (likely FtsN)[%]	0	0.00E+00	0	0.00E+00	2	8.46E+05	0	0.00E+00	N/A	N/A
Ribonuclease HII	0	0.00E+00	0	0.00E+00	2	4.09E+05	0	0.00E+00	N/A	N/A
Sulfatase domain-containing protein	0	0.00E+00	0	0.00E+00	2	5.53E+06	0	0.00E+00	N/A	N/A
Carbamoyl-phosphate synthase small chain	1	2.01E+04	0	0.00E+00	2	7.35E+04	0	0.00E+00	2.24	2.14
Phage associated protein	0	0.00E+00	0	0.00E+00	2	1.01E+06	0	0.00E+00	N/A	N/A
Phosphate acyltransferase	1	6.75E+04	0	0.00E+00	2	1.75E+06	0	0.00E+00	2.24	15.14
Uncharacterized protein	0	0.00E+00	0	0.00E+00	2	1.74E+05	0	0.00E+00	N/A	N/A
Pilin (Fragment)	0	0.00E+00	0	0.00E+00	2	1.11E+06	0	0.00E+00	N/A	N/A
Cytosine-specific methyltransferase	0	0.00E+00	0	0.00E+00	2	8.68E+06	0	0.00E+00	N/A	N/A
Transferrin-binding protein B	1	3.32E+04	1	9.44E+04	2	1.15E+06	0	0.00E+00	1.17	6.27
Uncharacterized protein conserved in bacteria	1	7.82E+04	1	5.72E+04	2	5.52E+05	0	0.00E+00	1.17	2.62
Uncharacterized protein	0	0.00E+00	0	0.00E+00	2	1.21E+06	0	0.00E+00	N/A	N/A
DNA ligase	0	0.00E+00	0	0.00E+00	2	2.12E+05	0	0.00E+00	N/A	N/A
Myo-inositol transport system permease	0	0.00E+00	0	0.00E+00	2	1.42E+07	0	0.00E+00	N/A	N/A
Uncharacterized protein	0	0.00E+00	0	0.00E+00	2	9.82E+05	0	0.00E+00	N/A	N/A

Ribosome association toxin RatA	0	0.00E+00	0	0.00E+00	2	1.06E+06	0	0.00E+00	N/A	N/A
Transcriptional regulator	0	0.00E+00	0	0.00E+00	2	2.06E+06	0	0.00E+00	N/A	N/A
DNA-directed RNA polymerase subunit omega	0	0.00E+00	0	0.00E+00	2	3.69E+06	0	0.00E+00	N/A	N/A
Bacterioferritin	0	0.00E+00	0	0.00E+00	2	1.18E+06	0	0.00E+00	N/A	N/A
2-amino-4-hydroxy-6-hydroxymethyldihydropteridine pyrophosphokinase	0	0.00E+00	0	0.00E+00	2	2.24E+06	0	0.00E+00	N/A	N/A
Mobilization protein A	0	0.00E+00	0	0.00E+00	2	4.64E+06	0	0.00E+00	N/A	N/A
Magnesium chelatase (Fragment)	0	0.00E+00	0	0.00E+00	2	1.28E+06	0	0.00E+00	N/A	N/A
Uncharacterized protein	0	0.00E+00	0	0.00E+00	2	3.79E+06	0	0.00E+00	N/A	N/A
Variant P9 pilE (Fragment)	0	0.00E+00	0	0.00E+00	2	9.76E+05	0	0.00E+00	N/A	N/A
Uncharacterized protein	0	0.00E+00	0	0.00E+00	2	9.60E+05	0	0.00E+00	N/A	N/A
Adenosylmethionine-8-amino-7-oxononanoate aminotransferase	0	0.00E+00	0	0.00E+00	2	2.34E+07	0	0.00E+00	N/A	N/A
Variant P9 pilE (Fragment)	0	0.00E+00	0	0.00E+00	2	9.83E+05	0	0.00E+00	N/A	N/A
1-deoxy-D-xylulose-5-phosphate synthase	0	0.00E+00	0	0.00E+00	2	1.23E+06	0	0.00E+00	N/A	N/A
Exodeoxyribonuclease VII large subunit	1	1.47E+06	0	0.00E+00	2	6.09E+06	1	1.65E+07	0.08	0.03
Uncharacterized protein	0	0.00E+00	0	0.00E+00	2	2.02E+06	0	0.00E+00	N/A	N/A
Uncharacterized protein rth39	0	0.00E+00	0	0.00E+00	2	7.18E+05	0	0.00E+00	N/A	N/A

Uncharacterized protein	0	0.00E+00	0	0.00E+00	2	3.42E+05	0	0.00E+00	N/A	N/A
ABC transporter permease, polyamine	0	0.00E+00	0	0.00E+00	2	6.05E+04	0	0.00E+00	N/A	N/A
Chlorophyllide reductase iron protein subunit X (Fragment)	0	0.00E+00	1	3.21E+04	2	1.72E+05	0	0.00E+00	2.46	4.00
Serine hydrolase family protein	0	0.00E+00	0	0.00E+00	2	6.86E+04	0	0.00E+00	N/A	N/A
Zn_Tnp_IS1 domain-containing protein	0	0.00E+00	0	0.00E+00	2	6.03E+06	0	0.00E+00	N/A	N/A
Uncharacterized protein (Fragment)	0	0.00E+00	0	0.00E+00	2	7.78E+06	0	0.00E+00	N/A	N/A
Phosphate starvation protein PhoH	0	0.00E+00	0	0.00E+00	2	1.58E+06	0	0.00E+00	N/A	N/A
LysR family transcriptional regulator (Fragment)	0	0.00E+00	0	0.00E+00	2	5.09E+04	0	0.00E+00	N/A	N/A
Electron transfer flavoprotein-ubiquinone oxidoreductase	0	0.00E+00	0	0.00E+00	2	1.26E+05	0	0.00E+00	N/A	N/A
Crispr-associated protein cas4	0	0.00E+00	0	0.00E+00	2	1.36E+05	0	0.00E+00	N/A	N/A
Toxin CdiA	0	0.00E+00	0	0.00E+00	2	7.84E+06	0	0.00E+00	N/A	N/A
TraK	0	0.00E+00	0	0.00E+00	2	2.30E+06	0	0.00E+00	N/A	N/A
Uncharacterized protein	0	0.00E+00	0	0.00E+00	2	4.23E+06	0	0.00E+00	N/A	N/A
Uncharacterized protein	0	0.00E+00	1	9.39E+06	2	1.95E+07	0	0.00E+00	2.46	1.55
Thiamine biosynthesis protein ThiS	0	0.00E+00	0	0.00E+00	2	2.91E+06	0	0.00E+00	N/A	N/A
Penicillin-binding protein 2 (FtsI)	5	1.03E+07	3	1.83E+06	1	1.50E+05	0	0.00E+00	0.15	0.01

Putative cell-division protein (likely FtsK)[%]	0	0.00E+00	0	0.00E+00	1	7.43E+05	0	0.00E+00	N/A	N/A
Putative cell-division protein (likely FtsK)[%]	0	0.00E+00	0	0.00E+00	1	2.95E+04	0	0.00E+00	N/A	N/A
Penicillin binding protein (Fragment) (FtsI)	4	3.47E+06	0	0.00E+00	0	0.00E+00	0	0.00E+00	0.00	0.00
Probable peptidoglycan D,D-transpeptidase PenA (FtsI)	4	2.55E+06	3	1.83E+06	0	0.00E+00	0	0.00E+00	0.00	0.00
Cell division protein FtsN	3	2.32E+06	2	1.58E+06	0	0.00E+00	0	0.00E+00	0.00	0.00
Cell division protein FtsB	1	1.94E+06	0	0.00E+00	0	0.00E+00	0	0.00E+00	0.00	0.00

SpC, spectral count; I, intensity

[$]N/A = fold change value is not applicable. This note occurs when the spectral-based or intensity-based fold change is calculated for proteins which have no peptides and no intensity values recorded for all negative control samples. The fold change is calculated by dividing the NSAF for the A3B3 sample by the average NSAF for the negative controls (i.e., $NSAF_{(A3B3)}/NSAF_{AVG(A1B1, A2B2, A4B4)}$). When the negative controls have a spectral count and intensity value of 0, then the average NSAF for the negative controls will be zero.

[%]The likely identity of these non-specific cell division proteins was determined through BLASTp (Appendix B).

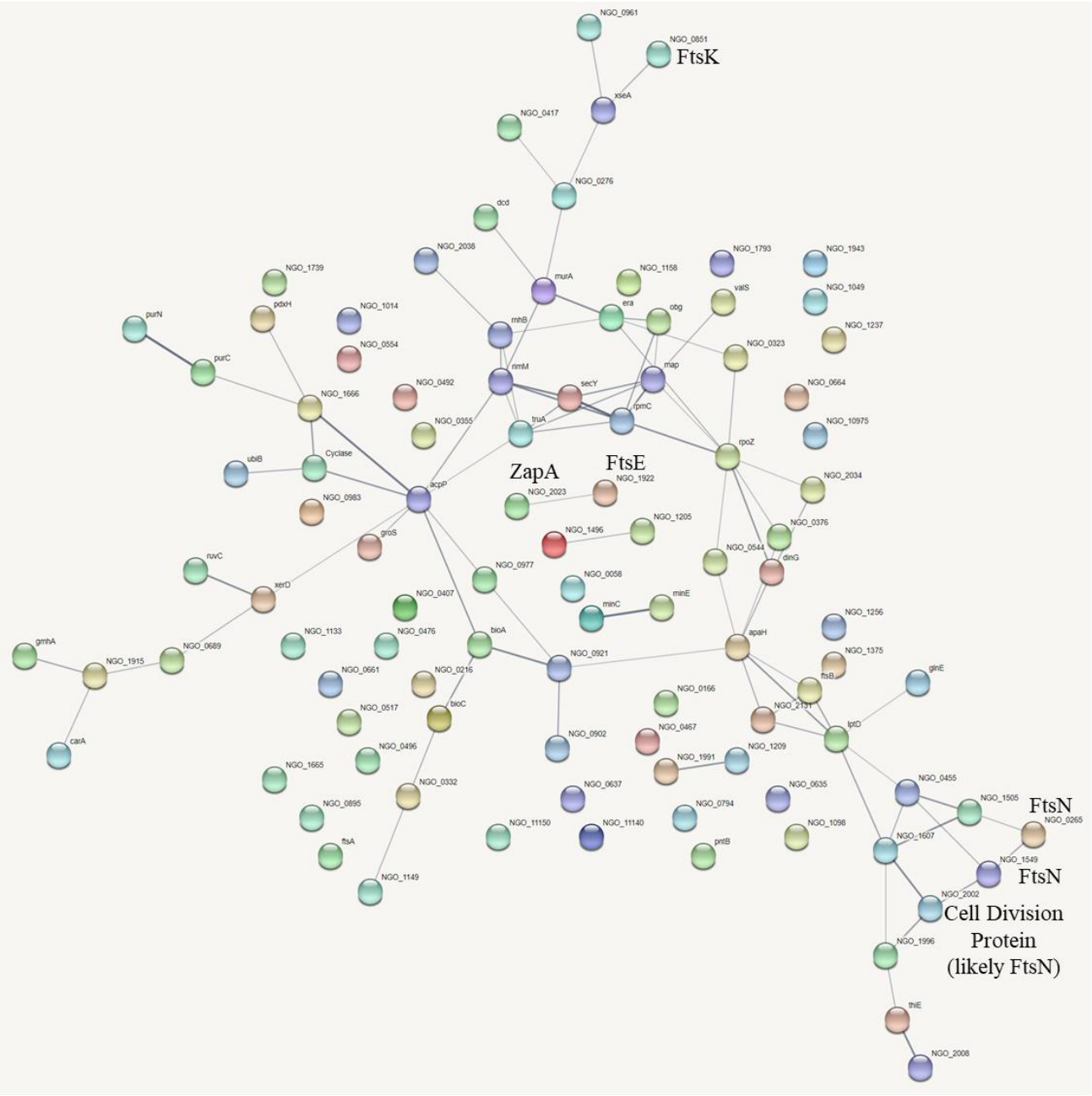

Figure B.2: STRING Network Examining Predicted Protein-Protein Intearctions for the 305 Proteins Identified in AP-MS Experiments. STRING analysis was performed on the 305 proteins identified in AP-MS experiments. The minimum interaction score was set to 0.4 and all interaction sources were included except the text-mining data source. The line thickness is indicative of the strength of the predicted interaction; thicker lines indicate more confidence in the prediction. The cell division cluster is indicated by a box. The permament URL for this network is provided: https://version-11-5.string-db.org/cgi/network?networkId=bII27POJWy8w

Table B.3: List of Additional Cell Division Proteins for STRING Analysis

	Protein or *gene* Names	**FA1090 Accession Number**
Identified in AP-MS Experiments	FtsZ	Q5F6M3
	ZipA	Q5F9Z8
	FtsX	Q5F5K3
	FtsI (*penA*)	Q5F6K9
	MinD	A0A0H4IVK1
Not Identified in AP-MS Experiments	FtsQ	Q5F6M1
	FtsL	Q5F6K8
	FtsW	Q5F6L7

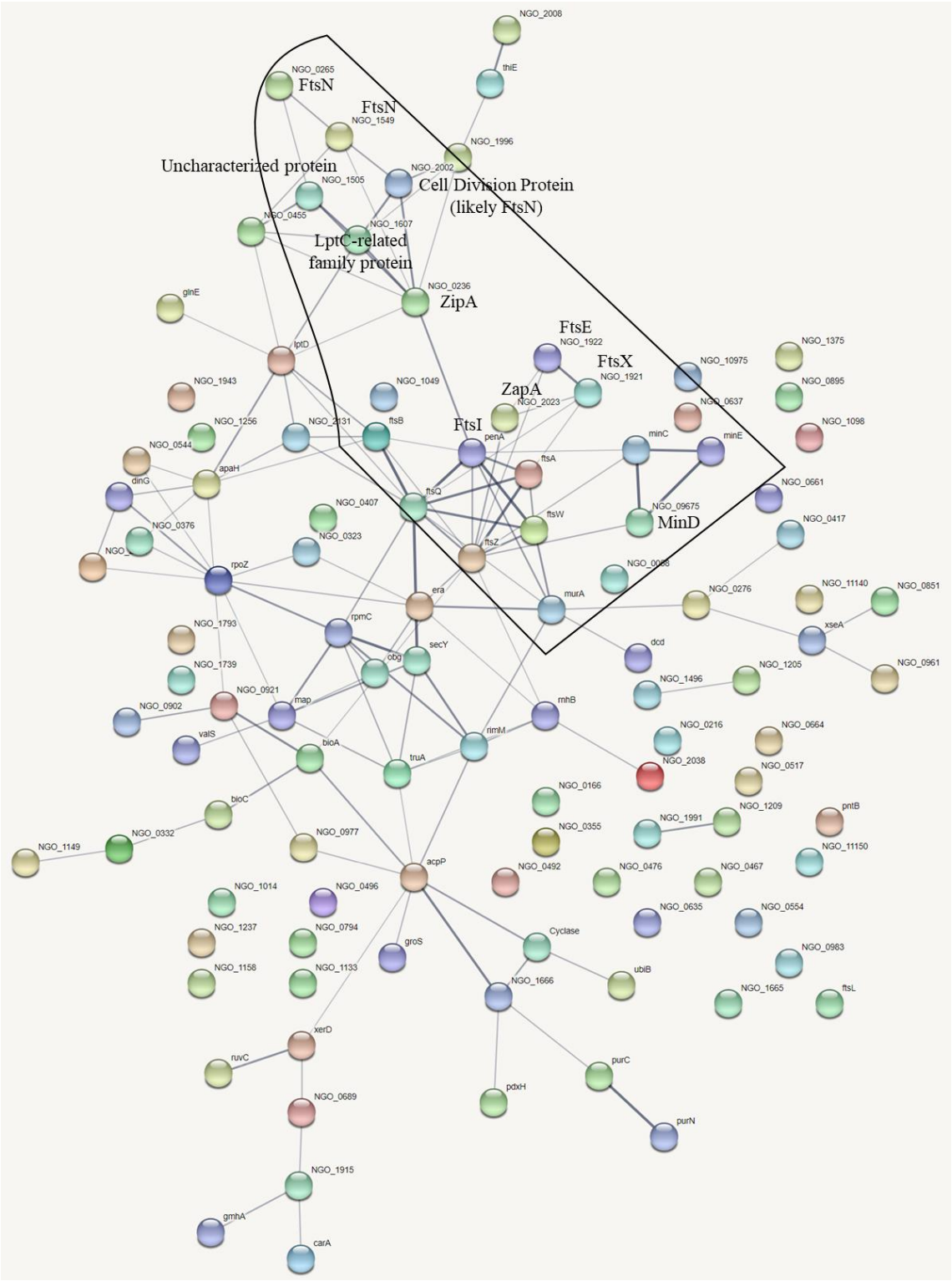

Figure B.4: STRING Network for the 305 Proteins Identified in AP-MS Experiments with the Inclusion of Additional Cell Division Proteins. Without text-mining data source. STRING analysis was performed on the 305 proteins identified in AP-MS experiments. The minimum interaction score was set to 0.4 and all interaction sources were included except the text-

mining data source. The cell division cluster is indicated (black box). The line thickness is indicative of the strength of the predicted interaction; stronger predicted interactions. The permanent URL is provided: https://version-11-5.string-db.org/cgi/network?networkId=bASNiDPcJrUn

BLASTp Analysis for Identifying Homologs of Non-Specific Cell Division Proteins

The potential identity of the 3 non-specific "cell division proteins" and the 2 non-specific "putative cell division proteins" was determined through BLASTp search. Table B.5 summarizes the results of the BLASTp search. One of the cell division proteins (Uniprot accession number: A0A2X1VIK0) is now considered an obsolete entry and a BLASTp search could not be performed. However, this protein is a homolog to one of the other "cell division proteins" (Uniprot accession number: A0A378VVM6). According to BLASTp results, this "cell division protein" has 92.21% identity with a Fic/DOC family protein. The third "cell division protein" (Uniprot accession number: Q5F5C7), was identified to have 99.64% identity to a SPOR domain-containing protein. This non-specifically identified cell division protein is most likely FtsN because the *E. coli* FtsN homolog is known to have a SPOR domain in its C-terminus (Gerding *et al.*, 2009). Lastly, the two "putative cell division proteins" were found to have 100% identity to the cell division protein FtsK. Therefore, these putative cell division proteins are most likely FtsK.

Table B.5: BLASTp Results for Identifying Homologs for the Non-Specific Cell Division Proteins

Name	Uniprot Accession Number	BLASTp Results				
		Description	Species	E Value	% Identity	NCBI Accession Number
Cell Division Protein	A0A2X1VIK0*					
Cell Division Protein	A0A378VVM6	Fic/DOC Family Protein	*N. gonorrhoeae*	3e-99	92.21%	AKP12939.1
Cell Division Protein	Q5F5C7	SPOR domain-containing Protein	*N. gonorrhoeae*	0.0	99.64%	WP_192214476.1
Putative Cell-division protein	A0A378VWI6	Cell division protein FtsK	*N. gonorrhoeae*	2e-13	100%	WP_115176784.1
Putative Cell-division protein	A0A378VW48	Cell division protein FtsK	*N. gonorrhoeae*	1e-17	100%	WP_169335710.1

*Accession number A0A2X1VIK0 is now an obsolete entry in the Uniprot database.

Venn Diagram to Examine the Location of Proteins Identified During AP-MS Experiments

A Venn diagram was created to examine the relationship between the 305 proteins identified during AP-MS experiments (Figure B.6). The Venn diagram determines the number of proteins unique to the four sample groups and the number of proteins that are common to one or more groups. The four large ovals each represent their own sample group, either the interaction sample A3B3 (i.e., resin + GST-FtsE + Ng lysate) or one of the 3 control samples: A1B1 (i.e., resin + Ng lysate), A2B2 (i.e., resin + GST + Ng lysate), or A4B4 (i.e., resin + interaction buffer). Each oval contains an area where there is no overlap with any other group. This area represents the proteins that are unique to this group and have not been identified in any other sample. In addition, each oval has areas that overlap with each of the other 3 sample groups. These overlapping regions represent the proteins that are common to multiple sample groups (i.e., "common" proteins).

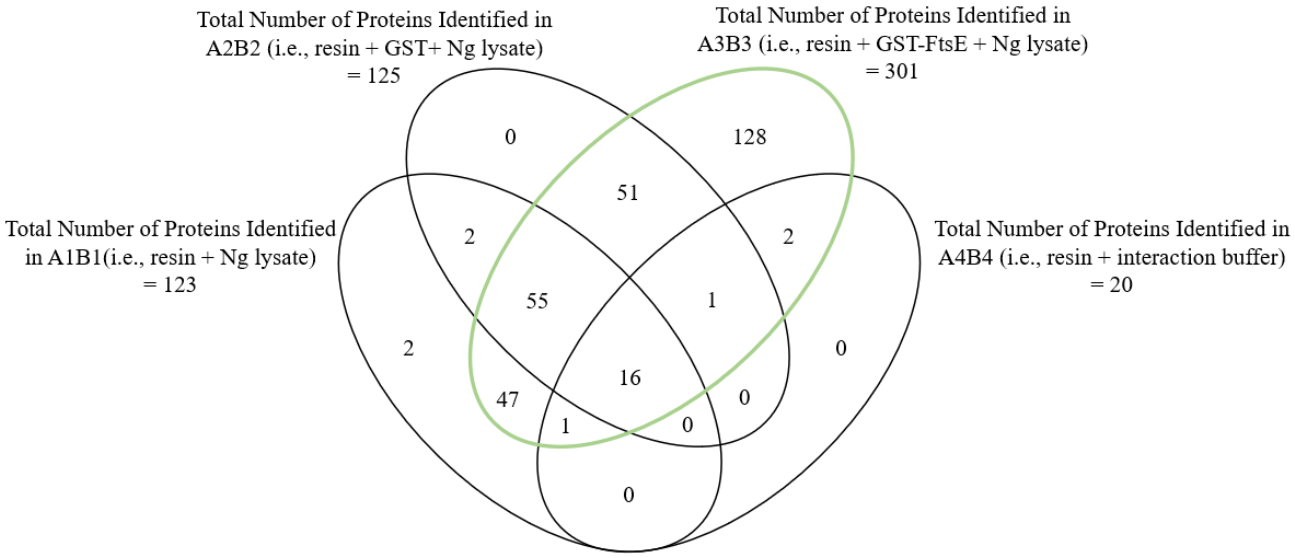

Figure B.6: Venn Diagram Illustrating the Relationship Between the Sample Groups from AP-MS Experiments. The 3 negative control samples (i.e., A1B1, A2B2, and A4B4) are shown in black while the interaction sample (i.e., A3B3) is shown in green.

The Venn diagram in Figure B.6 is a visual representation of the location of where these 305 proteins are found amongst the 4 sample groups (i.e., A1B1, A2B2, A3B3 and A4B4). Figure B.6 shows that 301 of the 305 proteins (98%) are found in A3B3 (i.e., resin + GST-FtsE + Ng

lysate). From these 301 proteins identified in A3B3, 128 (42.5%) are unique to the interaction sample A3B3 while the remaining 173 (57.4%) are common between the interaction sample and the negative controls (i.e., A1B1, A2B2, and A4B4). The largest number of common proteins was found in the intersection between the two negative controls A1B1 (i.e., resin + Ng lysate), A2B2 (i.e., resin + GST + Ng lysate), and the interaction sample A3B3 (i.e., resin + GST-FtsE + Ng lysate) with 55 proteins at this intersection. This is most likely because all three sample groups included the addition of the *N. gonorrhoeae* lysate to their samples while the remaining negative control A4B4 (i.e., resin + interaction buffer) did not include the addition of the *N. gonorrhoeae* lysate.

REFERENCES

Aarsman, M.E.G., Piette, A., Fraipont, C., Vinkenvleugel, T.M.F., Nguyen-Distèche, M., and den Blaauwen, T. (2005). Maturation of the *Escherichia coli* divisome occurs in two steps. Mol. Microbiol. *55*, 1631–1645. https://doi.org/10.1111/j.1365-2958.2005.04502.x.

Addinall, S.G., and Lutkenhaus, J. (1996). FtsA is localized to the septum in an FtsZ-dependent manner. J. Bacteriol. *178*, 7167–7172. https://doi.org/10.1128/jb.178.24.7167-7172.1996.

Addinall, S.G., Cao, C., and Lutkenhaus, J. (1997). FtsN, a late recruit to the septum in *Escherichia coli*. Mol. Microbiol. *25*, 303–309. https://doi.org/10.1046/j.1365-2958.1997.4641833.x.

Aebersold, R., and Mann, M. (2003). Mass spectrometry-based proteomics. Nature. *422*, 198–207. https://doi.org/10.1038/nature01511.

Alexeeva, S., Gadella, T.W.J., Verheul, J., Verhoeven, G.S., and Den Blaauwen, T. (2010). Direct interactions of early and late assembling division proteins in *Escherichia coli* cells resolved by FRET. Mol. Microbiol. *77*, 384–398. https://doi.org/10.1111/j.1365-2958.2010.07211.x.

Arends, S.J.R., Kustusch, R.J., and Weiss, D.S. (2009). ATP-binding site lesions in FtsE impair cell division. J. Bacteriol. *191*, 3772–3784. https://doi.org/10.1128/JB.00179-09.

Aussel, L., Barre, F.-X., Aroyo, M., Stasiak, A., Stasiak, A.Z., and Sherratt, D. (2002). FtsK is a DNA motor protein that activates chromosome dimer resolution by switching the catalytic state of the XerC and XerD recombinases. Cell. *108*, 195–205. https://doi.org/10.1016/S0092-8674(02)00624-4.

Ayala, J.A., Garrido, T., De Pedro, M.A., and Vicente, M. (1994). Molecular biology of bacterial septation. In, New Comprehensive Biochemistry, R. Hakenbeck, and J.-M. Ghuysen, eds. (Elsevier), pp. 73–101.

Barbour, A.G. (1981). Properties of penicillin-binding proteins in *Neisseria gonorrhoeae*. Antimicrob. Agents Chemother. *19*, 316–322. https://doi.org/10.1128/AAC.19.2.316.

Begg, K.J., and Donachie, W.D. (1985). Cell shape and division in *Escherichia coli*: experiments with shape and division mutants. J. Bacteriol. *163*, 615–622. https://doi.org/10.1128/jb.163.2.615-622.1985.

Begg, K.J., Dewar, S.J., and Donachie, W.D. (1995). A new *Escherichia coli* cell division gene, *ftsK*. J. Bacteriol. *177*, 6211–6222. https://doi.org/10.1128/jb.177.21.6211-6222.1995.

Berezuk, A.M., Glavota, S., Roach, E.J., Goodyear, M.C., Krieger, J.R., and Khursigara, C.M. (2018). Outer membrane lipoprotein RlpA is a novel periplasmic interaction partner of the cell division protein FtsK in *Escherichia coli*. Sci. Rep. *8*, 12933. https://doi.org/10.1038/s41598-018-30979-5.

Berezuk, A.M., Roach, E.J., Seidel, L., Lo, R.Y., and Khursigara, C.M. (2020). FtsA G50E mutant suppresses the essential requirement for FtsK during bacterial cell division in *Escherichia coli*. Can. J. Microbiol. *66*, 313–327. https://doi.org/10.1139/cjm-2019-0493.

Berggård, T., Linse, S., and James, P. (2007). Methods for the detection and analysis of protein–protein interactions. Proteomics. *7*, 2833–2842. https://doi.org/10.1002/pmic.200700131.

Bernatchez, S. (1997). Molecular cloning and characterization of the *ftsEX* genes of *Neisseria gonorrhoeae* CH811 encoding a putative ABC transporter and identification of their flanking genes. Doctoral dissertation. University of Ottawa.

Bernatchez, S., Francis, F.M., Salimnia, H., Beveridge, T.J., Li, H., and Dillon, J.-A.R. (2000). Genomic, transcriptional and phenotypic analysis of *ftsE* and *ftsX* of *Neisseria gonorrhoeae*. DNA Res. *7*, 75–81. https://doi.org/10.1093/dnares/7.2.75.

Bi, E., and Lutkenhaus, J. (1991). FtsZ ring structure associated with division in *Escherichia coli*. Nature. *354*, 161–164. https://doi.org/10.1038/354161a0.

den Blaauwen, T., and Luirink, J. (2019). Checks and balances in bacterial cell division. MBio. *10*, e00149-19. https://doi.org/10.1128/mBio.00149-19.

den Blaauwen, T., Andreu, J.M., and Monasterio, O. (2014). Bacterial cell division proteins as antibiotic targets. Bioorganic Chem. *55*, 27–38. https://doi.org/10.1016/j.bioorg.2014.03.007.

de Boer, P., Crossley, R., and Rothfield, L. (1992). The essential bacterial cell-division protein FtsZ is a GTPase. Nature. *359*, 254–256. https://doi.org/10.1038/359254a0.

de Boer, P.A., Cook, W.R., and Rothfield, L.I. (1990). Bacterial cell division. Annu. Rev. Genet. *24*, 249–274. https://doi.org/10.1146/annurev.ge.24.120190.001341.

Bork, P., Sander, C., and Valencia, A. (1992). An ATPase domain common to prokaryotic cell cycle proteins, sugar kinases, actin, and hsp7O heat shock proteins. Proc. Natl. Acad. Sci. U. S. A. *89*, 7290–7294. https://doi.org/10.1073/pnas.89.16.7290.

Botta, G.A., and Park, J.T. (1981). Evidence for involvement of penicillin-binding protein 3 in murein synthesis during septation but not during cell elongation. J. Bacteriol. *145*, 333–340. https://doi.org/10.1128/jb.145.1.333-340.1981.

Bowler, L.D., and Spratt, B.G. (1989). Membrane topology of penicillin-binding protein 3 of *Escherichia coli*. Mol. Microbiol. *3*, 1277–1286. https://doi.org/10.1111/j.1365-2958.1989.tb00278.x.

Boyle, D.S., Khattar, M.M., Addinall, S.G., Lutkenhaus, J., and Donachie, W.D. (1997). *ftsW* is an essential cell-division gene in *Escherichia coli*. Mol. Microbiol. *24*, 1263–1273. https://doi.org/10.1046/j.1365-2958.1997.4091773.x.

Bramhill, D. (1997). Bacterial cell division. Annu. Rev. Cell Dev. Biol. *13*, 395–424. https://doi.org/10.1146/annurev.cellbio.13.1.395.

Brandt, C., McFie, P.J., Vu, H., Chumala, P., Katselis, G.S., and Stone, S.J. (2019). Identification of calnexin as a diacylglycerol acyltransferase-2 interacting protein. PLoS One. *14*, e0210396. https://doi.org/10.1371/journal.pone.0210396.

Brymora, A., Valova, V.A., and Robinson, P.J. (2004). Protein-protein interactions identified by pull-down experiments and mass spectrometry. Curr. Protoc. Cell Biol. *22*, 17.5.1-17.5.51. https://doi.org/10.1002/0471143030.cb1705s22.

Buddelmeijer, N., and Beckwith, J. (2002). Assembly of cell division proteins at the *E. coli* cell center. Curr. Opin. Microbiol. *5*, 553–557. https://doi.org/10.1016/S1369-5274(02)00374-0.

Buddelmeijer, N., and Beckwith, J. (2004). A complex of the *Escherichia coli* cell division proteins FtsL, FtsB and FtsQ forms independently of its localization to the septal region. Mol. Microbiol. *52*, 1315–1327. https://doi.org/10.1111/j.1365-2958.2004.04044.x.

Busiek, K.K., Eraso, J.M., Wang, Y., and Margolin, W. (2012). The early divisome protein FtsA interacts directly through its 1c subdomain with the cytoplasmic domain of the late divisome protein FtsN. J. Bacteriol. *194*, 1989–2000. https://doi.org/10.1128/JB.06683-11.

Cho, H., Wivagg, C.N., Kapoor, M., Barry, Z., Rohs, P.D.A., Suh, H., Marto, J.A., Garner, E.C., and Bernhardt, T.G. (2016). Bacterial cell wall biogenesis is mediated by SEDS and PBP polymerase families functioning semi-autonomously. Nat. Microbiol. *1*, 16172. https://doi.org/10.1038/nmicrobiol.2016.172.

Cian, M.B., Giordano, N.P., Mettlach, J.A., Minor, K.E., and Dalebroux, Z.D. (2020). Separation of the cell envelope for gram-negative bacteria into inner and outer membrane fractions with technical adjustments for *Acinetobacter baumannii*. J. Vis. Exp. 60517. https://doi.org/10.3791/60517.

Condon, S.G.F., Mahbuba, D.-A., Armstrong, C.R., Diaz-Vazquez, G., Craven, S.J., LaPointe, L.M., Khadria, A.S., Chadda, R., Crooks, J.A., Rangarajan, N., et al. (2018). The FtsLB subcomplex of the bacterial divisome is a tetramer with an uninterrupted FtsL helix linking the transmembrane and periplasmic regions. J. Biol. Chem. *293*, 1623–1641. https://doi.org/10.1074/jbc.RA117.000426.

Corbin, B.D., Wang, Y., Beuria, T.K., and Margolin, W. (2007). Interaction between cell division proteins FtsE and FtsZ. J. Bacteriol. *189*, 3026–3035. https://doi.org/10.1128/JB.01581-06.

Dai, K., Xu, Y., and Lutkenhaus, J. (1993). Cloning and characterization of *ftsN*, an essential cell division gene in *Escherichia coli* isolated as a multicopy suppressor of *ftsA12*(Ts). J. Bacteriol. *175*, 3790–3797. https://doi.org/10.1128/jb.175.12.3790-3797.1993.

Dai, K., Xu, Y., and Lutkenhaus, J. (1996). Topological characterization of the essential *Escherichia coli* cell division protein FtsN. J. Bacteriol. *178*, 1328–1334. https://doi.org/10.1128/jb.178.5.1328-1334.1996.

Di Lallo, G., Ghelardini, P., and Paolozzi, L. (1999). Two-hybrid assay: construction of an *Escherichia coli* system to quantify homodimerization ability *in vivo*. Microbiology. *145*, 1485–1490. https://doi.org/10.1099/13500872-145-6-1485.

Di Lallo, G., Castagnoli, L., Ghelardini, P., and Paolozzi, L. (2001). A two-hybrid system based on chimeric operator recognition for studying protein homo/heterodimerization in *Escherichia coli*. Microbiology. *147*, 1651–1656. https://doi.org/10.1099/00221287-147-6-1651.

Di Lallo, G., Fagioli, M., Barionovi, D., Ghelardini, P., and Paolozzi, L. (2003). Use of a two-hybrid assay to study the assembly of a complex multicomponent protein machinery: bacterial septosome differentiation. Microbiology. *149*, 3353–3359. https://doi.org/10.1099/mic.0.26580-0.

Dillon, J.-A.R., Parti, R.P., and Thakur, S.D. (2015). Antibiotic resistance in *Neisseria gonorrhoeae*: Will infections be untreatable in the future? Culture. *35*, 1–8.

Draper, G.C., McLennan, N., Begg, K., Masters, M., and Donachie, W.D. (1998). Only the N-terminal domain of FtsK functions in cell division. J. Bacteriol. *180*, 4621–4627. https://doi.org/10.1128/JB.180.17.4621-4627.1998.

Du, S., and Lutkenhaus, J. (2017). Assembly and activation of the *Escherichia coli* divisome: The *E. coli* divisome. Mol. Microbiol. *105*, 177–187. https://doi.org/10.1111/mmi.13696.

Du, Y., and Arvidson, C.G. (2003). Identification of ZipA, a signal recognition particle-dependent protein from *Neisseria gonorrhoeae*. J. Bacteriol. *185*, 2122–2130. https://doi.org/10.1128/JB.185.7.2122-2130.2003.

Du, S., Pichoff, S., and Lutkenhaus, J. (2016). FtsEX acts on FtsA to regulate divisome assembly and activity. Proc. Natl. Acad. Sci. U. S. A. *113*, E5052–E5061. https://doi.org/10.1073/pnas.1606656113.

Du, S., Henke, W., Pichoff, S., and Lutkenhaus, J. (2019). How FtsEX localizes to the Z ring and interacts with FtsA to regulate cell division. Mol. Microbiol. *112*, 881–895. https://doi.org/10.1111/mmi.14324.

D'Ulisse, V., Fagioli, M., Ghelardini, P., and Paolozzi, L. (2007). Three functional subdomains of the *Escherichia coli* FtsQ protein are involved in its interaction with the other division proteins. Microbiology. *153*, 124–138. https://doi.org/10.1099/mic.0.2006/000265-0.

Dunham, W.H., Mullin, M., and Gingras, A.-C. (2012). Affinity-purification coupled to mass spectrometry: Basic principles and strategies. Proteomics. *12*, 1576–1590. https://doi.org/10.1002/pmic.201100523.

Egan, A.J.F., and Vollmer, W. (2013). The physiology of bacterial cell division. Ann. N. Y. Acad. Sci. *1277*, 8–28. https://doi.org/10.1111/j.1749-6632.2012.06818.x.

van den Ent, F., and Löwe, J. (2000). Crystal structure of the cell division protein FtsA from *Thermotoga maritima*. EMBO J. *19*, 5300–5307. https://doi.org/10.1093/emboj/19.20.5300.

Erickson, H.P. (1995). FtsZ, a prokaryotic homolog of tubulin? Cell. *80*, 367–370. https://doi.org/10.1016/0092-8674(95)90486-7.

Eswara, P.J., and Ramamurthi, K.S. (2017). Bacterial cell division: Nonmodels poised to take the spotlight. Annu. Rev. Microbiol. *71*, 393–411. https://doi.org/10.1146/annurev-micro-102215-095657.

Fraipont, C., Alexeeva, S., Wolf, B., van der Ploeg, R., Schloesser, M., den Blaauwen, T., and Nguyen-Distèche, M. (2011). The integral membrane FtsW protein and peptidoglycan synthase PBP3 form a subcomplex in *Escherichia coli*. Microbiology. *157*, 251–259. https://doi.org/10.1099/mic.0.040071-0.

Francis, F., Ramirez-Arcos, S., Salimnia, H., Victor, C., and Dillon, J.-A.R. (2000). Organization and transcription of the division cell wall (*dcw*) cluster in *Neisseria gonorrhoeae*. Gene. *251*, 141–151. https://doi.org/10.1016/S0378-1119(00)00200-6.

Gerding, M.A., Liu, B., Bendezú, F.O., Hale, C.A., Bernhardt, T.G., and de Boer, P.A.J. (2009). Self-enhanced accumulation of FtsN at division sites and roles for other proteins with a SPOR domain (DamX, DedD, and RlpA) in *Escherichia coli* cell constriction. J. Bacteriol. *191*, 7383–7401. https://doi.org/10.1128/JB.00811-09.

Ghuysen, J.M. (1991). Serine beta-lactamases and penicillin-binding proteins. Annu. Rev. Microbiol. *45*, 37–67. https://doi.org/10.1146/annurev.mi.45.100191.000345.

Gill, D.R., and Salmond, G.P.C. (1987). The *Escherichia coli* cell division proteins FtsY, FtsE and FtsX are inner membrane-associated. Mol. Gen. Genet. *210*, 504–508. https://doi.org/10.1007/BF00327204.

Gingras, A.-C., Gstaiger, M., Raught, B., and Aebersold, R. (2007). Analysis of protein complexes using mass spectrometry. Nat. Rev. Mol. Cell Biol. *8*, 645–654. https://doi.org/10.1038/nrm2208.

Gingras, A.-C., Abe, K.T., and Raught, B. (2019). Getting to know the neighborhood: using proximity-dependent biotinylation to characterize protein complexes and map organelles. Curr. Opin. Chem. Biol. *48*, 44–54. https://doi.org/10.1016/j.cbpa.2018.10.017.

Goehring, N.W., and Beckwith, J. (2005). Diverse paths to midcell: Assembly of the bacterial cell division machinery. Curr. Biol. *15*, R514–R526. https://doi.org/10.1016/j.cub.2005.06.038.

Goehring, N.W., Gonzalez, M.D., and Beckwith, J. (2006). Premature targeting of cell division proteins to midcell reveals hierarchies of protein interactions involved in divisome assembly: Assembly of *Escherichia coli* division apparatus. Mol. Microbiol. *61*, 33–45. https://doi.org/10.1111/j.1365-2958.2006.05206.x.

Gonzalez, M.D., and Beckwith, J. (2009). Divisome under construction: distinct domains of the small membrane protein FtsB are necessary for interaction with multiple cell division proteins. J. Bacteriol. *191*, 2815–2825. https://doi.org/10.1128/JB.01597-08.

Gonzalez, M.D., Akbay, E.A., Boyd, D., and Beckwith, J. (2010). Multiple interaction domains in FtsL, a protein component of the widely conserved bacterial FtsLBQ cell division complex. J. Bacteriol. *192*, 2757–2768. https://doi.org/10.1128/JB.01609-09.

Grant, S.G., Jessee, J., Bloom, F.R., and Hanahan, D. (1990). Differential plasmid rescue from transgenic mouse DNAs into *Escherichia coli* methylation-restriction mutants. Proc. Natl. Acad. Sci. U. S. A. *87*, 4645–4649. https://doi.org/10.1073/pnas.87.12.4645.

Greco-Stewart, V., Ramirez-Arcos, S., Liao, M., and Dillon, J.R. (2007). N terminus determinants of MinC from *Neisseria gonorrhoeae* mediate interaction with FtsZ but do not affect interaction with MinD or homodimerization. Arch. Microbiol. *187*, 451–458. https://doi.org/10.1007/s00203-007-0210-4.

Grenga, L., Luzi, G., Paolozzi, L., and Ghelardini, P. (2008). The *Escherichia coli* FtsK functional domains involved in its interaction with its divisome protein partners. FEMS Microbiol. Lett. *287*, 163–167. https://doi.org/10.1111/j.1574-6968.2008.01317.x.

Gundry, R.L., White, M.Y., Murray, C.I., Kane, L.A., Fu, Q., Stanley, B.A., and Van Eyk, J.E. (2009). Preparation of proteins and peptides for mass spectrometry analysis in a bottom-up proteomics workflow. In, Current Protocols in Molecular Biology, F.M. Ausubel, R. Brent, R.E. Kingston, D.D. Moore, J.G. Seidman, J.A. Smith, and K. Struhl, eds. (Hoboken, NJ, USA: John Wiley & Sons, Inc.), p. 10.25.1-10.25.23.

Guzman, L.-M., Barondess, J.J., and Beckwith, J. (1992). FtsL, an essential cytoplasmic membrane protein involved in cell division in *Escherichia coli*. J. Bacteriol. *174*, 7716–7728. .

Hale, C.A., and de Boer, P.A.J. (1997). Direct binding of FtsZ to ZipA, an essential component of the septal ring structure that mediates cell division in *E. coli*. Cell. *88*, 175–185. https://doi.org/10.1016/S0092-8674(00)81838-3.

Hale, C.A., and de Boer, P.A.J. (1999). Recruitment of ZipA to the septal ring of *Escherichia coli* is dependent on FtsZ and independent of FtsA. J. Bacteriol. *181*, 167–176. https://doi.org/10.1128/JB.181.1.167-176.1999.

Hale, C.A., and de Boer, P.A.J. (2002). ZipA is required for recruitment of FtsK, FtsQ, FtsL, and FtsN to the septal ring in *Escherichia coli*. J. Bacteriol. *184*, 2552–2556. https://doi.org/10.1128/JB.184.9.2552-2556.2002.

Harper, S., and Speicher, D.W. (2011). Purification of proteins fused to glutathione S-transferase. In, Protein Chromatography: Methods and Protocols, D. Walls, and S.T. Loughran, eds. (Totowa, NJ: Humana Press), pp. 259–280.

Hedrick, V.E., LaLand, M.N., Nakayasu, E.S., and Paul, L.N. (2015). Digestion, purification, and enrichment of protein samples for mass spectrometry. Curr. Protoc. Chem. Biol. *7*, 201–222. https://doi.org/10.1002/9780470559277.ch140272.

Henriques, A.O., Glaser, P., Piggot, P.J., and Moran Jr, C.P. (1998). Control of cell shape and elongation by the rodA gene in *Bacillus subtilis*. Mol. Microbiol. *28*, 235–247. https://doi.org/10.1046/j.1365-2958.1998.00766.x.

Karimova, G., Pidoux, J., Ullmann, A., and Ladant, D. (1998). A bacterial two-hybrid system based on a reconstituted signal transduction pathway. Proc. Natl. Acad. Sci. U. S. A. *95*, 5752–5756. https://doi.org/10.1073/pnas.95.10.5752.

Karimova, G., Ullmann, A., and Ladant, D. (2000). A bacterial two-hybrid system that exploits a cAMP signaling cascade in *Escherichia coli*. In, Applications of Chimeric Genes and Hybrid Proteins - Part C: Protein-Protein Interactions and Genomics, J. Thorner, S.D. Emr, and J.N. Abelson, eds. (Academic Press), pp. 59–73.

Karimova, G., Ladant, D., and Ullmann, A. (2002). Two-hybrid systems and their usage in infection biology. Int. J. Med. Microbiol. *292*, 17–25. https://doi.org/10.1078/1438-4221-00182.

Karimova, G., Dautin, N., and Ladant, D. (2005). Interaction network among *Escherichia coli* membrane proteins involved in cell division as revealed by bacterial two-hybrid analysis. J. Bacteriol. *187*, 2233–2243. .

Kellogg, D.S., Peacock, W.L., Deacon, W.E., and Pirkle, C.I. (1963). *Neisseria Gonorrhoeae* I: Virulence genetically linked to clonal variation. J. Bacteriol. *85*, 1274–1279. https://doi.org/10.1128/jb.85.6.1274-1279.1963.

Khadria, A.S., and Senes, A. (2013). The transmembrane domains of the bacterial cell division proteins FtsB and FtsL form a stable high-order oligomer. Biochemistry. *52*, 7542–7550. https://doi.org/10.1021/bi4009837.

Kim, S.-Y., and Hakoshima, T. (2019). GST pull-down assay to measure complex formations. In, The Hippo Pathway: Methods and Protocols, A. Hergovich, ed. (New York, NY: Springer New York), pp. 273–280.

LaPointe, L.M., Taylor, K.C., Subramaniam, S., Khadria, A., Rayment, I., and Senes, A. (2013). Structural organization of FtsB, a transmembrane protein of the bacterial divisome. Biochemistry. *52*, 2574–2585. https://doi.org/10.1021/bi400222r.

Lara, B., and Ayala, J.A. (2002). Topological characterization of the essential *Escherichia coli* cell division protein FtsW. FEMS Microbiol. Lett. *216*, 23–32. https://doi.org/10.1111/j.1574-6968.2002.tb11409.x.

de Leeuw, E., Graham, B., Phillips, G.J., ten Hagen-Jongman, C.M., Oudega, B., and Luirink, J. (1999). Molecular characterization of *Escherichia coli* FtsE and FtsX. Mol. Microbiol. *31*, 983–993. https://doi.org/10.1046/j.1365-2958.1999.01245.x.

Lenz, J.D., and Dillard, J.P. (2018). Pathogenesis of *Neisseria gonorrhoeae* and the host defense in ascending infections of human fallopian tube. Front. Immunol. *9*, 2710. https://doi.org/10.3389/fimmu.2018.02710.

Li, Y. (2011). Role of FtsA in cell division in *Neisseria gonorrhoeae*. Doctoral dissertation. University of Saskatchewan.

Liu, G., Draper, G.C., and Donachie, W.D. (1998). FtsK is a bifunctional protein involved in cell division and chromosome localization in *Escherichia coli*. Mol. Microbiol. *29*, 893–903. https://doi.org/10.1046/j.1365-2958.1998.00986.x.

Liu, G., Tang, C.M., and Exley, R.M. (2015). Non-pathogenic *Neisseria*: members of an abundant, multi-habitat, diverse genus. Microbiology. *161*, 1297–1312. https://doi.org/10.1099/mic.0.000086.

Liu, Z., Mukherjee, A., and Lutkenhaus, J. (1999). Recruitment of ZipA to the division site by interaction with FtsZ. Mol. Microbiol. *31*, 1853–1861. https://doi.org/10.1046/j.1365-2958.1999.01322.x.

Lock, R.L., and Harry, E.J. (2008). Cell-division inhibitors: new insights for future antibiotics. Nat. Rev. Drug Discov. *7*, 324–338. https://doi.org/10.1038/nrd2510.

Loughran, S.T., and Walls, D. (2011). Purification of poly-histidine-tagged proteins. In, Protein Chromatography: Methods and Protocols, S.T. Loughran, and D. Walls, eds. (Totowa, NJ: Humana Press), pp. 311–335.

Löwe, J., and Amos, L.A. (1998). Crystal structure of the bacterial cell-division protein FtsZ. Nature. *391*, 203–206. https://doi.org/10.1038/34472.

Luo, L., King, N.P., Yeo, J.C., Jones, A., and Stow, J.L. (2014). Single-step protease cleavage elution for identification of protein-protein interactions from GST pull-down and mass spectrometry. Proteomics. *14*, 19–23. https://doi.org/10.1002/pmic.201300315.

Lutkenhaus, J. (1993). *Escherichia coli* cell division. Curr. Opin. Genet. Dev. *3*, 783–788. https://doi.org/10.1016/S0959-437X(05)80099-1.

Lutkenhaus, J. (2009). Min oscillation in bacteria. In, Cellular Oscillatory Mechanisms, M. Maroto, and N.A.M. Monk, eds. (New York, NY: Springer New York), pp. 49–61.

Lutkenhaus, J., and Du, S. (2017). *E. coli* cell cycle machinery. In, Prokaryotic Cytoskeletons, J. Löwe, and L.A. Amos, eds. (Cham: Springer International Publishing), pp. 27–65.

Ma, X., and Margolin, W. (1999). Genetic and functional analyses of the conserved C-terminal core domain of *Escherichia coli* FtsZ. J. Bacteriol. *181*, 7531–7544. https://doi.org/10.1128/JB.181.24.7531-7544.1999.

Madigan, M.T., Martinko, J.M., and Parker, J. (2003). Microbial growth. In, Brock Biology of Microorganisms, (Upper Saddle River, NJ: Prentice Hall), pp. 137–166.

Maggi, S., Massidda, O., Luzi, G., Fadda, D., Paolozzi, L., and Ghelardini, P. (2008). Division protein interaction web: identification of a phylogenetically conserved common interactome between *Streptococcus pneumoniae* and *Escherichia coli*. Microbiology. *154*, 3042–3052. https://doi.org/10.1099/mic.0.2008/018697-0.

Margolin, W. (2000). Themes and variations in prokaryotic cell division. FEMS Microbiol. Rev. *24*, 531–548. https://doi.org/10.1111/j.1574-6976.2000.tb00554.x.

Meeske, A.J., Riley, E.P., Robins, W.P., Uehara, T., Mekalanos, J.J., Kahne, D., Walker, S., Kruse, A.C., Bernhardt, T.G., and Rudner, D.Z. (2016). SEDS proteins are a widespread family of bacterial cell wall polymerases. Nature. *537*, 634–638. https://doi.org/10.1038/nature19331.

Mehmood, S., Allison, T.M., and Robinson, C.V. (2015). Mass spectrometry of protein complexes: From origins to applications. Annu. Rev. Phys. Chem. *66*, 453–474. https://doi.org/10.1146/annurev-physchem-040214-121732.

Mercer, K.L.N., and Weiss, D.S. (2002). The *Escherichia coli* cell division protein FtsW is required to recruit its cognate transpeptidase, FtsI (PBP3), to the division site. J. Bacteriol. *184*, 904–912. https://doi.org/10.1128/jb.184.4.904-912.2002.

Mingorance, J., Tamames, J., and Vicente, M. (2004). Genomic channeling in bacterial cell division. J. Mol. Recognit. *17*, 481–487. https://doi.org/10.1002/jmr.718.

Miroux, B., and Walker, J.E. (1996). Over-production of proteins in *Escherichia coli*: Mutant hosts that allow synthesis of some membrane proteins and globular proteins at high levels. J. Mol. Biol. *260*, 289–298. https://doi.org/10.1006/jmbi.1996.0399.

Miura, K. (2018). An overview of current methods to confirm protein-protein interactions. Protein Pept. Lett. *25*, 728–733. https://doi.org/10.2174/0929866525666180821122240.

Mohammadi, T., van Dam, V., Sijbrandi, R., Vernet, T., Zapun, A., Bouhss, A., Diepeveen-de Bruin, M., Nguyen-Distèche, M., de Kruijff, B., and Breukink, E. (2011). Identification of FtsW as a transporter of lipid-linked cell wall precursors across the membrane: FtsW transports lipid II across the membrane. EMBO J. *30*, 1425–1432. https://doi.org/10.1038/emboj.2011.61.

Mohammadi, T., Sijbrandi, R., Lutters, M., Verheul, J., Martin, N.I., den Blaauwen, T., de Kruijff, B., and Breukink, E. (2014). Specificity of the transport of lipid II by FtsW in *Escherichia coli*. J. Biol. Chem. *289*, 14707–14718. https://doi.org/10.1074/jbc.M114.557371.

Mukherjee, A., and Lutkenhaus, J. (1994). Guanine nucleotide-dependent assembly of FtsZ into filaments. J. Bacteriol. *176*, 2754–2758. https://doi.org/10.1128/jb.176.9.2754-2758.1994.

Mukherjee, A., and Lutkenhaus, J. (1998). Dynamic assembly of FtsZ regulated by GTP hydrolysis. EMBO J. *17*, 462–469. https://doi.org/10.1093/emboj/17.2.462.

Nair, M., Jagadeeshan, S., Katselis, G., Luan, X., Momeni, Z., Henao-Romero, N., Chumala, P., Tam, J.S., Yamamoto, Y., Ianowski, J.P., et al. (2021). Lipopolysaccharides induce a RAGE-mediated sensitization of sensory neurons and fluid hypersecretion in the upper airways. Sci. Rep. *11*, 8336. https://doi.org/10.1038/s41598-021-86069-6.

Natale, P., Pazos, M., and Vicente, M. (2013). The *Escherichia coli* divisome: born to divide. Environ. Microbiol. *15*, 3169–3182. https://doi.org/10.1111/1462-2920.12227.

Nikolaichik, Y.A., and Donachie, W.D. (2000). Conservation of gene order amongst cell wall and cell division genes in eubacteria, and ribosomal genes in eubacteria and eukaryotic organelles. Genetica. *108*, 1–7. https://doi.org/10.1023/a:1004077806910.

Ortiz, C., Natale, P., Cueto, L., and Vicente, M. (2016). The keepers of the ring: regulators of FtsZ assembly. FEMS Microbiol. Rev. *40*, 57–67. https://doi.org/10.1093/femsre/fuv040.

Ouellette, S.P., Karimova, G., Davi, M., and Ladant, D. (2017). Analysis of membrane protein interactions with a bacterial adenylate cyclase–based two-hybrid (BACTH) technique. Curr. Protoc. Mol. Biol. *118*. https://doi.org/10.1002/cpmb.36.

Park, K.-T., Du, S., and Lutkenhaus, J. (2020). Essential role for FtsL in activation of septal peptidoglycan synthesis. MBio. *11*, e03012–e03020. https://doi.org/10.1128/mBio.03012-20.

Park, K.-T., Pichoff, S., Du, S., and Lutkenhaus, J. (2021). FtsA acts through FtsW to promote cell wall synthesis during cell division in *Escherichia coli*. Proc. Natl. Acad. Sci. U. S. A. *118*, e2107210118. https://doi.org/10.1073/pnas.2107210118.

Picard, F.J., and Dillon, J.R. (1989). Cloning and organization of seven arginine biosynthesis genes from *Neisseria gonorrhoeae*. J. Bacteriol. *171*, 1644–1651. https://doi.org/10.1128/JB.171.3.1644-1651.1989.

Pichoff, S., and Lutkenhaus, J. (2002). Unique and overlapping roles for ZipA and FtsA in septal ring assembly in *Escherichia coli*. EMBO J. *21*, 685–693. https://doi.org/10.1093/emboj/21.4.685.

Pichoff, S., and Lutkenhaus, J. (2005). Tethering the Z ring to the membrane through a conserved membrane targeting sequence in FtsA: Membrane tethering of Z ring by FtsA. Mol. Microbiol. *55*, 1722–1734. https://doi.org/10.1111/j.1365-2958.2005.04522.x.

Pichoff, S., and Lutkenhaus, J. (2007). Identification of a region of FtsA required for interaction with FtsZ. Mol. Microbiol. *64*, 1129–1138. https://doi.org/10.1111/j.1365-2958.2007.05735.x.

Pichoff, S., Du, S., and Lutkenhaus, J. (2018). Disruption of divisome assembly rescued by FtsN–FtsA interaction in *Escherichia coli*. Proc. Natl. Acad. Sci. U. S. A. *115*, E6855–E6862. https://doi.org/10.1073/pnas.1806450115.

Pichoff, S., Du, S., and Lutkenhaus, J. (2019). Roles of FtsEX in cell division. Res. Microbiol. *170*, 374–380. https://doi.org/10.1016/j.resmic.2019.07.003.

Pla, J., Dopazo, A., and Vicente, M. (1990). The native form of FtsA, a septal protein of *Escherichia coli*, is located in the cytoplasmic membrane. J. Bacteriol. *172*, 5097–5102. https://doi.org/10.1128/jb.172.9.5097-5102.1990.

Platt, T., Müller-Hill, B., and Miller, J.H. (1972). Assay of β-galactosidase. In, Experiments in Molecular Genetics, J.H. Miller, ed. (Cold Spring Harbor, New York: Cold Spring Harbor Laboratory), pp. 352–355.

Powell, A.J., Tomberg, J., Deacon, A.M., Nicholas, R.A., and Davies, C. (2009). Crystal structures of penicillin-binding protein 2 from penicillin-susceptible and -resistant strains of *Neisseria gonorrhoeae* reveal an unexpectedly subtle mechanism for antibiotic resistance. J. Biol. Chem. *284*, 1202–1212. https://doi.org/10.1074/jbc.M805761200.

Ramirez-Arcos, S., Szeto, J., Beveridge, T.J., Victor, C., Francis, F., and Dillon, J.-A.R. (2001). Deletion of the cell-division inhibitor MinC results in lysis of *Neisseria gonorrhoeae*. Microbiology. *147*, 225–237. https://doi.org/10.1099/00221287-147-1-225.

Ramirez-Arcos, S., Szeto, J., Dillon, J.-A.R., and Margolin, W. (2002). Conservation of dynamic localization among MinD and MinE orthologues: oscillation of *Neisseria gonorrhoeae* proteins in *Escherichia coli*. Mol. Microbiol. *46*, 493–504. https://doi.org/10.1046/j.1365-2958.2002.03168.x.

RayChaudhuri, D., and Park, J.T. (1992). *Escherichia coli* cell-division gene *ftsZ* encodes a novel GTP-binding protein. Nature. *359*, 251–254. https://doi.org/10.1038/359251a0.

Reddy, M. (2007). Role of FtsEX in cell division of *Escherichia coli*: Viability of *ftsEX* mutants is dependent on functional SufI or high osmotic strength. J. Bacteriol. *189*, 98–108. https://doi.org/10.1128/JB.01347-06.

Rico, A.I., García-Ovalle, M., Mingorance, J., and Vicente, M. (2004). Role of two essential domains of *Escherichia coli* FtsA in localization and progression of the division ring: Role of essential domains of FtsA. Mol. Microbiol. *53*, 1359–1371. https://doi.org/10.1111/j.1365-2958.2004.04245.x.

Robichon, C., Karimova, G., Beckwith, J., and Ladant, D. (2011). Role of leucine zipper motifs in association of the *Escherichia coli* cell division proteins FtsL and FtsB. J. Bacteriol. *193*, 4988–4992. https://doi.org/10.1128/JB.00324-11.

Ropp, P.A., and Nicholas, R.A. (1997). Cloning and characterization of the *ponA* gene encoding penicillin-binding protein 1 from *Neisseria gonorrhoeae* and *Neisseria meningitidis*. J. Bacteriol. *179*, 2783–2787. https://doi.org/10.1128/jb.179.8.2783-2787.1997.

Rothfield, L.I., and Justice, S.S. (1997). Bacterial cell division: The cycle of the ring. Cell. *88*, 581–584. https://doi.org/10.1016/S0092-8674(00)81899-1.

Rothfield, L., Justice, S., and García-Lara, J. (1999). Bacterial cell division. Annu. Rev. Genet. *33*, 423–448. https://doi.org/10.1146/annurev.genet.33.1.423.

Salimnia, H., Radia, A., Bernatchez, S., Beveridge, T.J., and Dillon, J.R. (2000). Characterization of the *ftsZ* cell division gene of *Neisseria gonorrhoeae*: expression in *Escherichia coli* and *N. gonorrhoeae*. Arch. Microbiol. *173*, 10–20. https://doi.org/10.1007/s002030050002.

Sambrook, J., and Russell, D.W. (2001a). Plasmids and their usefulness in molecular cloning. In, Molecular Cloning: A Laboratory Manual, (Cold Spring Harbor Laboratory Press, Cold Spring Harbor, New York), p. 1.116-1.118.

Sambrook, J., and Russell, D.W. (2001b). Commonly used techniques in molecular cloning. In, Molecular Cloning: A Laboratory Manual, (Cold Spring Harbor Laboratory Press, Cold Spring Harbor, New York), p. A8.40-A8.49.

Sánchez, M., Valencia, A., Ferrándiz, M.J., Sander, C., and Vicente, M. (1994). Correlation between the structure and biochemical activities of FtsA, an essential cell division protein of the actin family. EMBO J. *13*, 4919–4925. https://doi.org/10.1002/j.1460-2075.1994.tb06819.x.

Sánchez-Pulido, L., Devos, D., Genevrois, S., Vicente, M., and Valencia, A. (2003). POTRA: a conserved domain in the FtsQ family and a class of beta-barrel outer membrane proteins. Trends Biochem. Sci. *28*, 523–526. https://doi.org/10.1016/j.tibs.2003.08.003.

Sass, P., and Brötz-Oesterhelt, H. (2013). Bacterial cell division as a target for new antibiotics. Curr. Opin. Microbiol. *16*, 522–530. https://doi.org/10.1016/j.mib.2013.07.006.

Sauvage, E., Kerff, F., Terrak, M., Ayala, J.A., and Charlier, P. (2008). The penicillin-binding proteins: structure and role in peptidoglycan biosynthesis. FEMS Microbiol. Rev. *32*, 234–258. https://doi.org/10.1111/j.1574-6976.2008.00105.x.

Schäfer, F., Seip, N., Maertens, B., Block, H., and Kubicek, J. (2015). Purification of GST-tagged proteins. In, Methods in Enzymology, J.R. Lorsch, ed. (Academic Press), pp. 127–139.

Schmidt, K.L., Peterson, N.D., Kustusch, R.J., Wissel, M.C., Graham, B., Phillips, G.J., and Weiss, D.S. (2004). A predicted ABC transporter, FtsEX, is needed for cell division in *Escherichia coli*. J. Bacteriol. *186*, 785–793. https://doi.org/10.1128/JB.186.3.785-793.2004.

Sherratt, D.J., Lau, I.F., and Barre, F.-X. (2001). Chromosome segregation. Curr. Opin. Microbiol. *4*, 653–659. .

Skoog, K., and Daley, D.O. (2012). The *Escherichia coli* cell division protein ZipA forms homodimers prior to association with FtsZ. Biochemistry. *51*, 1407–1415. https://doi.org/10.1021/bi2015647.

Smits, A.H., and Vermeulen, M. (2016). Characterizing protein–protein interactions using mass spectrometry: challenges and opportunities. Trends Biotechnol. *34*, 825–834. https://doi.org/10.1016/j.tibtech.2016.02.014.

Snyder, L., Peters, J.E., Henkin, T.M., and Champness, W. (2013). The bacterial chromosome: DNA structure, replication and segregation. In, Molecular Genetics of Bacteria, (Washington, DC: ASM Press), pp. 42–43.

Snyder, L.A.S., Saunders, N.J., and Shafer, W.M. (2001). A putatively phase variable gene (*dca*) required for natural competence in *Neisseria gonorrhoeae* but not *Neisseria meningitidis* is located within the division cell wall (*dcw*) gene cluster. J. Bacteriol. *183*, 1233–1241. https://doi.org/10.1128/JB.183.4.1233-1241.2001.

Snyder, L.A.S., Shafer, W.M., and Saunders, N.J. (2003). Divergence and transcriptional analysis of the division cell wall (*dcw*) gene cluster in *Neisseria* spp. Mol. Microbiol. *47*, 431–442. https://doi.org/10.1046/j.1365-2958.2003.03204.x.

Söderström, B., and Daley, D.O. (2017). The bacterial divisome: more than a ring? Curr. Genet. *63*, 161–164. https://doi.org/10.1007/s00294-016-0630-2.

Söderström, B., Chan, H., Shilling, P.J., Skoglund, U., and Daley, D.O. (2018). Spatial separation of FtsZ and FtsN during cell division. Mol. Microbiol. *107*, 387–401. https://doi.org/10.1111/mmi.13888.

Spence, J.M., Wright, L., and Clark, V.L. (2008). Laboratory maintenance of *Neisseria gonorrhoeae*. Curr. Protoc. Microbiol. *8*, 4A.1.1-4A.1.26. https://doi.org/10.1002/9780471729259.mc04a01s8.

Steen, H., and Mann, M. (2004). The abc's (and xyz's) of peptide sequencing. Nat. Rev. Mol. Cell Biol. *5*, 699–711. https://doi.org/10.1038/nrm1468.

Stefanova, M.E., Tomberg, J., Olesky, M., Höltje, J.-V., Gutheil, W.G., and Nicholas, R.A. (2003). *Neisseria gonorrhoeae* penicillin-binding protein 3 exhibits exceptionally high carboxypeptidase and β-lactam binding activities. Biochemistry. *42*, 14614–14625. https://doi.org/10.1021/bi0350607.

Stefanova, M.E., Tomberg, J., Davies, C., Nicholas, R.A., and Gutheil, W.G. (2004). Overexpression and enzymatic characterization of *Neisseria gonorrhoeae* penicillin-binding protein 4. Eur. J. Biochem. *271*, 23–32. https://doi.org/10.1046/j.1432-1033.2003.03886.x.

Studier, F.W., Rosenberg, A.H., Dunn, J.J., and Dubendorff, J.W. (1990). Use of T7 RNA polymerase to direct expression of cloned genes. In, Methods in Enzymology, (Academic Press), pp. 60–89.

Sweet, R. and Walker (2011). Gonorrhea infection in women: prevalence, effects, screening, and management. Int. J. Womens Health. *3*, 197–206. https://doi.org/10.2147/IJWH.S13427.

Szeto, J., Ramirez-Arcos, S., Raymond, C., Hicks, L.D., Kay, C.M., and Dillon, J.-A.R. (2001). Gonococcal MinD affects cell division in *Neisseria gonorrhoeae* and *Escherichia coli* and exhibits a novel self-interaction. J. Bacteriol. *183*, 6253–6264. https://doi.org/10.1128/JB.183.21.6253-6264.2001.

Szklarczyk, D., Gable, A.L., Lyon, D., Junge, A., Wyder, S., Huerta-Cepas, J., Simonovic, M., Doncheva, N.T., Morris, J.H., Bork, P., et al. (2019). STRING v11: protein–protein association networks with increased coverage, supporting functional discovery in genome-wide experimental datasets. Nucleic Acids Res. *47*, D607–D613. https://doi.org/10.1093/nar/gky1131.

Thakur, S.D., Levett, P.N., Horsman, G.B., and Dillon, J.-A.R. (2018). Association of *Neisseria gonorrhoeae* genogroups and specific PBP2/MtrR/PorB mutation patterns with susceptibility to penicillin in a susceptible gonococcal population. J. Antimicrob. Chemother. *73*, 2682–2686. https://doi.org/10.1093/jac/dky233.

Turriziani, B., Garcia-Munoz, A., Pilkington, R., Raso, C., Kolch, W., and von Kriegsheim, A. (2014). On-beads digestion in conjunction with data-dependent mass spectrometry: A shortcut to

quantitative and dynamic interaction proteomics. Biology. *3*, 320–332. https://doi.org/10.3390/biology3020320.

Typas, A., and Sourjik, V. (2015). Bacterial protein networks: properties and functions. Nat. Rev. Microbiol. *13*, 559–572. https://doi.org/10.1038/nrmicro3508.

Typas, A., Banzhaf, M., Gross, C.A., and Vollmer, W. (2012). From the regulation of peptidoglycan synthesis to bacterial growth and morphology. Nat. Rev. Microbiol. *10*, 123–136. https://doi.org/10.1038/nrmicro2677.

Unemo, M., and Ison, C. (2013). Gonorrhoea. In, Laboratory Diagnosis of Sexually Transmitted Infections, Including Human Immunodeficiency Virus, M. Unemo, R. Ballard, C. Ison, D. Lewis, F. Ndowa, and R. Peeling, eds. (World Health Organization), pp. 21–54.

Unemo, M., and Shafer, W.M. (2014). Antimicrobial resistance in *Neisseria gonorrhoeae* in the 21st century: Past, evolution, and future. Clin. Microbiol. Rev. *27*, 587–613. https://doi.org/10.1128/CMR.00010-14.

Unemo, M., Fasth, O., Fredlund, H., Limnios, A., and Tapsall, J. (2009). Phenotypic and genetic characterization of the 2008 WHO *Neisseria gonorrhoeae* reference strain panel intended for global quality assurance and quality control of gonococcal antimicrobial resistance surveillance for public health purposes. J. Antimicrob. Chemother. *63*, 1142–1151. https://doi.org/10.1093/jac/dkp098.

Unemo, M., Seifert, H.S., Hook, E.W., Hawkes, S., Ndowa, F., and Dillon, J.-A.R. (2019a). Gonorrhoea. Nat. Rev. Dis. Primer. *5*, 79. https://doi.org/10.1038/s41572-019-0128-6.

Unemo, M., Golparian, D., and Eyre, D.W. (2019b). Antimicrobial resistance in *Neisseria gonorrhoeae* and treatment of gonorrhea. In, *Neisseria Gonorrhoeae*: Methods and Protocols, M. Christodoulides, ed. (New York, NY: Springer New York), pp. 37–58.

Ursinus, A., van den Ent, F., Brechtel, S., de Pedro, M., Höltje, J.-V., Löwe, J., and Vollmer, W. (2004). Murein (peptidoglycan) binding property of the essential cell division protein FtsN from *Escherichia coli*. J. Bacteriol. *186*, 6728–6737. https://doi.org/10.1128/JB.186.20.6728-6737.2004.

Van De Putte, P., Van Dillewijn, J., and Rörsch, A. (1964). The selection of mutants of *Escherichia coli* with impaired cell division at elevated temperature. Mutat. Res. *1*, 121–128. https://doi.org/10.1016/0027-5107(64)90014-4.

Varnaitė, R., and MacNeill, S.A. (2016). Meet the neighbors: Mapping local protein interactomes by proximity-dependent labeling with BioID. Proteomics. *16*, 2503–2518. https://doi.org/10.1002/pmic.201600123.

Vega, D.E., and Margolin, W. (2018). Direct interaction between the two Z Ring membrane anchors FtsA and ZipA. J. Bacteriol. *201*, e00579-18. https://doi.org/10.1128/JB.00579-18.

Vicente, M., Gomez, M.J., and Ayala, J.A. (1998). Regulation of transcription of cell division genes in the *Escherichia coli dcw* cluster. Cell. Mol. Life Sci. *54*, 317–324. https://doi.org/10.1007/s000180050158.

Villanelo, F., Ordenes, A., Brunet, J., Lagos, R., and Monasterio, O. (2011). A model for the *Escherichia coli* FtsB/FtsL/FtsQ cell division complex. BMC Struct. Biol. *11*, 28. https://doi.org/10.1186/1472-6807-11-28.

Vollmer, W. (2006). The prokaryotic cytoskeleton: a putative target for inhibitors and antibiotics? Appl. Microbiol. Biotechnol. *73*, 37–47. https://doi.org/10.1007/s00253-006-0586-0.

Wang, L., and Lutkenhaus, J. (1998). FtsK is an essential cell division protein that is localized to the septum and induced as part of the SOS response. Mol. Microbiol. *29*, 731–740. https://doi.org/10.1046/j.1365-2958.1998.00958.x.

Wang, L., Khattar, M.K., Donachie, W.D., and Lutkenhaus, J. (1998). FtsI and FtsW are localized to the septum in *Escherichia coli*. J. Bacteriol. *180*, 2810–2816. https://doi.org/10.1128/JB.180.11.2810-2816.1998.

Wang, X., Huang, J., Mukherjee, A., Cao, C., and Lutkenhaus, J. (1997). Analysis of the interaction of FtsZ with itself, GTP, and FtsA. J. Bacteriol. *179*, 5551–5559. https://doi.org/10.1128/jb.179.17.5551-5559.1997.

Westling-Häggström, B., Elmros, T., Normark, S., and Winblad, B. (1977). Growth pattern and cell division in *Neisseria gonorrhoeae*. J. Bacteriol. *129*, 333–342. https://doi.org/10.1128/JB.129.1.333-342.1977.

Wissel, M.C., and Weiss, D.S. (2004). Genetic analysis of the cell division protein FtsI (PBP3): Amino acid substitutions that impair septal localization of FtsI and recruitment of FtsN. J. Bacteriol. *186*, 490–502. https://doi.org/10.1128/JB.186.2.490-502.2004.

Wissel, M.C., Wendt, J.L., Mitchell, C.J., and Weiss, D.S. (2005). The transmembrane helix of the *Escherichia coli* division protein FtsI localizes to the septal ring. J. Bacteriol. *187*, 320–328. https://doi.org/10.1128/JB.187.1.320-328.2005.

Wissmueller, S., Font, J., Liew, C.W., Cram, E., Schroeder, T., Turner, J., Crossley, M., Mackay, J.P., and Matthews, J.M. (2011). Protein-protein interactions: Analysis of a false positive GST pulldown result. Proteins. *79*, 2365–2371. https://doi.org/10.1002/prot.23068.

Workowski, K.A., Bachmann, L.H., Chan, P.A., Johnston, C.M., Muzny, C.A., Park, I., Reno, H., Zenilman, J.M., and Bolan, G.A. (2021). Sexually transmitted infections treatment guidelines, 2021. MMWR Recomm. Rep. *70*, 1–187. https://doi.org/10.15585/mmwr.rr7004a1.

World Health Organization (2020). WHO guidelines for the treatment of *Neisseria gonorrhoeae* (Geneva: World Health Organization).

World Health Organization (2021). Global progress report on HIV, viral hepatitis and sexually transmitted infections, 2021 (Geneva: World Health Organization).

Yang, D.C., Peters, N.T., Parzych, K.R., Uehara, T., Markovski, M., and Bernhardt, T.G. (2011). An ATP-binding cassette transporter-like complex governs cell-wall hydrolysis at the bacterial cytokinetic ring. Proc. Natl. Acad. Sci. U. S. A. *108*, E1052–E1060. https://doi.org/10.1073/pnas.1107780108.

Yim, L., Vandenbussche, G., Mingorance, J., Rueda, S., Casanova, M., Ruysschaert, J.-M., and Vicente, M. (2000). Role of the carboxy terminus of *Escherichia coli* FtsA in self-interaction and cell division. J. Bacteriol. *182*, 6366–6373. https://doi.org/10.1128/JB.182.22.6366-6373.2000.

Yu, X., Tran, A.H., Sun, Q., and Margolin, W. (1998). Localization of cell division protein FtsK to the *Escherichia coli* septum and identification of a potential N-terminal targeting domain. J. Bacteriol. *180*, 1296–1304. https://doi.org/10.1128/JB.180.5.1296-1304.1998.

Yugandhar, K., Gupta, S., and Yu, H. (2019). Inferring protein-protein interaction networks from mass spectrometry-based proteomic approaches: A mini-review. Comput. Struct. Biotechnol. J. *17*, 805–811. https://doi.org/10.1016/j.csbj.2019.05.007.

Zhou, M., Li, Q., and Wang, R. (2016). Current experimental methods for characterizing protein-protein interactions. ChemMedChem. *11*, 738–756. https://doi.org/10.1002/cmdc.201500495.

Zou, Y., Li, Y., and Dillon, J.-A.R. (2017a). The distinctive cell division interactome of *Neisseria gonorrhoeae*. BMC Microbiol. *17*, 232. https://doi.org/10.1186/s12866-017-1140-1.

Zou, Y., Li, Y., Ekanayake, S.B., and Dillon, J.-A.R. (2017b). An *Escherichia coli* expression model reveals the species-specific function of FtsA from *Neisseria gonorrhoeae* in cell division. FEMS Microbiol. Lett. *364*, 1–9. https://doi.org/10.1093/femsle/fnx078.